Mitochondrial modulators of hypoxia related pathways in tumours.

Cameron Edward Snell

Submitted for the Degree of D.Phil in Clinical Laboratory Sciences
Hiliary Term 2013.

Abstract

The Lon protease is a mitochondrial matrix quality-control protease belonging to the family of AAA+ proteins (ATPases associated with many cellular activities). We had previously found Lon to be upregulated in lung tumours with a non-angiogenic phenotype in a microarray study comparing these to conventional angiogenic tumours. In this project I set out to investigate whether Lon had any role in modulating the hypoxic response of tumour cells. Using a novel monoclonal antibody against Lon, I found that upregulation of Lon was present in breast and lung tumours and that higher levels of Lon are correlated with shorter overall survival in breast cancer patients. Targeting Lon with siRNA and shRNA in tumour cell lines reduced the normoxic and hypoxic stabilisation of HIF-α subunits. This is mediated through a mechanism independent of the activity of HIF-prolyl hydroxylases and independent of any changes in mitochondrial transcription. I found that the pre-imported form of Lon could bind and chaperone VHL in the cytoplasm potentially modulating VHL activity. In cell lines and human tumours, I observed that the proline-hydroxylated form of HIF-1α is induced by hypoxia and the hydroxylated form of HIF-1α is associated with shorter overall survival in breast cancer patients. This observation supports the notion that higher levels of Lon is associated with poor survival by downregulating VHL leading to higher levels of hydroxylated HIF. Finally I show that targeting Lon in cell lines is able to inhibit growth in a cell-line dependent fashion and partially reverses the Warburg effect, increasing oxygen consumption and reducing lactate production. In conclusion, I have demonstrated the broad therapeutic potential of targeting the Lon protease in tumours and highlighted a mechanism of post-hydroxylation HIF-regulation that has not been previously recognised in VHL competent tumours.

Acknowledgements

I would like to acknowledge the contribution of the Nuffield Dominions Trust for supporting my research and the opportunity to travel to Oxford from Australia to produce the work presented here.

My supervisors Professor Francesco Pezzella and Professor Kevin Gatter have been instrumental in my development as a scientist and have been an ongoing source of guidance and support in producing this work. I am very grateful for their time and enthusiasm for translational research. Professor Adrian Harris has been especially supportive and I have benefitted greatly from his intellectual input and help from members of his laboratory.

I am indebted to those who have given their time to teach me laboratory techniques, most especially Helen Turley and her great expertise in producing antibodies and performing immunohistochemistry. Karl Morten has been a very good source of discussion and has helped with assays relating to mitochondrial function. Massimo Masiero and Demin Li, who helped me on a daily basis with molecular biology. Vishwas Agashi, for very helpful discussion on mitochondrial unfolded proteins. Alan McIntyre, Simon Lord and Dean Singleton for help with cell lines, reagents and other techniques. Ji-Liang Li for help with *in vivo* work, which is ongoing.

Members of the laboratory and department have been also been very helpful, including Russell Leek, Graham Steers and Kingsley Micklem who assisted me with confocal and other imaging.

This work would not have been possible without the support of my wife Felicity during the many hours that performing and writing this research occupied. This was all the more helpful given the birth of our son Sebastian in my final year. Thanks too to David Murphy for proof-reading. I am grateful for the life-long support of my parents Greg and Marianne and their encouragement to pursue my goal of contributing to the care of patients with cancer.

Table of Contents

Abbreviations

AAA	ATPases associated with many cellular activities
ALAS	5-Aminolevulinic Acid
AMP	Adenosine monophosphate
ATFS	Activating transcription factor associated with stress
ATP	Adenosine triphosphate
BCA	Bicinchoninic acid
CCRC	Clear cell renal cell carcinoma
CDDO	2-cyano-3,12-dioxooleana-1,9-dien-28-oic acid
CHOP	C/EBP homology protein
CODD	C-terminal oxygen-dependent degradation domain
COX	Cytochrome C oxidase
CTAD	C-terminal transactivation domain
DAB	3,3'-Diaminobenzidine
DMEM	Dulbecco's Modified Eagle Medium
DNA	Dexyrubonucleic acid
DPAA	Diphenylarsinic acid
ELISA	Enzyme-linked immunosorbent assay
ER	Oestrogen receptor
ERUPR	Endoplasmic reticulum unfolded protein response
FDG	Fluorodeoxyglucose
FFPE	Formalin-fixed paraffin embedded
FIH	Factor inhibiting HIF
FITC	Fluorescein isothiocyanate
FOXO	class O of forkhead box transcription factors
GAC	Glutaminase C
GFP	Green fluorescent protein
HA	Haemagluttinin
HIF	Hypoxia inhibitory factor
HIV	Human immunodeficiency virus
HRP	Horseradish peroxidase
HSP	Heat-shock protein
LDHA	Lactate dehydrogenase A
LDS	Lithium dodecyl sulfate
MTS	3-(4,5-dimethylthiazol-2-yl)-5-(3-carboxymethoxyphenyl)-2-(4-sulfophenyl)-2H-tetrazolium
NRF	Nuclear factor-like
NSCLC	Non-small cell lung cancer
NTAD	N-terminal activation domain
ORF	Open reading frame
PAS	Per-Arnt-Sim
PBS	Phosphate buffered saline
PCR	Polymerase chain reaction
PET	Positron emission tomography
PHD	Proline Hydroxylase
PLA	Proximity Ligation Assay

PTEN	Phosphatase and tensin homolog
RNA	Ribonucleic acid
ROS	Reactive oxygen species
SDHB	Succinate dehydrogenase, mitochondrial
SDHC	Succinate dehydroxygenase complex C
SDHD	Succinate dehydroxygenase complex D
SUMO	Small ubiquitin-like modifier
TFAM	Transcription factor A, mitochondrial
TMA	Tissue microarray
UPR	Unfolded protein response
VBC	VHL-elongin BC complex
VEGF	Vascular endothelial growth factor
VHL	Von-Hippel Lindau

Chapter 1 : Introduction

Angiogenesis and Cancer

Tumour cells can survive and proliferate in an environment that is limited in nutrients and oxygen by exploiting innate physiological mechanisms that change their metabolic profile and recruit new blood vessels. The results of these adaptations can be seen in histological sections as vascular proliferation, and, where growth has exceeded adaptive ability, areas of necrosis.

The hypothesis that 'tumour growth is angiogenesis-dependent' was published in 1971 (Folkman, 1971), and was primarily based on the observation that metastases of retinoblastoma to the vitreous and aqueous humour remained avascular and less than $1mm^3$ in size, due to their distance from the vascular bed (Figg & Folkman, 2008). This observation was reinforced by experiments in which mouse melanomas were implanted into isolated rabbit and canine thyroid glands, yet proliferated only up to $\sim 1mm^3$ (Folkman *et al.*, 1963) (Folkman *et al.*, 1966). These results suggested that in the absence of neo-angiogenesis, tumours would stop growing at this size.

Proangiogenic molecules from tissues and tumours began to be purified and identified in the early 1980s, the first of which was basic fibroblast growth factor (Esch *et al.*, 1985). Vascular endothelial growth factor (VEGF) was identified as a

pro-angiogenic factor in 1989 (Ferrara & Henzel, 1989), and in 1995 it was recognised that this factor was induced in response to hypoxia (Liu *et al.*, 1995).

In the multistep development of human tumours, the ability to induce angiogenesis has been recognised as one of the hallmark capabilities a malignancy must acquire (Hanahan & Weinberg, 2011). The 'angiogenic switch' stimulates normally quiescent vasculature to sprout new vessels to help sustain neoplastic growth (Hanahan & Folkman, 1996). However, there are discrete examples of tumours that are able to grow in the absence of detectable neo-angiogenesis, which have been termed 'non-angiogenic' (Ribatti *et al.*, 2003).

Angiogenic and non-angiogenic tumours

Non-angiogenic tumours that grow beyond approximately $1mm^3$ in size rely on the pre-existing vascular network of the host tissue. A number of different mechanisms have been described which allow for tumour perfusion in the absence of sprouting angiogenesis. *Vascular mimicry* is a phenomenon whereby tumour cells are thought to adopt properties of endothelial cells, forming vascular channels that are lined by tumour cells (Paulis *et al.*, 2010). *Intussusceptive microvascular growth* is a suggested mechanism of vascular network formation whereby pre-existing vascular lumens are split by the invasion of tumour cells (Patan *et al.*, 1996). The most readily detectable mechanism of non-angiogenic growth by histological analysis is, however, *vessel co-option,* whereby the tumour cells appear to grow along existing vascular networks.

Characteristic primary tumours that show non-angiogenic growth include brain glioblastomas (Wesseling *et al.*, 1994), NSCLC (Pezzella *et al.*, 1997), oral squamous cell carcinoma (Shieh *et al.*, 2004) and melanoma (Maniotis *et al.*, 1999). Tumours that metastasise to certain highly vascularised tissues such as brain, lung and liver may display entire or focal areas of non-angiogenic growth, even if the primary tumour was capable of neo-angiogenesis (Van den Eynden *et al.*, 2012) (Carbonell *et al.*, 2009) (Evidence for novel non-angiogenic pathway in breast-cancer metastasis. Breast Cancer Progression Working Party, 2000).

The clinical consequences of having a tumour with a non-angiogenic pattern of growth are not clear. Although it has been hypothesised that non-angiogenic tumours may be resistant to anti-angiogenic therapies, this has not been established either in prospective or retrospective trials. In fact, primary non-angiogenic NSCLC has been associated with a higher incidence of distant metastasis and shorter disease-free status after resection (Pezzella *et al.*, 1997). Patients treated with the VEGF receptor tyrosine kinase inhibitor cediranib show tumour histology consistent with increased vascular co-option (di Tomaso *et al.*, 2011), suggesting that non-angiogenic growth may allow escape from anti-angiogenic therapy.

The physiological response to hypoxia includes angiogenesis, so a reasonable hypothesis is that non-angiogenic tumours simply have enough oxygen to support their growth in the host vascular bed, or, as will become an ongoing theme in this thesis, do not exhibit a significantly aberrant hypoxic response. The

differential expression of genes comparing angiogenic and non-angiogenic cancers from the same vascular bed (Hu *et al.*, 2005) may identify genes that influence the hypoxic response of tumours, and as a consequence determine the angiogenic phenotype.

Non-angiogenic growth in lung cancer is readily identified histologically as filling alveolar spaces, with the pre-existing capillary network forming a 'chicken-wire' appearance (Adighibe *et al.*, 2006). A gene expression signature for non-angiogenic NSCLC was published in 2005, derived by comparing the expression of mRNA transcripts by microarray in 12 non-angiogenic and 30 angiogenic tumours (Hu *et al.*, 2005). 62 genes were found to separate the two types of tumour, 40 of which were more highly expressed in non-angiogenic tumours. These included genes involved in mitochondrial metabolism, transcription, protein synthesis and the cell cycle. The gene PRSS15, encoding a mitochondrial protein called the Lon protease, was one of the genes identified as being expressed at a higher level in non-angiogenic tumours. The gene PRSS15 was reported as being approximately 1.5 times more highly expressed in non-angiogenic than angiogenic tumours.

Mitochondria and metabolism in cancer

Recently described as an 'emerging hallmark' of cancer, metabolic reprogramming in tumour cells allows for sustained proliferation (Hanahan & Weinberg, 2011). The characteristic metabolic phenotype of cancer cells is the

use of glucose in glycolysis, rather than for oxidative phosphorylation in conditions of sufficient oxygen, termed 'aerobic glycolysis' or the 'Warburg effect' (Warburg *et al.*, 1926). Both rapidly proliferating normal and tumour cells use glycolysis, although the extent to which this contributes ATP appears to be limited to 50-60%, even in highly aggressive tumours and ascites (Berridge *et al.*, 2010). Aerobic glycolysis is inefficient, producing only 2 molecules of ATP compared to 32 with aerobic respiration. The relative diversion to aerobic glycolysis is the basis of diagnostic PET scanning that identifies uptake of [^{18}F]fluorodeoxy-D-glucose (FDG) in metastatic cancer.

The switch to aerobic glycolysis is mediated in part by HIF-1α, through the regulation of four factors: PDK1, LDHA, BNIP3 and BNIP3L (Semenza, 2012). PDK1 (pyruvate dehydrogenase kinase 1) phosphorylates and inactivates pyruvate dehydrogenase, preventing the conversion of pyruvate to acetyl coenzyme A for entry into the tricarboxylic acid cycle (Kim *et al.*, 2006). LDHA (lactate dehydrogenase A) converts pyruvate to lactate, favouring glycolysis over respiration (Semenza *et al.*, 1996). Hypoxia in tumours has been shown to trigger a specialised form of autophagy that eliminates mitochondria, dependent on HIF-1α and mediated by BNIP3 (Zhang *et al.*, 2008) and BNIP3L (Bellot *et al.*, 2009). A switch in isoforms of subunit 4 of cytochrome c oxidase is also mediated by HIF-1α, improving efficiency of the electron transfer chain under hypoxia (Fukuda *et al.*, 2007).

HIF-1α may promote the change to glycolysis in tumours, but it is not the only factor to do so. HIF-1β deficient Hepa-1 cells (a mouse hepatoma cell line) show

similar FDG uptake to wild-type cells when grown as an allograft (Golinska *et al.*, 2011). The lower ratio of ATP to AMP may allosterically activate phosphofructokinase 1 and promote glycolysis (Golinska *et al.*, 2011). The switch to glycolysis in hypoxia that is seen in normal cells (the Pasteur effect) may be thought of as an adaptation to conditions where oxygen is limited. However, at 1% oxygen, mouse embryonic fibroblasts (MEFs) deficient in HIF-1α have higher ATP levels than wild type cells at 20% oxygen (Zhang *et al.*, 2008). This suggests that at 1% oxygen, the level of oxygen is not rate-limiting for ATP production. The switch to glycolysis by HIF-1α may be to prevent the toxic accumulation of reactive oxygen species (ROS) that otherwise damage and potentially kill the cells, as occurs with HIF-1α -/- MEFs (Zhang *et al.*, 2008) (Chandel *et al.*, 1998). Increased intermediate products of glycolysis can be shunted into biosynthetic pathways required for serine and nucleotide synthesis (Schulze & Harris, 2012).

Lon protease

The human mitochondrial Lon protease is encoded by the gene *Lonp1*, located on the short (p) arm of Chromosome 19 at band 1, sub-band 3 and sub-sub-band 2 (19p13.2). Transcribed mRNA has 18 coding exons and a spliced exon length of 3111 bp, encoding a protein of 959 amino acids. The gene has been sequenced in 97 tumour samples to date (by the Cancer Genome Project), and 6 mutations have been detected; 5 missense mutations, and one mutation predicted to produce a stop codon (Forbes *et al.*, 2008). These mutations occur in exons,

distributed along all 3 domains of the protein. The Lon protease is often abbreviated to Lon, and also has the alternative name of serine protease 15.

Classification

ATPases are proteins that are capable of turning chemical energy into biological events. The most common ATPase in the cell is the Walker-type ATPase, defined by conserved Walker A and B motifs which mediate ATP-binding and hydrolysis. AAA+ superfamily proteins (ATPases associated with diverse cellular activities), of which Lon is a member, constitute a subfamily of Walker-type ATPases, and these contain a conserved ATPase domain spanning approximately 200-250 amino acids (the AAA+ module) (Confalonieri & Duguet, 1995).

AAA+ proteases contain a regulatory ATPase (AAA+ module) and a proteolytic subunit. They include ClpAP, ClpXP, ClpCP, HslUV and Lon in bacteria and their homologues in mitochondria and chloroplasts (Ogura & Wilkinson, 2001). The regulatory subunits of ClpA, ClpX and HslU also function as chaperones. Members of the Lon family are highly conserved and ubiquitous in bacteria, archea and eukaryotes where they are found in chloroplasts (Ostersetzer *et al.*, 2007), mitochondria (Willingham & Gottesman…, 1993) and peroxisomes (Kikuchi *et al.*, 2004). A comparison of the amino acid sequences from Lon in human, mouse, drosophila, yeast and bacteria is shown in Figure 1.1 highlighting the degree of conservation. Lon family AAA+ proteases contain both regulatory and proteolytic components on a single polypeptide, while other AAA+ family members have distinct subunits. Orthologues of Lon are divided into two subgroups: A type Lons (A-Lons) have a large multilobed N-terminal domain,

whereas B type Lons (B-Lons) lack this, instead having a membrane anchoring region (Rotanova *et al.*, 2006). B-Lons are limited to Archea, whereas A-Lons are present in all bacteria and eukaryotic cell organelles.

Humans contain two AAA+ Lon proteases; located in peroxisomes (encoded by the gene *Lonp2*), one regulates fatty acid β-oxidation (Okumoto *et al.*, 2011), while the other is found in mitochondria. The cytosolic protein cereblon (a thalidomide-binding protein (Ito *et al.*, 2010)) contains a LON domain (N-terminal domain of Lon protease), but does not contain ATP-binding and catalytic domains, and is therefore not a AAA+ protease. Cereblon is part of an E3 ubiquitin ligase complex.

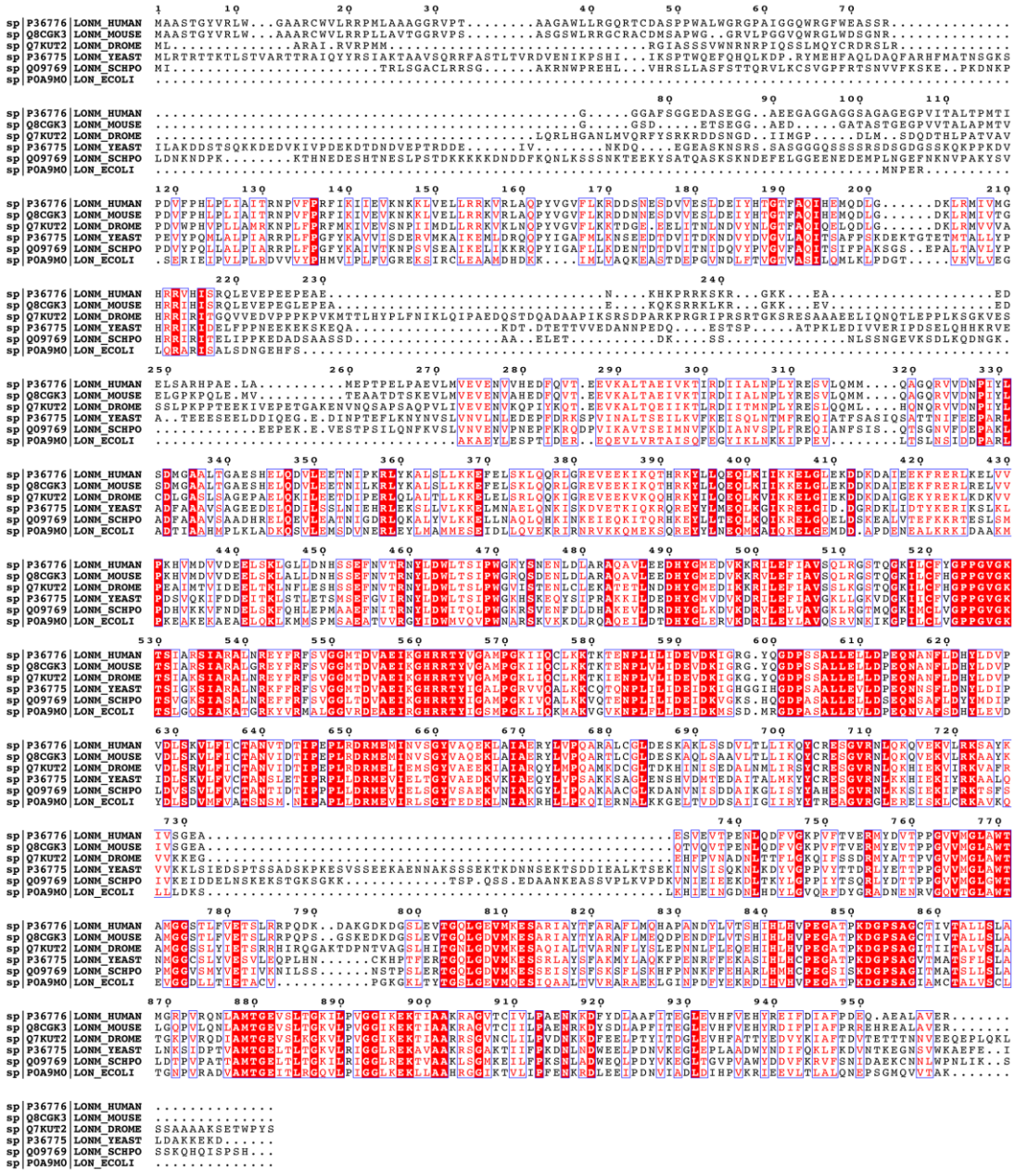

Figure 1.1 Amino acid sequence alignment of the Lon protease from diverse organisms. From top to bottom, sequences are from *H. sapiens*, *M. muscularis*, *D. melanogaster*, *S. cerevisiae*, *S. pombe* and *E. coli*. Sequences were retrieved from Uniprot (www.uniprot.org) and aligned using Clustal Omega (Sievers *et al.*, 2011). Figure assembled using ESPRIPT (http://espript.ibcp.fr/). White lettering within a red box identifies identical amino acids, red lettering denotes similar amino acids using the Risler matrix (Risler *et al.*, 1988). A blue frame identifies a similar group of amino acids.

Structure

Like *E. coli* Lon protease (*Ec*Lon), human Lon protease (*Hs*Lon) contains three domains. The N-terminal domain is thought to be involved with the selective

binding of substrates and oligomeric assembly of the protease (Lee *et al.*, 2004). The ATPase (AAA+) domain is composed of two subdomains: a larger N-terminal nucleotide-binding domain (α/β domain) and a smaller C-terminal domain (α domain, also known as Substrate Sensor and Discriminatory domain). The function of this domain appears to be the ATP-dependent unfolding of substrate proteins before their cleavage by the proteolytic domain (Rasulova *et al.*, 1998a). The ATPase domain is also implicated in binding to mitochondrial DNA (Lee *et al.*, 2004). The C-terminal proteolytic domain contains a functional Ser-Lys dyad at the active site (Rotanova *et al.*, 2004). The domain structure is shown in Figure 1.2.

The human Lon protease is a nuclear-encoded, mitochondrial matrix protein that forms a ring-shaped structure of six identical subunits in humans (García-Nafría *et al.*, 2010). The precursor polypeptide is synthesised in the cytoplasm with an amino-terminal mitochondrial targeting sequence (approximately AA 1-67) which is cleaved off on import into the matrix (Yamamoto *et al.*, 2005) (Figure 1.2C).

A

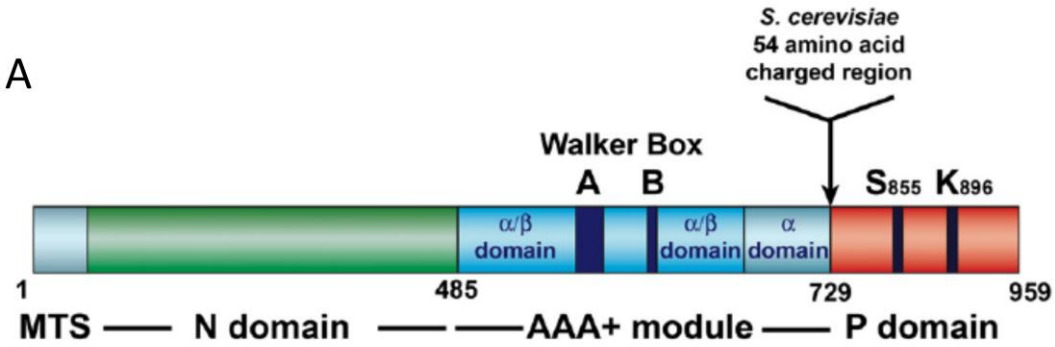

B

Significant Pfam-A Matches

Show or hide all alignments.

Family	Description	Entry type	Clan	Envelope		Alignment		HMM		Bit score	E-value	Predicted active sites
				Start	End	Start	End	From	To			
LON	ATP-dependent protease La (LON) domain	Family	CL0178	123	368	124	368	2	205	109.2	1.9e-31	n/a
AAA	ATPase family associated with various cellular activities (AAA)	Family	CL0023	519	661	519	656	1	127	85.2	3.8e-24	n/a
Lon_C	Lon protease (S16) C-terminal proteolytic domain	Domain	CL0329	736	949	737	947	2	203	232.4	2.7e-69	898,855

C

MitoProt II - v1.101

```
Input sequence length : 959 aa

                VALUES OF COMPUTED PARAMETERS

Net charge of query sequence                  : -13
Analysed region                               :  69
Number of basic residues in targeting sequence :   9
Number of acidic residues in targeting sequence :   1
Cleavage site                                 :  59
Cleaved sequence                              : MAASTGYVRLWGAARCWVLRRPMLAAAGGRVPTAAGAWLLRGQRTCDASPPWALWGRG
```

Figure 1.2 Domain structure of Lon protease. A. Overall domain organisation. MTS, the mitochondrial targeting sequence is part of the precursor protein that binds the mitochondrial translocation machinery and directs matrix import. The Lon N terminal domain proposed to be involved in substrate recognition and binding. The AAA+ module containing Walker Box A and B motifs for ATP-binding and hydrolysis. The P (proteolytic) domain contains the serine (S) and lysine (K) residues that form the catalytic dyad at the active site. Reproduced (Venkatesh *et al.*, 2011). **B.** Screen-grab of domain matches from Pfam (pfam.sanger.ac.uk), using human Lon protease as the query sequence, identifying matches for the three domains, and their positions. **C.** Predicted length of the mitochondrial targeting sequence of Lon protease as determined by a computational method (Mitoprot II) (Claros & Vincens, 1996).

Similar to other AAA+ proteases, the active sites of the six assembled Lon monomers are sequestered within the chamber, and are inaccessible to the exterior. The atomic structure of human Lon has not been solved, but X-ray

structures have been published from the P-domain (García-Nafría *et al.*, 2010). Crystal structures of the bacterial holoenzymes from *Bacillus subtilis* and *Thermococcus onnurineus* NA1 confirm the overall architecture (Cha *et al.*, 2010) (Duman & Löwe, 2010) (Figure 1.3). Structures of N-domain, part of the AAA+ domain and P-domain have been published for *Ec*Lon, and these are expected to be highly conserved (Botos *et al.*, 2004) (Li *et al.*, 2005c) (Rasulova *et al.*, 1998b). The isolated catalytic domains appear to be catalytically inactive in the absence of the ATPase domain, while the ATPase activity is reduced by certain mutations around the proteolytic active site (Rasulova *et al.*, 1998b). This suggests there is co-ordination between ATPase and proteolytic activity, and both are required for Lon catalysis.

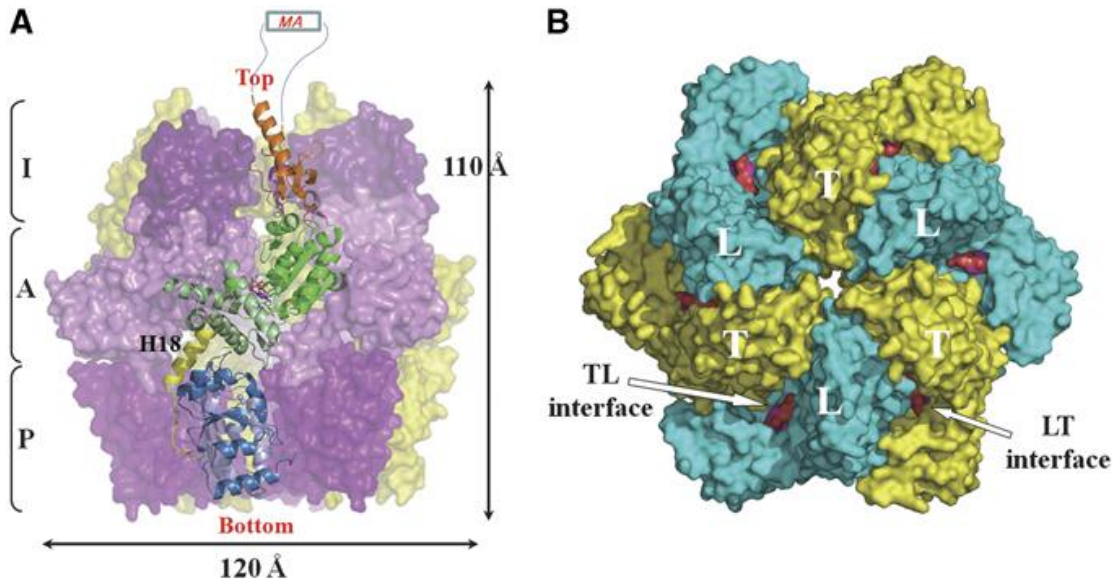

Figure 1.3 Overall struture of Lon protease from *Thermococcus onnurineus*. A. The Lon protease forms a hexamer of six identical subunits, one subunit is represented as a ribbon, the others as a surface representation. The Lon protease is a B type Lon protease composed of apical insertion domain (I), AAA+ domain (A) and proteolytic domain (P). MA is the putative membrane-anchoring region. **B.** Surface representation showing the top view of the hexamer (putative substrate entry view), with bound ADPs coloured red. T- and L- monomers are labelled. Figure reproduced (Cha *et al.*, 2010). Structural identity with human Lon is 36% (Venkatesh *et al.*, 2011).

Function of Lon protease

As the Lon protease is such a conserved protein, and as mitochondria are derived from endosymbiotic prokaryotes, it is worth reviewing some of the literature regarding the significant insights into Lon biology that have been made in organisms other than human cells.

Prokaryotes

The ATP-dependent Lon (La) protease is named after the phenotype of *E. coli* with mutations in Lon. This mutant (K-12 F-) was grows in long (LONg) forms after irradiation or when propagated in nutrient without aeration (hypoxia) (HOWARD-FLANDERS *et al.*, 1964). UV sensitivity of Lon mutants was subsequently shown to be due to the stabilisation of SulA, a cell division inhibitor (Wu *et al.*, 1999). Another phenotype of Lon-deficient bacteria was the abnormal accumulation of cell wall components, giving mucoid colonies. This was shown to be due to the accumulation of another substrate, RcsA, a positive regulator for the transcription of genes involved in capsule production (Wu *et al.*, 1999). *E. coli* Lon mutants are also unable to adapt to a nutritional downshift, as they are unable to degrade free ribosomal proteins which would normally lead to the production of adaptive enzymes (Kuroda *et al.*, 2001).

In bacteria, Lon has a role in protein quality control, degrading misfolded proteins that would otherwise aggregate. Aggregation is prevented by the cooperation of chaperones (DnaK system, alternatively named Heat shock protein 70) (Tomoyasu *et al.*, 2001). Substrate discrimination appears to be

conferred by protein structure, the common features of which may be non-globular conformation (Van Melderen *et al.*, 1996). There is some redundancy in substrate specificity between Lon and ClpYQ (HslUV), as both can degrade SulA at elevated temperatures (Wu *et al.*, 1999).

Forced overexpression of Lon in *E. coli* is lethal, and so the endogenous expression is normally tightly controlled by the heat-shock regulon (Phillips & VanBogelen…, 1984). In prokaryotes, molecular chaperones and ATP-dependent proteases downregulate their own synthesis by modulating the activity of their transcription factors – in *E. coli* this factor is σ^{32} (Tsilibaris *et al.*, 2006). σ^{32} is degraded under normal conditions by DnaK (HSP 70) and the ATP-dependent protease HflB. Degradation is inhibited when this chaperone and protease system is overwhelmed by the stress of heat shock. In this way, Lon appears to be regulated by the load of unfolded protein within a cell.

Eukaryotes

Yeast

The eukaryotic yeast *S. cerevisiae* deficient in Lon protease (also named Pim1 – proteolysis into mitochondria) are respiratory deficient and contain a non-functional mitochondrial genome (Suzuki *et al.*, 1994). They also accumulate electron-dense intra-mitochondrial inclusion bodies, which may be aggregated proteins from the loss of Lon proteolysis (Bender *et al.*, 2011). In yeast Lon is the only ATP-dependent protease in the mitochondrial matrix, while in metazoans, the two component ClpXP protease is also present. Yeast Lon also differs from

other organisms as it is heptameric in *S. cerevisiae* (Stahlberg *et al.*, 1999), and hexameric in bacteria (Cha *et al.*, 2010) and *H. Sapiens* (García-Nafría *et al.*, 2010). As the only AAA+ protease, there are a number of aggregated proteins that accumulate in its absence, described as endogenous substrates of Lon (Major *et al.*, 2006). One study lists the approximate number of endogenous substrates as 19 – these include mitochondrial stress proteins, mitochondrial metabolic enzymes, respiratory chain subunits, and the mitochondrial ribosomal protein 20 (Bayot *et al.*, 2010). The scaffold protein Isu, important for assembly of iron-sulphur clusters, has also been recently identified as an endogenous Lon substrate in *S. cerevisiae* (Song *et al.*, 2012).

In *S. pombe*, deletion of Lon leads to inhibition of growth at 37 °C (but not at 30 °C), absence of growth on glycerol, electron-dense deposits in the matrix and some loss of mitochondrial membrane potential (Guha *et al.*, 2011). Whole-genome microarray analysis on *S. pombe* Lon deficient cells showed a very specific upregulation of 12 genes, including 9 of the 11 protein-coding genes of the mitochondrial genome (Guha *et al.*, 2011). This was despite there being no change in the mtDNA copy number. Similarly, deletion of Lon in *S. cerevisiae* leads to defects in the synthesis of Cox1 and Cob1 mitochondrial encoded proteins containing introns, and also leads to defects in splicing the introns in these mRNA transcripts (van Dyck *et al.*, 1998).

In addition to proteolysis, Lon has been shown to exhibit chaperone-like activity in yeast. Defects in cytochrome c oxidase (COX2) assembly can be overcome by over-expression of a wild-type or proteolytic inactive mutant of Lon (Rep *et al.*,

1996). This activity was dependent on the ATPase domain remaining functional, suggesting an ATP-dependent chaperone-like activity in protein complex assembly, independent of proteolytic activity (Fu *et al.*, 1997).

Drosophila Melanogaster

Drosophilia Schneider cells (macrophage-like), treated with small interfering RNA (siRNA) against Lon, exhibit a phenotype of increased abundance of mitochondrial transcription factor A (TFAM), and mtDNA copy number (Matsushima *et al.*, 2010). Conversely, overexpression reduced TFAM levels and mtDNA copy number, suggesting that TFAM was an endogenous substrate of Lon (Matsushima *et al.*, 2010). As TFAM is essential for mtDNA transcription, it appears that Lon may have a role in modulating the expression of mitochondrial-encoded genes, via this substrate (Matsushima *et al.*, 2010) (Bernstein *et al.*, 2012).

Homo Sapiens

Depletion of Lon by anti-sense morpholino oligonucleotides in lung fibroblasts results in loss of mitochondrial membrane potential, reduction in oxygen consumption, reduction of mitochondrial mass with accumulation of electron-dense granules and apoptotic cell death (Bota *et al.*, 2005). This death phenotype was not reproduced when an inducible shRNA construct against Lon was stably integrated in a colorectal cell line (Lu *et al.*, 2007), nor when siRNA was used in SK-HEP-1 cells (Lee *et al.*, 2011) (derived from the ascitic fluid of a patient with liver adenocarcinoma, although it has a phenotype more commonly associated

with endothelial cells (Heffelfinger *et al.*, 1992)). In SK-HEP-1 cells, siRNA against Lon induced a phenotype consistent with insulin resistance, accompanied by decreases in cellular ATP and mitochondrial membrane potential (Lee *et al.*, 2011). Reported phenotypic differences in reducing levels of Lon may be dependent on cell type, or be cell line-specific.

The endogenous substrates of human Lon comprise a diverse group of proteins, with differing levels of evidence to prove they are indeed substrates. Lon degrades oxidised mitochondrial aconitase (Bota & Davies, 2002), subunits of cytochrome c oxidase (Fukuda *et al.*, 2007) and the steroidogenic acute regulatory protein (StAR) (Granot *et al.*, 2007). Described endogenous substrates of mammalian Lon are summarised with published evidence (Table 1). In contrast to Lon, there are no known endogenous mammalian ClpXP substrates (the other matrix AAA+ protease), but it has been recently associated with mouse PDIP38 and p32 (Lowth *et al.*, 2012).

Recently, Lon has been shown to degrade TFAM in human cells when it is phosphorylated by cAMP-dependent protein kinase in mitochondria (Lu *et al.*, 2012). Only in cells that have severe mtDNA defects (by culturing in the presence of ethidium bromide), does shRNA targeting of Lon been demonstrated to cause upregulation of mitochondrial transcription by TFAM, and TFAM bound to mtDNA is resistant to degradation (Lu *et al.*, 2012).

Table 1.1 Described substrates of Lon protease in metazoans

Substrate	Function	Evidence	References
Oxidised aconitase (mitochondrial)	Krebs cycle enzyme, catalyses conversion of citrate to isocitrate	Purified Lon degrades oxidised aconitase *in vitro*. Morpholino oligonucleotide against Lon in cells leads to accumulation of aconitase in cells.	(Bota & Davies, 2002)
Cytochrome c oxidase (COX) subunit 4, isoform 1 (COX4i1)	Essential subunit of the respiratory chain, isoform 1 is proposed to be most efficient under aerobic conditions, isoform 2 under hypoxia.	shRNA against Lon resulted in the persistence of COX4i1 in conditions of hypoxia or on addition of $CoCl_2$ in cells.	(Fukuda *et al.*, 2007)
Steroidogenic Acute Regulatory (StAR) protein	Transfers cholesterol from the outer to inner mitochondrial membranes.	Lon degrades StAR *in vitro*, and cleavage sites identified. Overexpression or siRNA knockdown of Lon changes levels of StAR protein in cells.	(Granot *et al.*, 2007) (Ondrovicová *et al.*, 2005)
Mitochondrial 5-Aminolevulinic Acid (ALAS-1)	First and rate-limiting step of heme bioxynthesis.	Heme normally decreases mitochondrial ALAS-1 through proteolysis. This effect is reduced with siRNA against Lon.	(Tian *et al.*, 2011a)
Mitochondrial Calpain 10	Ca^{2+}-activated cysteine protease ubiquitously expressed in cytosol, mitochondria and nucleus. Cleaves respiratory chain components reducing respiration after Ca^{2+} overload.	Putative Lon-specific inhibitors slow the degradation of calpain 10 in isolated mitochondria (but is not ATP dependent).	(Smith & Schnellmann, 2011)
Mitochondrial transcription factor A (TFAM)	Mitochondrial DNA transcription, maintenance and copy number.	Lon degrades TFAM *in vitro,* and blocked with specific inhibitor. *D.melanogaster* Lon levels correlate with TFAM in cells.	(Bernstein *et al.*, 2012) (Matsushima *et al.*, 2010) (Lu *et al.*, 2012)
Glutaminase C (GAC)	Catalyses conversion of glutamine to glutamate.	Putative specific Lon inhibitors inhibit DPAA mediated GAC degradation	(Kita *et al.*, 2012)

Substrate	Function	Evidence	References
	Diphenylarsinic acid (DPAA) promotes degradation.	in HepG2 cells. siRNA against Lon inhibits DPAA mediated GAC degradation.	
C. Elegans Activating transcription factor associated with stress-1 (ATFS-1) Some similarity to mammalian ATF5 (Haynes *et al.*, 2010).	Slowed import of ATFS-1 into mitochondria; occurs in the mitochondrial unfolded protein response. If not imported, acts as a transcription factor upregulating mitochondrial stress genes. Once signalling peptide of ATFS cleaved in matrix, it is degraded by Lon.	*C. Elegans* fed *E. coli* that express siRNA against Lon protease show increased quantities of endogenous and exogenous-tagged ATFS-1.	(Nargund *et al.*, 2012)

DNA binding of Lon protease

Prokaryotic and eukaryotic Lon is a DNA-binding protein, in addition to its role in proteolysis and as a chaperone. Prokaryotic Lon appears to bind to different DNA sequences without apparent sequence similarity (Nomura *et al.*, 2004). The relationship between DNA binding, proteolysis and ATP hydrolysis is unclear. One study suggested that DNA stimulates enzyme activity (Chung & Goldberg, 1982), while another reported that it inhibits proteolysis but not ATPase activity (Charette *et al.*, 1984). As many of the substrates in *E. coli* are proteins involved in transcription and DNA methylation, binding of Lon may be a mechanism to bring the enzyme and substrate into closer proximity (Lee & Suzuki, 2008).

The mitochondrial genome is small and circular, encoding 13 proteins involved in oxidative phosphorylation, 2 ribosomal RNAs and 22 transfer RNAs. The endosymbiotic event that gave rise to mitochondria was accompanied by a large

migration of genes to the nucleus (approximately 900) (Gray *et al.*, 1999). There are various theories suggesting why a small subset of genes remains encoded on the mitochondrial genome, including the ability to rapidly regulate translation and assembly, and protein hydrophobicity requiring direct membrane insertion (Allen, 2003). As a circular genome, there are two strands that comprise mtDNA; heavy- and light-, with the heavy strand being GT-rich and encoding all proteins except one. The control region carries the heavy- and light- strand promoters which mediate mtDNA transcription and replication.

Human Lon protease binds to specifically single-stranded DNA and RNA oligonucleotides (Fu & Markovitz, 1998) (Liu *et al.*, 2004). Binding is promoted by G-rich sequences with a propensity to form parallel G-quartets, as found in the control region at the light strand promoter of mitochondrial DNA (Lu *et al.*, 2007) (Chen *et al.*, 2008). In intact cells, protein substrate stimulates DNA binding of Lon, whereas ATP-binding inhibits this interaction (Liu *et al.*, 2004).

Cellular levels of Lon can alter the sensitivity of mtDNA to oxidative stress. Hydrogen peroxide added to cells increases the rate of mitochondrial mutations, but to a much lesser extent if levels of Lon are reduced by shRNA (Lu *et al.*, 2007). It is possible that Lon depletion leads to higher levels of anti-oxidant or repair proteins, or that Lon blocks lesion repair, although there is no evidence for these hypotheses.

Factors affecting Lon expression

Lon is up-regulated in hypoxia by the hypoxia inducible factor-1α (HIF-1α) (Fukuda *et al.*, 2007) (Hori *et al.*, 2002). Lon is also up-regulated by endoplasmic reticulum (ER) stress, which is triggered by the accumulation of mis- and unfolded proteins in the ER lumen (Hori *et al.*, 2002). Increasing the levels of a mitochondrial protease as part of the ER response to stress would seem to be a misdirected adaptation, though ER stress inhibits cytosolic protein synthesis (Koumenis, 2006). This may lead to decreased protein import and conditions of stress in mitochondria, and Lon may function to degrade abnormal proteins created by ER stress (Bernstein *et al.*, 2012).

In cell culture, the expression of Lon is induced by hydrogen peroxide, heat stress and serum starvation (Ngo & Davies, 2009). In tissues, Lon is increased in malignant lymphoma cells (Bernstein *et al.*, 2012), and also in the adipose tissue of patients with lipodystrophy, a side effect of chronic intake of antiretroviral drugs for the treatment of HIV infection (Pinti *et al.*, 2010b). One of the antiretroviral drugs (HIV is always treated with combinations of drugs), stavudine (d4T), is incorporated into mtDNA causing chain termination and mtDNA depletion (Brinkman *et al.*, 1999). The consequent increase in intracellular reactive oxygen species (ROS), rather than depletion of mtDNA, causes this increase in Lon levels with stavudine (Pinti *et al.*, 2010b).

An analysis of the promoter of human Lon identified binding sites for the transcription factors NRF-2, NF-κB, Nkx-2 and Lyf-1 (Pinti *et al.*, 2010a). Three of these transcription factors (NRF-2, NF-κB and Nkx-2) are induced by oxidative

stress, confirming that Lon has a role in the response to stress. NRF-2 is a crucial transcription factor for mitochondrial biogenesis, in addition to the response to stress, and is positively regulated by PGC-1α, a gene central to mitochondrial biogenesis (Scarpulla, 2008).

Substrate recognition and catalysis by Lon

Studies of Lon in *E. coli* suggest that solvent-exposed hydrophobic patches in an unfolded protein act as substrate recognition tags for proteolysis (Gur & Sauer, 2009) (Gur & Sauer, 2008). Mutation of critical sites required for recognition appears to stabilise these proteins (Gonzalez *et al.*, 1998) (Gur & Sauer, 2009). A study into the degradation of HUβ showed that recognition and binding with Lon are independent of the initial cleavage site (Liao *et al.*, 2010). Lon binds both HUβ and HUα (DNA-binding histone-like proteins), while only HUβ contains a cleavage site and is degraded (Liao *et al.*, 2010). This suggests that while features of proteins such as hydrophobicity may stimulate binding, degradation will only proceed if the correct cleavage pattern is presented.

Human Lon protease can degrade the yeast mitochondrial processing peptidase (MPPα) *in vitro*, only when in a native confirmation, and is trypsin-resistant (Ondrovicová *et al.*, 2005). The cleavage sites are at hydrophobic residues exposed at the surface. This suggests that substrate recognition by the Lon protease may not be entirely restricted to abnormal proteins which are unfolded or damaged (Venkatesh *et al.*, 2011).

The general process of ATP-dependent proteolysis also likely applies to the mitochondrial Lon protease (Venkatesh *et al.*, 2011). Firstly, recognition and binding of substrate occurs at the N-domain and AAA+ module in an ATP-independent manner. ATP-binding and hydrolysis provides the energy for conformational changes allowing for unfolding of substrates, and allows movement into the proteolytic chamber. Peptide bond cleavage occurs, generating peptides from ~5 to 20 amino acids. Degradation in Lon proceeds, as shown for StAR and MPPα (Ondrovicová *et al.*, 2005).

Inhibitors of Lon

Certain proteasomal inhibitors, such as the peptidyl aldehyde MG132, can diffuse into the mitochondria and inhibit the degradation of StAR (Granot *et al.*, 2003). Inhibitors that target both the Lon protease and the proteasome, as determined *in vitro*, also include MG262 (a peptide boronate), lactacystin and β-lactone, suggesting some similarity in their proteolytic mechanism (Bayot *et al.*, 2008) (Frase *et al.*, 2006). The proteosome inhibitor Bortezomib has recently been shown to be an inhibitor of Lon (Lu *et al.*, 2012), and also causes mitochondrial damage by an unknown mechanism (Ling *et al.*, 2003).

Recently, the first Lon specific inhibitor was identified as the synthetic triterpenoid CDDO (Bernstein *et al.*, 2012). Inhibition of Lon with CDDO promotes the accumulation of electron-dense aggregates within mitochondria, and lymphoma cell death *in vitro* (Bernstein *et al.*, 2012). However, this agent

has also been reported to be a ligand for the nuclear receptor PPARγ, so off-target effects may contribute to this phenotype (Wang *et al.*, 2000).

Recombinant human Lon protease has been used in *in vitro* assays, where it can degrade FITC labelled casein, in an ATP-dependent manner (Liu *et al.*, 2004) (Bayot *et al.*, 2008). A fluorescent peptide reporter substrate that is selective for Lon degradation in mitochondria has been described, based on a peptide from the bacteriophage protein λN, although this substrate is also degraded by the proteasome (Fishovitz *et al.*, 2011).

Protein quality control in the mitochondrial matrix

Mitochondria have a dedicated repertoire of proteins for the assembly, folding and complex formation within the organelle. Chaperones are required for import and folding, and the matrix proteases degrade misfolded proteins. The mitochondrial chaperones include the mitochondrial Hsp70, the orthologues to *E. coli* GroEL and GroES (Hsp60 and Hsp10), which are all nuclear encoded (Haynes & Ron, 2010).

The protein folding environment of the mitochondria is unique, with proteins being encoded, folded and assembled from two separate genomes (mtDNA and nuclear DNA) in the presence of protein-altering reactive oxygen species. It is clear that perturbations such as increased energy demands, hypoxia and mutations can negatively impact the protein-folding environment. Studies in *C.elegans* and mammalian cell lines have demonstrated that the protein-folding

capacity of mitochondria are dynamic and can be upregulated to deal with unfolded or misfolded proteins (Zhao *et al.*, 2002) (Yoneda *et al.*, 2004).

The earliest experiments that demonstrated a distinct mitochondrial unfolded protein response (mtUPR) pathway involved transfecting a mutant mitochondrial matrix protein into cells and demonstrating increased transcription of the mitochondrial chaperones Hsp60, Hsp10, mtDNAJ (Tid1/DNAJA3) and the mitochondrial protein ClpP (Zhao *et al.*, 2002). Importantly, this was specific to mitochondria, as ER-specific chaperones were not induced.

The first component identified for HSP60 upregulation was the transcription factor CHOP (C/EBP homology protein), as a binding site was found in the HSP60 promoter, and overexpression of CHOP led to increased HSP60 expression (Zhao *et al.*, 2002). CHOP has a dimerisation partner C/EBPβ, and both exhibit increased transcription in response to mitochondrial stress (Zhao *et al.*, 2002).

Much of the current understanding of mtUPR has come from studies in *C. elegans*, including reporter animals that express GFP under the control of the mitochondrial chaperone gene promoter of hsp60 (Yoneda *et al.*, 2004). Ethidium bromide treatment of transgenic reporter animals resulted in increased activity of the hsp60 promoter, as a consequence of depleting mitochondrial DNA-encoded proteins (Yoneda *et al.*, 2004). A genome-wide RNAi screen was undertaken in this transgenic *C. elegans* model to identify components required to signal the mtUPR response. This identified four genes

required for activation of mtUPR; ClpP, DVE-1, UBL-5 and ATFS-1 (Haynes *et al.*, 2007).

ClpP is the protease component of the two-component AAA+ protease ClpXP, and is the other intra-matrix AAA+ protease besides Lon. ClpXP is required to upregulate the genes involved in mtUPR and, in its absence, proteolysis of unfolded mitochondrial proteins is impaired (Haynes *et al.*, 2007). This suggests that ClpP may have a role in transmitting mtUPR signals to the cytosol (Haynes *et al.*, 2007) (Haynes & Ron, 2010).

The mitochondrial inner membrane ABC transporter HAF-1 was also shown to be required for mtUPR in *C. elegans* (Haynes *et al.*, 2010). Most recently, ATFS-1 (activating transcription factor associated with stress-1) has been reported to be important for the mtUPR – a protein that is mitochondrial-imported yet also a nuclear transcription factor (Nargund *et al.*, 2012). This study showed that during mitochondrial stress, mitochondrial import of ATFS-1 was slowed, allowing it to accumulate in the cytosol, traffic to the nucleus and activate a transcriptional program of mitochondrial protection (Nargund *et al.*, 2012). HAF-1 was determined to inhibit the general import of AFTS-1 during mitochondrial stress and may be required to upregulate mtUPR in this way (Nargund *et al.*, 2012). Unfortunately, AFTS-1 does not have a direct mammalian homologue, but does have a distant similarity to ATF5 (Haynes *et al.*, 2010). There are no reports of ATF5 eliciting a program of mtUPR, nor of being imported to mitochondria, so the mechanism of mtUPR in mammalian mitochondria is yet to be elucidated.

The general mechanism of protein import being slowed under mitochondria stress may, however, still apply.

In *C. elegans*, reducing the levels of Lon by RNAi appears to not induce mtUPR, as determined by visualising transgenic animals expressing GFP under the control of the hsp-60 promoter (Nargund *et al.*, 2012). Lon, however, does appear to degrade ATFS-1 once it has been imported by mitochondria (Nargund *et al.*, 2012). This is despite the fact that in human cell lines, decreasing levels of Lon cause the accumulation of electron-dense mitochondrial inclusions, likely aggregated misfolded and damaged proteins (Bernstein *et al.*, 2012) (Bota *et al.*, 2005). The RNAi process in *C.elegans* may be limited by its efficiency, and Lon knockout animals have not been reported.

A recurring biological theme, in the unfolded protein or heat shock response, is that chaperone occupancy regulates signalling. This is true as much for bacteria, as discussed earlier for the bacterial transcription factor α^{32} (Tsilibaris *et al.*, 2006), as it is for the mammalian cytoplasmic heat shock response (Hsp 70 sequesters the HSF family of transcription factors) (Haynes & Ron, 2010). Organelle-specific UPR is complicated due to the compartmentalisation of the stress and response, but for the most conserved branch of endoplasmic reticulum (ER) UPR, when the ER chaperone BiP binds to an excess of unfolded ER, it allows for the oligomerization of IRE1, which can splice and ligate XBP1 mRNA (a transcription factor) and allow for the upregulation of ERUPR genes (Haynes & Ron, 2010). The fact that mthsp70 plays a central role in the import of proteins into the mitochondria (Becker *et al.*, 2012) suggests that, again,

chaperones may mediate the transcriptional response, especially, in the case of ATFS-1, as the slow imported protein is itself a transcription factor (Nargund *et al.*, 2012).

Oxygen sensing in metazoans

Sophisticated homeostatic mechanisms that detect and respond to the level of oxygen have evolved in metazoan organisms. These mechanisms are designed to ensure appropriate use and delivery of oxygen to cells, and exist both within individual cells and on a paracrine (such as angiogenesis) and endocrine (erythropoietin) scale. Central to the cellular response to hypoxia is the transcription factor HIF (hypoxia-inducible factor) (Figure 1.4).

HIF is a heterodimer of two basic helix-loop-helix/PAS proteins, and consists of an unstable alpha subunit (such as HIF-1α) and a constitutively present and stable beta subunit (such as HIF-1β). The dimer binds to DNA at specific locations called hypoxic response elements (HREs) and elicits a transcriptional upregulation of genes required to respond appropriately to the oxygen deficit (Mole *et al.*, 2009). There are three HIF-α subunits, of which HIF-1α and HIF-2α have been most studied.

The HIF-α subunits are continually degraded under normoxic conditions. The degradation of HIF-1α begins with the hydroxylation within its oxygen-dependent degradation domain (proline 402 and 564) by oxygen-dependent

prolyl hydroxylase domain (PHD) proteins (1-3). Hydroxylation at either of these sites generates a recognition site for the von Hipple-Lindau (pVHL) tumour suppressor protein, which is part of a larger, E3 ubiquitin ligase complex. Recognition of the VHL complex leads to ubiquitination of HIF-1α and proteasomal degradation (Kaelin & Ratcliffe, 2008).

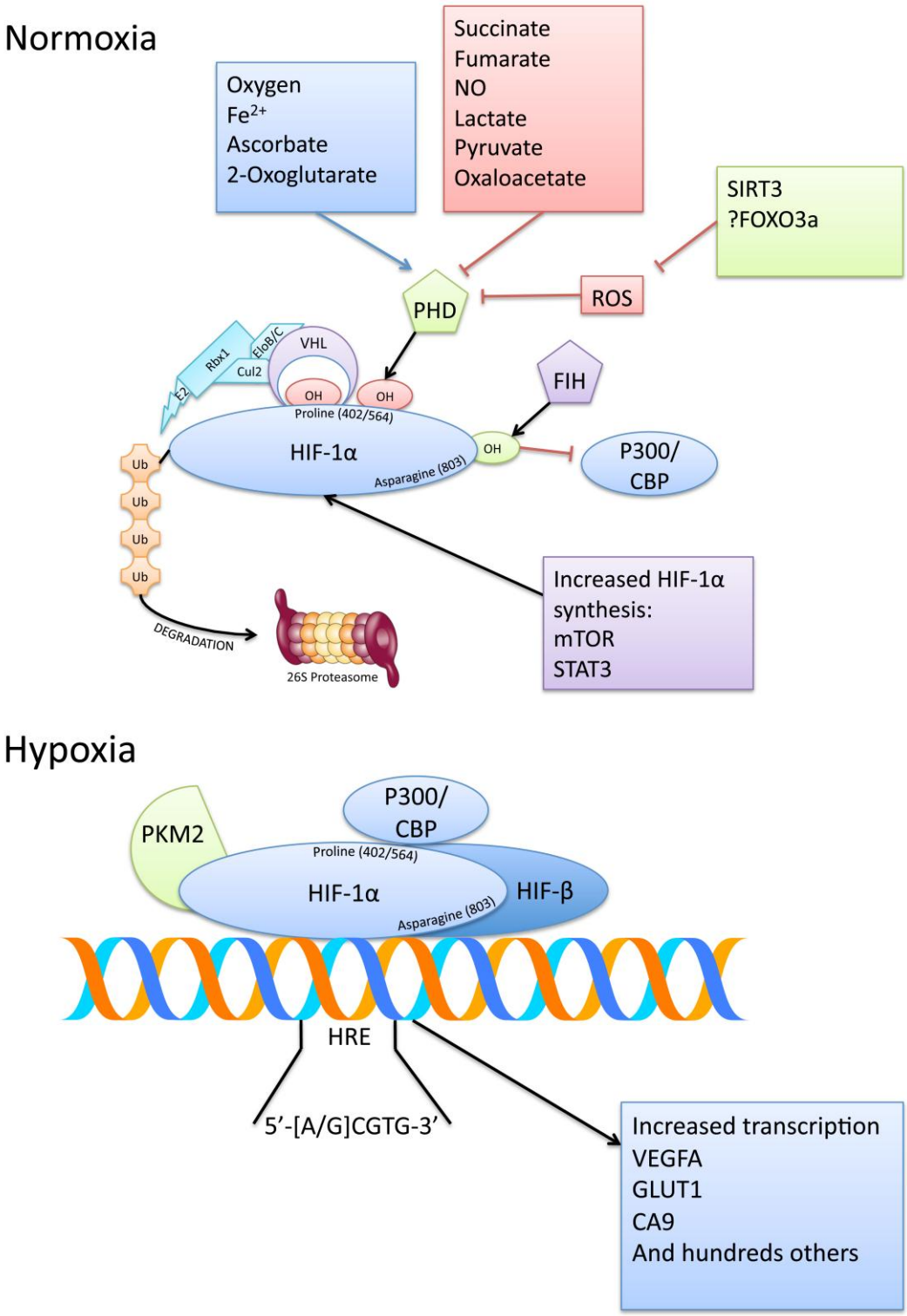

Figure 1.4 Model of HIF-1α regulation. Under conditions of normal oxygen tension, HIF-1α is subject to oxygen-dependent proline hydroxylation that allows for VHL complex recognition, ubiquitination and degradation by the 26S proteasome. The activity of the PHDs is regulated by a number of factors, including ROS, which is modulated by SIRT3. The binding of the co-activator p300/CBP is inhibited by HIF-1α asparagine hydroxylation by FIH. In conditions of low oxygen tension, HIF-1α escapes proline hydroxylation and associates with HIF-β. The heterodimer binds to hypoxia response elements (HREs) in the promoter of target genes and initiates transcription.

PHD enzymes as the cellular oxygen sensor

The PHD proteins belong to a superfamily of Fe(II) and 2-oxoglutarate-dependent oxygenases, which have an absolute requirement for oxygen. One oxygen atom is used in the oxidative decarboxylation of 2-oxoglutarate producing succinate and CO_2, whilst the other oxygen atom is incorporated into the amino-acid of HIF-1α (McNeill *et al.*, 2002). Under conditions of hypoxia, HIF-1α prolyl hydroxylation is inhibited (Tian *et al.*, 2011b).

A number of studies have attempted to measure the relationship between HIF hydroxylase activity and oxygen concentration. It appears that the K_M for oxygen (the concentration of oxygen which achieves a half-maximal enzyme activity) depends on the length of the peptide substrate *in vitro*, as short HIF-1α fragments report a higher K_M than longer, perhaps more physiological, polypeptides (Hirsilä *et al.*, 2003) (Ehrismann *et al.*, 2007). The most accurate estimation of the K_M (oxygen) for PHD2 is 81±28 μM for HIF-1α CODD polypeptide *in vitro* (Ehrismann *et al.*, 2007).

This value is well above the estimated oxygen concentration in tissues, which is in the range of 10-30μM (Kaelin & Ratcliffe, 2008). This would suggest that in all cells, *in vivo*, the oxygen concentration is already limiting for PHD activity, and that any small pertubation in oxygenation would lead to a further inhibition of HIF-1α degradation. HIF-1α prolyl hydroxylation is therefore limiting to degradation within the physiological range of cellular oxygen, as well as being

amenable to alteration through intracellular signals that can influence the hydroxylation reaction (Kaelin & Ratcliffe, 2008).

Factor inhibiting HIF (FIH) is also an Fe(II)- and 2-oxoglutarate-dependent dioxygenase, which hydroxylates an asparaginyl residue (Asn803) within the C-terminal transactivation domain (CTAD) in HIF-1α and HIF-2α, which inhibits the interaction with p300 and CBP (Schofield & Ratcliffe, 2004). In doing so, it can repress the transcriptional activity of the HIF dimer (Lando *et al.*, 2002).

In vitro, the hydroxylation sites of HIF-1α have differential sensitivities to oxygen. Proline 402 (within the NTAD) is most sensitive, being 80% hydroxylated in RCC4 cells at 1% oxygen, with Proline 564 being 80% hydroxylated at 0.5% oxygen (Tian *et al.*, 2011b). Asparagine 803 is most resistant, requiring oxygen concentrations of approximately 0.1% to observe inhibition of hydroxylation (Tian *et al.*, 2011b). FIH is more sensitive to peroxide than PHDs, and may be the mechanism by which oxidant stress signals through the HIF transcriptional program (Masson *et al.*, 2012).

Studies using hypoxia in cultured cells show an increase in HIF-1α exponentially from 6% oxygen (Jiang *et al.*, 1996). This observation led a leading author on hypoxia to state that increases in HIF-1α at higher oxygen tensions "cannot be explained by known biochemical properties of the hydroxylases" (Semenza, 2012). Despite this recent assertion, many authors have described mechanisms by which the PHD enzymes' activity might be modulated.

Reactive oxygen species (ROS) and the hypoxic response

The concept that ROS could modulate the hypoxic response was published as a mechanism of oxygen sensing, before it was known that HIF was regulated by hydroxylation (Chandel *et al.*, 1998). The mechanism and source of ROS remains controversial, not helped by directly contradictory reports in the literature. In hypoxia, increased ROS formation from the Q_O site of complex III has been proposed to be required for hypoxic signalling via ROS (Bell *et al.*, 2007). The increase in ROS in hypoxia is paradoxical, as oxygen is a substrate for ROS generation. In some studies, mitochondrial ROS generation is reported to decrease during hypoxia (Hoffman *et al.*, 2007).

Despite these controversies, exogenous application of H_20_2 increases hypoxic signalling (Chandel *et al.*, 2000), and murine embryonic cells lacking cytochrome c cannot stabilise HIF-α subunits at 1.5% oxygen (Mansfield *et al.*, 2005). Peroxide-based ROS can inhibit PHD catalytic activity *in vitro*, possibly by oxidizing PHD-bound Fe(II) (Pan *et al.*, 2007). Complex III produces ROS which are directed towards both the mitochondrial matrix and the intermembrane space (Brand, 2010), and there is the possibility that ROS may act indirectly on ascorbate, Fe(II), or Krebs cycle intermediates.

Krebs cycle intermediates and PHD activity

The PHDs and HIF require the Krebs cycle intermediate 2-oxoglutarate as a co-substrate for hydroxylation, and ascorbate to keep the iron centre in a reduced state (Schofield & Ratcliffe, 2004). The PHDs have been reported to be inhibited

by fumarate and succinate by competing with 2-oxoglutarate (Isaacs *et al.*, 2005) (Selak *et al.*, 2005). Lactate, pyruvate and oxaloacetate appear to inhibit HIF hydroxylation in an ascorbate-reversible manner (Lu *et al.*, 2005).

Changes in metabolic intermediates may affect the hypoxic response, but the most compelling evidence of this occurring *in vivo* is in tumours that have mutations in fumurate hydratase (Isaacs *et al.*, 2005) or succinate hydrogenase (Pollard *et al.*, 2005). Recent evidence suggests that the cancer-predisposing phenotype associates with fumarate hydratase mutations is not due to activation of HIF pathways, but rather due to constitutive activation of the NRF2 pathway (Adam *et al.*, 2011).

Mechanisms of aberrant activation of the HIF pathway in cancer

It is clear that multiple inputs regulate the stability of HIF-α subunits. Apart from those already mentioned, HIF-1α mRNA levels can be reduced by the expression of microRNA-155 (Bruning *et al.*, 2011) and also by the expression of the RNA destabilising protein tristetraprolin (Chamboredon *et al.*, 2011). Both of these mechanisms lead to decreased HIF-1α levels and transcriptional activity. Post-translational modifications of HIF-1α, including small ubiquitin-like modifier (SUMO)ylation, leads to increased stability (Carbia-Nagashima *et al.*, 2007), while acetylation appears to inactivate the transcriptional activity of HIF-1α (Lim *et al.*, 2010). Recent advances in mitochondrial-related proteins that influence the hypoxic response in tumours warrant particular focus in this review.

The mitochondrial deacetylase sirtuin-3 (SIRT3). SIRT3 was recognised to have a tumour suppressor function when *SIRT3-/-* cells were found to have altered metabolism, decreased mitochondrial integrity and promoted an invasive and tumourigenic phenotype compared to wild-type cells (Kim *et al.*, 2010). Mice knockout for SIRT3 have an elevated glucose uptake and express a higher level of genes associated with the response to hypoxia (Finley *et al.*, 2011). Over the period of two years, SIRT3-/- mice develop mammary gland tumours that are oestrogen and progesterone receptor positive, similar to those that develop in older women (Kim *et al.*, 2010).

SIRT3 destabilises HIF-1α in a PHD-dependent manner, by increasing ROS production (Finley *et al.*, 2011) (Bell *et al.*, 2011), although direct inhibition of PHD activity was not clearly shown (Greer *et al.*, 2012). The metabolic phenotype of SIRT3-/- cells (increased glucose uptake and lactate production) can be reversed by stable knockdown of HIF-1α (Finley *et al.*, 2011). In human breast cancer, a least one copy of SIRT3 is deleted in 40%, and 87% show decreased immunohistochemical staining for SIRT3 (Finley *et al.*, 2011). Although it is not clear how SIRT3 suppresses ROS production, it does have several deacetylation targets, including superoxide dismutase (Tao *et al.*, 2010). SIRT3 has also been reported to deacetylate mitochondrial ribosomal protein L10 (MRPL10), the major acetylated protein in the mitochondrial ribosome (Yang *et al.*, 2010). Increased acetlyation of MRPL10 leads to increased translational activity in SIRT3-/- mice (Yang *et al.*, 2010), leading to increased synthesis of proteins encoded by mtDNA, a similar phenotype to Lon-deficient drosophila Schneider cells (Matsushima *et al.*, 2010).

FOXO3a. Forkhead transcription factor of the O class (FOXO) proteins is a family of four transcription factors (Foxo1, Foxo3a, Foxo4 and Foxo6). FOXO factors have been described as tumour suppressors in several systems (Dansen & Burgering, 2008). FOXO3a induces the expression of inhibitors of c-Myc, which itself is a regulator of mitochondrial biogenesis (see below) (Zhang *et al.*, 2007). Specifically, FOXO3a activation causes the upregulation of several members of the Mad/Mxd family of transcriptional repressors, particularily Mxi1, which leads to efficient c-Myc transcriptional repression and cell cycle arrest (Delpuech *et al.*, 2007).

FOXO3a activation and repression of c-Myc driven mitochondrial biogenesis leads to a reduction in mitochondrial DNA copy number, expression of mitochondrial proteins and a reduction in cellular ROS production (Ferber *et al.*, 2011). As a consequence of these changes, cells with activated FOXO3a reduced the amount of HIF-1α induced by hypoxia, an effect dependent on c-Myc (Ferber *et al.*, 2011). FOXO3a also induces manganese-containing superoxide dismutase (SOD2) (Kops *et al.*, 2002), which can detoxify ROS, but the ROS-suppressing effect of FOXO3a is independent of SOD2 (Ferber *et al.*, 2011).

In a study of resected nasopharyngeal carcinomas, FOXO3a expression was inversely correlated with HIF-1α, and low FOXO3a or high HIF-1α predicted poorer prognosis (Shou *et al.*, 2012). This suggests that HIF-1α stability may be affected by FOXO3a *in vivo*.

Independent of effects on the mitochondria, FOXO3a represses the transcriptional activity of HIF-1α by complexing with it and p300 on the Glut-1 (a HIF-1α target gene) promoter (Emerling *et al.*, 2008). This may be particularly relevant in cells deficient in PTEN activity, which have high constitutive AKT signalling that can phosphorylate and inactivate FOXO3a (Emerling *et al.*, 2008). Glioma and prostate cell lines with loss of PTEN have increased HIF-1α stability and activity (Zundel *et al.*, 2000) (Zhong *et al.*, 2000).

The M2 isoform of pyruvate kinase (PKM2). Pyruvate kinase catalyses the final step in glycolysis, regulating the availability of pyruvate to mitochondria. Four pyruvate kinase isoforms exist in mammals; the L and R isoforms are expressed in liver and red blood cells, M1 is ubiquitously expressed in normal tissues, and M2, an alternatively spliced isoform, is exclusively expressed during embryonic development (Christofk *et al.*, 2008). Cancer cells exclusively express the M2 isoform of pyruvate kinase, which has lower activity, and contributes to the lower use of pyruvate by mitochondria (Christofk *et al.*, 2008).

PKM2 is induced by HIF-1α, and it can also act as a coactivator of HIF-1α, suggesting it is involved in a positive feedback loop, increasing the activity of both under hypoxia (Luo *et al.*, 2011). PKM2 interacts directly with HIF-1α, HIF-2α and enhances binding and p300 recruitment to hypoxic response elements (Luo *et al.*, 2011). By increasing the transcription of proglycolytic genes such as *LDHA* and *SLC2A1*, PKM2 can promote a shift towards anaerobic metabolism.

The switch in isoforms from M1 to M2 is mediated by three heterogenous nuclear ribonucleoprotein proteins, which are upregulated by c-Myc (David *et al.*, 2010). Additonally, mTOR activation is reported to promote the expression of PKM2 by enhancing the transcription of HIF-1α, mimicking the effect of hypoxia, even under normoxic conditions (Sun *et al.*, 2011).

CHCHD4. CHCHD4 encodes 2 alternatively spliced isoforms, one of which, CHCHD4.1, is identical to Mia40, a component of the mitochondrial electron transfer system which regulates electron transport to cytochrome C (Yang *et al.*, 2012). Modulating the expression of CHCHD4 in tumour cells by shRNA reduced levels of stabilised HIF-1α in moderate hypoxia (1% oxygen), which translated to decreased growth and angiogenesis in mouse tumour xenografts. The expression of CHCHD4 (by mRNA) also correlates with a hypoxic gene signature (Yang *et al.*, 2012). The exact mechanism of this effect is not clear, although this may be similar to that described for other components of the electron transport chain, such as mitochondrial complex III (Brunelle *et al.*, 2005), attributed to changes in ROS.

c-Myc. Ectopic expression of the oncogene c-Myc is capable of immortalising primary human prostate epithelial cells (Gil *et al.*, 2005) and it is overexpressed in approximately 30% of human cancers (Dang *et al.*, 2008). Myc promotes glycolysis by the transcriptional induction of glycolytic enzymes and LDH-A (Kim *et al.*, 2004).

Myc also has a central role in promoting mitochondrial biogenesis, and the induction of Myc signalling leads to increased oxygen consumption, mitochondrial mass and function in the P493-6 human B-cell line (Li *et al.*, 2005a). Myc increases the expression of 175 nuclear-encoded mitochondrial genes, including TFAM, key to transcription and replication of mtDNA (Li *et al.*, 2005a).

HIF-1α and c-Myc can regulate the activity of each other. HIF-1α can inhibit c-Myc by two mechanisms; HIF-1α activates transcription of the c-Myc repressor MXI1, and HIF-1α also promotes the proteasome-dependent degradation of c-Myc (Zhang *et al.*, 2007). In this way, HIF-1α can inhibit mitochondrial biogenesis and respiration in VHL-deficient cells, an effect that is reversed when VHL is re-introduced (Hervouet *et al.*, 2005). In cell lines with dysregulated c-Myc, HIF-1α promotes the induction of hexokinase 2, which enhances glycolysis, and induces pyruvate dehydrogenase kinase 1, which inactivates pyruvate dehydrogenase and inhibits mitochondrial respiration (Kim *et al.*, 2007).

c-Myc can also induce the expression of HIF-1α in breast cancer cell lines, affecting stability, but not transcription of HIF-1α (Doe *et al.*, 2012). The accumulation of HIF-1α in this setting is transcriptionally active and proline-hydroxylated, suggesting that there is a diminished activity of VHL with c-Myc overexpression. This is despite the expression of all components of the VCB complex being increased in response to c-Myc overexpression (Doe *et al.*, 2012). The mechanism for this phenomenon remains unresolved, although the authors demonstrate dysfunction of the VHL complex, as VCB complex proteins appear to

be disassociated with co-immunoprecipitation of VHL (Doe *et al.*, 2012). Reducing the levels of c-Myc in multiple myeloma cells using siRNA has also been shown to reduce the stability of HIF-1α (Zhang *et al.*, 2009).

The von Hippel Lindau protein and mitochondria

VHL-deficient cell lines derived from clear cell renal cell carcinoma (CCRC) have mitochondrial impairment that can be restored with re-expression of wtVHL (Hervouet *et al.*, 2005). This has the effect of increasing mtDNA, TFAM and respiratory chain protein contents (Hervouet *et al.*, 2005). The effect is not specific to modulating levels of HIF-1α, as restored respiratory chain subunit content also occurs in CCRC cell line 786-o, which is devoid of HIF-1α (Hervouet *et al.*, 2008). In this case, the restoration of mitochondrial function can also be achieved by siRNA against HIF-2α (Hervouet *et al.*, 2008).

A single report has identified VHL as being localised to mitochondria (Shiao *et al.*, 2000). In this study, rat kidney epithelial-like cells (NRK-52E) were transfected with plasmids encoding rat VHL and rat VHL fused to GFP (Shiao *et al.*, 2000). These overexpressed proteins were demonstrated to localise to mitochondria by the fluorescent detection of GFP, and immunogold electron microscopy for the unfused and GFP-fused VHL (Shiao *et al.*, 2000). Importantly, endogenous VHL was not reported as being localised to mitochondria, and there is no other published evidence for the localisation of VHL in mitochondria.

VHL has been found to be associated with the mitochondrial DnaJ protein Tid1, long isoform (Bae *et al.*, 2005). The authors demonstrated that over-expression of Tid1 in cells or rabbit reticulocyte lysate promoted the interaction between VHL and HIF-1α (Bae *et al.*, 2005). HSP70s always require the co-operative activity of a J protein to mediate polypeptide folding, and Tid1 (DNAJA3) is described as having promiscuous client binding (Kampinga & Craig, 2010). Tid1 is predominantly mitochondrial, although some distributes to the cytoplasm, and other interactions include p53 (Ahn *et al.*, 2010), STAT1 and STAT3 (Copeland *et al.*, 2011) (Lu *et al.*, 2006). Indeed, the mechanism by which p53 translocates to mitochondria is via the interaction with Tid1 (Ahn *et al.*, 2010) (Trinh *et al.*, 2010). There are, however, no other published findings, including yeast two-hybrid screens, that corroborate the finding that VHL and Tid1 interact.

VHL assembly

A functional VHL requires assembly in a complex composed of elongin B, elongin C, cullin 2 and Rbx1 (Okumura *et al.*, 2012). Greater than 70% of the mutations in VHL responsible for VHL disease-associated and sporadic clear cell renal cell carcinoma are in the region that binds elongins B and C (the BC box – amino acids 157-172) (Feldman *et al.*, 1999) (Kishida *et al.*, 1995). Elongins B and C are ubiquitous adaptor proteins that interact with several other regulatory proteins in addition to VHL, including elongin A and members of the suppressors of cytokine signalling (SOCS) proteins (Okumura *et al.*, 2012).

Acquisition of the correct folding structure of proteins is critical for their function. It is well recognised that this is an active process that requires the assistance of molecular chaperones. The folding of VHL in cells is well characterised and mediated by a chaperone pathway consisting of Hsp70 and the chaperonin TRiC (also called CCT), which is the eukaryotic orthologue of the bacterial chaperonin GroEL (Feldman *et al.*, 1999) (Melville *et al.*, 2003). The Hsp70 and TRiC appear to function sequentially in the folding of VHL, with the newly formed VHL polypeptide first requiring the folding activity of Hsp70 (Melville *et al.*, 2003). VHL release from the TRiC requires association with elongins B and C (Feldman *et al.*, 1999). TRiC binding requires two β strands within the β domain of VHL. Some tumours contain VHL mutations that prevent this binding, and thus prevent VHL assembly (Feldman *et al.*, 2003). Association of the VHL-elonginB/C complex with cullin-2 and Rbx1 appears to occur subsequent to TRiC release (Hansen *et al.*, 2002).

VHL degradation requires the activity of different chaperones than for assembly (McClellan *et al.*, 2005). Degradation of misfolded VHL is reported to be mediated by the proteasome (Schoenfeld *et al.*, 2000), and VHL is ubiquitinated (Cai & Robertson, 2010). Hsp70 and Hsp90 are required for VHL degradation, but Hsp90 is dispensable for folding (McClellan *et al.*, 2005).

Expression of HIF in tissues

The expression of HIF-1α and HIF-2α by immunohistochemistry is detectable in most types of primary tumours and their metastases, and within malignancies is

usually detected in a small subset of tumour cells (<10%) (Talks *et al.*, 2000). Peri-necrotic accentuation of nuclear HIF-α staining is seen in tumours, consistent with these areas having the lowest oxygen concentrations (Talks *et al.*, 2000). Intra-tumoural measurements of oxygen concentration demonstrate lower levels in breast tumours compared to normal breast tissue (Vaupel, 2004), and negative correlation between HIF-1α levels and oxygen concentration in cervical cancer (Hutchison *et al.*, 2004).

In normal tissues, very little expression of HIF-1α or HIF-2α is seen, one exception being abundant cytoplasmic HIF-2α in tumour-associated and bone marrow macrophages (Talks *et al.*, 2000). In normal lymph nodes, weak and occasional cellular positivity for HIF-1α and HIF-2α is present (Giatromanolaki *et al.*, 2008).

Increased levels of HIF-1α and HIF-2α proteins in cancer cells can be the result of the loss of function of many different tumour suppressors. This may lead either to the increased synthesis of HIF-1α or impaired degradation. A summary of the effects on HIF-1α of loss of function of selected tumour suppressors are presented (Table 2).

Table 2.1 Effect on HIF-1α due to loss of function of tumour suppressor genes in cancer

Tumour suppressor gene	Effect on HIF-1α	Tumour types	Reference
VHL	Decreased ubiquitination	Renal carcinoma, haemangioblastoma, phaeochromocytoma	(Maher *et al.*, 2011)
SIRT3	Decreased hydroxylation	Breast carcinoma	(Kim *et al.*, 2010) (Finley *et al.*, 2011)
FOXO3a	Decreased hydroxylation	Breast carcinoma, Nasopharyngeal carcinoma	(Accili & Arden, 2004) (Ferber *et al.*, 2011) (Shou *et al.*, 2012)
P53	Decreased ubiquitination	Many	(Ravi *et al.*, 2000)
PTEN	Increased synthesis	Glioblastoma, breast, endometrial and prostate adenocarcinoma	(Zhong *et al.*, 2000) (Keniry & Parsons, 2008)
SDHB, SDHC, SDHD	Decreased hydroxylation	Paraganglioma	(Selak *et al.*, 2005)
FH	Decreased hydroxylation	Renal carcinoma, leiomyoma	(Isaacs *et al.*, 2005)
IDH1	Decreased hydroxylation	Glioblastoma	(Zhao *et al.*, 2009)
TSC2	Increased synthesis	Tuberous sclerosis	(Brugarolas *et al.*, 2003)
LKB1	Increased synthesis	Gastrointestinal hamartoma	(Shackelford *et al.*, 2009)

Whilst reduced levels of all of these tumour suppressor genes have been implicated in increasing the levels of HIF-1α, which promotes cancer progression (Semenza, 2010a), a high proportion of renal carcinomas do not express HIF-1α, through truncated transcripts and transcriptional silencing (Shinojima *et al.*,

2007). In xenograft models of renal cell carcinoma, expression of HIF-1α suppresses growth (Kondo *et al.*, 2003), and can act in specific contexts as a tumour suppressor (Keith *et al.*, 2012).

The association between HIF-1α and HIF-2α expression and clinical outcome

Many clinical studies have established the correlation between expression of increased levels of HIF-1α and HIF-2α with increased patient mortality in different tumour types (Semenza, 2010a). These studies include, but are not limited to, tumours of the breast (Yamamoto *et al.*, 2008), lung (Swinson *et al.*, 2004), colorectal (Schmitz *et al.*, 2009) and cervical carcinomas (Birner *et al.*, 2000). However, increased expression of HIF-1α confers a favourable prognosis in renal cell carcinoma (Lidgren *et al.*, 2005) and neuroblastoma (Noguera *et al.*, 2009). High levels of HIF-2α have never been reported to confer favourable prognosis, and have been reported only in association with increased patient mortality (Keith *et al.*, 2012).

Enhanced expression of HIF-α proteins contribute to cancer progression

The HIF-α subunits elicit a transcriptional program by binding to HREs within promoters of hundreds of target genes. The proteins that are produced in response have key roles in every aspect of cancer biology, including those involved in genetic instability (Huang *et al.*, 2007), angiogenesis (Couvelard *et al.*, 2005), metabolism (Finley *et al.*, 2011), pH regulation (Swietach *et al.*, 2007), invasion, metastasis, epithelial-mesenchymal transition (Lu & Kang, 2010) and radiation resistance (Moeller *et al.*, 2007).

Increased transcription can be demonstrated by the direct binding of HIF-1α to promoters of target genes. However, binding is not observed for hypoxia-repressed genes, suggesting an indirect HIF-1α mediated mechanism for repression (Mole *et al.*, 2009).

Rationale and described links between Lon and hypoxic signalling pathways

The Lon protease has been previously linked to the hypoxic response of tumour cells, by degrading isoform 2 of cytochrome c oxidase subunit 4 (COX4i1) (Fukuda *et al.*, 2007). This paper also provides evidence that Lon is a HIF target gene, induced in hypoxia consequent to a HRE within the promoter (Fukuda *et al.*, 2007), although this finding was not replicated in a subsequent bioinformatic analysis of the Lon promoter (Pinti *et al.*, 2010a). Under hypoxia, there is an isoform switch in COX4 from isoform 1 to 2, which optimises the COX activity under hypoxic conditions (Fukuda *et al.*, 2007). This response is highly evolutionary conserved, occurring also in yeast, which does not have an orthologous HIF system (Kwast *et al.*, 1998), suggesting this is a fundamental response of eukaryotic cells to hypoxia.

The recent description of Lon-degrading mitochondrial TFAM has a less obvious link to the hypoxic response (Bernstein *et al.*, 2012) (Matsushima *et al.*, 2010). The phenotype of Lon-deficient Drosophila Schneider cells includes increased mitochondrial DNA copy number and rate of mitochondrial transcription, and

these are attributed to the increased levels of TFAM (Matsushima *et al.*, 2010). These phenotypes are characteristic of increased mitochondrial biogenesis, which also occur when clear cell renal cell carcinomas, deficient in VHL, have VHL re-introduced (Hervouet *et al.*, 2005). Clearly, there are a number of pathways and transcription factors that can influence the level of mitochondrial biogenesis, including HIF-1α through the negative regulation of c-Myc (Zhang *et al.*, 2007). However, the findings to be outlined establish that these studies may both be describing the same effect, due to loss of repression of mitochondrial biogenesis through activation of the hypoxic response.

Another paper more directly suggests a link between Lon and VHL by studying the genome of *Takifugu rubripes* (pufferfish) (Sikora & Godzik, 2004). In pufferfish, the VHL orthologue is predicted to be a multidomain 1127 amino acid protein with a Lon-N domain and M24-like peptidase domain (Sikora & Godzik, 2004). Proteins that interact in one species may be part of a larger multi-domain protein in another. This paper suggests that VHL may therefore interact with a Lon-N domain-containing protein (Sikora & Godzik, 2004). This may be the Lon protease, however the VHL pufferfish does not contain the other domains comprising the Lon protease.

A fundamental role for Lon in the response to hypoxia is also suggested by the inability of Lon-deficient *E. coli* to respond to growth under non-aerated conditions (HOWARD-FLANDERS *et al.*, 1964), although this may be partly due to modification of the heat-shock response.

These links, as well as the finding of up-regulated Lon mRNA in tumours with a non-angiogenic phenotype (Hu *et al.*, 2005), suggest that there may be a role for Lon in modulating the hypoxic response of tumour cells. Investigating whether this is the case is the prime aim of this project.

Chapter 2 : The expression of Lon protease in normal and malignant tissue

To begin our investigation into whether the mitochondrial Lon protease plays a pathophysiological role in cancer, we raised and characterised a monoclonal antibody against Lon. We then used this validated antibody to determine the expression of Lon in normal and malignant tissue, and evaluated its use as a biomarker in breast cancer.

Outline

The mitochondrial Lon protease is a AAA+ (ATP-ase associated with various cellular activities) protease that degrades abnormally folded and certain regulatory proteins (Venkatesh *et al.*, 2011). Recently, it has also been found to control mitochondrial transcription by degrading mitochondrial transcription factor A (TFAM) (Lu *et al.*, 2012). Lon was previously identified as one of 62 genes that formed a gene expression signature for non-angiogenic lung cancer (Hu *et al.*, 2005). The expression of Lon is induced by hypoxia, oxidative and endoplasmic reticulum stress, and has been shown to increase in malignant compared to resting B cells (Bernstein *et al.*, 2012). Using a novel mouse monoclonal antibody, validated for formalin-fixed paraffin embedded (FFPE) immunohistochemistry, we find that Lon is ubiquitously expressed in normal tissue, with significantly increased levels found in columnar epithelium and adrenal medulla. Lon expression is significantly increased in breast and lung cancer compared to normal tissues. High levels of Lon are associated with poorer

overall survival in ER-positive breast cancer. This is the first study to evaluate the expression of the Lon protease as a biomarker, and the availability of our monoclonal antibody will allow further evaluation of Lon expression in cancer and other diseases.

Introduction

Increased expression of the mitochondrial Lon protease has been linked to malignant transformation of cells - human mammary epithelial cells overexpressing ErbB2 express significantly higher levels of Lon (Zhu *et al.*, 2002), and malignant B cells show higher levels of Lon that resting B cells (Bernstein *et al.*, 2012). The study of Lon expression in tumour cells has been limited by the lack of specific antibodies against the Lon protease to allow conventional immunohistochemical evaluation *in vivo.* We sought to produce a monoclonal antibody against Lon and to determine whether it was upregulated in human solid malignancies, and whether it was useful as a prognostic factor or correlated with other hypoxic markers in tumours (Fukuda *et al.*, 2007).

Materials and methods

Monoclonal antibody production

To generate a Lon antibody, the peptide immunogen *N*-CEKDDKDAIEEKFRERLKE-*C* was produced by the Protein & Peptide Chemistry Laboratory (CRUK facility at Lincoln's Inn Fields, London). 20mg of peptide was

coupled to the carrier protein keyhole limpet haemocyanin (KLH) (20mg) by using the Imject mcKLH kit (Pierce). Conjugate was dialysed to remove unconjugated peptide and salts against PBSA. The KLH-peptide conjugate was diluted 1:1 with TiterMax Gold adjuvant (Sigma) and 25µl (10µg protein) was injected subcutaneously into the groin of two CD1 mice (Charles River). Mice were immunized with three further doses without adjuvant at 10 day intervals intraperitoneally, with the fourth dose given four days prior to the mice being culled and spleens harvested.

Spleen cells were disaggregated mechanically and with gentle trituration using a pipette. They were then fused to the mouse myeloma cell line NS0 (available from Sigma) using PEG 15,000 (Sigma) as the fusing agent. Hybrid cells were selected by incubating cells in hypoxanthine-aminopterin-thymidine (HAT) medium (Köhler & Milstein, 1975). β-Aminopterin blocks the *de novo* synthesis of purine nucleotides and thymidylates, so the salvage pathway has to be used. This utilises HGPRT (hypoxanthine-guanine phosphoribosyltransferase) with an absolute requirement for thymidine to synthesize thymidylate and hypoxanthine to synthesize purine nucleotides. The HGPRT gene is mutated to be non-functional in the fusion partner cells NS0, so they will die in conditions that block the *de novo* pathway. The mouse spleen cells can divide only a limited number of times before they die in culture. Thus only hybrids between the two can survive. Colonies were individually extracted (with a Pasteur pipette) and plated into wells of a 24 well plate. Wells were tested for antibody by enzyme-linked immunosorbent assay (ELISA), using the KLH-coupled peptide as the immobilised antigen (96 well ELISA plate – BD Falcon) alongside a control plate

of KLH-coupled to an irrelevant peptide. The presence of reactive antibody was detected by adding goat anti-mouse HRP conjugated secondary antibody (Dako) and the HRP substrate ABTS (Roche).

Wells containing ELISA-positive Lon antibody were subsequently tested for immunoreactivity by immunohistochemistry on FFPE 293T cell pellets transfected with PCMV6-Entry Lon (Origene). Positive hybridoma colonies were selected for cloning. The colony was diluted and plated at a concentration of one cell per well in a 96 well plate. Clones were tested by ELISA, and selected positive clones by cell pellet immunohistochemistry. Cloning was repeated and the final clone expanded, and hybridoma supernatant collected and stored. The final clone-producing antibody used for this project was Lon 20H1.

Immunohistochemistry

4μM sections were deparaffinised by sequential washing (xylene 2 x 5 minutes, 100% ethanol 2 x 5 minutes, 70% ethanol 5 minutes, 50% ethanol 5 minutes, running water to rinse). Antigen retrieval was performed by placing slides in specified buffer within a pressurised decloaking chamber (Biocare Medical). Sections were blocked with 2.5% normal horse serum (Vector Laboratories) for 15 minutes. Slides were tapped off and primary antibody, diluted in RPMI, was incubated overnight at 4°C. Primary antibody was removed and slides were rinsed with two washes of PBS for five minutes. Bound antibody was detected by addition of a secondary detection reagent with peroxidase (as per Table 2.1). A

chromogenic signal was produced by addition of diaminobenzidine (DAB) (Dako), producing a brown product at the site of the target antigen.

Table 2.1 Conditions and antibodies used for immunohistochemistry

Target antigen	Antibody supplier (clone)	Retrieval and dilution	Detection
Lon	In-house (20H1)	Dako S1699 1:2	Impress (Vector Laboratories)
HIF-1α	BD (54/HIF-1α)	0.1mM EDTA pH 8, 1:100	Impress (Vector Laboratories)
CA9	Gift from J. Pastorek, Institute of Virology, Slovak Republic. (M75) (Pastoreková *et al.*, 1992)	Tris-EDTA pH 9, 1:50	Envision kit (DAKO)
Glut1	Dako (Rabbit polyclonal)	0.01M citrate pH 6 1:100	Impress (Vector Laboratories)
VHL	BD (Ig32)	0.01M citrate pH 6 1:500	Impress (Vector Laboratories)
Ki-67	BD (MIB-1)	0.01M citrate pH 6 1:50	Envision kit (Dako)

For Lon staining on TMA cores, slides were scored semi-quantitatively (0, 1, 2 or 3) on the basis of signal intensity by two pathologists, and discrepancies were resolved by review and consensus. 5% of cores were had divergent scoring requiring review. All tumour cells within a core showed a similar degree of staining for Lon. For HIF-1α, cores were scored as positive if there was any detectable nuclear staining. CA9 was scored positive if there was membranous staining within a least 10% of tumour cells within a core. Glut1 and VHL was scored semi-quantitatively on the basis of signal intensity (0, 1, 2 or 3). For Ki-67, the proportion of epithelial tumour cells was used to assign a proliferative index (score 1 <10%, 2 10-50%, 3 >50%).

Patients and tissue samples

FFPE tissues were obtained for 287 sequential patients with breast carcinoma who underwent surgery between 1989 and 1998 at the John Radcliffe Hospital, Oxford (Table 2.3). The number of patient samples stained by immunohistochemistry was limited by core exhaustion. Patients had been treated by wide local excision and postoperative radiotherapy, or by mastectomy with or without postoperative radiotherapy. Postoperative chemotherapy (600 mg/m^2 cyclophosphamide, 40 mg/m^2 methotrexate and 600 mg/m^2 5-fluorouracil IV on day 1 of a 21 day cycle, repeated for six cycles) and hormonal therapy were offered according to local protocols. The sample size was determined by the availability of tissue with clinical follow-up data and ethical approval. Two cases had no clinical follow up. Follow-up data was correct as of January 2008. The median follow-up time was 10 years, with a medial overall survival of 14.5 years and a median relapse free survival of 13.1 years. Oestrogen receptor (ER) status was determined by ELISA (Abbott Laboratories) and considered positive if greater than 10 fmol/mg cytosolic protein (Leclercq *et al.*, 1986). Human epidermal growth factor receptor-2 (HER-2) status was determined using the HercepTest (Dako).

Tissue microarrays (TMAs) were assembled by taking three 1mm cores of tumour from tumour blocks and placing into a pre-cored wax block of 120 cores (Bubendorf *et al.*, 2001). Approval for use of tissue was obtained from the local research ethics committee (C02.216). The study was designed to comply with the REMARK criteria (McShane *et al.*, 2005).

For a comparison of tumour and matched normal tissues, whole sections of tumours were requested and the expression in the tumour was compared to the expression in normal adjacent structures. For the comparative expression of normal human tissue expression, a TMA slide of normal tissue was used so that all cores were equally treated.

Cell pellets

Cells were trypsinized and resuspended in 10% neutral buffered formalin (4% w/v paraformaldehyde, John Radcliffe Histopathology department) and fixed overnight in a 1.5 ml tube. Cells were then spun down and resuspended in 2% agarose dissolved in 10% formalin at 60°C in a water bath. Cells formed a pellet when the cell and agarose mixture was briefly centrifuged, and the agarose was allowed to solidify on ice. The tip of the 1.5ml tube was cut off using a razor blade and the cell pellet removed by applying positive pressure to the cut end with the use of a syringe. The cell pellet was processed overnight in a cassette in the same way as routine histological samples.

Statistics

Pearson's χ^2 test was used to test for associations between immunohistochemical scores and clinical parameters that were categorical variables. Cases were omitted from analyses if there was missing data. Survival analyses refer to overall survival times, where the death from any cause represents an event. Patients were censored according to the last date of follow-up by a doctor. Cox regression analysis was used to identify prognostic factors. Two-sided *p* values <0.05 were considered significant. Mean survival times were estimated from

Kaplan-Meier curves. Associations between ordinal immunohistochemical scores were examined using Pearson's correlation coefficient. All statistical analyses were performed with SPSS statistics (version 21.0, IBM). Bar graphs were assembled using Prism 4.0 (Graphpad).

For cells, cell culture and western blotting methods, see Chapter 3.

Results

Validation of Lon antibody

We validated the mouse monoclonal Lon antibody, Lon 20H1, for use in immunohistochemistry and western blotting. To verify that the antibody recognised Lon in FFPE tissue, 293T cells were transfected with a flag-tagged overexpression vector. The antibody produced a strong brown DAB precipitate with cells transfected with the Lon vector while cells transfected with the control vector showed only a few cytoplasmic dots (of endogenous Lon) (Figure 2.1A). The proportion of cells that stained positively with the Lon antibody was similar to that see with anti-flag antibody.

To determine that the antibody has sufficient sensitivity to detect endogenous levels of Lon, and to confirm the staining was specific, U87 cells were transfected with siRNA, targeted against the Lon protease (siLonp1.1) or a control sequence (siControl) and made into a FFPE cell pellet. U87 cells showed moderate cytoplasmic granular positivity, which was completely absent when the Lon

protease was targeted by siRNA (Figure 2.1B). This confirms sensitivity to detect endogenous Lon and specificity for use in FFPE.

Validation of the antibody for use in western blotting was achieved in a similar way. Targeting the Lon protease by siRNA resulted in the loss of an immunoreactive band at approximately 110 kDa which was present in the control transfected or mock transfected U87 cells (Figure 2.1C). No other bands were seen on the western blot.

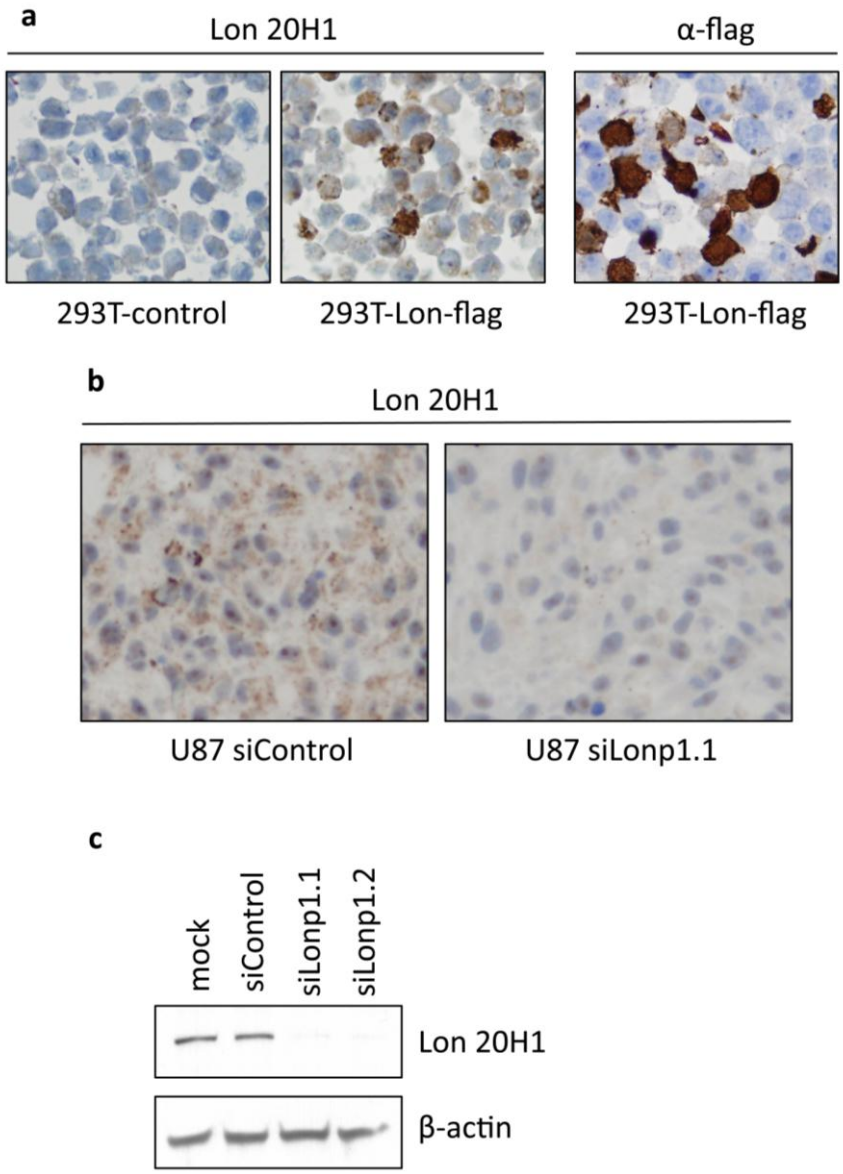

Figure 2.1 Validation of the Lon protease for use in FFPE and western blotting. A. 293T cells were transfected with either a control (pCMV6-Entry REDD1) or Lon-flag tagged (pCMV6-Entry Lonp1) overexpression vector, then created into a cell pellet and stained by immunohistochemistry using the antibodies indicated. **B.** U87 cells were transfected with siRNA against the Lon protease (siLonp1.1) or a control sequence (siControl), turned into a cell pellet and stained using the Lon 20H1 monoclonal antibody, **C.** U87 cells were transfected with siRNA against the Lon protease (siLonp1.1 and siLonp1.2) or a control sequence (siControl) or transfection reagent alone (mock) and then western blotted with Lon 20H1 and a loading control antibody (β-actin).

The expression of Lon in normal tissue

In order to establish the expression of Lon in normal tissues we stained a TMA compiled from various normal human tissues (Figure 2.2). Lon was ubiquitously expressed in all tissues and more highly expressed in endocrine and epithelial

tissues. Lon was expressed with a granular and cytoplasmic pattern, suggestive of organelle staining. There was membranous-type staining in the epithelium of the fallopian tube, gallbladder and colon. Nuclear staining was not observed. Within lymphoid tissues, discrete cells within the germinal centre showed stronger staining, and these were likely activated B cells. Strong staining was noted in the adrenal medulla. Within the kidney, strong staining was seen in the cells of collecting ducts, with weaker staining of proximal tubules and glomerular cells. Normal breast epithelium showed weak staining in myoepithelial cells and slightly increased staining in luminal cells in ducts and lobules. Staining is summarised in Table 2.2.

Table 2.2 Lon protease immunohistochemical staining patterns in normal human tissues. (c) indicates cytoplasmic, (m) membranous, -/+ equivocal staining, +, ++, +++ and ++++ indicate increasing intensity of staining of tissue. Epithelium abbreviated to ep.

Central Nervous system		Breast	
Neuronal cells	+/++ (c)	Lobular ep.	+ (c)
Endothelial cells	+ (c)	Ductal ep.	++ (c)
Glial cells	+ (c)	Myoepithelial cells	+ (c)
Purkinje cells	++ (c)	Adipocytes	-/+ (c)
Granular layer cells	+ (c)	Female reproductive system	
Molecular layer cells	+ (c)	Ovarian stroma	+ (c)
Blood and immune system		Follicle cells	+ (c)
Bone marrow	+/++ (c)	Fallopian tube cells	+++ (c/m)
Germinal centre cells	+++ (c)	Uterine stroma	+ (c)
Non-germinal centre cells	+ (c)	Uterine ep.	++ (c)
Spleen – white pulp	++ (c)	Cervical ep.	+/++ (c)
Spleen – red pulp	+ (c)	Placenta	
Liver and pancreas		Syncytiotrophoblast	+++ (c/m)
Hepatocytes	+ (c)	Cytotrophoblast	++ (c)
Cells of bile ducts	++ (c/m)	Male reproductive tissue	
Gallbladder epithelium	+++ (c/m)	Seminiferus duct cells	++ (c)
Exocrine pancreas cells	+ (c)	Leydig cells	+ (c)
Exocrine duct cells	++ (c/m)	Seminal vesicle ep.	+++ (c/m)
Endocrine pancreas	++ (c)	Prostatic ep.	+ (c)
Gastro-intestinal tract		Urinary tract	
Oesophagus ep.	+ (c)	Glomerular cells	+ (c)
Stomach ep.	+/++ (c)	Renal tubules	++/+++ (c)
Small intestine ep.	+/++ (c)	Urothelial cells	+ (c)
Colonic epithelium	++ (c)	Skin and soft tissue	
Smooth muscle	+ (c)	Keratinocytes	+ (c)
Stroma	-/+ (c)	Melanocytes	+/++ (c)
Respiratory system		Fibroblasts	+/- (c)
Alveolar ep.	+ (c)	Striated muscle	+ (c)
Macrophages	++/+++ (c)	Adipocytes	+/- (c)
Tracheal chondrocytes	+ (c)	Peripheral nerve	+/- (c)
Endocrine system		Smooth muscle	+ (c)
Thyroid follicular cells	+ (c)		
Adrenal cortex	++(c)		
Adrenal medulla	++++ (c)		

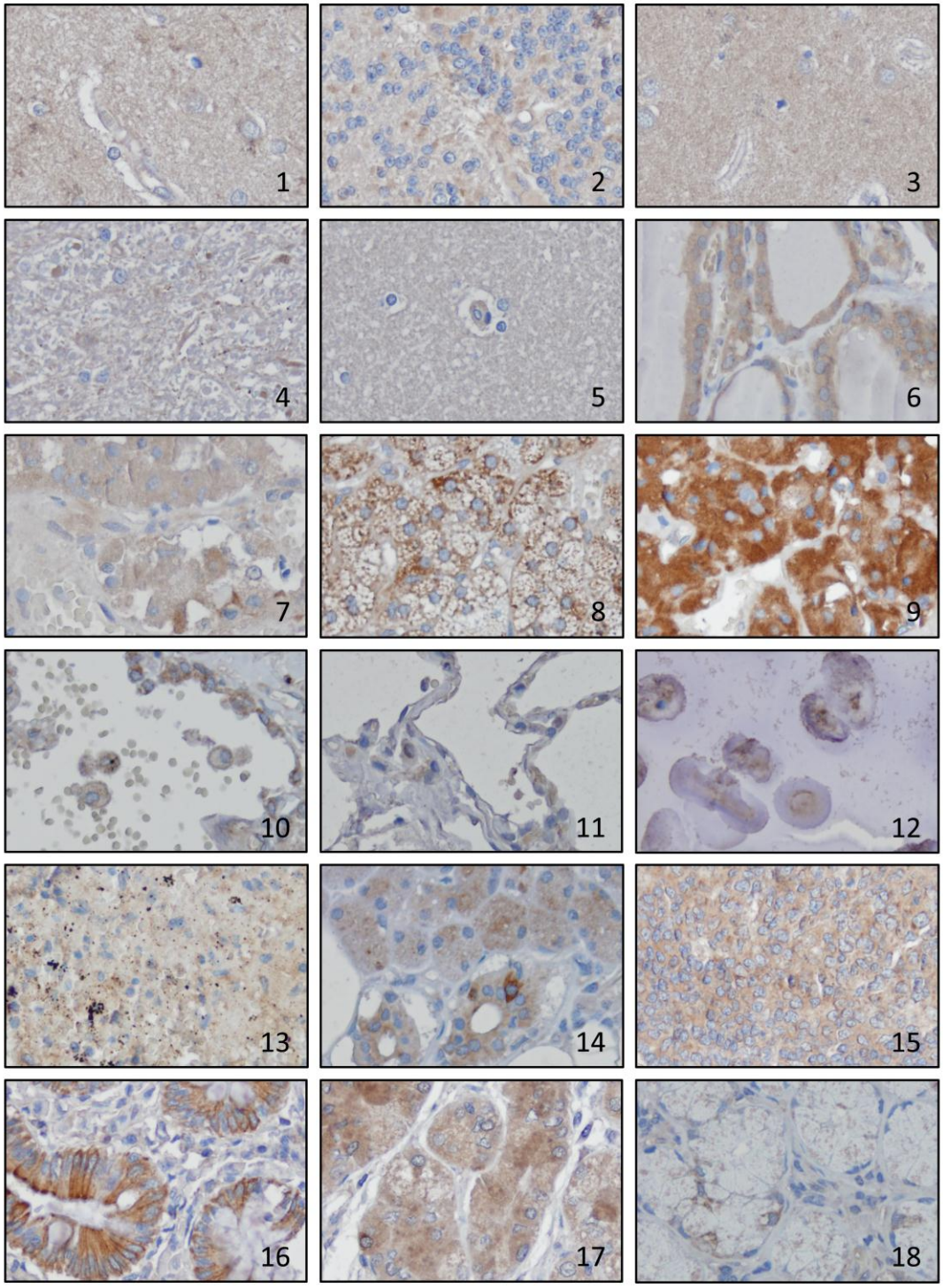

Figure 2.0.1 Representative immunohistochemistry for Lon protease in normal human tissues. Brown staining with diaminobenzidine indicates immunoreactivity.

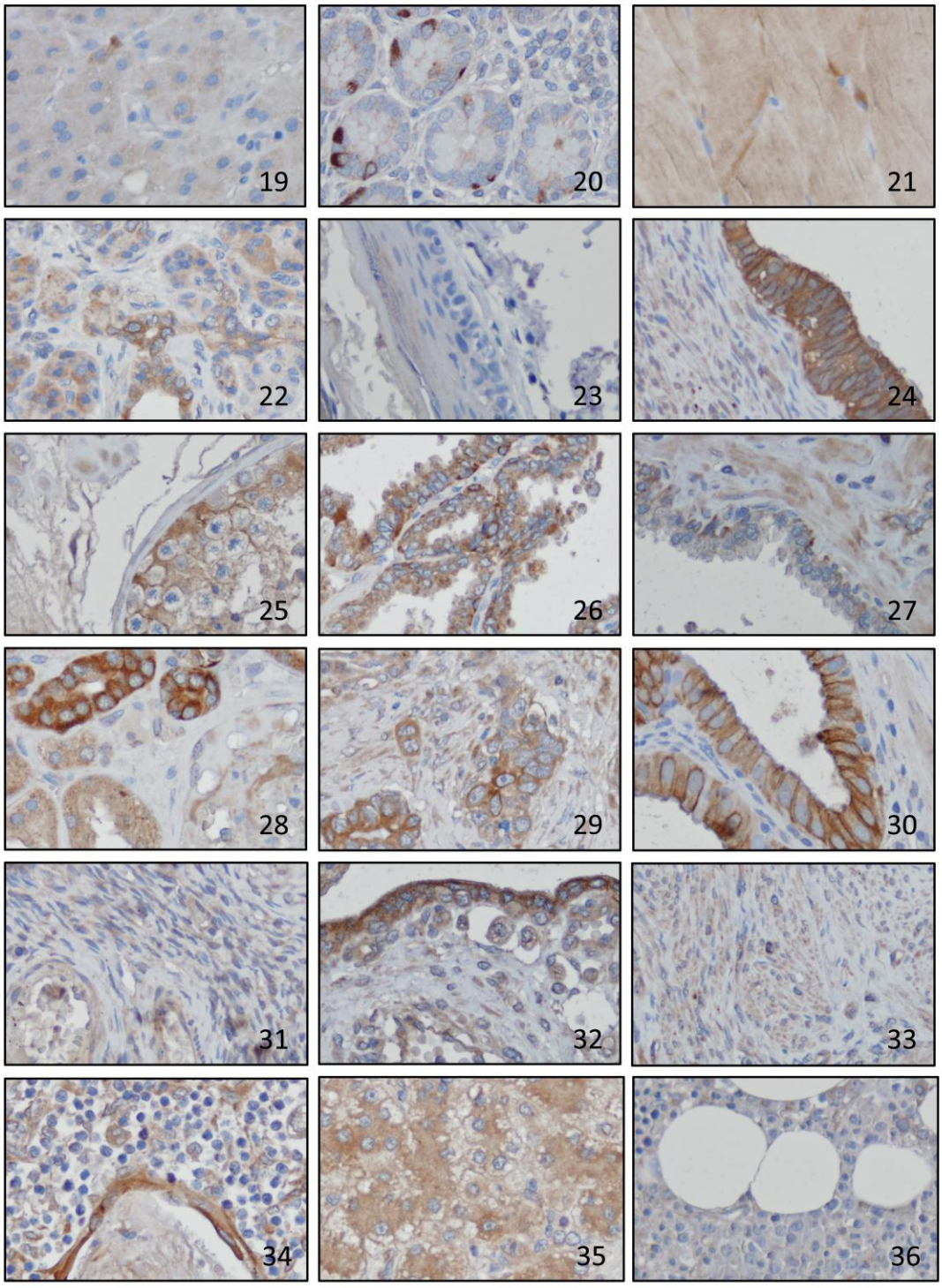

19. Liver
20. Ileum
21. Striated muscle
22. Pancreas
23. Skin
24. Fallopian tube
25. Testicle
26. Seminal vesicle
27. Prostate
28. Kidney
29. Breast
30. Gallbladder
31. Ovary
32. Placenta
33. Uterine muscle
34. Thymus
35. Foetal liver
36. Bone marrow

Figure 2.2 (Continued) Representative immunohistochemistry for Lon protease in normal human tissues.

The expression of Lon in tumour versus matched normal tissues

To determine whether the expression of Lon may play a pathophysiological role in carcinogenesis we first assessed whether it was increased in tumour cells compared to the matched normal tissue of patients with breast and lung cancer. For this analysis, we assessed 20 patients with lung cancer and 15 with breast cancer.

The expression of Lon was significantly higher in both breast and lung cancer (Figure 2.3). The pattern of Lon expression in tumour cells was predominantly granular and cytoplasmic, and there was considerable variation in expression between different tumours.

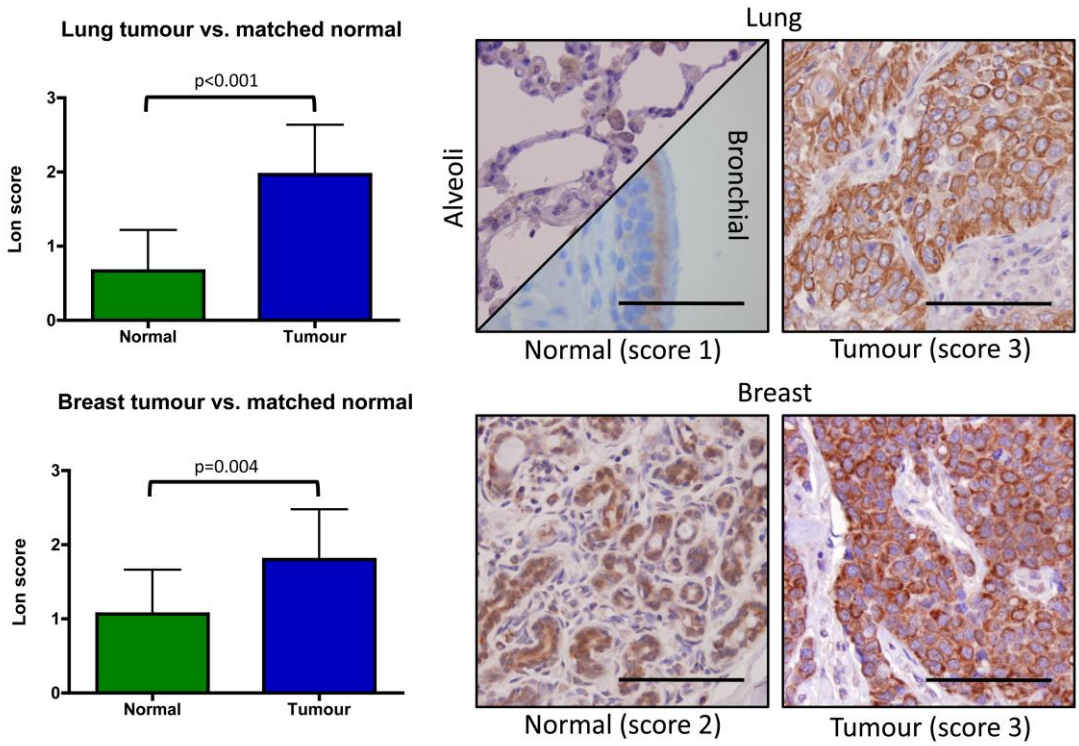

Figure 2.3 The expression of Lon is upregulated in tumour compared to normal originating tissue. Whole sections of tumour and normal tissue from either breast or lung were stained and scored for the expression of Lon. Graphs show mean and standard deviation of expression in normal and tumour tissue. *P* values quoted are the result of the paired t-test and error bars indicate standard deviation (N = 20 for lung; 15 for breast tumours). Right, representative sections of normal and tumour from breast and lung. Normal lung panel is split to

show representative staining in alveolar and bronchial epithelium. Brown staining with diaminobenzidine indicates immunoreactivity. Scale bar equals 100μM.

The expression of Lon as a predictor of outcome in breast cancer

Having determined that Lon was upregulated in breast cancer, we examined the expression in a series of patients with breast cancer treated with tumour resection at the John Radcliffe Hospital with clinical follow up data. Of 287 patients, 181 were scored for expression of Lon (due to TMA core exhaustion). The patient demographics of tumours analysed with Lon were representative of the entire cohort (Table 2.3).

We assessed whether Lon expression was an adverse prognostic factor in a univariate analysis of overall survival by Cox regression (Table 2.3). Only the presence of lymph node metastases, age greater than 50 years, tumour diameter greater than 2cm, and patients treated with radiotherapy and chemotherapy were significant prognostic factors impacting overall survival ($p < 0.05$). The expression of Lon score 2 vs. 1 was not significant for adverse survival ($p = 0.057$). Although there were few cases of breast cancer that scored 1 for expression of Lon (28 patients, 16% of cohort), the lower expression of Lon shows a non-significant trend towards better survival.

In a χ^2 (Pearson's) test of association between Lon expression and categorical variables of clinicopathological data, Lon was significantly correlated with ER positivity ($p = 0.004$) and HER2 positivity ($p = 0.007$), but with none of the other variables tested (Table 2.4).

To assess the impact of Lon expression on survival in breast cancer over time, we plotted Kaplan-Meier curves of overall survival for patients sub-grouped according to Lon expression (Figure 2.4B and statistics 2.4C). Representative images of the Lon immunohistochemistry scores assigned to tumours are shown in Figure 2.4A. There were no significant differences in survival between the patients that scored 1, 2 or 3 as determined by the log rank test comparing each pair (Figure 2.4C).

The survival curves for patients with tumours that scored 2 and 3 for Lon expression overlapped, whilst patients with a Lon score of 1 appeared to show better survival. This trend appears to hold true only until approximately 4000 days (Figure 2.4B), after which time the curves (representing Lon scores 1, 2 and 3) appear to decrease at the same rate. One possible interpretation of this is that the expression of Lon may be only predictive of prognosis within the first ten years post resection. Higher levels of Lon may be associated with an earlier adverse prognosis in the primary resected tumour.

To determine whether Lon expression may be predictive of earlier survival, we censored all observations at 10 years and re-evaluated the significance of differences in overall survival between patients with tumours with low (score 1) or high (score 2 or 3) levels of Lon (Figure 2.4). This dichotomised pattern exhibits the best fit with the differential clinical outcome between groups, based on expression of Lon.

The expression of higher levels of Lon in breast cancer is significantly associated with a shorter overall survival at 10 years follow-up (Figure 2.5). Patients with tumours with low expression of Lon have an estimated 3231 days survival (95% C.I. 2866-3598), whereas those with high levels (score 2 or 3) have 2808 days survival (95% C.I. 2617-2999, $p = 0.048$).

Table 2.3 Patient demographics of breast tumours analysed for Lon expression

Marker	Total	Lonp1
Total, n	287	181
Age, years		
Mean	58	57
Range	26-90	26-83
Female, n	287	181
Histology, n		
Ductal	224	136
Lobular	38	27
Mixed	15	11
Other	10	7
Diameter, n		
≤2 cm	117	72
>2 cm	169	108
Missing	1	1
Lymph Nodes, n		
Involved	117	75
Uninvolved	169	101
Missing	1	5
Grade, n		
1	28	18
2	115	75
3	94	55
Missing	50	33
ER, n		
Negative	69	39
Positive	205	131
Missing	13	11
HER2, n		
Negative	221	144
Positive	20	11
Missing	46	26
Radiotherapy		
Not Received	49	35
Received	238	146
Missing	0	0
Chemotherapy		
Not Received	238	148
Received	49	33
Missing	0	0
Hormonal Therapy		
Not Received	82	42
Received	205	139
Missing	0	0

Table 2.4 Cox regression analysis – univariate analysis of overall survival

Variable	n	Events	Hazard ratio	95% CI	p
Lymph nodes					
- Negative	175	63	1.00		
- Positive	104	60	2.030	1.425-2.893	**<0.001**
Lon (score)					
- 1	28	8	1.00		
- 2	56	29	2.142	0.978-4.690	0.057
- 3	95	44	1.859	0.857-3.949	0.107
Grade					
- 1	27	9	1.00		
- 2	115	50	1.270	0.624-2.584	0.509
- 3	93	46	1.664	0.814-3.400	0.163
Histology					
- Ductal	222	99	1.00		
- Lobular	38	14	0.762	0.436-1.335	0.342
- Mixed	15	9	1.534	0.775-3.037	0.219
- Other	10	4	0.697	0.256-1.896	0.480
Age					
- <50	84	19	1.00		
- ≥50	201	107	3.014	1.848-4.917	**<0.001**
Diameter					
- <2cm	117	40	1.00		
- ≥2cm	168	86	1.872	1.285-2.727	**0.001**
ER					
- Negative	68	32	1.00		
- Positive	204	87	0.815	0.543-1.223	0.332
HER2					
- Negative	220	95	1.00		
- Positive	19	8	0.943	0.458-1.942	0.874
Radiotherapy					
- No	47	27	1.00		
- Yes	238	99	0.640	0.418-0.981	**0.040**
Chemotherapy					
- No	237	108	1.00		
- Yes	48	18	1.235	0.750-2.035	0.407
Hormonal therapy					
- No	82	31	1.00		
- Yes	203	95	1.525	1.012-2.298	**0.044**

Table 2.5 Statistical significance of association between Lon expression and categorical clinical variables

		Age	Grade	Nodes	ER	HER2	Chemo	RT	Hormonal
Lon	χ^2	1.049	3.127	2.214	**11.254**	**10.027**	2.859	.8	5.18
	p	.308	.537	.330	**.004**	**.007**	.239	.670	.075
	N	181	148	176	**170**	**155**	181	181	181

A

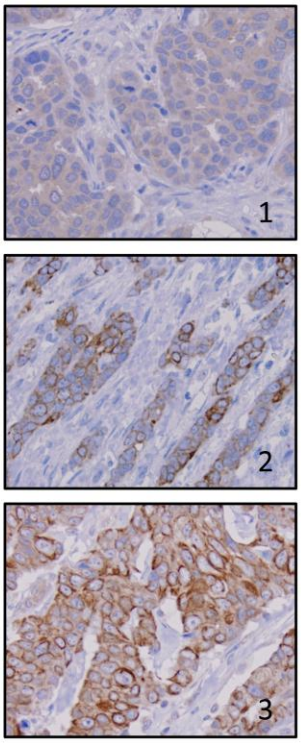

B

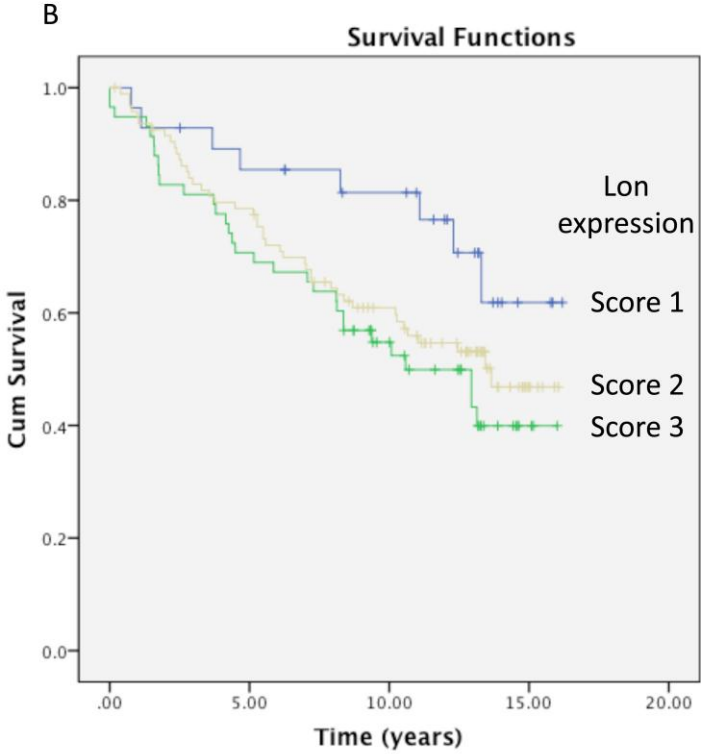

C

Pairwise Comparisons

	Lon expression	1		2		3	
		Chi-Square	Sig.	Chi-Square	Sig.	Chi-Square	Sig.
Log Rank (Mantel-Cox)	1			3.835	.050	2.674	.102
	2	3.835	.050			.331	.565
	3	2.674	.102	.331	.565		

Figure 2.4 Higher levels of Lon expression in breast cancer is associated with a trend towards poorer overall survival. A. Representative immunostaining for Lon in breast cancer showing variability of expression (number indicates score of Lon expression). **B.** Kaplan-Meier curve showing overall survival of breast cancer patients sub-grouped according to Lon expression. Censored patients indicated by a cross. **C.** Log rank statistics between sub-groups according to Lon expression. Cum(ulative) survival indicates the proportion of patients alive at time.

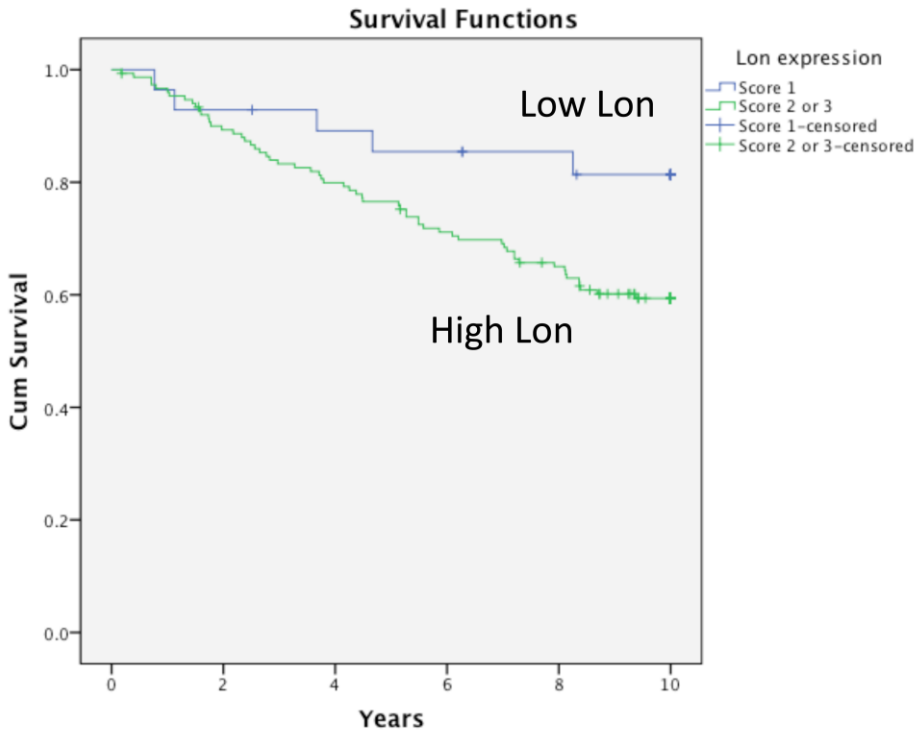

Case Processing Summary

Lon expression	Total N	N of Events	Censored	
			N	Percent
Score 1	28	5	23	82.1%
Score 2 or 3	151	60	91	60.3%
Overall	179	65	114	63.7%

Pairwise Comparisons

	Lon expression	Score 1		Score 2 or 3	
		Chi-Square	Sig.	Chi-Square	Sig.
Log Rank (Mantel-Cox)	Score 1			3.908	.048
	Score 2 or 3	3.908	.048		

Figure 2.5 High Lon expression in breast cancer is significantly associated with poorer overall survival at 10 years follow-up. Kaplan-Meier curves shows overall survival of patients grouped according to high (score 2 or 3) or low (score 1) expression of Lon.

Lon expression only predicts overall survival in ER positive breast cancer

As we had determined there was a significant correlation between higher Lon expression and ER positivity we looked at whether Lon expression was a stronger predictor of survival when stratified by ER status. Patients with tumours that were ER negative tended to have a shorter overall survival, although this was not significant ($p = 0.321$) (when censored at 10 years, $p = 0.067$) (Figure 2.6). When stratified by ER status, higher (score 2 or 3) Lon

expression was predictive of shorter overall survival in ER positive tumours, but not in ER negative tumours.

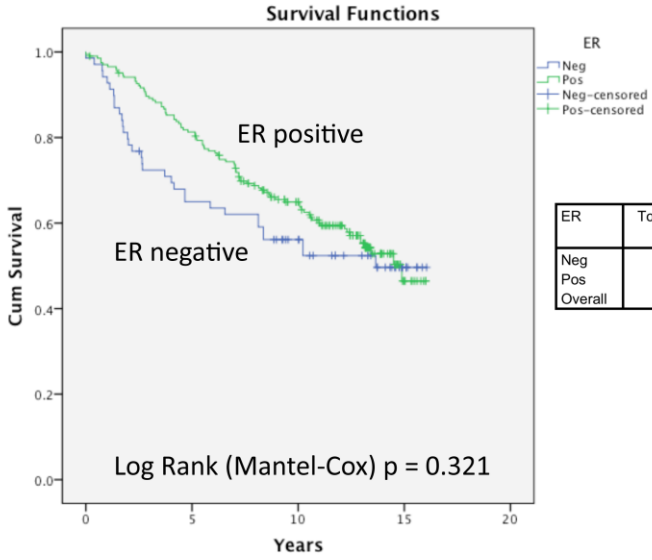

Case Processing Summary

ER	Total N	N of Events	Censored	
			N	Percent
Neg	68	32	36	52.9%
Pos	204	87	117	57.4%
Overall	272	119	153	56.3%

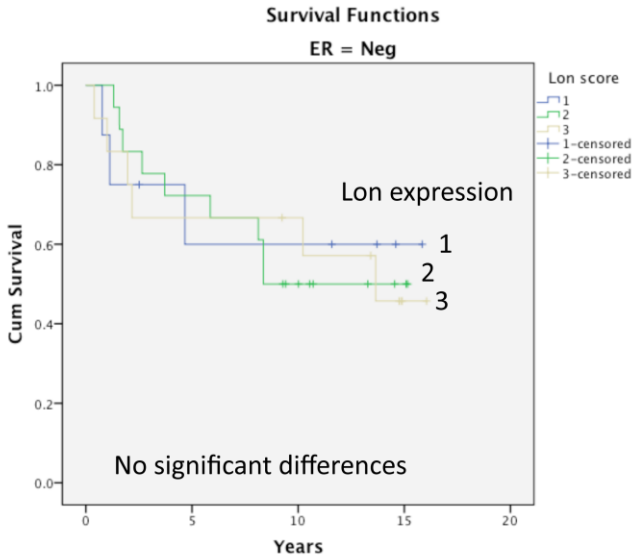

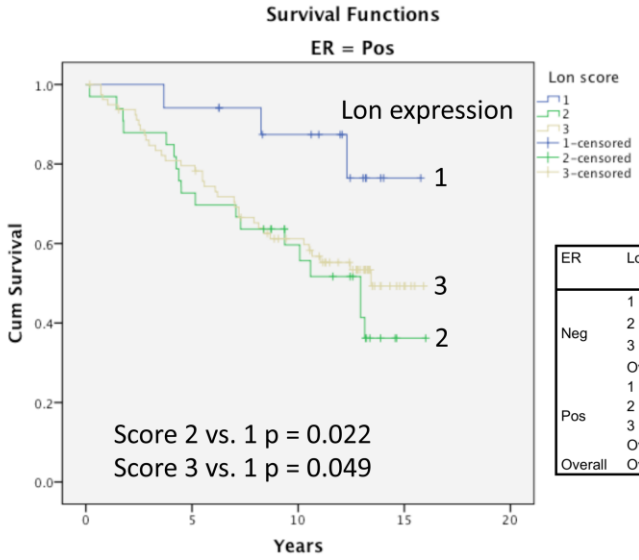

Case Processing Summary

ER	Lon score	Total N	N of Events	Censored	
				N	Percent
Neg	1	8	3	5	62.5%
	2	18	9	9	50.0%
	3	12	6	6	50.0%
	Overall	38	18	20	52.6%
Pos	1	17	3	14	82.4%
	2	33	18	15	45.5%
	3	80	36	44	55.0%
	Overall	130	57	73	56.2%
Overall	Overall	168	75	93	55.4%

Figure 2.6 Higher expression of Lon is predictive of shorter overall survival in ER-positive but not ER-negative breast cancer. Kaplan-Meier curves show the differences in overall survival in patients with ER positive and negative tumours (top). Patients were then stratified

according to ER status and effect of Lon expression was determined (ER negative, middle; ER positive, bottom). Table indicates numbers of patients in each subgroup. *P* values are the result of the long-rank test.

The correlation of Lon with other immunohistochemical markers

As Lon had been identified as being differentially regulated (at the mRNA) level according to the level of angiogenesis observed in lung cancer (Hu *et al.*, 2005), we evaluated whether there was any relationship between the expression of Lon and HIF-1α, or the hypoxic markers CA9 and GLUT1 in patients with breast cancer. Lon is also reportedly upregulated in hypoxia (Fukuda *et al.*, 2007). We included VHL in this analysis, as it is responsible for the degradation of HIF-1α (Maxwell *et al.*, 1999) (Table 2.6). The exhaustion of cores in TMA blocks limited the number of samples available for analysis.

Lon expression was only significantly correlated with VHL in this analysis (Table 2.6). CA9 expression positively and significantly correlated with GLUT1 (p=0.033). As both CA9 and GLUT1 are both surrogate markers of hypoxia (as both are induced by hypoxia) we would expect these two markers to be co-expressed and this association has been previously reported in breast cancer (Pinheiro *et al.*, 2011). The expression of Glut1 and CA9 only weakly (non-significantly) correlated with HIF-1α in this series.

The expression of Ki-67 has been repeatedly confirmed as a robust prognostic indicator in breast cancer in several clinical studies (Colozza *et al.*, 2005). We evaluated whether the expression of Lon correlated with levels of hypoxic markers or Lon. No significant correlation was found.

Table 2.6 Correlations between Lon and hypoxic biomarkers and Ki-67 in breast cancer. Correlations calculated using Pearson's correlation coefficient (*r*) and 2-tailed significance (*p*). N indicates number of samples available for correlation. ■ = significant positive correlation.

Pearson's correlation (r)		CA9	Glut1	Hif-1α	VHL	Ki-67
Lon	*r*	-0.059	-0.161	-0.079	**0.161**	-0.055
	p	*.632*	*.259*	*.392*	***.033***	*.648*
	N	68	51	120	**175**	71
CA9	*r*		**0.271**	0.212	0.086	0.021
	p		***.033***	*.087*	*.506*	*.811*
	N		**62**	66	62	128
Glut1	*r*			0.231	-0.099	0.164
	p			*.164*	*.493*	*.209*
	N			38	50	60
Hif-1α	*r*				0.085	0.107
	p				*.363*	*.399*
	N				116	64
VHL	*r*					0.110
	p					*.383*
	N					65

The expression of Lon in a panel of cell lines in normoxia and hypoxia

We investigated whether we could demonstrate the hypoxic induction of Lon in hypoxia, previously demonstrated only at the transcript level (Fukuda *et al.*, 2007). We incubated MCF7 (breast), HCT116 (colorectal), MG63 (osteosarcoma), A549 (lung) and U87 (glioblastoma) cells in the presence or absense of 1% hypoxia for 16 hours (Figure 2.6).

We were able to demonstrate slight Lon upregulation only in MCF7 and A549 cells (Figure 2.6). There was wide variation in Lon expression between different cell lines. MG63 had the lowest level of Lon expression, followed by A549, MCF7, U87 and HCT116 with the most. HIF-1α was stabilised in hypoxia to different extents between different cell lines, despite loading the same amount of protein

from each cell line. There was some degree of correlation between the level of Lon expression and the amount of HIF-1α stabilised in hypoxia in this limited panel of cell lines. The two cell lines with low levels of Lon (MG63 and A549) showed the least stabilisation of HIF-1α in hypoxia, compared to the three cell lines with higher levels of Lon (MCF7, HCT116 and U87). This observation raises the possibility that the amount of Lon may regulate the amount of HIF-1α stabilised in hypoxia (Chapter 3).

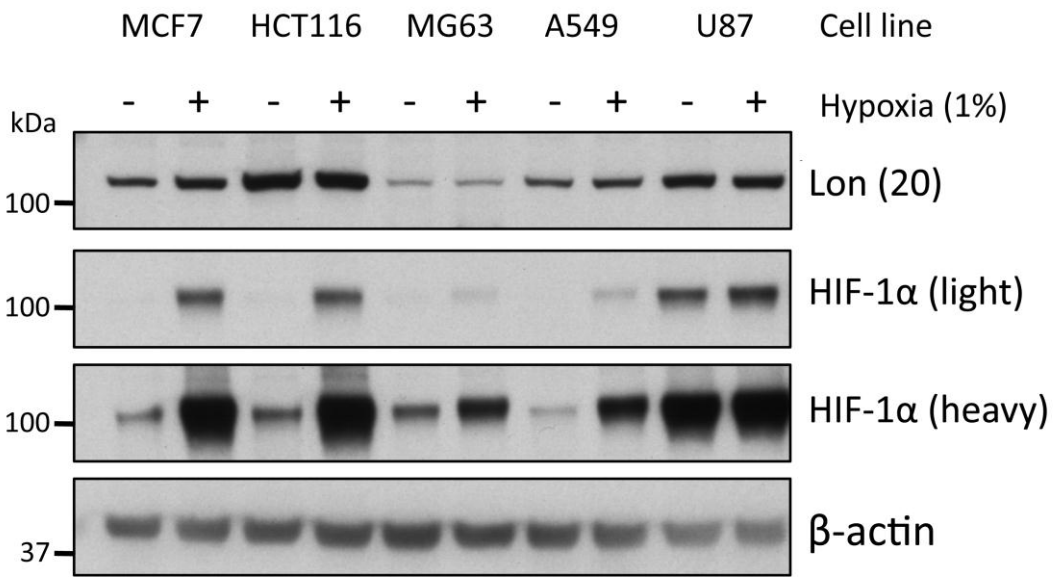

Figure 2.6 The expression of Lon and HIF-1α in normoxia and 1% hypoxia in a panel of cell lines. The cell lines indicated were incubated in 1% hypoxia for 16 hours, lysed and western blotted for the indicated proteins. Lon and HIF-1α immunoblots were on separate membranes and β actin is representative of both.

Discussion

This chapter has described the production of the first monoclonal antibody demonstrated to be specific for human Lon protease and validated for use in FFPE immunohistochemistry and western blotting. We find that Lon is

upregulated in breast and lung tumours, and that low levels of Lon may predict favourable prognosis in breast cancer (up to 10 years).

Lon expression in normal tissues

In normal tissues, Lon is ubiquitously expressed with a granular cytoplasmic positivity consistent with its mitochondrial localisation. Lon is expressed at higher levels in columnar epithelial tissues, including the epithelial lining of the gastro-intestinal tract, male and female reproductive organs and abluminal breast epithelial cells. The tubules of the kidney and the adrenal medulla also have notably high expression of Lon. These cell types have in common a very high metabolic requirement; for epithelial cells the high metabolic requirement is for active transport, renal tubular cells for resorbtion of glomerular filtrate, and for adrenal glands the active process of synthesising and secreting catecholamines. The increased metabolic requirements of these cells may necessitate higher levels of proteins involved in the stress response, specifically those able to deal with the higher levels of mitochondrial ROS that are formed as a by-product of mitochondrial metabolism.

The evaluation of oxidative stress in tissues by immunohistochemistry can be achieved by either detecting the presence of certain end-products of oxidative stress or by assaying for proteins involved in the antioxidant response. DNA damaged by ROS leads to (among many other changes) 8-hydroxydeoxyguanosine (8-OHdG) adduct formation, and the levels of this can be detected by immunohistochemistry as a surrogate marker of oxidative stress

(Yarborough *et al.*, 1996). This marker has been widely evaluated as a marker of oxidative stress, and higher levels appear to have a negative prognostic effect in ovarian carcinoma (Karihtala *et al.*, 2009), colorectal carcinoma (Sheridan *et al.*, 2009) and melanoma (Murtas *et al.*, 2010). In breast cancer, expression of 8-OHdG correlates inversely with survival – negative expression is prognostic for earlier breast-cancer specific death (Sova *et al.*, 2010).

Immunohistochemical markers of proteins involved in the oxidative stress response include the mitochondrial manganese superoxide dismutase (SOD2), which converts superoxide to hydrogen peroxide (Zelko *et al.*, 2002), and thioredoxin, which plays a critical role in redox regulation (Baker *et al.*, 1997). Increased expression of both has been observed in several human primary tumours including cervical, lung, colorectal and squamous cell carcinoma (Kinnula & Crapo, 2004) (Raffel *et al.*, 2003). Higher levels of both also predict poorer survival in patients with gastrointestinal carcinoma (Kinnula & Crapo, 2004; Raffel *et al.*, 2003). The increased expression of selected markers of oxidative stress (8-OHdG) and proteins involved in responding to oxidative stress correlate with the development of tumours and also predict adverse prognosis. In a similar way, higher levels of Lon expression may facilitate the survival and adaptation of tumour cells by neutralising proteotoxic stresses linked to oncogenesis, such as hypoxia and oxidative stress (Bernstein *et al.*, 2012).

Although a comprehensive study on the expression of the ROS surrogate marker 8-OHdG has not been reported to date, normal breast (Karihtala *et al.*, 2011) and

prostate epithelium (Oberley *et al.*, 2000) and renal tubules (Tsai *et al.*, 2011) have been shown to have high levels of expression. We detected Lon more highly expressed in all of these tissues, supporting the notion that it is expressed in normal tissues that have higher levels of oxidative stress.

Increased Lon expression in malignancy

The increased expression of Lon in breast and lung cancer may enable a tumour to cope with the increased mitochondrial proteolytic load that tumours with increased levels of oxidative stress may be expected to have. The primary site of ROS formation is from the electron transport chain, much of which is directed internally towards matrix located proteins (Brand, 2010). Lon can degrade proteins affected by oxidative damage and therefore maintain the protein-folding environment of the mitochondrial matrix (Bota & Davies, 2002). Our results are consistent with a previous report that demonstrated higher expression of Lon in malignant B cells compared to normal resting B cells (Bernstein *et al.*, 2012).

Lon expression in a series of breast cancer

Statistically significant prognostic factors that were associated with a worse overall survival in breast cancer included the established variables of age, increased tumour size and the presence of lymph node metastasis. The worse prognostic effect of patients treated with radiotherapy or hormonal therapy may be a function of these patients being more intensively treated for clinically more aggressive disease.

The higher expression of Lon showed a trend towards being prognostic for shorter overall survival in the full follow-up period. The follow-up period in this dataset is particularly long (median 10 years), and the prognostic power of biomarkers may be time-dependent in a disease that is genetically unstable, such as in cancer. When we artificially reduced the observation period, high Lon expression was associated with shorter overall survival, suggesting the prognostic impact was significant only in the first 10 years. The limitation of this analysis is the small number of patients that had low expression of Lon (16%) and the high proportion of these that had censored observations (82%). The evaluation of Lon expression in other clinical series is required to more fully establish its prognostic value.

We found that Lon expression was significantly correlated with oestrogen receptor positivity, and when stratified according to ER status, higher expression of Lon was only significantly correlated with worse overall survival in ER-positive tumours. Recently, tumour mtDNA levels (compared to normal tissue) have been shown to be significantly higher in breast ER positive tumours compared to ER negative tumours (Bai *et al.*, 2011), and oestrogen signalling can promote mitochondrial biogenesis (Mattingly *et al.*, 2008). ER positive tumours may therefore represent a group of tumours with enhanced mitochondrial activity. If this activity is associated with proteotoxic stress leading to enhanced Lon expression, the tumour may have a more aggressive phenotype contributing to a short overall survival.

Higher Lon expression correlated with HER2 positivity in this data set, as all 11 HER2 positive tumours had Lon scores of 2 or 3. The more aggressive growth of these tumours may be associated with mitochondrial proteotoxic or ER stress, but the small numbers involved preclude drawing conclusions about the role of Lon in HER2 positive breast cancer.

We were not unable to demonstrate a correlation between Lon expression and HIF-1α expression in breast cancer, nor did we find any correlation between the expression of Lon and the HIF target genes CA9 or Glut1. We did find a significant correlation between Lon and VHL levels, which may have biologic significance and is further explored in Chapter 3. The induction of Lon in hypoxia has previously been shown only at the transcript level (Fukuda *et al.*, 2007) and thus overall changes in protein content may be too small for immunohistochemistry to detect. There are also factors other than hypoxia that may influence overall levels of Lon to a greater extent (Pinti *et al.*, 2010a). We were able to detect only very modest increases in Lon expression in hypoxia in 2/5 cell lines, suggesting that the induction of Lon in hypoxia may also be cell-line dependent. The differential induction of HIF-1α in hypoxia in tumour cell lines with differing levels of Lon led us to question whether Lon itself may possibly have a role in HIF-α subunit stabilisation.

In conclusion, by creating and validating a novel monoclonal antibody against the Lon protease we have established the normal tissue expression and determined that Lon is associated with the development of tumours in the lung and breast. Within different tumours, there are widely different levels of

expression of Lon, and this raises the possibility that Lon may have a pathophysiological role in mediating certain tumour phenotypes, such as the metabolic phenotype. Higher levels of Lon may also be a poor prognostic factor in breast cancer.

Chapter 3 : Lon protease and the hypoxic response of cells

In response to the claimed links between Lon and the hypoxic-response of cells, as outlined in Chapter 1, we sought to establish a direct link experimentally. This was greatly facilitated by having produced an antibody against the Lon protease, as detailed in Chapter 2.

Outline

The Lon protease, a mitochondrial localised AAA+ protease with quality control and chaperone activities as earlier outlined, plays an important role in facilitating the aberrant stabilisation of HIF-α subunits in tumour cells. We find that reducing the levels of Lon by siRNA and shRNA reduces the level and transcriptional activity of HIF-1α and HIF-2α in tumour cell lines. Our findings are consistent with a model in which the mitochondrial unfolded protein response may modulate the hypoxic response of cells. We present evidence that Lon binds and chaperones VHL and consequently inactivates it, causing an accumulation of proline hydroxylated HIF-1α. This activity relies primarily on the chaperone activity of Lon, rather than its proteolytic activity. This mechanism of reducing HIF-α levels is unique and has not previously been recognised as a mechanism for altering hypoxic signalling. This is also the first described mechanism of mtUPR signalling in mammalian cells via an extra-mitochondrial role of Lon.

Introduction

Mitochondria of murine embryonic cells knockout for cytochrome c gene are unable to stabilise HIF-1α and HIF-2α in response to 1.5% oxygen, although wild-type and heterozygote cells do (Mansfield *et al.*, 2005). The mitochondrial respiratory chain has been proposed to influence oxygen sensing via the production of ROS at complex 3, and evidence for this includes the observation that HIF-α subunits are stabilised by exogenous treatment of cells with hydrogen peroxide (Chandel *et al.*, 2000). Recent evidence suggests that hydrogen peroxide may affect asparaginyl hydroxylation of HIF-α by FIH to a much greater extent than proline hydroxylation, and in this way selectively affect HIF transcriptional output rather than HIF-α levels (Masson *et al.*, 2012). This suggests that oxygen radicals, derived from mitochondria or elsewhere, are not the primary mechanism by which hypoxia affects the HIF hydroxylases and HIF-α stabilisation (Masson *et al.*, 2012). Together, these observations highlight the unresolved question of how mitochondria influence oxygen sensing.

The physiological mechanisms by which mitochondria influence stability of the HIF-α subunits may be exploited by tumour cells to aberrantly stabilise HIF-α subunits in normoxia, in order to gain the selective advantage that increased HIF signalling in tumours confer (Semenza, 2010a). We sought to determine the mechanisms by which tumours aberrantly stimulate angiogenesis, normally a hypoxia driven process, by comparing the gene expression profiles of angiogenic and non-angiogenic lung cancers. We selected one gene, the Lon protease, as potentially having a pathophysiologic role in orchestrating this phenotype (Hu *et al.*, 2005).

Materials and methods

Cells and cell culture

MCF7, U87-MG, A549, MG63, HCT116, MDA-MB-468 and HEK293T cells were selected from laboratory stocks, originally acquired from ATCC. RCC4 cells stably transfected with empty vector (RCC4-VHL) or pcDNA3 expressing VHL (RCC4+VHL) were created in Oxford by the Ratcliffe group (Maxwell *et al.*, 1999). Cells were cultured in Dulbecco's Modified Eagle Medium (Lonza) supplemented with 2mM L-glutamine (Lonza) and 10% foetal calf serum (South American origin, EU approved, Invitrogen). No antibiotics were used in cell culture apart from those used for cell selection. Mycoplasma testing was performed routinely (at least monthly) using the Mycoalert mycoplasma detection kit (Lonza). To facilitate passage, cells were briefly rinsed with PBS and trypsinized using 0.25% w/v trypsin-EDTA (Sigma).

siRNA

siRNA duplexes were purchased pre-annealed and lyophilised from Qiagen (pre-deigned sequences) and Eurogentec (for custom sequences). The control, non-targeted siRNA duplex used for all experiments was AllStars Negative Control siRNA from Qiagen. This proprietary sequence has been validated (by the company) by gene expression array to ensure that there are no nonspecific effects on gene expression and phenotype. For siRNA target DNA sequences and nomenclature, see Figure 3.2.

DNA transfection

Transfection of siRNA into cells was performed by using a reverse transfection protocol. To do so, siRNA duplexes were diluted in the serum-free media Optimem (Invitrogen) in a tissue culture dish and the lipid-based transfection reagent Lipofectamine RNAiMAX (Invitogen) was added. The solutions were mixed and incubated for 20 minutes. Cells prepared in a single cell suspension in full media containing no antibiotics were added to the transfection mix. A final concentration of 10nM siRNA was used for cellular assays. For a $10cm^2$ dish this required 2mls of Optimem, 25µl of Lipofectamine RNAiMAX and 1×10^6 cells in 10mls of DMEM. These amounts were scaled as required.

Plasmids

The plasmid CMV6-Entry containing the open reading frame (ORF) of Lon protease, Myc-DDK (Flag) tagged, was acquired from Origene. Plasmid pcDNA3 containing the ORF of vHL with a haemaglutinin (HA) tag was a kind gift from Norma Masson (Maxwell *et al.*, 1999). The plasmid containing eGFP (pEGFP-N1) was a kind gift from Demin Li (LLR/CRUK Haemato-oncology Group, NDCLS, Oxford) and was originally acquired from Clontech. Plasmids required for lentiviral production, psPAX2 and pMD2.G, were acquired from Addgene. Plasmids for creating VHL overexpression lentivirus were the donor vector pDONR221 and the destination vector pLenti6/V5-DEST, both from Invitrogen.

Plasmid mutagenesis

Plasmid mutagenesis was performed using the QuikChange XL kit (Stratagene). Briefly, the original plasmid was used as a template and PCR amplification was performed using primers containing the mutation required. Primers were designed using the QuikChange primer design program (https://www.genomics.agilent.com) (Table 3.1). PCR amplification was performed using a high fidelity polymerase with proofreading properties (*Pfu*Turbo DNA polymerase). The reaction was performed in a thermal cycler (MJ research) after which the template strand was digested with the enzyme *Dpn* I (specific for methylated and hemimethylated DNA). 2µl of the reaction mixture was used to transform XL-10 Gold Ultracompetent cells (Agilent technologies). Colonies were screened for the presence of the mutation by sequencing.

Table 3.1 Primers used for plasmid mutagenesis

Lon S855A	CCCAAGGACGGCCCAGCCGCAGGCTGCAC
Lon S855A antisense	GTGCAGCCTGCGGCTGGGCCGTCCTTGGG
Lon K529N	CCCCCCTGGCGTGGGTAATACCAGCATTG
Lon K529N antisense	CAATGCTGGTATTACCCACGCCAGGGGGG
Lon Δ1-59	CGCGATCGCCATGCCGGCAATTGGGG
Lon Δ1-59 antisense	CCCCAATTGCCGGCATGGCGATCGCG
VHL 1-154	TTTGCCAATATCACACTGCCACCCGGGTACCC
VHL 1-154 antisense	GGGTACCCGGGTGGCAGTGTGATATTGGCAAA

Plasmid transfection

Plasmid transfection was performed using Turbofect (Thermo Scientific). For a $10cm^2$ dish, 10µg of DNA was diluted in 1ml of Optimem and mixed. 20µl of Turbofect was added and the mixture was briefly vortexed and incubated for 15 minutes before being added to the 10mls of media in the dish. Transfected cells were incubated for three days prior to harvesting.

Lentiviral vector production

The overexpression lentiviral vectors producing VHL-HA and GFP were produced by a one-step PCR amplification reaction of the gene from pcDNA3 and pEGFP-N1 using primers that had attB1 and attB2 sequences at the 5' and 3' ends of the gene fragment respectively (Landy, 1989). The PCR product was run on a 1% agarose gel containing 0.5µg/ml ethidium bromide. The PCR product was excised under ultraviolet light and the DNA purified using the Wizard SV Gel and PCR Clean-Up System (Promega). The purified DNA was used in the BP recombination reaction with pDONR 221 and Gateway BP Clonase II enzyme mix (Invitrogen). The BP reaction was then used to transform competent *E. coli* cells (TOP10, Invitrogen) and plated onto lysogeny broth (LB) agar plates containing 50 µg/ml kanamycin. Five colonies were selected, expanded in 5mls of LB containing 25 µg/ml for 16 hours and plasmid DNA extracted using the Miniprep kit (Qiagen). DNA was sequenced to determine the correct insertion of sequence within the vector. This DNA was subsequently used to shuttle the insert into the destination lentiviral vector (pLenti6/V5-Dest) using Gateway LR Clonase II enzyme mix (Invitrogen).

A second round of transformation and selection was performed, this time using ampicillin (100 µg/ml) as the selection antibiotic and the competent cells One Shot Stbl3 (Invitrogen) (these cells are better suited to cloning unstable DNA with long terminal repeats (LTRs) as exist in lentiviral vectors). Clones were selected, expanded and DNA extracted as previously outlined. The correct insertion of the DNA was determined by restriction digest using the enzymes *Afl* II and *Xho* I (New England BioLabs). Aberrent LTR recombination was detected in some clones (these were discarded). Clones with the correct restriction digest pattern were sequenced and the DNA re-transformed into Stbl3 cells. To produce DNA for lentiviral production, cells were grown in 250 mls of LB for 16 hours and DNA extracted using the Purelink HiPure Plasmid Filter Maxiprep Kit (Invitrogen).

Lentiviral production

Lentiviral particles were produced in 293T cells by co-transfection of the pLenti6 vector containing either VHL-HA or GFP, with the packaging plasmids psPAX2 and pMD2.G. Transfection was performed using calcium phosphate as the transfection agent. 6.5 x 10^6 293T cells were plated into a T-175 flask and transfected the next day with 30µg lentiviral vector and 30µg packaging mix (440µg psPAX2 : 180µg pMD2.G). The plasmids were diluted in 192.73µl of 2M $CaCl_2$ and diluted with water up to 1.54ml. The plasmid $CaCl_2$ mixture was added dropwise to 1.54mls 2X Hepes Buffered Saline (0.28M NaCl, 0.05M HEPES, 1.5mM Na_2HPO_4, pH 7.05 with NaOH) while bubbling air through the solution.

The transfection mixture was allowed to stand for 10 minutes before adding dropwise to the cells. Media was changed the following day with 20mls fresh DMEM + 10% FCS + 10mM L-Glutamine, and virus-containing media was harvested daily for three days.

Lentiviral titring

Lentiviral supernatant was titred by p24 ELISA using the Lenti-X p24 Rapid Titer Kit (Clontech). The immunoreactivity of the lentivirus supernatant to p24 was compared to a known standard of p24 concentration (in kit) in a sandwich ELISA. Signal was produced by streptavidin-HRP induced substrate colour change and measured by the absorbance at 450nm on a plate-reading spectrophotometer. We assumed that each lentiviral particle contained 2000 molecules of p24 to determine an absolute number for lentiviral particles. We determined infectious units (IFU) based on killing with the selectable marker Blasticidin (Invitrogen) and estimated that approximately 100 lentiviral particles were required to produced one functional IFU. All transductions were performed using a multiplicity of infection of 3 (3 IFU per cells transduced). Titred stocks were frozen at -80°C in aliquots to avoid freeze-thaw degradation.

Cell lysis

Cell lysis for western blotting was performed by rinsing cells once with PBS and adding Lysis-M reagent containing Complete mini protease inhibitor cocktail tablet and PhosStop (Roche) directly to the tissue culture dish. Cells were agitated in lysis buffer for five minutes before transfer to a 1.5 ml tube, and

centrifuged for 3 minutes at 10,000 rpm. For immunoprecipitation experiments, cells were lysed in Igepal lysis buffer (10mM Tris pH 7.5, 0.25M NaCl, 0.5% v/v Igepal CA630 (Sigma) with Complete mini protease inhibitor cocktail).

Protein quantification

Protein concentration was quantified using the bicinchoninic acid (BCA) kit (Pierce). An aliquot of protein was added to the BCA reagent, incubated for 30 minutes at 37°C, and the absorbance at 562nm was quantified using the Nanodrop spectrophotometer. The absorbance of the sample was plotted onto a standard curve of known protein concentrations (of bovine serum albumin) to determine sample concentration.

Western blotting

Cell lysates were denatured by incubation at 70°C for 10 minutes in the presence of 1x LDS Sample Buffer (Invitrogen) with 2.5% β-mercaptoethanol (Sigma). Samples were loaded onto 4-12% Bis-Tris 1.5mm pre-cast gels (Life Technologies) and run at 200V for approximately 45 minutes. Separated proteins were transferred to nitrocellulose membrane by assembling a sandwich flanked either side by blotting paper and submerged in transfer buffer (wet transfer technique) (Towbin Buffer 25mM Tris, 192mM glycine, 20% v/v methanol). Transfer cassettes were assembled and placed in a Mini Trans-Blot electrophoretic transfer cell as per the manufacturer's instructions (Bio-Rad). Transfer was run at 100V for 90 minutes. Transfer efficiency was assessed by staining the membrane with Ponceau S solution (0.1% w/v in 5% acetic acid,

Sigma). Membranes were saturated with 5% w/v non-fat milk (Marvel) dissolved in PBS 0.1% Tween-20 (Sigma) for one hour. Primary antibodies were diluted in milk-PBS solution and applied overnight. Washing was performed three times (1x15 minutes, 2x5 minutes) in PBS 0.1% Tween-20. Secondary antibodies were HRP conjugated (Dako) and diluted the same way. Signal was detected using Amersham ECL reagents (GE healthcare) and film (Santa Cruz). For densitometry, film was scanned using a GS-800 calibrated densitometer (Bio-Rad). Bands were quantified using the gel analysis tool in ImageJ (http://rsbweb.nih.gov/ij/).

Antibodies

Table 3.2 Antibodies used

Antibody against	**Supplier, Clone (Catalogue Number)**	**Use (WB = western blotting), IHC (immunohistochemistry), IP (immunoprecipitation)**	**Dilution**
Lon protease	Created, 20H1 (see chapter 2)	WB, IHC	WB – 1/5, IHC – 1/2,
HIF-1α	BD, 54 (610959)	WB, IHC	WB – 1:1000, IHC – 1:100
HIF-2α	Created by lab, 190b (Talks *et al.*, 2000)	WB	WB – 1/5 (hybridoma supernatant)
VHL	CST, polyclonal (2738S)	WB	1:100
VHL	BD, Ig32 (556347)	IHC	1:500 Dako S1699
β-actin	Sigma AC-74 (A5316)	WB	1:10,000
HIF-1α-OH Pro406	Millipore polyclonal (07-1585)	WB, IHC	WB - 1:1000, IHC – 1:1000 Dako S1699
HIF-1α-OH Pro564	CST D43B5 (2738S)	WB, IHC	WB – 1:1000, IHC – 1:800 Dako S1699

Antibody against	Supplier, Clone (Catalogue Number)	Use (WB = western blotting), IHC (immunohistochemistry), IP (immunoprecipitation)	Dilution
COX-II	Santa Cruz 12C4 (sc-65239)	WB	1:500
COX-IV	Invitrogen 10G8 (A21347)	WB	1:1000
Flag	Sigma M2 (F1804)	WB, IP	WB - 1:10,000
HA	Santa Cruz, polyclonal (sc805)	WB, IP	WB - 1:1000
GFP	Abcam polyclonal (ab290)	WB	1:10,000
Tid1	CST RS-13 (4775S)	WB	1:1000
Elongin C	BD 56 (610760)	WB	1:1000

RNA extraction

Cells were lysed in Trizol reagent (Invitrogen) and RNA was precipitated using the manufacturer's instructions. Cells were lysed in a six-well plate; 1ml was used per well. Lysed cells were transferred to a 1.5ml tube and 200µl of chloroform (Sigma) was then added. The mixture was centrifuged in a refrigerated microcentrifuge at 12,000xg for 15 minutes at 4°C. The top (aqueous) phase was transferred to a clean 1.5ml tube, and 0.5ml isopropanol (Sigma) added, mixed and incubated for 10 minutes. The mixture containing RNA was centrifuged at 12,000xg for 10 minutes at 4°C, and RNA formed a pellet. The RNA pellet was washed with 1ml 75% ethanol, repelleted and then resuspended in 50µl molecular biology grade water (DEPC treated) (Sigma). RNA quantification was performed using the Nanodrop spectrophotometer.

Real time quantitative PCR

Reverse transcription of RNA to produce cDNA was performed with 1µg of extracted RNA and using the High Capacity RNA-to-cDNA kit (Applied BIosystems) according to the manufacturer's instructions. The resulting cDNA was diluted in 100µl water, and 5µl used per PCR reaction, totalling 20µl. PCR reactions were duplexed, amplifying both the control gene RLPO and the interrogated gene within the same reaction using Taqman assays with different fluorophores (Applied Biosystems) to allow for quantification independent of template pipetting errors. PCR reactions contained '1x TaqMan Universal PCR Master Mix, No Amperase UNG' (Applied Biosystems), template and a predesigned gene expression assay together with endogenous control (RLPO) assay.

Table 3.3 Taqman Gene Expression Assays used (Applied Biosystems)

Gene Symbol	NCBI Gene Reference	Assay ID	Reporter Dye
HIF1A	NM_181054.2	Hs00153153_m1	FAM
EPAS1	NM_001439.4	Hs01026149_m1	FAM
LONP1	NM_004793.2	Hs00270514_m1	FAM
VHL	NM_000551.3	Hs03046964_s1	FAM
CA9	NM_001216.2	Hs00154208_m1	FAM
SLC2A1	NM_006516.2	Hs00892681_m1	FAM
VEGFA	NM_001025366.2	Hs00900055_m1	FAM
RLPO (control)	NM_001002.3	4326314E	VIC

Reactions were run in a 96 well PCR plate and cycled on a *MJ Research Chromo4* Real Time 4-color 96-well PCR system connected to a PC running Opticon Monitor software version 3.1 (Bio-Rad). The thermal cycler was programmed to

initially heat to 95°C for 10 minutes, and then cycled at 95°C for 15s and 60°C for 1 minute, and repeated 40 times (40 cycles). Serial dilutions of template were run to obtain amplification efficiencies of duplexed reactions.

Real time analysis

Using efficiencies of target and control gene expression calculated from serial dilutions of template, relative quantification was performed using the method described by MW Pfaffl (Pfaffl, 2001). Each well was normalised for control gene expression (RLPO). Three independent biologic replicates were used to calculate a mean and standard deviation of expression compared to control.

Immunoprecipitation

Immunoprecipitation was performed using Protein G Dynabeads (Invitrogen) with a DynaMag-2 magnet (Invitrogen). 5µg of antibody was bound to the beads diluted in 200µl of Igepal lysis buffer (see cell lysis) by incubation with rotation at room temperature for 10 minutes. Beads were washed once with Igepal lysis buffer and then cell lysate was added to the beads on ice. They were incubated with lysate for 30 minutes with rotation at 4°C. Beads were washed three times with 200µl Igepal lysis buffer, and then transferred to a new tube. Elution was performed by incubating beads in 1xLDS Sample Buffer (Invitrogen) at 70°C for 10 minutes. Beads were elevated from solution between washes, and applied to the magnet to allow retrieval of eluted proteins.

Cell fractionation

Mitochondrial and cytoplasmic fractionation was performed by using the Qproteome Mitochondria Isolation Kit (Qiagen). Cells were lysed using the provided lysis buffer and centrifuged at 1000 x *g* for 10 minutes at 4°C. The supernatant was predominantly cytoplasmic proteins. The pellet was further disrupted by shearing with a 23G needle and syringe, and purified by differential centrifugation. High purity mitochondria were obtained by density-based purification and lysed in Igepal lysis buffer. Fractions were quantified for protein content (as previously outlined) and equal amounts loaded for western blot.

Spheroid production

Spheroids were produced by trypsinizing and counting cells (U87 and MCF7) and diluting to a final concentration of 25,000 cells per ml in complete media. To MCF7 cells, Matrigel (BD Biosciences) was added at a final concentration of 25µl per ml of media and placed on ice. 200µl of this mixture (5000 cells) was added to each well of an ultra-non-adherent 96-well plate (Corning) on ice and then centrifuged at 1800 rpm for 10 minutes at 4°C. Cells initially form an aggregate at the base of each well of the plate, but establish a spheroid morphology after one day in culture. U87 cells do not require matrigel, while MCF7 and MDA-MB-468 cells do require it.

Spheroid embedding

Spheroids were collected from each well of the plate by using a 200µl pipette with the tip cut off. Several spheroids were fixed in 10% formalin (John Radcliffe Hospital histopathology department) in a 50ml falcon tube overnight. The

formalin was aspirated away, leaving the spheroids in the conical base of the tube. Molten 2% w/v agarose dissolved in 10% formalin at 60°C was carefully pipetted over the spheroids and the falcon tube briefly centrifuged to ensure spheroids remained at the horozontal cut-off tip of the conical base of the tube. Agarose was then allowed to solidify by placing the tube on ice. The agarose cone containing spheroids was removed from the tube, and the tip containing the spheroids was cut off and placed within an embedding cassette. The spheroid agarose pellet was processed overnight in the same manner as tissue samples processed for histopathology (John Radcliffe Hospital). Agarose pellets containing spheroids were embedded in wax the next day, sectioned on a microtome at 4μM and the sections placed onto slides for staining or immunohistochemistry. Immunohistochemistry was performed as described in Chapter 2.

Reactive oxygen species assays

Cells were trypsinized and stained with MitoSox (Invitrogen) at a final concentration of 5μM for 10 minutes at 37°C. For DCFH-DA (Sigma) staining the concentration was 25μM with the same conditions. Cells were washed three times in PBS and staining was detected using a FACSCalibur flow cytometer (BD Biosciences) using the PE (MitoSox) and FITC (DCFH-DA) channels. Data were analysed and histograms produced using FlowJo (http://www.flowjo.com).

Proximity ligation assay

Cells and spheroids were assembled into FFPE blocks as previously described and 4μM sections were antigen retrieved, blocked and primary antibody added (as per methods Chapter 2). Two primary antibodies were applied to the sections, these were mouse anti-VHL (BD) and rabbit anti-Lon (Prestige antibodies, Sigma) both at 1:100 dilution overnight. Anti-rabbit and anti-mouse oligonucleotide-linked secondary antibodies were used (Olink biosciences). Duolink in situ detection reagents (Red) was used to produce a signal (Olink biosciences) according to manufacturers protocol. Slides were mounted and coverslipped using aqueous mounting media containing DAPI (Vector Laboratories).

Chemicals

Chloramphenicol was sourced from Sigma, MG132 from Merck Millipore and Bortezomib from Cell Signalling Technologies.

Results

The Lon protease is required for the normoxic expression of HIF-α subunits in tumour cell lines

A microarray study on lung cancers suggested that tumours with higher levels of Lon protease correlated with the non-angiogenic phenotype (Hu *et al.*, 2005). Hypoxia, acting through stabilised HIF-α, stimulates the production of angiogenic

growth factors (such as VEGF-A) and angiogenesis. To address whether there might be a causal relationship between the levels of Lon protease and stabilisation of HIF-α, we used small-interfering RNAs to transiently reduce the level of Lon protease and assayed for the quantity of stabilised HIF. In contrast to the microarray results, we observed that knocking down the Lon protease reduced the amount of HIF-1α and HIF-2α in normoxia (Figure 3.1 A). This result was confirmed using two cells lines, the breast cancer line MCF-7 and glioblastoma cell line U-87. U87 cells have both more HIF and more Lon in normoxia. Western Blots of three independent experiments were quantified by image densitometry and the reduction in HIF-α levels was statistically significant (Figure 3.1 B). The levels of VHL appeared unaltered with siRNA targeted against the Lon protease (Figure 3.1 A).

In a large-scale screening of siRNA designed to identify novel regulators of the HIF pathway, multiple 'hits' were the result of off-target gene silencing (Lin *et al.*, 2005). Although none of our siRNA sequences contained the 7 nt motif, AGGCAGT described that is present in the HIF-1α mRNA, we were acutely aware that off-target gene silencing could affect the sensitive HIF pathway. In order to establish that multiple sequences against the Lon protease were not attributed to off-target effects, we used U87 cells and seven different siRNA sequences against Lon, to assay effects on HIF-1α. We established that despite substantial depletion of the protein levels of Lon protease, there was heterogeneity in terms of the amount of HIF-1α present, using different sequences (Figure 3.2). Six out of seven sequences demonstrated reductions in the level of HIF-1α, although there were significant variations between different sequences. This result suggests

that only extremely efficient siRNA knockdown is able to affect levels of HIF-1α. Indeed, small differences in efficiency, not detectable by western blotting, can entirely abrogate the effect (as observed with siRNA duplex number 7, Figure 3.2). The differences between siRNA duplexes is possibly related to the peak efficacy. If the effect is due to the cytoplasmic levels of this Lon (a phenomenon that is described later in this chapter), which would be expected to be a small component of overall protein, then substantially reduced protein levels may not produce an effect. If small levels of cytoplasmic Lon are expressed, as may occur with resumption of Lon protein synthesis (a siRNA duplex sequence-dependent process), then no effect on HIF-1α may be seen despite the absence of Lon protease on the western blot.

Lon targeted RNAi does not significantly alter mRNA levels of HIF-1α or HIF-2α

Cells transfected with either control (siC) or Lon-targeted siRNA were analysed for HIF-1α and HIF-2α mRNA transcript levels. No significant differences in HIF-α subunits were detected, suggesting that transcriptional changes were not responsible for the lowered levels of HIF-1α and HIF-2α proteins seen with siRNA against Lon protease (Figure 3.1).

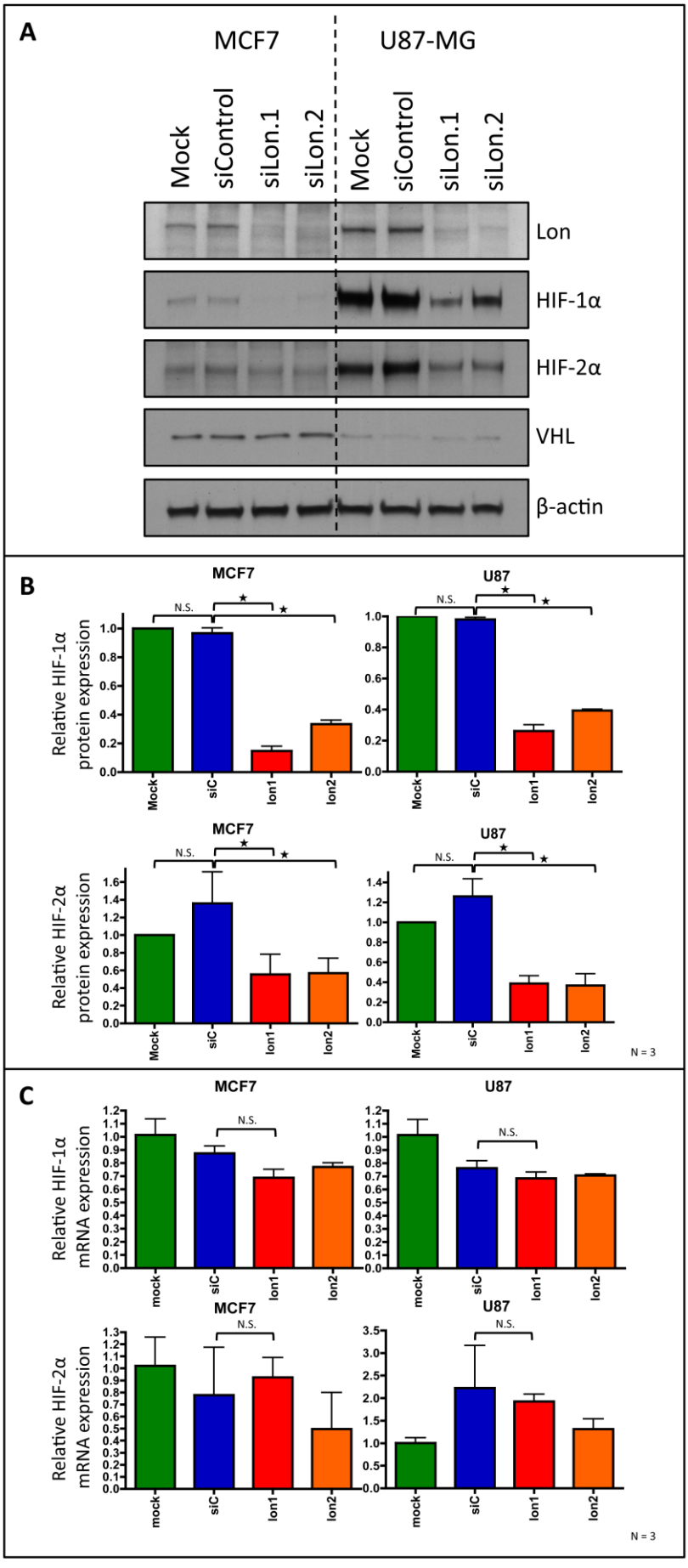
A
MCF7
U87-MG
Mock
siControl
siLon.1
siLon.2
Mock
siControl
siLon.1
siLon.2
Lon
HIF-1α
HIF-2α
VHL
β-actin
B
MCF7
U87
Relative HIF-1α protein expression
Relative HIF-2α protein expression
N.S.
Mock
siC
lon1
lon2
N = 3
C
MCF7
U87
Relative HIF-1α mRNA expression
Relative HIF-2α mRNA expression
N.S.
mock
siC
lon1
lon2
N = 3

Figure 3.1 Targeting the Lon protease with siRNA reduces the level of HIF-1α without affecting mRNA levels. MCF7 and U87 cells were transfected with either negative control (siControl) or one of two different sequences against the Lon protease (siLon.1 and siLon.2) or with transfection reagent alone (Mock). Lysates were probed by western blot with the indicated antibodies (A). Three replicated blots were quantified by densitometry and the relative expression and standard deviation represented. Protein expression is relative to β-actin (B). RNA levels of HIF-1α and HIF-2α were determined by real-time qPCR (C). Graphs represent average relative expression and standard deviation. Statistical significance determined by unpaired T-test (N.S. not significant, indicates $p < 0.05$).

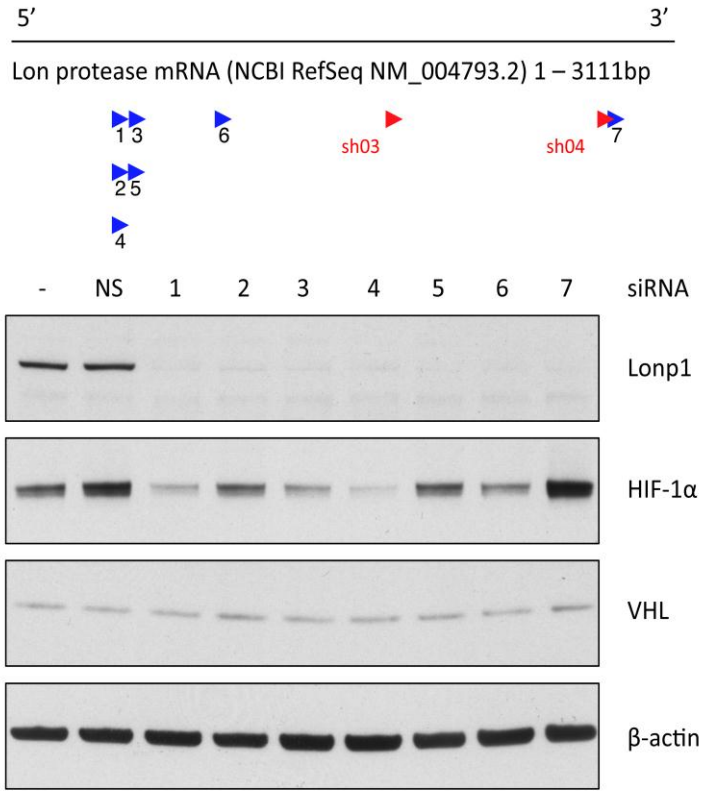

siRNA	Supplier (+catalogue No.)	Target Sequence	Named in experiments as
NS	Qiagen (1022076)	Proprietary	siControl, siC
1	Eurogentec (custom)	CGCGCTTTATCAAGATTAT	Not used
2	Eurogentec (custom)	CCGCGCTTTATCAAGATTA	Not used
3	Eurogentec (custom)	GTCGGCGTCTTTCTAAAGA	Not used
4	Qiagen (SI00068488)	CCCGCGCTTTATCAAGATTAT	siLon.1, Lon1, siLonp1, siLonp1.1
5	Qiagen (SI00068495)	CAGCCTTATCTCGGCGTCTTT	Not used
6	Qiagen (SI00068509)	CCGGGACATCATTGCCTTGAA	siLon.2, Lon2, siLonp1.2
7	Qiagen (SI03097297)	CTGGAGGTGCACTTCGTGGAA	Not used

Figure 3.2 Different siRNA sequences targeting the Lon protease have variable efficacy at reducing levels of HIF-1α in U87 cells. U87 cells were transfected with siRNA targeting the Lon protease (siRNA 1-7, supplier and sequences as in table) or a control, non-specific (NS) sequence, or with transfection reagent alone (-) (Mock). The location of the target sequence in relation to the Lonp1 transcript is illustrated above, and the target sequence in the table below. Lysates were probed for levels of Lon, HIF-1α, VHL and β-actin by western blot. The location of shRNA

sequences sh03 and sh04 illustrate location of targeted sequences used for proliferation experiments in Chapter 4.

Targeting the Lon reduces levels of HIF-1α in normoxia and hypoxia

Transfection of siRNA targeted against the Lon protease reduces levels of HIF-1α, compared to control transfected cells, in normoxia and in cells incubated in hypoxia for 16 hours (Figure 3.3C). In these conditions of hypoxia, MCF7 cells show robust increases in the levels of HIF-1α, while U87 cells show no significant increase in the levels of HIF-1α over normoxia. This phenomenon is repeatedly seen with this cell line (see Chapter 4). A slight increase in the levels of Lon is seen in cells cultured in hypoxia compared to normoxia, consistent with a previous report (Fukuda *et al.*, 2007).

The effect of reducing levels of Lon protease on a gradient hypoxia spheroid model

Using a rapid spheroid culture model to generate a gradient of hypoxia, we embedded and stained U87 spheroids to determine the contribution that Lon protease makes to HIF-1α stabilisation (Figure 3.3A). Using this technique, U87 cells can be formed into spheroids for formalin fixation and paraffin embedding three days after siRNA transfection. The distance of CA9 membranous staining from the spheroid edge (a HIF-1α inducible protein (Wykoff *et al.*, 2000)) increased three-fold from 20μM to 60μM (Figure 3.3B) in Lon protease knockdown spheroids, and the reduction in nuclear HIF-1α staining is clearly seen (Figure 3.3A). An increase in Lon staining towards the hypoxic core of the spheroid is not apparent.

Reducing levels of Lon reduces the transcriptional levels of genes dependent on hypoxic signalling in spheroids

Although embedding and staining MCF7 tumour spheroids causes a high level of disaggregation during processing producing poor sections for immunohistochemistry, these spheroids can be lysed and RNA extracted. The spheroid model recapitulates the physiologic gradient of hypoxia expected in a solid tumour and the induction of hypoxic-regulated genes occurs with a gradient of effect, unlike cells in 2-d culture placed in a hypoxic incubator. Generating spheroids of similar sizes with cells transfected with either control of Lon-targeted siRNA provides a measure of the likely transcriptional effect of targeting Lon in a solid tumour.

We find that the levels of CA9 and GLUT1 are decreased in both U87 and MCF7 tumour spheroids (Figure 3.3D), consistent with a reduction in the level of HIF-1α transcription upon which expression of these genes is dependent (Wykoff *et al.*, 2000) (Chen *et al.*, 2001). There was no significant change in HIF-1α expression in U87 and MCF7 spheroids with siRNA targeting Lon. The mRNA levels of VEGFA were significantly reduced in MCF7 spheroids, but this was not observed in U87 spheroids. Potentially, the threshold of HIF-1α suppression required for a decrease in VEGFA levels is not achieved with Lon knockdown in U87 cells as it is in MCF7 cells. Levels of VHL were unchanged.

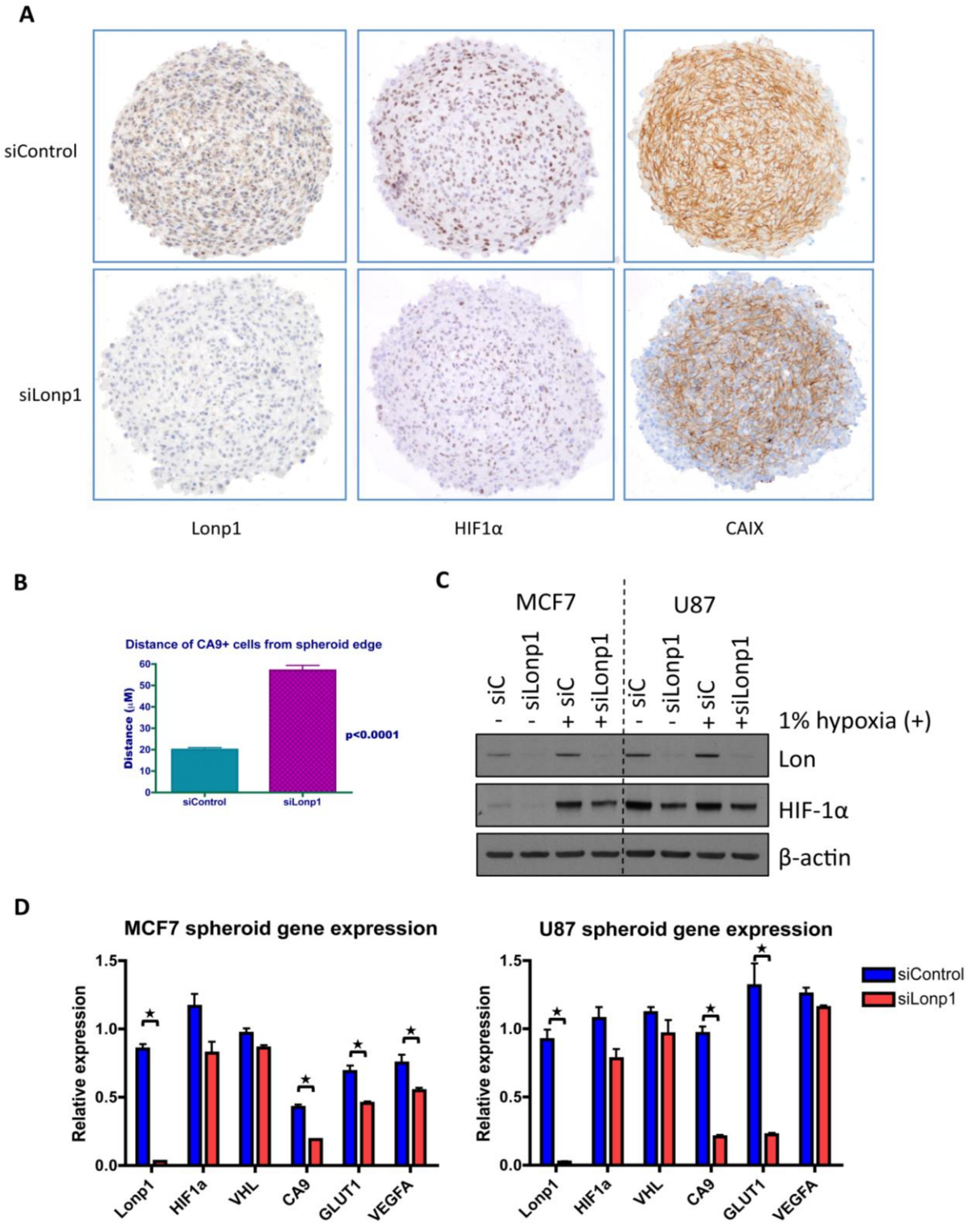

Figure 3.3. Reducing levels of Lon protease by siRNA reduces normoxic and hypoxic levels of HIF-1α and reduces HIF-1α target genes in spheroids. A. U87 cells were transfected with siRNA targeted against the Lon protease (siLonp1) or a control sequence (siControl) and spheroids were created. Spheroids were FFPE and immunohistochemistry was performed using the indicated antibodies. **B.** The distance of CAIX immunoreactivity from the edge of the spheroid was calculated from 3 biologic replicates (each of at least 9 spheroids) and represented as a bar chart. **C.** MCF7 and U87 cells were transfected with siRNA as indicated and incubated in hypoxia for 16 hours prior to lysis and lysates probed by western blot for the indicated antibodies. **D.**

RNA from MCF7 and U87 spheroids were quantified by qPCR for the genes indicated. Error bars represent standard deviation and statistical significance determined by unpaired T-test (indicates p <0.05, unlabelled not significant).

Inhibitor studies suggest that siRNA against the Lon protease mediates changes in HIF-1α stability independent of proline hydroxylase enzyme activity

To determine the mechanism by which targeting the Lon protease with siRNA reduces levels of normoxic HIF-1α, we selectively inhibited enzymes involved in HIF-1α degradation. We used the prolyl hydroxylase inhibitor dimethloxalylglcine (DMOG) to inhibit HIF-1α hydroxylation, and the proteasomal inhibitor MG132. This approach has been used to determine that SIRT3 increased the rate of HIF-1α hydroxylation (Finley *et al.*, 2011), and a similar approach was used to prove that fumarate hydratase deficiency inhibited HIF-1α hydroxylation (O'Flaherty *et al.*, 2010).

With application of 1mM DMOG for four hours to cells transfected with control or Lon-targeted siRNA, the levels of HIF-1α were normalised in MCF7 and U87 cells (Figure 3.4A). The normalisation of HIF-1α levels with inhibition of HIF hydroxylation suggests that the levels of transcription and translation are similar, and confirm the previous mRNA results previously described. This result suggests that the levels of HIF-1α are largely modulated by degradation of HIF-1α.

With application of MG-132, levels of HIF-1α are largely normalised in U87 cells, but, strikingly, are still reduced in MCF7 with siRNA against Lon (Figure 3.4A). This result has a number of possible interpretations. siRNA directed against Lon may promote the non-proteasomal degradation of HIF-1α. Non-proteasomal

degradation of HIF-1α has been suggested as a component of altering HIF-1α levels with treatment of cells with methylglyoxal, a byproduct of glycolysis produced in conditions of high glucose (Bento *et al.*, 2010). Methylglycoxal reduces levels of HIF-1α by recruiting Carboxyl terminus of Hsc70-interacting protein (CHIP) as the E3 ubiquitin ligase, an effect independent of proline-hydroxylation and VHL (Bento *et al.*, 2010). Lon is unlikely to affect CHIP recruitment to HIF-1α, as the levels of HIF-1α are largely normalised with inhibition of hydroxylation (DMOG).

The disparity in the levels of HIF-1α in MCF7 cells treated with MG132 can be explained by an alternative mechanism. Cells are transfected three days with siRNA three days prior to the application of drug, which is then applied for four hours. At the beginning of drug treatment, ***if*** **HIF-1α that is present in normoxia is proline-hydroxylated**, then on application of DMOG for four hours the hydroxylated HIF would largely be degraded (as DMOG does not prevent degradation of hydroxylated HIF), and the amount of HIF that accumulates in this time would be newly translated (no differences in DMOG treated cells indicate no differences in rate of translation in HIF-1α). However, on application of MG132, in cells treated with siRNA against Lon, the amount of HIF-1α is already lower than in control siRNA-treated cells (as per Figure 2.1). Over the period of four hours (with MG132), control siRNA treated cells accumulate newly translated HIF-1α on top of the previous normoxic level of HIF-1α. Cells treated with siRNA against Lon, however, had much less HIF-1α on starting treatment with MG132, and by the end of the four hours still had less. The differences were more apparent in MCF7 cells than in U87 cells, owing to U87 cells having much

higher rates of HIF-1α translation consequent to having a mutation in PTEN (Pore *et al.*, 2006).

On application of MG132 to both cell lines, with or without Lon, the accumulation of HIF-1α was accompanied by an increase in proline-hydroxylated HIF-1α (Figure 3.4A). The ratio of proline-hydroxylated HIF-1α to total HIF-1α was the same whether the cells were treated with control or Lon-targeted siRNA. This suggests that siRNA targeted against the Lon protease does not alter the activity of the proline-hydroxylase enzymes. This is the first described mitochondrial protein to affect HIF-1α levels independent of PHD activity.

Lon-targeted siRNA does not affect levels of reactive oxygen species

Mitochondria have been proposed to alter the hypoxic response of cells via generating reactive oxygen species (ROS) from the respiratory chain which inhibit the activity of the PHD enzymes (Kaelin & Ratcliffe, 2008). To determine whether reducing levels of Lon may modulate ROS levels, we assayed ROS using the two intracellular fluorescent reporters 2',7'-dichlorfluorescein-diacetate (DCFH-DA) and MitoSOX red.

We were unable to detect any significant changes in ROS in control transfection or Lon siRNA transfected cells (Figure 3.4B). This is consistent with Lon knockdown affecting HIF-α subunit stability via a mechanism independent of PHD activity.

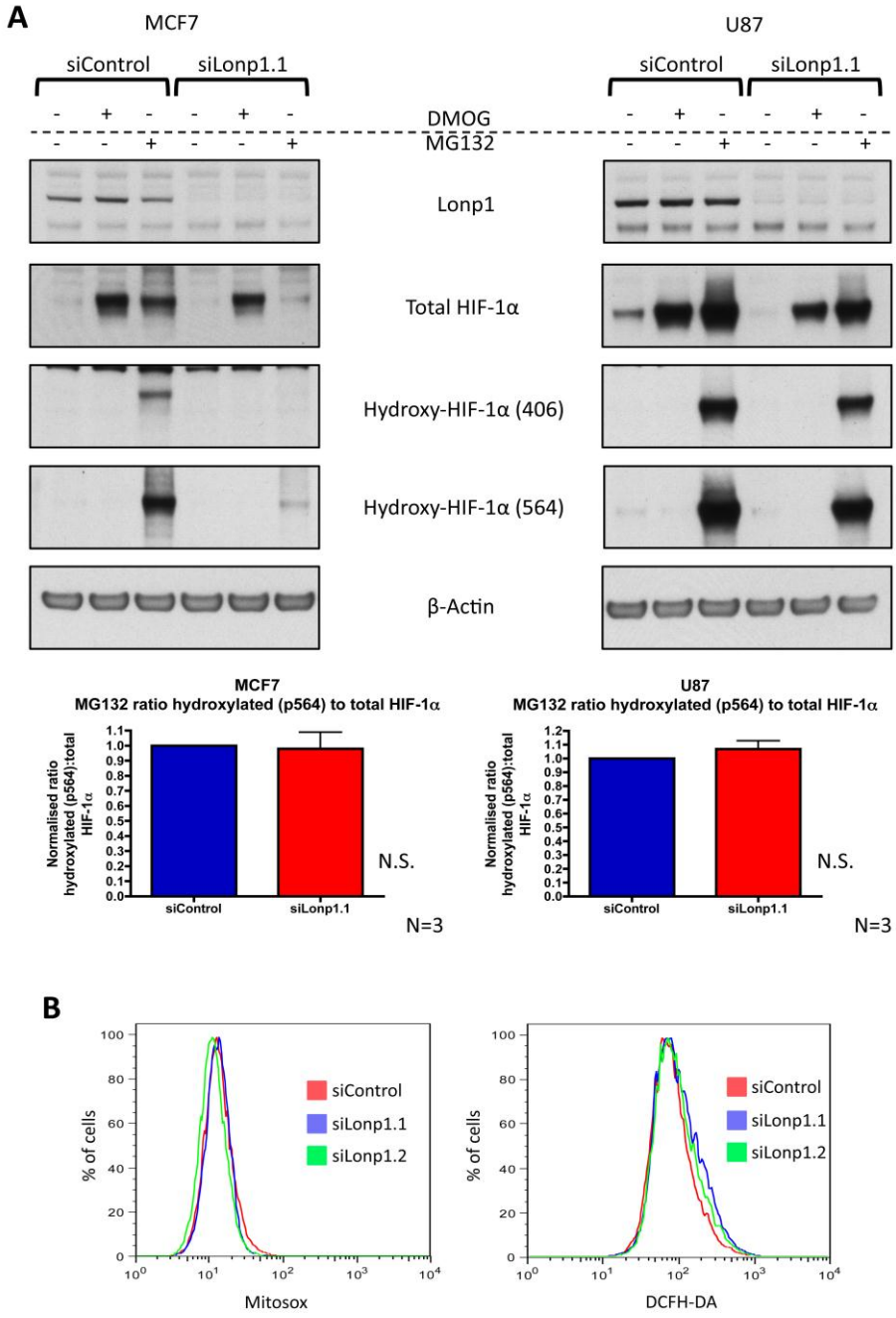

Figure 3.4 Reducing levels of the Lon protease by siRNA reduces HIF-1α stability independent of HIF-proline hydroxylase enzyme activity. MCF7 cells and U87 cells were transfected with siRNA targeting the Lon protease (siLonp1.1) or a control sequence (siControl) and treated for 4 hours with DMOG (1mM) or MG132 (10μM). Western blot was performed on the lysates and probed for the proteins indicated. The lower graphs represent the ratio (of 3 biologic replicates) between HIF-1α proline hydroxylated at Pro564 and total HIF-1α (a surrogate measure of HIF-PHD activity). Error bars indicate standard deviations and significance determined by unpaired T test (N.S. = not significant) (A). Representative histogram of assay for

reactive oxygen species using the dye MitoSox (left) and DCFH-DA (right). Cells were transfected with siRNA as indicated (B).

Targeting the Lon protease reduces the normoxic expression of proline-hydroxylated HIF-1α

Having determined that targeting Lon reduced HIF-1α levels independent of proline-hydroxylation, we attempted to see if reduced levels of proline-hydroxylated HIF-1α occurred with siRNA targeting Lon (Figure 3.5). We found that reducing levels of Lon reduced the levels of proline-hydroxylated HIF-1α in normoxia at both hydroxylation sites (Pro402 and Pro564) in U87 cells. In MCF7 cells, reduced levels of proline hydroxylated HIF-1α at Pro564 were seen, although we had difficulty detecting any proline-hydroxylated HIF-1α at Pro402 in this cell line. The HIF-1α Pro402 hydroxylation-specific antibody may not be sensitive enough by western blotting to detect this change. These findings are consistent with Lon affecting stability of proline-hydroxylated HIF-1α.

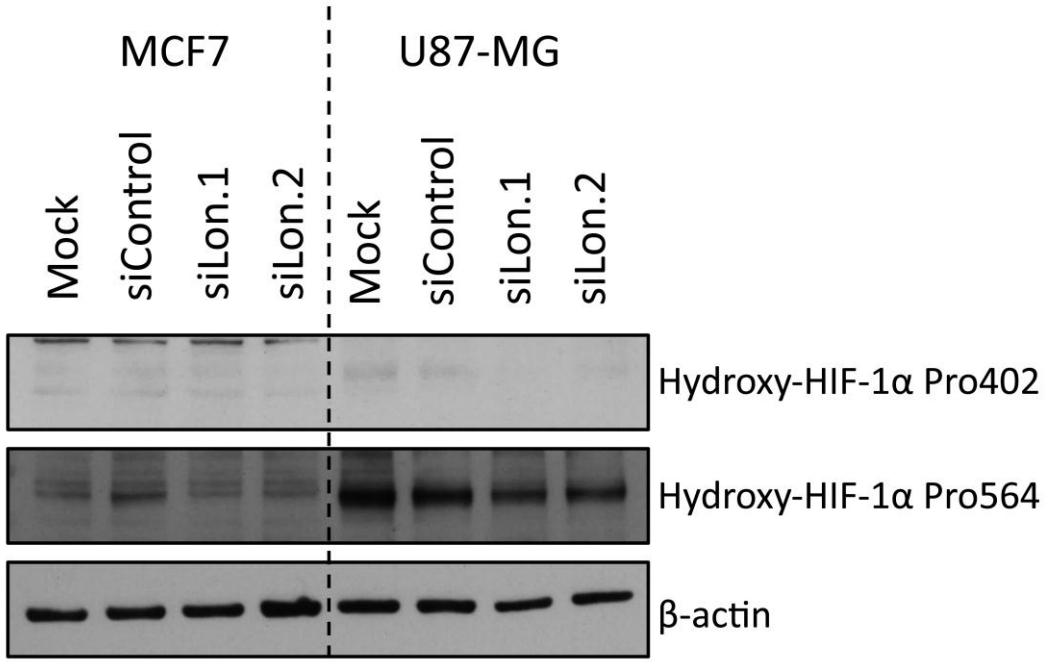

Figure 3.5 Targeting the Lon protease with siRNA reduces the expression of proline-hydroxylated HIF-1α in normoxia. MCF7 and U87 cells were transfected with the indicated siRNA duplexes. Cell lysates were probed by western blot with the indicated antibodies.

Targeting the Lon protease with siRNA reduces stabilised HIF-1α independent of changes in mitochondrial transcription

Recently, the mitochondrial transcription factor TFAM has been shown to be degraded by the Lon protease (Bernstein *et al.*, 2012) (Matsushima *et al.*, 2010). TFAM is phosphorylated by protein kinase A, rendering it unable to bind mtDNA and promotes proteolysis by Lon (Lu *et al.*, 2012). Reducing levels of Lon in the context of mtDNA deficits can cause increased mitochondrial transcription (Lu *et al.*, 2012). To determine whether increases in mitochondrial transcription elicited changes in the stability of HIF-1α secondary to Lon-targeted siRNA, we concurrently treated cells with the mitochondrial translational inhibitor chloramphenicol (Karbowski *et al.*, 1999). The effect of chloramphenicol was determined by blotting for the mitochondrial-encoded protein cytochrome c oxidase subunit II (COX2), one protein of the 13 protein complex of cytochrome c oxidase (complex IV) (Mick *et al.*, 2011). The levels of the nuclear encoded component COX4 (non-isoform specific) of the same complex were assessed to ensure the nuclear-encoded component was unaffected.

Chloramphenicol causes robust depletion of mitochondrial-encoded COX2 without affecting the levels of COX4 (Figure 3-5A). The decrease in levels of HIF-1α seen with siRNA targeted against Lon is present with treatment of chloramphenicol or vehicle (DMSO) alone. This suggests that the decrease in HIF-1α stabilisation is independent of increases in mitochondrial transcription.

Reducing levels of the Lon protease is associated with increased levels of COX2 as well as COX4 (most prominent in U87 cells, Figure 3-5A). This suggests there

may be increased synthesis of both nuclear and mitochondrial components of the respiratory chain in response to reduced levels of Lon. This may be consequent to reduced levels of HIF signalling, as reintroduction of VHL into VHL-deficient renal cell carcinoma cell lines causes increased levels of both of these proteins (Hervouet *et al.*, 2005). Alternatively, depleting Lon may cause an increase in TFAM levels and mediate an increase in mitochondrial transcription (Lu *et al.*, 2012).

Selective inhibition of mitochondrial translation with chloramphenicol appears to have a modest effect in reducing normoxic HIF-1α levels in U87 and MCF7 cells (Figure 3-5A). Chloramphenicol has been reported to increase ROS by decreasing the ratio of mitochondrial complex IV to cytochrome c (Ramachandran *et al.*, 2002). Alternatively, chloramphenicol treatment may inhibit the electron transport chain and reduce ROS and oxygen consumption, reducing possible HIF PHD inhibition (Kaelin & Ratcliffe, 2008). There are no reports on the effect on HIF-1α stabilisation with chloramphenicol treatment. The reduction in HIF-1α levels by depleting Lon is far more potent than with chloramphenicol treatment, suggesting that the mechanism of Lon mediated HIF-α stabilisation is independent of mitochondrial translation.

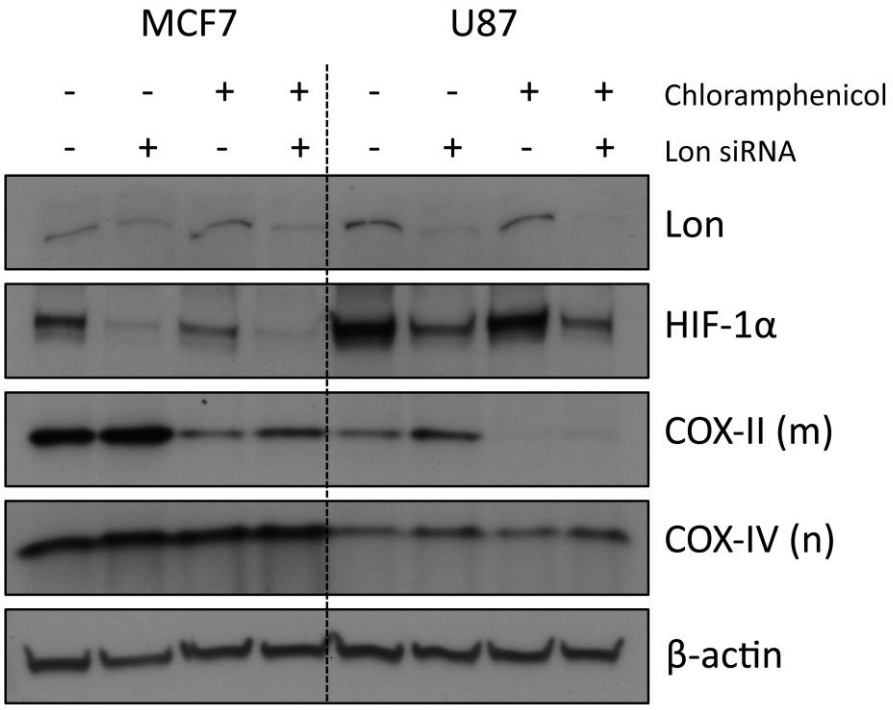

Figure 3.6 Targeting the Lon protease by siRNA reduces the levelof HIF-1α independent of any increases in mitochondrial transcription. MCF7 and U87 cells were transfected with either non-targeting control (-) or Lon-targeting siRNA in the presence of chloramphenicol (50μM) or vehicle (DMSO) alone. Drug was replaced each day for 3 days. Western blot performed for the indicated proteins. Representative of three similar experiments.

Targeting the Lon protease by siRNA in a renal cell carcinoma cell line does not alter HIF-1α stabilisation

To determine whether targeting the Lon protease by siRNA reduced HIF-1α stabilisation by modulating the activity of the VHL complex, we transfected RCC4 cells that have an inactivating mutation in VHL (RCC4-VHL) and high normoxic levels of HIF-1α. We compared this to RCC4 cells in which the VHL had been stably reintroduced by transfection (RCC4+VHL) (Figure 3.7).

We found that targeting the Lon protease by siRNA in RCC4 cells did not cause any change in the levels of HIF-1α whether they had mutant or wild-type reintroduced VHL (Figure 3.7). Although this is indicative that Lon's effect on HIF-1α may be dependent on VHL, we cannot exclude the possibility that the efficacy of Lon knockdown was not sufficient to elicit a change in HIF-1α levels, as we saw no change in HIF-1α levels in RCC4+VHL cells.

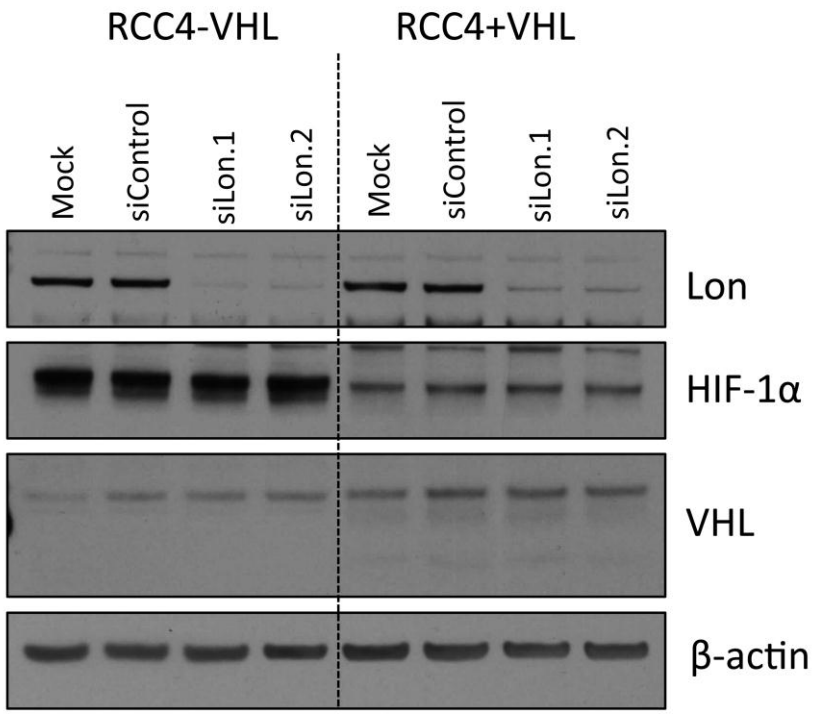

Figure 3.7 Transfection of siRNA targeted against the Lon protease does not reduce the levels of HIF-1α in RCC4 cells with or without functional VHL. RCC4 cells were stably transfected with pcDNA3 containing VHL (RCC4+VHL) or empty vector (RCC4-VHL). Cells were transfected with control siRNA (siControl), Lon targeted siRNA (siLon.1 and siLon.2) or transfection reagent alone (Mock). Western blot was performed and probed with antibodies against the proteins indicated. Results representative of three independent experiements.

Co-transfection of Lon and VHL in 293T cells causes reduced stability of exogenous VHL

At this point we had determined that the likely mechanism of reduced HIF-α subunit expression with transfection of Lon-targeted siRNA was by altering the rate of post-hydroxylation degradation. We therefore sought to determine whether there was any direct interaction between Lon and VHL. In Chapter 2 we had determined there was a significant correlation between levels of Lon and VHL in breast cancer. Despite this, we had previously observed that VHL levels were unchanged in cell lines with transfection of siRNA against Lon (Figures 3.1, 3.2, 3.3 and 3.7). A previous report had suggested that VHL may be mitochondrial when overexpressed in 293T cells (Shiao *et al.*, 2000), providing further evidence that VHL may interact in some way with mitochondria.

Initial attempts at co-expressing VHL and Lon using CMV-promoter driven tagged expression constructs failed, leading us to the conclusion that expression of VHL was impaired with co-expression of Lon (pilot experimental results not shown). We speculated that the proteolytic activity of Lon was responsible for impaired VHL stability and therefore generated a catalytic inactive Lon with the serine in the active site mutated to an alanine (s855a), as previously described (Liu *et al.*, 2004).

Co-transfection of Lon and the catalytic inactive mutant Lon s855a with either VHL or GFP was performed in 293T cells (Figure 3.8). The co-transfection of Lon or the catalytic inactive mutant resulted in no change in the level of GFP protein expressed, suggesting that there was no overall transcriptional or translational

changes as a result of Lon overexpression. The flag-tagged Lon s855a resulted in a wider band than the overexpressed catalytic active Lon. This could be the result of either higher quantities of Lon s855a protein than active Lon protein, or the result of impaired post-translational processing of the catalytic inactive Lon. Impaired processing could be the result of failure to efficiently import the Lon s855a into mitochondria (Wagner *et al.*, 1994) and this would prevent the mitochondrial targeting sequence from being cleaved by the matrix processing peptidase (MPP) (Becker *et al.*, 2012). This would lead to the presence of Lon occurring over a wider range of molecular weights, giving the appearance of a wider Lon band on the western blot. Alternatively, active Lon may cause the degradation of unassembled Lon subunits, in its role in protein quality control.

The co-transfection of Lon with VHL led to low levels of VHL compared to the transfection with the Lon s855a (Figure 3.8). When the ratio of active to inactive Lon was titred in sixths (as human Lon exists as a hexamer), the expression of VHL remained low until at 5 out of 6 subunits transfected were inactive subunits. The amount of VHL seen with co-transfection of 5/6 Lon catalytic inactive subunits (s855a) was still substantially lower than the level of VHL seen when transfected with just s855a inactive subunits. This suggests that the activity of Lon (with respect to the stability of VHL) requires significant suppression of proteolytic activity, and possibly the complex remains active with a substantial proportion of inactive subunits.

Interestingly, the width of the Lon band is not proportional to the amount of catalytic inactive or active Lon transfected into cells (Figure 3.8). The Lon band

(detected with an anti-flag antibody) is only wider when all six subunits transfected into cells are inactive, and this particular phenotype is rescued when just 1 out of 6 subunits transfected are catalytic active Lon. The co-expression of VHL correlates with the width of the Lon band, suggesting that impaired post-translational modification of Lon is associated with VHL stability in this model.

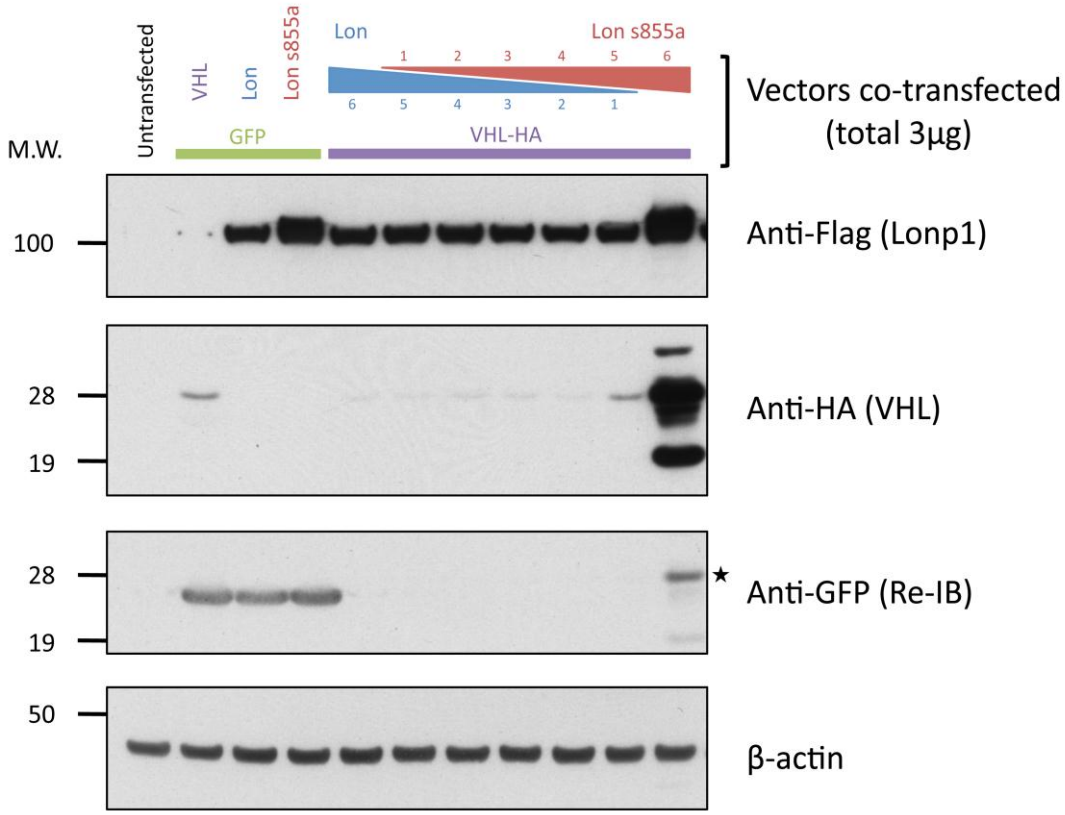

Figure 3.8 Co-transfection of Lon and VHL-HA causes lack of expression of VHL-HA in 293T cells and is reversed by co-transfection with a catalytically inactive Lon. 293T cells were co-transfected with 2 plasmids containing CMV-driven expression of the indicated proteins. Cells were lysed and assayed by western blot for the indicated proteins. Anti-GFP blot is re-immunoblotted (Re-IB) from the anti-HA blot above, so there is still residual visibility of anti-HA banding pattern seen (). Results representative of three similar experiments.

Reduced stability of VHL with Lon transfection is reversible with proteasomal inhibition

To demonstrate that the reduced levels of VHL when co-transfected with Lon were as a result of VHL degradation rather than reduced synthesis, we co-

transfected Lon and VHL and treated the cells with the proteasomal inhibitors MG132 and bortezomib (Figure 3.9). MG132 treatment did not increase levels of VHL, but bortezomib did, suggesting that VHL was proteolytically degraded when co-transfected with catalytically active Lon. The fact that MG132 did not increase levels of Lon raises the possibility that the degradation of VHL was mediated by a protease other than the proteasome. This could be mediated by the Lon protease, with which the VHL was co-transfected. Recently, Lon has been found to be inhibited by bortezomib and the related compound MG262, raising the possibility that Lon may degrade exogenously transfected VHL (Lu *et al.*, 2012).

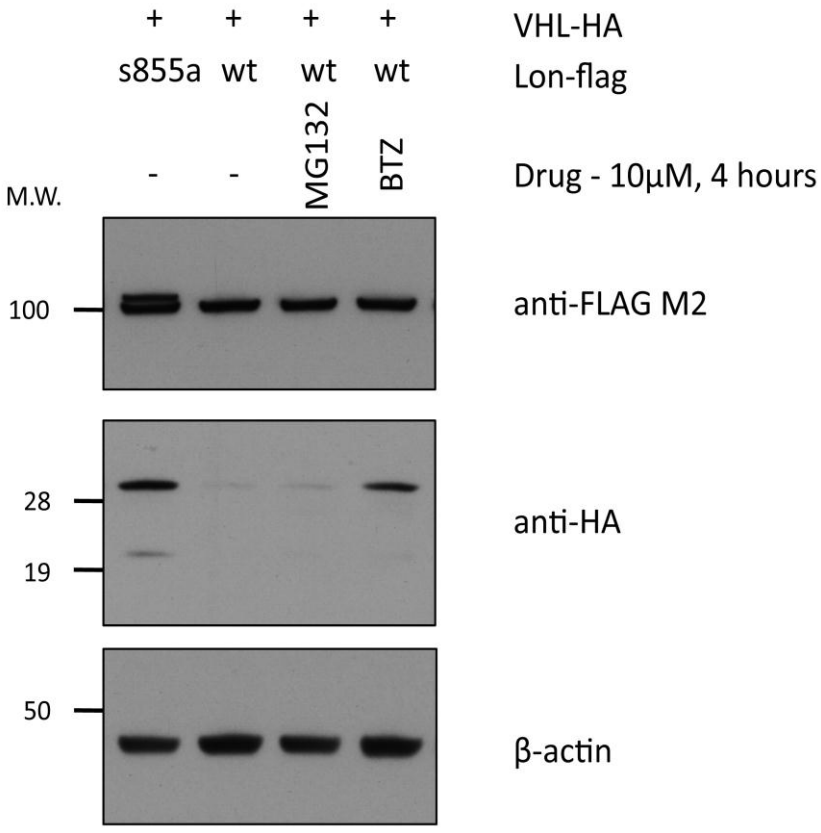

Figure 3.9 Reduced stability of VHL-HA with co-transfection of Lon is reversible with treatment with the proteasomal inhibitor bortezomib (BTZ). 293T cells were co-transfected with VHL-HA and either catalytic inactive Lon (s855a) or catalytically active Lon (wt) and treated

with 10μM of the proteasomal inhibitors MG132, bortezomib (BTZ) or vehicle (DMSO) alone for 4 hours. Cell lysates were assayed for levels of the indicated proteins by western blot.

The catalytic inactive Lon mutant (s855a) co-immunoprecipiates with exogenously transfected VHL

Initial attempts at co-immunoprecipitating Lon and VHL were unsuccessful with lysis buffer containing EDTA, however the switch to non-EDTA containing lysis buffer allowed for the following observations to be made. In 293T cells co-transfected with Lon catalytic inactive mutant (s855a) and VHL, both were able to be co-immunoprecipiated with pull-down of either tag (Flag or HA) (Figure 3.10). With anti-flag (Lon) immunoprecipiation, both long and short isoforms of VHL are seen (the short isoform arises from an internal translation initiation site (Iliopoulos *et al.*, 1998)). This suggests that the Lon s855a and VHL interaction is not dependent on the first 53 amino acids. A higher molecular weight band may be the result of post-translational modification of VHL. Sumolyation and ubiquitination of VHL has been shown to occur on lysine residues within the beta domain of VHL on lysines 171 and 196 (Cai & Robertson, 2010), and NEDDylation at lysine 159 (Stickle *et al.*, 2004). However, we still see a band corresponding to the same increase in molecular weight with a VHL-HA truncated at 154 creating an alpha-domain only VHL. This modification remains uncharacterised, but does not affect the ability of Lon s855a to immunoprecipitate VHL as it also pulls down with anti-flag.

Significantly, the catalytic active (WT) Lon did not co-immunoprecipiate with VHL, although the quantities of VHL immunoprecipiated were much less (due to a lower abundance of the protein) (Figure 3.10). There was no cross-reactivity of

antibodies and protein-tags, as Lon-flag was not immunoprecipitated with anti-HA antibody, and VHL-HA was not immunoprecipiated with anti-flag antibody. We were unable to co-immunoprecipitate endogenous Lon with VHL-HA transfected alone.

The ability to co-immunoprecipitate Lon catalytic inactive mutant (s855a) and exogenous VHL gives weight to the idea that these two proteins may interact physiologically, but the fact that this interaction cannot be detected with the catalytically active Lon is puzzling. Certainly, catalytically inactive Lon is not a protein that exists physiologically and it is possible that this interaction is due to the s855a mutation creating a novel VHL interacting site. Since these two proteins are widely reported to be sequestered in different cellular compartments (Lon in mitochondria (Wang *et al.*, 1993), and VHL in nucleus and cytoplasm (Duan *et al.*, 1995)), we could not be sure whether this interaction was actively formed in cells, or after cell lysis.

The catalytic inactive Lon mutant (s855a) coimmunoprecipiates with a truncated VHL, unable to assemble into VBC complex

VHL assembles into a complex containing elongins B and C, Cullin-2 and Rbx-1 to form a ubiquitin protein isopeptide ligase (E3) complex (Lewis & Roberts, 2004). The VHL protein acts as the substrate recognition component, and assembly into an E3 complex requires the alpha domain, specifically the "BC box" comprising amino acids 157-172 (Feldman *et al.*, 1999). To determine whether the interaction between the Lon catalytic inactive mutant and VHL was mediated

through one of the interacting proteins of the E3 complex we co-transfected Lon s855a and a VHL construct containing only the acidic and beta domain, truncated at amino acid 154 (labelled as '154' in Figure 3.10). Lon s855a could still co-immunoprecipitate with the truncated VHL-HA (154), suggesting the interaction with Lon was not dependent on assembly into a functional E3 complex. Since we have also shown that the interaction is not dependent on the first 53 amino acids, we have narrowed the region of interaction to within amino acids 54-154 of VHL (the beta domain). The beta domain of VHL is required for binding to the chaperonin TRiC (Feldman *et al.*, 1999) and for recognition of substrates, such as HIF-1α (Min *et al.*, 2002).

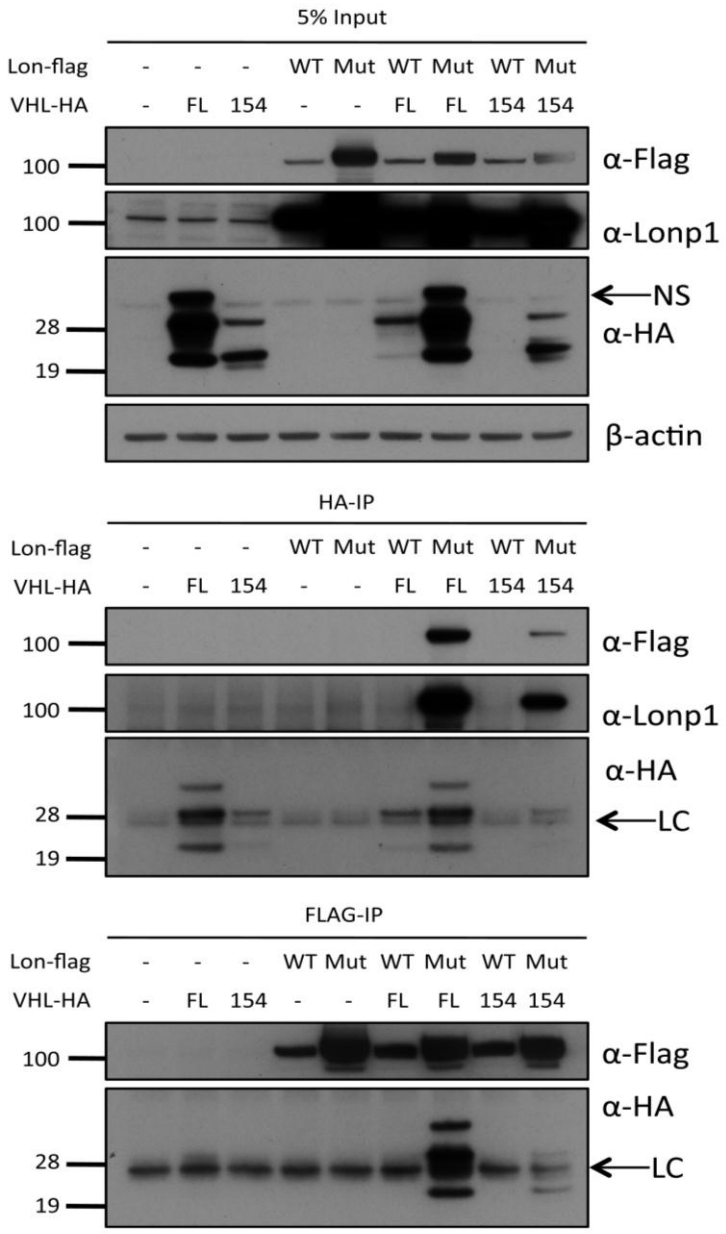

Figure 3.10 The catalytic inactive Lon mutant s855a (Mut) co-immunoprecipitates with VHL-HA (FL) and the acidic/β-domain only VHL construct truncated at amino acid 154 (154). 293T cells were cotransfected with either Lon (WT) or catalytic inactive Lon (Mut) and the full length VHL (FL) tagged with HA, or the acidic/β-domain only VHL construct (also HA tagged)(154). Input lysates are western blotted (top) with the indicated antibodies. NS denotes non-specific band. Lysates were immunoprecipitated against HA (middle) and Flag (bottom) and western blotted for the proteins indicated. LC denotes antibody light chain.

The physical association between catalytically inactive Lon (s855a) and VHL-HA occurs within cells, prior to cell lysis

To determine that the interaction we saw between the catalytic inactive Lon and VHL occurred in cells prior to lysis, we separately transfected plasmids of each into 293T cells and then mixed the cell lysates (Figure 3.11). Plasmids transfected at the same time for Lon s855a and VHL acted as the positive control. When immunoprecipitated using anti-HA antibody, Lon s855a could be pulled-down with VHL only if the two plasmids were co-transfected into cells and not in separately transfected lysates, which were subsequently mixed. This proves that this interaction occurs in cells and consequently the two proteins must exist in the same cellular compartment.

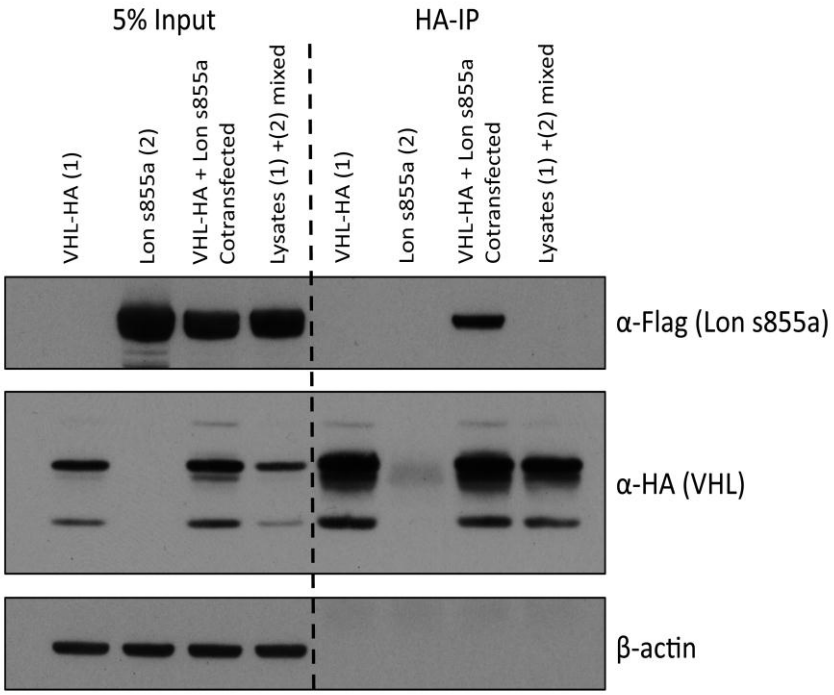

Figure 3.11 The interaction between Lon s855a and VHL-HA occurs in cells, prior to lysis. 293T cells were transfected individually with VHL-HA (1) and Lon s855a (2). In lane 3 293T cells were cotransfected with VHL-HA and Lon s855a. In lane 4 the individual lysates (1) and (2) were mixed. Each of these was immunoprecipitated against HA (right). Lysates and immunoprecipitates were western blotted and probed for the indicated proteins. Representative of three similar experiments.

Exogenously transfected VHL and catalytic inactive Lon s855a are present in cytoplasm and mitochondria, whereas catalytically active Lon is predominantly mitochondrial

To determine the potential sites of localisation of transfected VHL and Lon, we transfected plasmids into cells and performed cytoplasmic and mitochondrial fractionation (Figure 3.12). Endogenous Lon protease was present in the mitochondrial fraction and co-purified with the known mitochondrial protein Tid1 (Lu *et al.*, 2006). The endogenous VHL of 293T cells was not reliably seen after fractionation. Overexpressed VHL-HA was seen in cytoplasmic and mitochondrial compartments and the mitochondrial compartment enriched for the shorter (p19) isoform of VHL. Exogenously transfected VHL (untagged and GFP-N-terminally tagged) has been shown to localise to mitochondria (Shiao *et al.*, 2000), although this is the first demonstration of an enrichment for the p19 isoform. The functional difference between various VHL isoforms is unknown, although only the shorter isoform is conserved in mice.

Co-overexpression of VHL and Lon in 293T cells leads to a lack of VHL detectable in both mitochondrial and cytoplasmic compartments (Figure 3.12). The wild-type overexpressed Lon localises exclusively in the mitochondrial compartment. The co-expression of Lon catalytically inactive mutant (s855a) and VHL leads to the accumulation of VHL in both cytoplasm and mitchondria, also showing an enrichment of the p19 isoform in the mitochondria. The s855a Lon is present in the cytoplasm with a higher molecular weight than the wild-type mitochondrial

band, suggesting the cytoplasmic component is unprocessed Lon with an intact MTS (as occurs with catalytically inactive PIM1 in *S.cerevisiae* (Wagner *et al.*, 1997)).

The presence of an unprocessed component of Lon in the cytoplasm with transfection of the catalytic inactive mutant suggests that the 'thicker' band seen in previous western blots (Figures 3.8, 3.9 and 3.10) may be the result of cytoplasmic retention of Lon. The observation that Lon and VHL (when overexpressed) co-immunoprecipitate when Lon is catalytically inactive and not active raises the possibility that this interaction is occurring in the cytoplasm (as catalytically active Lon is exclusively mitochondrial).

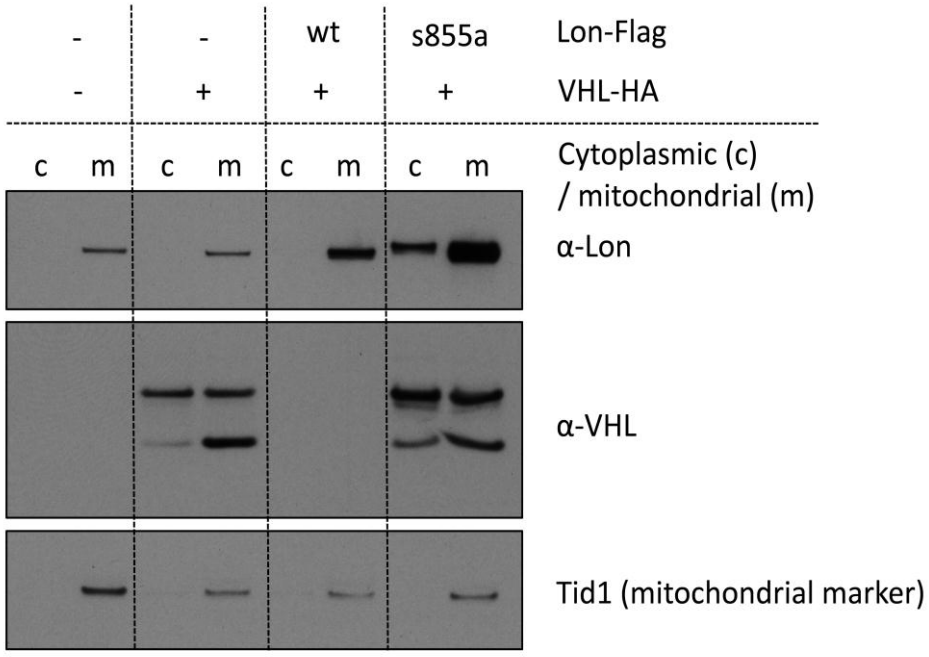

Figure 3.12 The Lon catalytic inactive mutant s855a exhibits impaired mitochondrial import, and exogenously transfected VHL accumulates in mitochondrial. 293T cells were transfected with Lon (wt), catalytic inactive Lon (s855a) with VHL-HA and cells were fractionated into cytoplasmic and mitochondrial fractions. Fractions were quantified and equal amounts of protein from each fraction western blotted and probed for the indicated proteins.

The interaction between Lon catalytic inactive mutant (s855a) and VHL occurs only with the unprocessed form

To determine the location of the interaction between Lon s855a and VHL-HA, we co-transfected cells with both of these vectors and performed mitochondrial and cytoplasmic fractionation prior to immunoprecipitation of VHL-HA (Figure 3.13). We found that only the heavy (pre-cleaved), unprocessed form of Lon s855a co-immunoprecipitated with VHL-HA in both the cytoplasmic and mitochondrial fractions.

This result may explain why exogenously transfected Lon (wt) is not co-immunoprecipitated with VHL-HA. The catalytically active Lon is efficiently imported and processed into mitochondria, not allowing for the interaction to be seen. This raises the issue as to whether the interaction between Lon and VHL is simply a consequence of impaired mitochondrial import and processing, and whether this occurs physiologically. However, we have presented (earlier) strong evidence to suggest that siRNA targeting Lon promotes VHL activity in MCF7 and U87 cells.

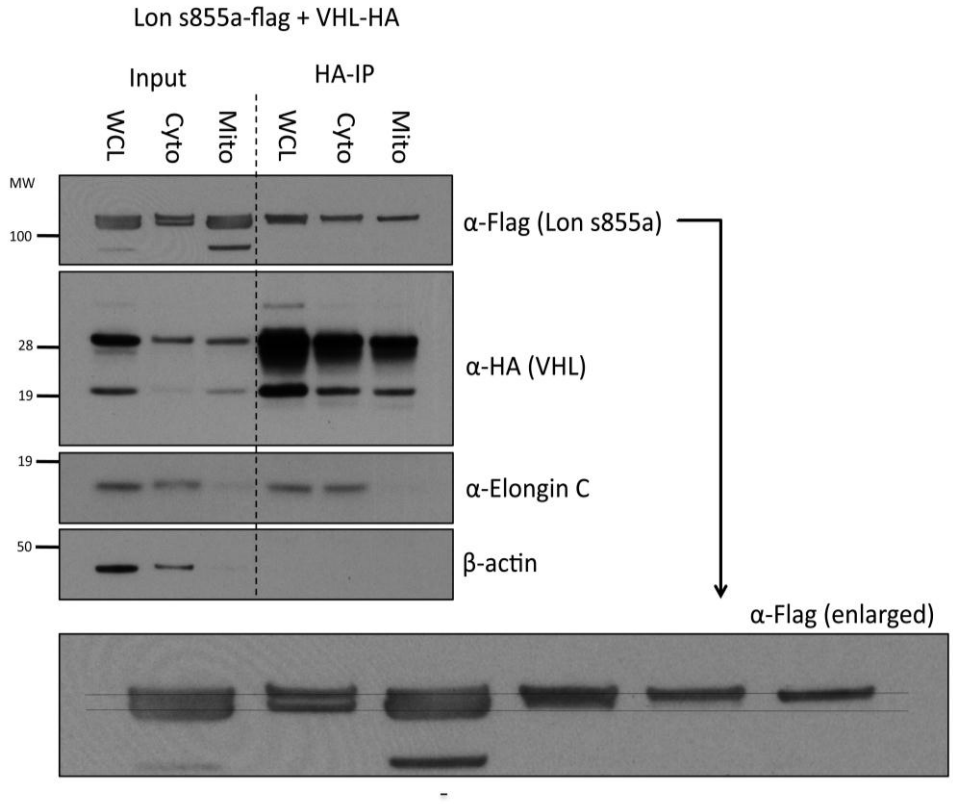

Figure 3.13 The interaction between Lon s855a and VHL-HA occurs only with the longer unprocessed form of Lon. 293T cells were co-transfected with Lon s855a and VHL-HA and fractionated into cytoplasmic (Cyto) and mitochondrial (Mito) fractions or kept as a whole cell lysate (WCL). Each of these was immunoprecipitated against anti-HA (right). Input and immunoprecipitates were western blotted and probed for the indicated proteins. The flag blot is enlarged and reproduced at the bottom with horizontal lines added to indicate unprocessed weight (top line) and processed weight (bottom line) of Lon s855a.

The interaction between exogenously transfected Lon and VHL is not dependent on mitochondrial localisation

As a result of our observation that the interaction between Lon (s855a) and VHL was able to occur in the cytoplasmic fraction, we created Lon and catalytically inactive Lon mutants that lacked the predicted MTS. The predicted MTS was between amino acids 1-59 (Δ1-59) (Claros & Vincens, 1996). Deletion of the MTS and cotransfection with VHL-HA led to the same destabilisation of VHL with the catalytic active Lon compared to the catalytically inactive Lon (s855a) (Figure 3-14; compare lanes 2, WT, 3 s855a and lanes 5 Δ1-59, 6 Δ1-59 s855a). This

suggests that the destabilisation of VHL when co-transfected with Lon is dependent on the cytoplasmic activity of Lon.

Lon s855a can co-immunoprecipitate with VHL-HA, whether it is targeted to the mitochondria (Figure 3.14 lane 10) or not (lane 14). The Lon s855a that co-immunoprecipitates with VHL-HA is shorter if it lacks the MTS, consistent with both being cytoplasmically located.

The interaction between Lon and VHL in the cytoplasm is intriguing, especially when considered together with our data suggesting that Lon promotes aberrant HIF-α subunit stabilisation in cancer cell lines without affecting VHL levels (Figure 3.1). Our hypothesis was that Lon was acting as a chaperone on VHL, causing it to be inactive. This might explain why different cell lines show varying levels of stabilised HIF-1α in normoxia that is proline-hydroxylated (Chapter 5). To prove the specific chaperone activity of Lon towards VHL, we inactivated the ATP-binding motif within the Walker A region. The replacement of lysine with asparagine reduces ATPase and proteolytic activities of Lon in *E.coli* (Fischer & Glockshuber, 1994). In yeast this mutation cannot rescue the respiratory incompetence of Δpim1 cells (Wagner *et al.*, 1997). The corresponding mutation in human Lon is k529n (Figure 3.14).

When co-transfected into 293T cells, Lon k529n (ATPase-ve) allows for stabilised expression of VHL-HA, and this is not further altered with the double mutation k529n s855a (Figure 3.14). Importantly, the co-immunoprecipitation of Lon with VHL is drastically reduced with mutation of the ATPase site,

compared to the catalytic inactive Lon (compare HA-IP s855a lane 10, with the next two lanes). This difference may be underestimated by western blot due to overexposure of the flag immunoblot, and the ponceau S stain is provided for quantitative visual assessment. The fact that Lon can be co-immunoprecipitated with k529n at all suggests that the interaction is not due to a novel site introduced by creation of the s855a mutant.

The abrogation of VHL binding by Lon when the k529 is mutated suggests that ATPase activity is required for this interaction (Panaretou *et al.*, 1998). This suggests that Lon is acting as an ATP-dependent chaperone towards VHL in the cytoplasm, prior to import and assembly.

Additional observations accompanying this experiment (not included in Figure 3.14) include the severe toxicity of the catalytic active mutant with deletion of the MTS (Δ1-59) and moderate toxicity of the catalytic active Lon targeted to mitochondria (WT). This raises the possibility that some differences in expression (Lon and VHL) may be associated with differential toxic effects.

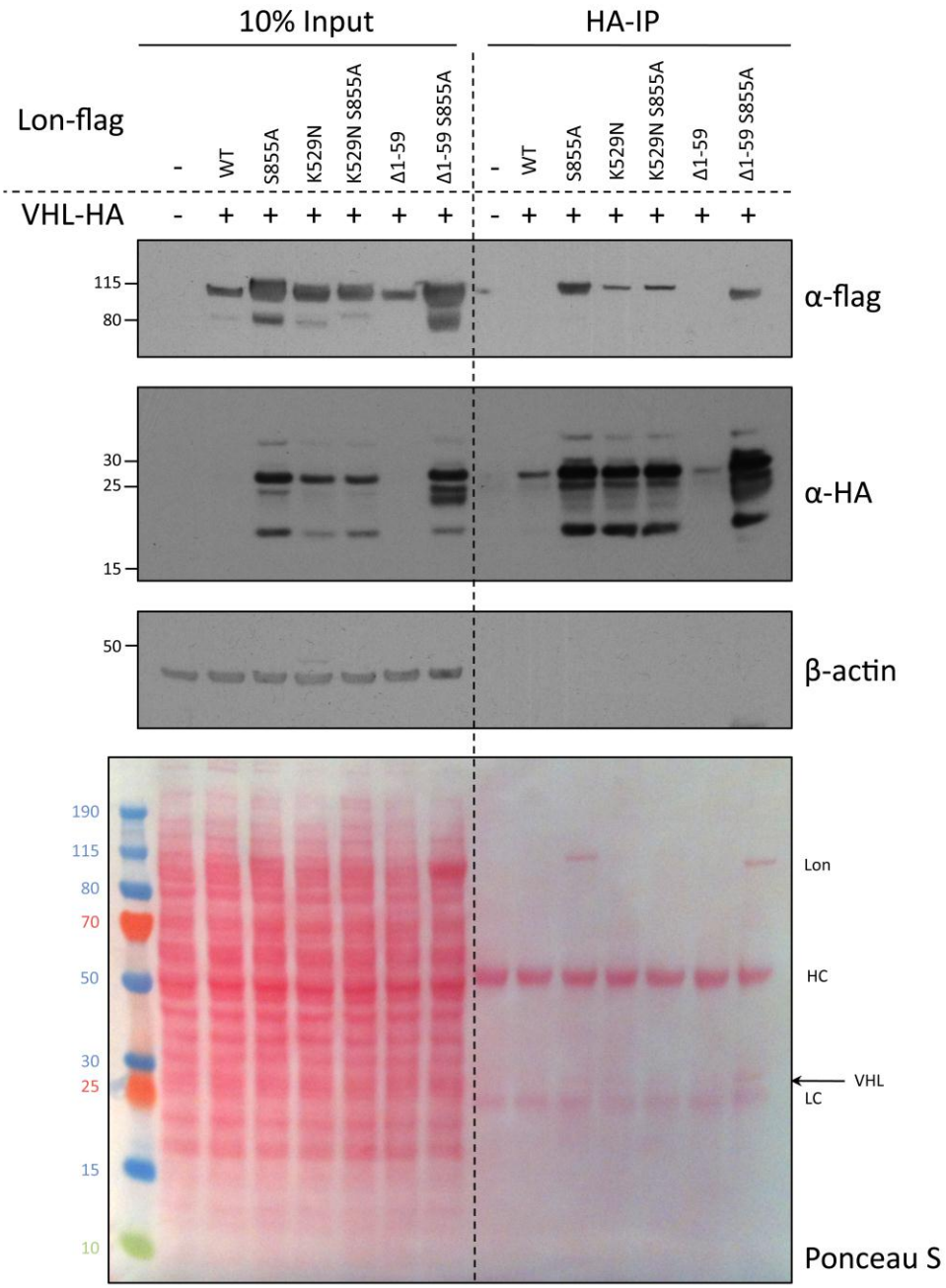

Figure 3.14 The catalytic inactive Lon protease (s855a) and VHLHA interaction is dependent on ATPase activity but not on mitochondrial localisation. 293T cells were co-transfected with VHL-HA and the Lon protease mutants as indicated. WT – Lon-flag vector, S855A – catalytic inactive Lon-flag, K529N – ATPase inactive Lon-flag, S855A K529N – double mutant, Δ1-59 – Lon-flag lacking MTS, Δ1-59 S855A – double mutant. The left side shows the total amount of protein used for the immunoprecipitation against anti-HA on the right. The western blot was probed with the antibodies indicated. The bottom panel shows the Ponceau S stain of the western blot providing visual evidence of the specificity of the VHLHA and Lon s855a

interaction, and the absence of any other significant interacting proteins. Heavy chain (HC) and light chain (LC) are from the anti-HA antibody.

No interaction detectable by immunoprecipiation between endogenous Lon and VHL-HA in U87 cells

Experiments in 293T cells had consistently failed to co-immunoprecipitate the catalytic active Lon and VHL (Figures 3.10 and 3.14). Mutations in Lon that promoted stability of VHL, both at the catalytic site and atpase site, allowed for Lon:VHL co-immunoprecipitation (Figure 3.14). However, catalytically active Lon lacking a MTS could still not co-immunoprecipitate with VHL, possibly due to lack of VHL in transfected cells. Detecting an interaction between Lon and VHL endogenously was likely to be difficult, due to the low levels of endogenous expression of VHL, poor VHL antibodies for immunoprecipitation, and the likely small amount of endogenous Lon that is unprocessed in the cytosolic compartment.

The nature of the Lon:VHL interaction, if it were to occur physiologically, would be transient, leading to a conformational change in VHL that would render it inactive towards proline-hydroxylated HIF-α subunits. In an attempt to prove the interaction between VHL and endogenous Lon protease, we used U87 cells, now known to have high levels of HIF-1α dependent on Lon expression, and transduced them with lentivirus containing VHL-HA or GFP control (Figure 3.15). The basal level of HIF-1α was the same with overexpression of either GFP or VHL-HA, suggesting that absolute levels of VHL are not responsible for normoxic expression of HIF-1α. Transfecting these cells with siRNA against the Lon protease reduced the level of HIF-1α in GFP and VHL-HAvexpressing cells

equally. Reducing the levels of Lon in VHL-HA expressing U87 cells appeared to reduce slightly the expression of VHL-HA. Immunoprecipitation of HA caused the pulldown of elongin C, but not of HIF-1α or Lon.

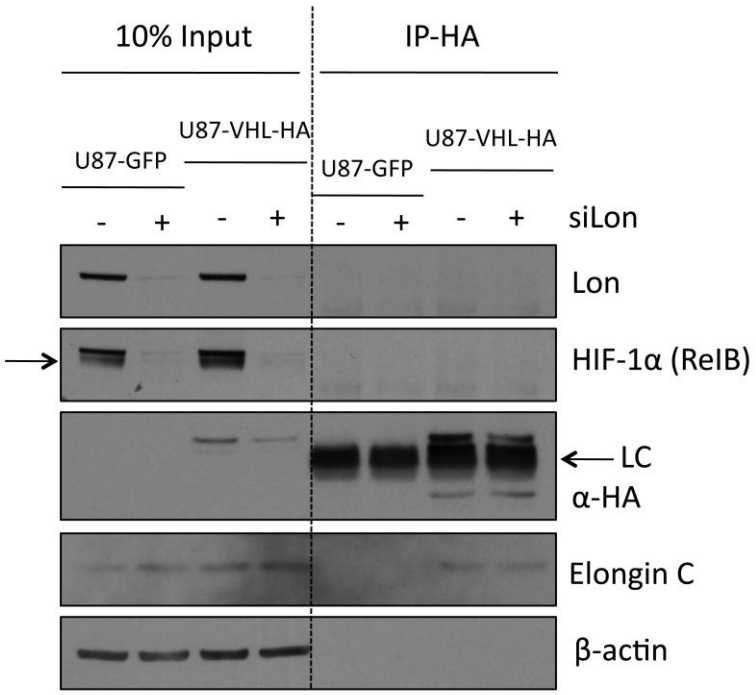

Figure 3.15 VHL-HA in U87 cells does not co-immunoprecipitate endogenous Lon protease or HIF-1α. U87 cells stably expressing either GFP or VHLHA were transfected with siRNA targeting the Lon protease. The input levels are represented on the left side and immunoprecipitation against HA on the right side. The western blot was probed with the indicated antibodies. The band representing HIF-1α is indicated with an arrow, the band just above is Lon protease, as the blot is re-immunoblotted after probing for Lon. The position of the antibody light chain (LC) at 25 KDa is indicated.

An interaction between Lon and VHL is detectable in cell line tumour spheroids by proximity ligation assay (PLA)

Transient or weak interactions between proteins may not be detectable by immunoprecipitation but are nevertheless important for diverse biological processes (Ozbabacan *et al.*, 2011). Transient interactions can be demonstrated *in situ* using the highly sensitive proximity ligation assay (PLA) (Söderberg *et al.*,

2006). We assayed for the endogenous interaction between Lon and VHL in U87 and MDA-MB-468 FFPE tumour spheroids and found they interacted in cells across the spheroid (Figure 3.16). There was no detectable increase in the level of Lon-VHL interaction towards the hypoxic core of the spheroid.

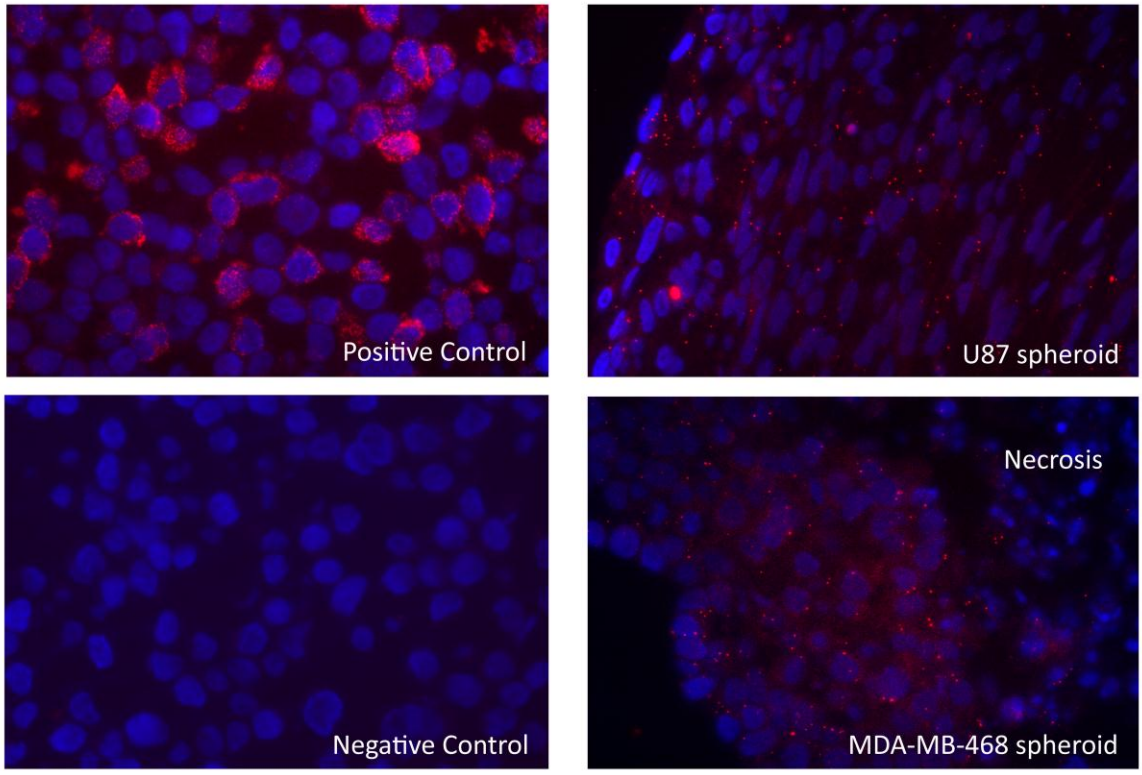

Figure 3.16 The interaction between endogenous Lon and VHL is demonstrated using the proximity ligation assay (PLA). Positive control is a FFPE cell pellet of 293T cells co-transfected with vectors encoding Lon catalytic inactive mutant (S855A) and VHL-HA. Negative control is a cell pellet co-transfected with Lon (catalytically active) and VHL-HA. These controls have been previously validated for the interaction by immunoprecipitation in Figure 3.14. On the right, the same conditions demonstrate VHLLon interaction in U87 and MDA-MB-468 FFPE spheroids. A red dot indicates a positive signal for the interaction. Counterstained with DAPI.

Discussion

The Lon protease is required for the aberrant expression of HIF-1α in VHL competent tumour cells

We have demonstrated that targeting the Lon protease by siRNA reduces the level of aberrantly stabilised HIF-α subunits in tumour cell lines in normoxia and hypoxia, and also reduces the expression of HIF-dependent genes. This important discovery points to an involvement of Lon in the mitochondrial control of hypoxic signalling and a pathophysiological mechanism for the aberrant stabilisation of HIF-α subunits in tumours, as Lon levels are increased in the majority of tumours (Chapter 2).

The threshold for achieving this phenotype appears to be quite high, as demonstrated by varied ability of different siRNA sequences to reduce levels of HIF-1α, despite all of them effectively reducing the protein levels of Lon (Figures 3.1 and 3.2). As later results suggest, it may be the cytoplasmic role of Lon that affects HIF-α signalling through a potential chaperone role with VHL. The differing ability of Lon targeted siRNAs to effect a change in HIF-α stability may therefore be more to do with the ability to produce a sustained reduction in Lon cytoplasm levels, rather than the more abundant mitochondrial Lon. Indeed, the endogenous Lon was only ever detected as a single band, suggesting that any cytoplasmic Lon is only ever present transiently.

We were acutely aware that off-target effects of siRNA have previously been described to effect HIF-1α levels (Lin *et al.*, 2005). However, we have demonstrated reduction in HIF-1α levels to varying extents in six different siRNA sequences and also in one shRNA sequence (Chapter 4), effectively ruling out this possibility.

Lon stabilises HIF-1α by inhibiting the degradation of proline-hydroxylated HIF-1α

The levels of HIF-α are modulated by the rate of transcription and translation, and proline hydroxylation. The mechanism by which siRNA targeted against the Lon protease reduces HIF-α expression appears to be through modulation of the rate of post-hydroxylation degradation.

We have shown that there are no significant differences in the rate of HIF-1α translation when targeting Lon with siRNA (Figure 3.4). We were unable to demonstrate any increase in the rate of hydroxylation of HIF-1α with proteasomal inhibition as a measure of HIF-PHD activity. HIF-α subunit stability is modulated by mitochondria through ROS, and we were unable to detect any changes in ROS, consistent with a mechanism of HIF stability not dependent on PHD activity.

Recently, c-Myc overexpression in normal and tumour cells lines has been shown to increase the stability of proline-hydroxylated HIF-1α (Doe *et al.*, 2012). The mechanism was not fully elucidated, but levels of VHL were increased along with other components of the VCB complex. The authors concluded that there must be

a disruption of HIF-1α binding to the VCB complex or a post-translational modification, preventing the degradation of HIF-1α, that was transcriptionally active with overexpression of c-Myc. This situation is not unlike the model of regulation of HIF-α that is abrogated by siRNA targeting of the Lon protease. In the case of Lon, there is no detectable change in the levels of VHL, yet there is a decrease in the levels of hydroxylated HIF-1α when Lon levels are reduced.

VHL is the subject of post-translational modifications, including ubiquitination, sumoylation (Cai & Robertson, 2010) and neddylation (Stickle *et al.*, 2004). We did not see any change in the molecular weight of VHL that would be expected if these post-translational modifications were responsible for the effect of Lon on HIF-α. VHL phosphorylation (Roe *et al.*, 2011), expected to produce minimal changes in weight, could be a mechanism by which Lon modulates VHL activity.

Together our observations support the notion that a significant proportion of HIF-α stabilised in cells in normoxia is proline-hydroxylated. On this basis, we embarked on a study on the expression of proline-hydroxylated HIF-1α in tumours (Chapter 5).

The control of mitochondrial transcription may be modulated by Lon through HIF-α stability

The stabilisation of HIF-α subunits has previously been linked to mitochondrial biogenesis. Initial experiments involving transfecting wild type *VHL* into *VHL*-deficient renal cell carcinomas revealed an increase in mitochondrial DNA and

components of the respiratory chain, and allowed cells to grow in the absence of glucose (Hervouet *et al.*, 2005). The mechanism by which HIF-1 modulated mitochondrial biogenesis was later established by demonstrating that HIF-1 repressed the activity of C-MYC, also using renal cell carcinoma cell lines (Zhang *et al.*, 2007). HIF-1 promotes the expression of the *MXI1* gene, which encodes a repressor of C-MYC transcriptional activity, while at the same time HIF-1 can promote proteasomal degradation of C-MYC (Zhang *et al.*, 2007). HIF-mediated control of mitochondrial biogenesis is complicated by the finding that the pharmacological stabilisation of HIF-α subunits has different effects on mitochondrial biogenesis depending on the drug used. Stabilisation of HIF-α by cobalt chloride ($CoCl_2$) caused a reduction in mitochondrial complex subunits, but not if HIF-α is stabilised by desferrioxamine (DFO) (Hervouet *et al.*, 2008). DFO acts by preventing Fenton reactions by complexing iron (Tarpey *et al.*, 2004), so may directly inhibit HIF-PHDs as well as inhibiting the production of hydroxyl radicals. Notwithstanding, $CoCl_2$ induces HIF-α accumulation by inhibiting HIF-PHDs, but also inhibits the mitochondrial intermediate peptidase (MIP) that cleaves COX4 precursor protein (Hervouet *et al.*, 2006) and also increases reactive oxygen species (Hervouet *et al.*, 2008). This suggests that while HIF-α stabilisation is correlated with mitochondrial biogenesis, the pharmacological mechanism by which HIF is stabilised may be important in mediating these effects.

Two groups have reported the effect of increased mitochondrial biogenesis with depletion of Lon both in *Drosophila* (Matsushima *et al.*, 2010) and human cells (Lu *et al.*, 2012). Targeting Lon with siRNA increases the level of TFAM

(Matsushima *et al.*, 2010) and, similarly, TFAM levels are increased when VHL is reintroduced into VHL-negative cell lines (Hervouet *et al.*, 2005). We find that targeting Lon with siRNA reduces levels of HIF-α stabilisation, and therefore the changes in mitochondria may be consequent to levels of HIF in normoxia.

Another group has demonstrated that in cells with deficiencies in cytochrome *b*, targeting TFAM by shRNA reduces the amount of HIF-1α stabilised under hypoxia (Bell *et al.*, 2007). Reducing TFAM levels in these circumstances would reduce ROS and mitochondrial electron transport in cells that already did not consume oxygen (Bell *et al.*, 2007). There is unlikely to be any effect on HIF-1α resulting from global changes in mitochondrial translation, given our finding that chloramphenicol does not affect HIF-1α stabilisation (Figure 3.6), and the lack of any literature regarding effects of chloramphenicol on HIF signalling.

Our findings suggest that Lon may promote stabilisation of HIF independent of oxygen tension and consequently may reduce the level of mitochondrial biogenesis and increase levels of HIF target genes, including those involved in the shift to aerobic glycolysis such as GLUT1. Whilst having positive effects on HIF-α stabilisation and transcription, Lon can also degrade mitochondrial TFAM (Lu *et al.*, 2012), reducing the level of mitochondrial transcription. The combination of these two effects would induce a shift away from oxidative phosphorylation and a promotion of aerobic glycolysis (the Warburg effect), as shown in Chapter 4.

The direct interaction of VHL and Lon in the cytoplasm can be demonstrated by overexpression of Lon mutants in 293T cells

Lon appears to affect HIF-α stabilisation through mechanisms independent of proline hydroxylation, and proline-hydroxylated HIF-1α can be demonstrated to accumulate in VHL-competent tumours (Chapter 5.). These observations led us to investigate whether there was any direct interaction between Lon and VHL in transfected 293T cells.

We have been able to demonstrate an interaction through co-immunoprecipitation between cytoplasmic Lon protease and VHL by artificially promoting the cytoplasmic accumulation of Lon, whether by mutation of the ATPase domain or the catalytic active site (Figure 3.14). In addition, removing the mitochondrial targeting sequence did not inhibit the interaction in catalytically inactive Lon.

The co-overexpression of Lon and VHL resulted in destabilisation and degradation of VHL, which could be reversed by treatment with the proteasomal inhibitor bortezomib, but not MG132 (Figure 3.9). In purified recombinant form, Lon is inhibited by MG132 (Bayot *et al.*, 2008), MG262 and Bortezomib (Lu *et al.*, 2012). However, the lack of universally accepted substrates of Lon that are not also degraded by other proteases has limited the study of specific inhibitors in cells. Recently, TFAM degradation was shown to be inhibited by Bortezomib and MG262, but perhaps tellingly, MG132 was not tested (Lu *et al.*, 2012). MG132 requires a much higher concentration for inhibition of proteasomal active sites (K_i) of 0.004μM compared to MG262 0.00002μM (Bayot *et al.*, 2008), evidence

than MG132 may be a poorer inhibitor of Lon compared to MG262 or Bortezomib. The data we present is consistent with decreased exogenous VHL stability and proteolysis when co-transfected with Lon, suggestive of the degradation of VHL by Lon.

However, we consistently see unchanged levels of VHL with siRNA targeted against the Lon protease (Figures 3.1 and 3.2), which does not support the idea that Lon mediates changes in HIF-α stability secondary to VHL degradation. The selective destabilisation of VHL with Lon overexpression could reflect stability changes post-chaperone modification that Lon exerts on VHL.

The observation that the interaction between Lon and VHL is reduced by mutating the ATPase site of Lon suggests that the interaction is chaperone-type. The chaperone activity of Lon has been reported in *S. cerevisiae* (Rep *et al.*, 1996). Yeast with mutations in Afg3g and Rca1p (AAA proteins involved in assembly of multiprotein complexes at the inner mitochondrial membrane) have defects in respiratory-dependent growth and assembly of mitochondrial complexes, and can be rescued by overexpression of Lon and enhanced by catalytically inactive Lon (Rep *et al.*, 1996). An ATPase deficient Lon, however, prevented rescue (Rep *et al.*, 1996). The ATPase activity of Lon required for phenotypic rescue could be mediated within the cytoplasm, especially since the catalytic inactive mutant, known to be impaired in mitochondrial import, enhanced rescue (Rep *et al.*, 1996).

In conclusion, Lon may promote the stability of HIF-α by chaperone activity towards VHL in the cytoplasm. The failure to co-immunoprecipitate Lon with transduced (Figure 3.15) or endogenous (not shown) VHL is not surprising, since the nature of this interaction is likely to be transient. Transient protein-protein interactions are difficult to analyse (Ozbabacan *et al.*, 2011), and the 293T transfection with Lon mutants that promote cytosolic accumulation of Lon likely provide the increased frequency of interaction required for detection by immunoprecipitation. We are able to demonstrate the interaction *in situ* between Lon and VHL in U87 and MDA-MB-468 spheroids using the highly sensitive PLA, and have established that the interaction occurs outside of the nucleus, and is not induced by hypoxia.

Mitochondrial to nuclear signalling may be mediated by cytoplasmic retention of Lon

The levels of Lon increase in hypoxia (Figure 3.3) (Fukuda *et al.*, 2007) and also in response to increased oxidative stress, according to an analysis of the promoter of the *Lon* gene (Pinti *et al.*, 2010a). The upregulation of Lon may not be sufficient to mediate changes in HIF-α stability, since we have determined that cytoplasmic component of Lon may mediate changes in VHL activity. The delayed import of Lon would be predicted to exert a greater effect on VHL and promote the stabilisation of proline-hydroxylated HIF-α subunits. In effect, modulating the hypoxic response may be a balance between Lon production and mitochondrial import, and the two may be in equilibrium.

Delayed import of mitochondrial proteins has recently been identified as the mechanism by which mtUPR signals to elicit nuclear transcriptional changes in *C. elegans* (Nargund *et al.*, 2012). In this proof of principle, AFTS-1 has a mitochondrial targeting sequence and a nuclear localisation sequence, and when mitochondrial import is slowed, causes the transcription of nuclear genes, including those involved in a shift to glycolysis (Nargund *et al.*, 2012). ATFS-1 has no human homologue, but the mechanism of delayed import to mitochondria as a method to transmit signals resulting in transcriptional changes in the nucleus is likely to be conserved.

Impaired mitochondrial import of Lon as a mechanism of mtUPR signalling

In an RNAi screen in *C. elegans* to determine genes that when knocked-down induced the transcription of HIF-1, 26 out of 113 positive 'hits' were mitochondrial proteins, including mitochondrial respiratory chain genes *cco-1* (cytochrome c oxidase-1), *spg7*, *clk-1* and *isp-1* (Lee *et al.*, 2010). These four genes also induce mtUPR when knocked down with siRNA in *C. elegans* (Nargund *et al.*, 2012). The mechanism for inducing mtUPR is thought to be through impairment of the electron transport chain, the activity of which is important for mitochondrial protein import (Becker *et al.*, 2012). This suggests that activation of mtUPR may promote the stabilisation of HIF-α, although there is no evidence for this either in models of mtUPR in *C. elegans* or in any other organisms. The lack of established methods for inducing mtUPR in mammalian cell culture makes establishing this link difficult, although differences in mtUPR may account for differential stabilisation of HIF-α subunits between tumour cell lines.

The mechanism mammalian cells use to detect unfolded proteins within the mitochondrial matrix and transmit the signal to elicit cytoplasmic or nuclear responses is unknown (Pellegrino *et al.*, 2013). The possibility we present is that the impaired import of the Lon protease may negatively regulate the activity of VHL and impair HIF-α degradation. In this way, the energy requirements of the cell would shift from mitochondrial respiration to glycolysis, reducing ROS levels and promoting the clearance of mitochondrial unfolded proteins. Targeting Lon by siRNA in *C. elegans* does not cause mtUPR using genetic reporters (Nargund *et al.*, 2012) (as might be expected for a mitochondrial protease involved in quality control), consistent with the idea that reducing levels of Lon may promote mitochondrial matrix protein folding.

Whilst the role of cytoplasmic Lon in mediating mtUPR is speculative, given the lack of methods to induce and measure mtUPR in mammalian cells and our lack of evidence than endogenous Lon can act in the cytoplasm under physiologic conditions, the argument for such a signalling mechanism is compelling and fits with the limited current data. Aberrant HIF-α stabilisation caused by mtUPR in tumour cells is a focus for future investigation.

Chapter 4 : The functional effects of targeting the Lon protease in tumour cells

Having determined that Lon expression was increased in malignancy (Chapter 2) and that the increased expression was required for the level of stabilisation of HIF-α subunits in normoxia and hypoxia (Chapter 3), we sought to determine the functional consequences of depleting Lon in tumour cells.

Overview

The mitochondrial Lon protease is upregulated in tumours and predicts poorer overall survival in ER-positive breast cancer (Chapter 2). Depletion of the Lon protease reduces hypoxic signalling in cancer cell lines by reducing the stabilisation of HIF-α subunits (Chapter 3). HIF signalling is critical in tumorigenesis, mediating the metabolic change to glycolysis, angiogenesis, invasion and metastasis as well as promoting survival in hypoxic environments. Lon may be an important therapeutic target, and so we sought to determine the functional effect of reducing levels of Lon in cell lines *in vitro*. We find that reducing levels of Lon can inhibit the proliferation *in vitro* of tumour cells in two and three-dimensions, but this is cell-type dependent. We find that reducing Lon levels also reduces the cellular dependence on glucose, increases oxygen consumption and reduces lactate production, with no detectable change in ATP levels. In this way, targeting Lon appears to cause a partial reversal of the major

metabolic phenotype of cancer cells, known as the Warburg effect. We also find that the mitochondria fuse and form a more inter-connected network with Lon knockdown.

Introduction

The Lon protease degrades damaged (Bota & Davies, 2002) and certain regulatory proteins such as TFAM in the mitochondrial matrix (Lu *et al.*, 2012). Lon forms a homo-oligomeric ring-shaped complex that has similarities in structure to the 26S proteasome (García-Nafría *et al.*, 2010). Recently, the proteasomal inhibitor bortezomib has been shown to also inhibit the Lon protease and prevent the degradation of TFAM (Lu *et al.*, 2012). Interestingly, proteasomal inhibitors, in particular bortezomib, have been shown to reduce HIF signalling in tumour cells *in vitro* and *in vivo* (Birle & Hedley, 2007). Bortezomib reduces VEGF secretion from tumour cells in hypoxia with 50 times lower concentration than required for the same effect with MG132 (Birle & Hedley, 2007).

Our finding that reducing the levels of Lon reduces HIF-α stabilisation and transcriptional activity (Chapter 3) raises the possibility that pharmacological inhibition of Lon may also reduce HIF signalling. Previous reports demonstrating reduced HIF signalling in response to proteasomal inhibiton (Befani *et al.*, 2012) (Birle & Hedley, 2007) (Shin *et al.*, 2008) (Kaluz *et al.*, 2006) may be due to inhibition of Lon. Indeed, there is no consensus on the mechanism by which

proteasomal inhibition reduces HIF transcriptional activity, despite increasing the amount of HIF-α subunits by preventing degradation.

There is circumstantial evidence to implicate Lon inhibition in the mechanism by which proteasomal inhibitors reduce HIF signalling. We wished to evaluate the utility of developing Lon-specific inhibitors by determining the phenotype of tumour cells *in vitro* with short hairpin and short interfering RNA.

Methods

Lentiviral shRNA production and transduction

The lentiviral constructs for producing shRNA-mediated knockdown of Lon protease were purchased from Sigma. The hairpin sequence and TRC number are as below. Clones were purchased as frozen bacterial stocks. Bacterial stocks were streaked out on plates, a single clone expanded and Maxi-prep DNA extracted (Invitrogen). Lentiviral particles were produced and titrated as described in Chapter 3. An MOI of 3 was used for target cell transduction. After transduction, cells were selected using puromycin for a minimum of three days (U87 and MDA-MB-468 cells 1μg/ml media, and 0.7μg/ml for MCF7 cells).

Table 4.3 Lentiviral shRNA sequences used

shRNA target	TRC number	Hairpin sequence	Name
Lonp1	TRCN0000291803	CCGGCCAGTGTTTGAAGAAGACCAACTC GAGTTGGTCTTCTTCAAACACTGGTTTTTG	sh03
Lonp1	TRCN0000291804	CCGGCGAGAACAAGAAGGACTTCTACTC GAGTAGAAGTCCTTCTTGTTCTCGTTTTTG	sh04
Non-human control	SHC202	CCGGCAACAAGATGAAGAGCACCAACTC GAGTTGGTGCTCTTCATCTTGTTGTTTTT	shNS

Spheroid growth assay

Spheroids were produced in 96-well ultra non-adherent round-bottom plates (Corning) as described in Chapter 3. Spheroids formed after 24 hours in culture and were photographed on an inverted Nikon TMS microscope (4x magnification) using an attached Nikon Coolpix 950 camera. Photos of spheroids in culture were taken every two days. The camera was calibrated by photographing a Neubauer haemocytometer (1mm = 564 pixels). For calculating volume, the acquired images were processed in ImageJ (http://rsbweb.nih.gov/ij/) using the following macro to calculate pixel area occupied by a spheroid (written by the author).

```
run("8-bit");
setAutoThreshold("Default");
//run("Threshold...");
setThreshold(0, 99);
run("Convert to Mask");
run("Analyze Particles...", "size=10000-3000000 circularity=0.01-1.00
show=Outlines display exclude include in_situ");
```

This macro was run with the 'batch' function to allow for simultaneous processing of multiple spheroids. Once pixel area was acquired for each spheroid, the volume was calculated, making the assumption that each spheroid was spherical (i.e. a radius was calculated from measured area, which was then

used to calculate a volume). Spheroids were embedded, processed and sectioned as described in Chapter 3.

Proliferation assay

Proliferation was measured by using the CyQUANT reagent (Invitrogen). Cells were counted using a Neubauer haemocytometer and 2000 cells were plated per well in a 96-well plate (in quadruplicate). One plate was used per time point, either in a normal (normoxic) incubator (5% CO_2) or in a hypoxic (5% CO_2, 1% O_2 displaced with N_2) incubator. At each time point, the plate was removed, media tapped off and plate stored at -80°C. For quantification, 200µl of CyQUANT GR/cell lysis buffer was added to each well, mixed and incubated for five minutes, and fluorescence read using a FLUOstar OPTIMA plate reader (BMG labtech) (Ex480nm/Em520nm). Values obtained were converted to cell number by comparison with a cell number standard curve (for each cell line).

Oxygen consumption assay

Oxygen consumption was measured in cells by using an oxygen-sensitive fluorescent probe in the media, MitoXpress-Xtra (Luxcel Biosciences). This probe shows increased fluorescence with decreasing oxygen consumption. Cells were counted and 5×10^4 (for MCF7) or 1×10^5 (for U87) cells were added to each well of a black 96-well plate with clear bottoms (BD Falcon), and allowed to adhere overnight. Media was replaced with 6.25% (62.5nM) reconstituted MitoXpress-Xtra probe in 150µl of media and the wells sealed with mineral oil. Probe fluorescence was measured using a time-resolved fluorescent plate reader

(FLUOstar Omega – BMG labtech), with the plate incubated at 37°C. The probe was excited and emission read from the bottom of the plate (Ex380nm/Em650nm). Measurements were taken from each well every 90 seconds and plotted using MARS data analysis software (BMG Labtech). The maximum rate of change in the fluorescence of the probe was taken as the oxygen consumption (after 10 minutes), and relative rates were calculated for cells transfected with different siRNAs. In a matching seeded 96-well plate of cells (with a fifth the number of counted cells), actual cell number was determined using the CyQUANT assay to allow for normalisation of relative oxygen consumption (in practice there were less than 10% differences between conditions). Glucose-free conditions were achieved by using dialysed foetal calf serum (Sigma) and glucose-free DMEM (Invitrogen).

ATP assay

ATP levels were calculated using the CellTiter-Glo assay (Promega). 5000 cells were plated in 100µl in wells of a white 96-well plate (with opaque white bases). 100µl of reagent was added to each well, incubated for 10 minutes and luminescence read on a FLUOstar Optima. The signal was normalised to cell number (in a parallel black plate) using the CyQUANT assay.

Glucose uptake and lactate production

Timed glucose uptake was performed by collecting the media exposed to cells in a 96-well plate after a 12 hour incubation. The glucose content of the media was measured by a Siemens ADVIA Clinical Chemistry System (Clinical Biochemistry

at the John Radcliffe Hospital), using the glucose oxidase assay. Media lactate was measured in the same way using the lactate assay. Both assays gave absolute values which were normalised to cell number determined using the CyQUANT assay.

Mitochondrial morphology

MCF7 cells stably transfected with a vector encoding a fluorescent protein targeted to mitochondria (pDsRed2-Mito) was a kind gift from E. Favaro. Cells were plated in dishes with a coverslip for the base (MatTek), and imaged live using a laser scanning confocal microscope (Ziess LSM 510). Stacked images were transformed into a three-dimensional image using ImageJ. For analysis of mitochondrial elements, single slice images from individual cells were skeletonised, and the 10 longest mitochondrial elements were measured for length.

Statistics

Graphs and curves were assembled in Prism version 4.0 (Graphpad software). Statistical significance was calculated using the unpaired Student's t test.

For cells, culturing conditions and siRNA transfection, see Chapter 3.

Results

Targeting the Lon protease by shRNA severely reduces two- and three-dimensional growth in U87 cells but not MCF7 cells

In order to determine the effect of reducing levels of Lon on proliferation, we created lentiviral particles that, when transduced into cells, targeted the degradation of Lon RNA and stably reduced levels of Lon. We attempted this using a number of different suppliers of shRNA constructs and we sought to reproduce the reduced levels of stabilised HIF-1α described in Chapter 3. In western blots, in normoxia and hypoxia, one shRNA sequence (sh03) reduced the amount of HIF-1α detected compared to the non-targeting control (shNS) (Figure 4.1A, 4.2A). Both shRNA sequences sh03 and sh04 reduced levels of Lon to undetectable levels, however sh04 did not alter levels of HIF-1α. The locations of sh03 and sh04 binding with respect to the Lon sequence are illustrated in Chapter 3 (Figure 3.2).

Reducing the levels of Lon in U87 cells severely reduced the two-dimensional proliferation in normoxia and hypoxia (Figure 4.1C). When grown as spheroids, U87 cells deficient in Lon also show severely reduced growth compared to cells transduced with the non-targeting control (Figure 4.1B). The severely reduced levels of proliferation precluded the expansion and maintenance of a stable cell line deficient in Lon, and eventually resistant clones (with higher levels of Lon) became the predominant population (data not shown).

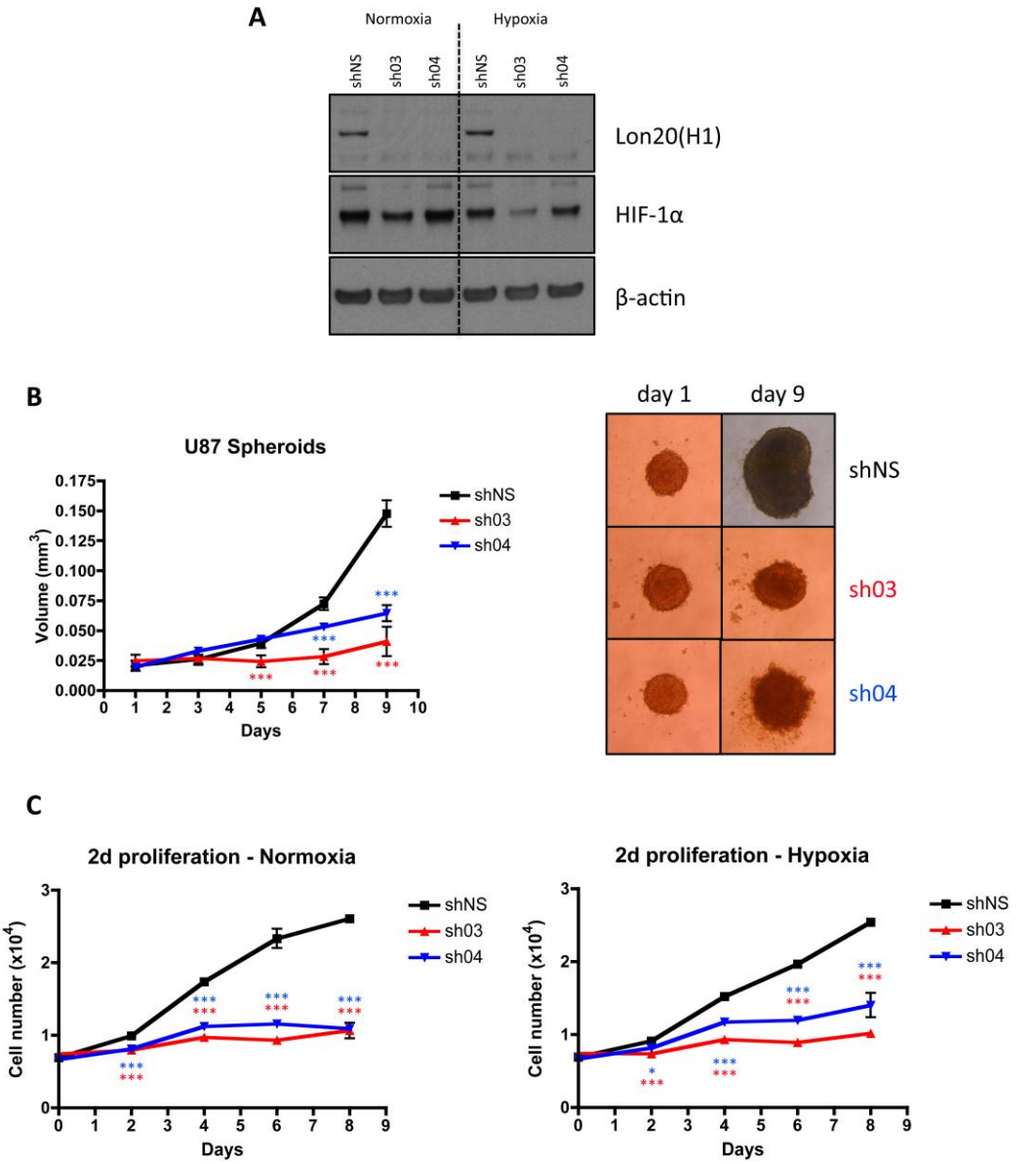

Figure 4.1 U87 cells transduced with shRNA targeting the Lon protease show reduced HIF-1α stabilisation and reduced two- and three-dimensional proliferation. A. U87 cells were transduced with lentiviral particles encoding shRNA targeted against the Lon protease and cultured in normoxia or hypoxia (1%) for 16 hours. Lysates were probed by western blot with the indicated antibodies. **B.** U87 cells stably expressing shRNA targeted against the Lon protease (sh03 and sh04) or a non-targeting control (shNS) were grown as spheroids and the size measured every two days (each point on the graph is the mean of 18 spheroids). Representative images of spheroids at day 1 and day 9. **C.** The same cells were also grown concurrently in two-dimensions, in normoxia (left) or 1% oxygen (right). Growth curves are representative of three similar experiments. Error bars indicate standard deviation. Significance was calculated using the unpaired Student's t-test (* = $p<0.05$, *** = $p<0.0001$).

When the same lentiviral stocks were used to transduce MCF7 cells, there was no significant difference in proliferation (in two- or three-dimensional growth) between cells with shRNA targeted against the Lon protease compared to the

non-targeting control (Figure 4.2B and C). This was despite the levels of Lon being reduced to non-detectable levels, and reduced stabilisation of HIF-1α in normoxia and hypoxia for sh03 (Figure 4.2A).

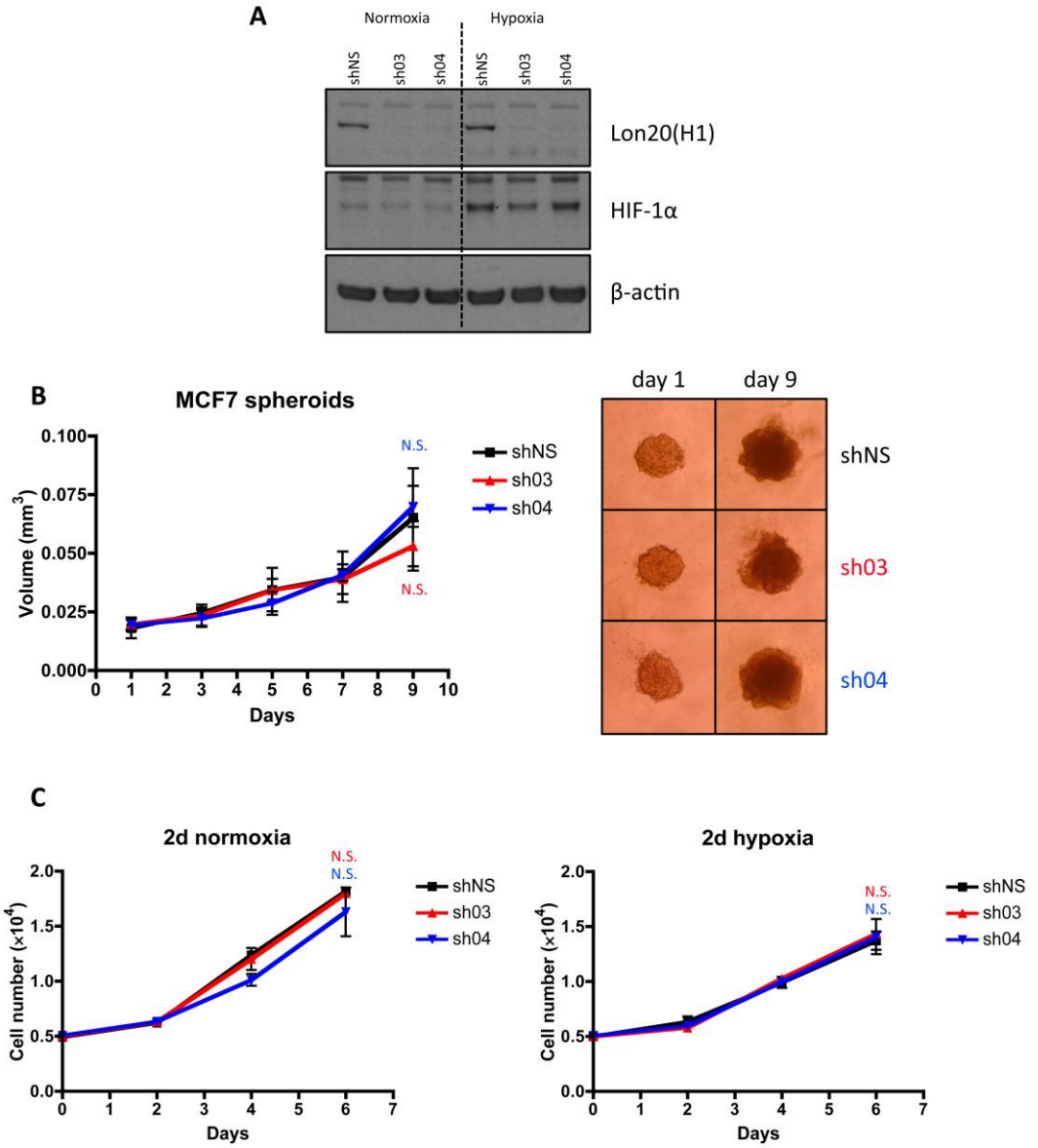

Figure 4.2 MCF7 cells transduced with shRNA targeting the Lon protease show reduced HIF-1α stabilisation and no significant differences in two- and three-dimensional proliferation. A. MCF7 cells were transduced with lentiviral particles encoding shRNA targeted against the Lon protease and cultured in normoxia or hypoxia (1%) for 16 hours. Lysates were probed by western blot with the indicated antibodies. **B.** MCF7 cells stably expressing shRNA targeted against the Lon protease (sh03 and sh04) or a non-targeting control (shNS) were grown as spheroids and the size measured every two days (each point on the graph is the mean of 18 spheroids). Representative images of spheroids at day 1 and day 9. **C.** The same cells were also grown concurrently in two-dimensions, in normoxia (left) or 1% oxygen (right). Growth curves are representative of three similar experiments. Error bars indicate standard deviation. Significance was calculated using the unpaired Student's t-test. N.S. = not significant ($p > 0.05$).

Reduced levels of Lon in MDA-MB-468 cells severely reduces two- and three-dimensional growth and hypoxic signalling in spheroids

We selected a third cell line, the breast cancer cell MDA-MB-468, to determine whether there were significant effects on growth with reduced levels of the Lon protease. In normoxia, MDA-MB-468 cells showed undetectable levels of HIF-1α (Figure 4.3A). With shRNA targeted against the Lon protease, there was reduced stabilisation of HIF-1α with shRNA sequence sh03, but not with sh04, compared to the non-silencing control (shNS (Figure 4.3A). There was a reduction in the level of Lon to non-detectable levels with both sh03 and sh04. This was similar to the effect seen in MCF7 and U87 cells. Additionally, the amount of the HIF-1α target gene, CA9, was reduced in hypoxia with sh03.

Both shRNA sequences targeting the Lon protease severely reduced the two-dimensional growth of MDA-MB-468 cells in normoxia and hypoxia compared to non-targeted control (Figure 4.3B). Similar to U87 cells, in prolonged culture resistant clones became established in cells transduced with shRNA targeted against the Lon protease.

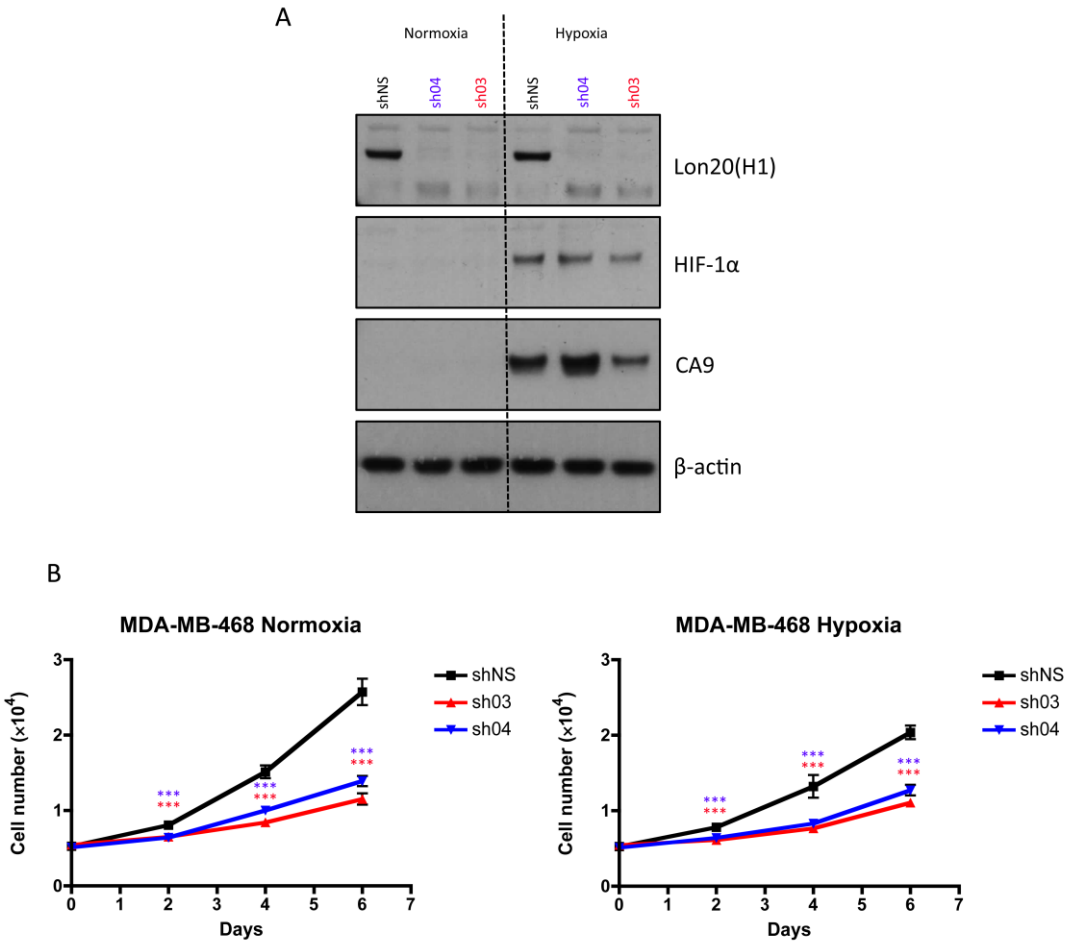

Figure 4.3 Targeting the Lon protease by shRNA in MDA-MB-468 cells reduces HIF-1α stabilisation in hypoxia and reduces two-dimensional growth in normoxia and hypoxia. A. MDA-MB-468 cells were transduced with lentiviral particles encoding shRNA targeted against the Lon protease and cultured in normoxia or hypoxia (1%) for 16 hours. Lysates were probed by western blot with the indicated antibodies. **B.** Growth of MDA-MB-468 cels with shRNA targeted against the Lon protease (sh03 and sh04) or a non-targeted control in normoxia (left) or 1% oxygen (right). Growth curves are representative of three similar experiments. Error bars indicate standard deviation. Significance was calculated using the unpaired Student's t-test (*** = $p<0.0001$).

When grown as spheroids, MDA-MB-468 cells also show severely reduced growth when stably expressing shRNA, targeted against the Lon protease (Figure 4.4). When spheroids were embedded, sectioned and stained, both spheroids stably expressing sh03 and sh04 showed reduced levels of HIF-1α staining and reduced CA9 expression in their central regions (Figure 4.4, bottom panels). In spheroids expressing the non-targeting control shRNA, CA9 expression was seen within 3-4 cells of the edge of the spheroid. In spheroids expressing shRNA

sequences sh03 and sh04, targeting the Lon protease, CA9 expression was seen approximately 10 cells from the edge of the spheroid. This shows that the more physiologic gradient of hypoxia within a spheroid can be used to demonstrate a greater effect of reduced HIF-α stabilisation with Lon targeted shRNA than in two-dimensional models (i.e. western blotting in a dish whether in normoxia and hypoxia).

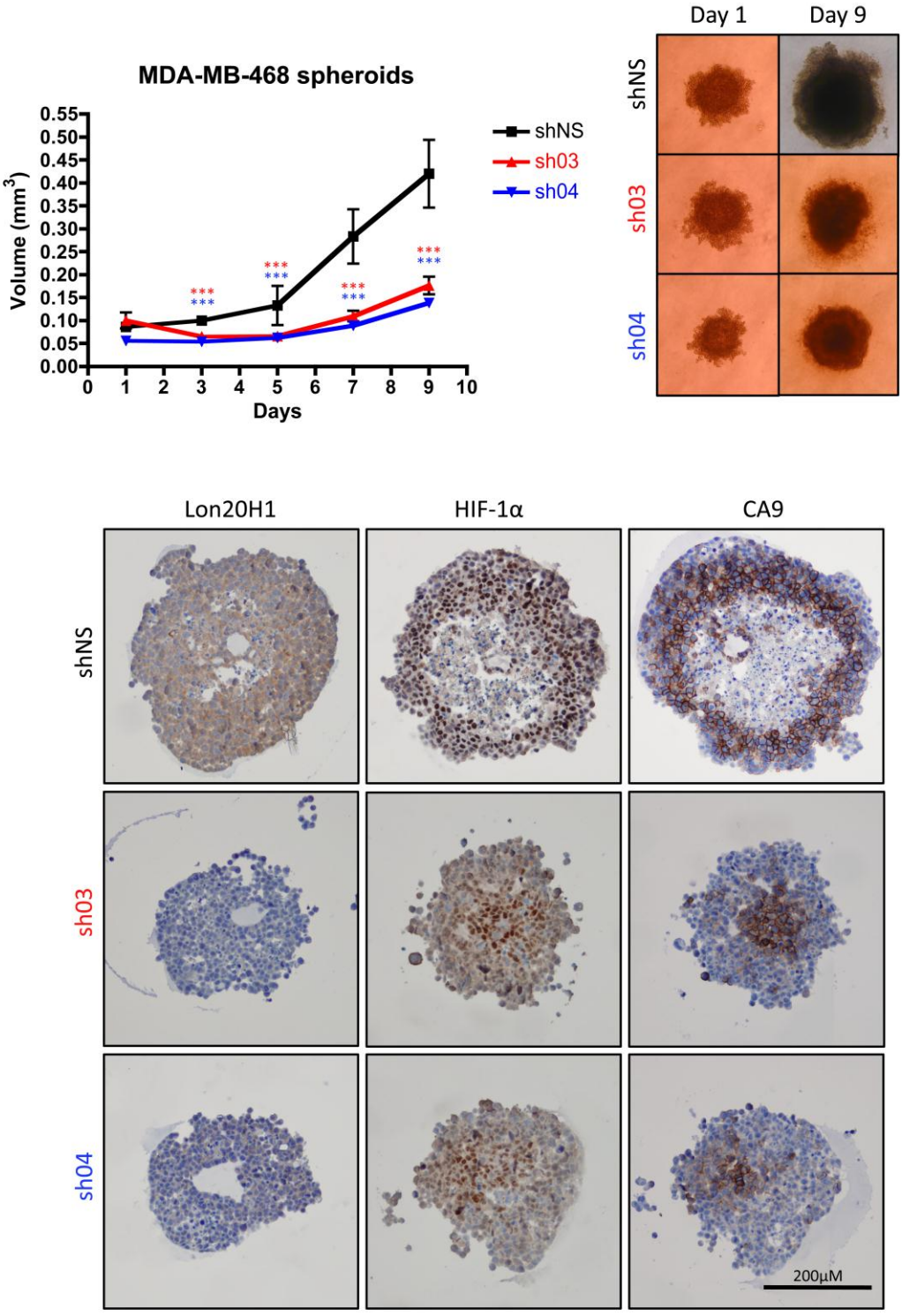

Figure 4.4 Targeting the Lon protease with shRNA reduces spheroid growth in MDA-MB-468 cells and reduces hypoxic signalling in spheroids. (Top) MDA_MB-468 cells stably expressing the shRNA sequences targeting the Lon protease (sh03 and sh04) or a non-targeting control (shNS) were grown as spheroids and measured every two days. Pictures (right) show typical spheroid size at day 1 and day 9. Each point represents the mean of 12 spheroids, error bars indicate standard deviation and significance determined using the unpaired Student's t-test. *** indicates $p < 0.0001$. Spheroid growth representative of three similar experiments. **(Bottom)**. MDA-MD-468 spheroids (at day 5) were harvested, sectioned and stained for the indicated antibodies by immunohistochemistry. Brown staining with diaminobenzidine indicates immunoreactivity.

Targeting Lon with siRNA increases oxygen consumption and reduces aerobic glycolysis without detectable changes in ATP levels in tumour cell lines

One particularly noticeable observation made whilst performing experiments in Chapter 3 was the propensity for cells treated with siRNA against Lon to fail to acidify the media (which contains phenol red as an indicator). This is the opposite of observations made in a previous report (Bota & Davies, 2002).

Using an oxygen-sensitive fluorescent probe (Hynes *et al.*, 2009) and timed media exposures, we were able to quantify oxygen consumption, lactate production and glucose uptake concurrently (although on different plates) (Figures 4.5 and 4.6). ATP was measured to determine if there was a shift in overall available cellular energy. Using this approach, we were able to determine that Lon knockdown produced an overall increase in oxygen consumption, whilst utilising less glucose and producing less lactic acid. ATP was not significantly altered. Whilst the oxygen consumption increased, the maximum oxygen consumption rate attainable in the absence of glucose was not significantly different between control and knockdown cells, suggesting that the capacity for oxygen consumption was not intrinsically different. These results were consistent across two cell lines MCF7 and U87 (Figure 4.5 for U87 and Figure 4.6 for MCF7). The second siRNA (siLonp1.2) in U87 cells did not produce significant changes in glucose uptake or lactate production, likely due to the smaller effect that targeting Lon had in these cells compared to MCF7 cells.

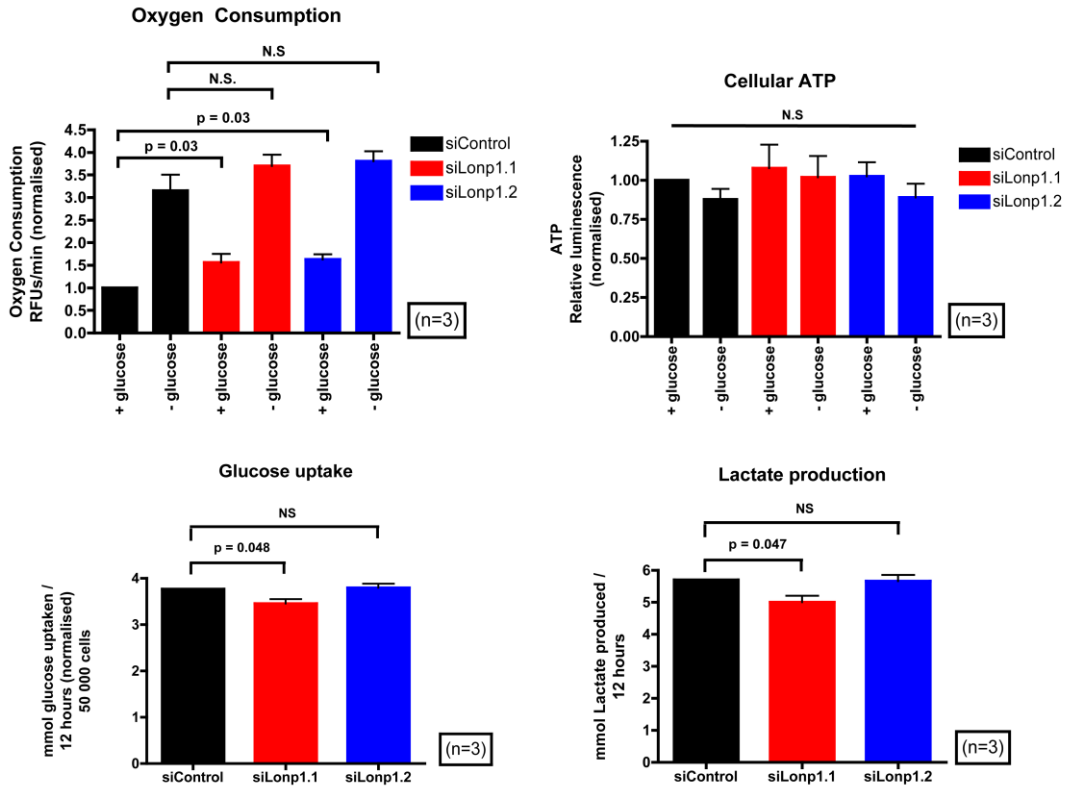

Figure 4.5 Reducing levels of Lon by siRNA in U87 cells increases oxygen consumption, decreases glucose uptake and lactate production without affecting overall ATP levels. For details, see Figure 4.6.

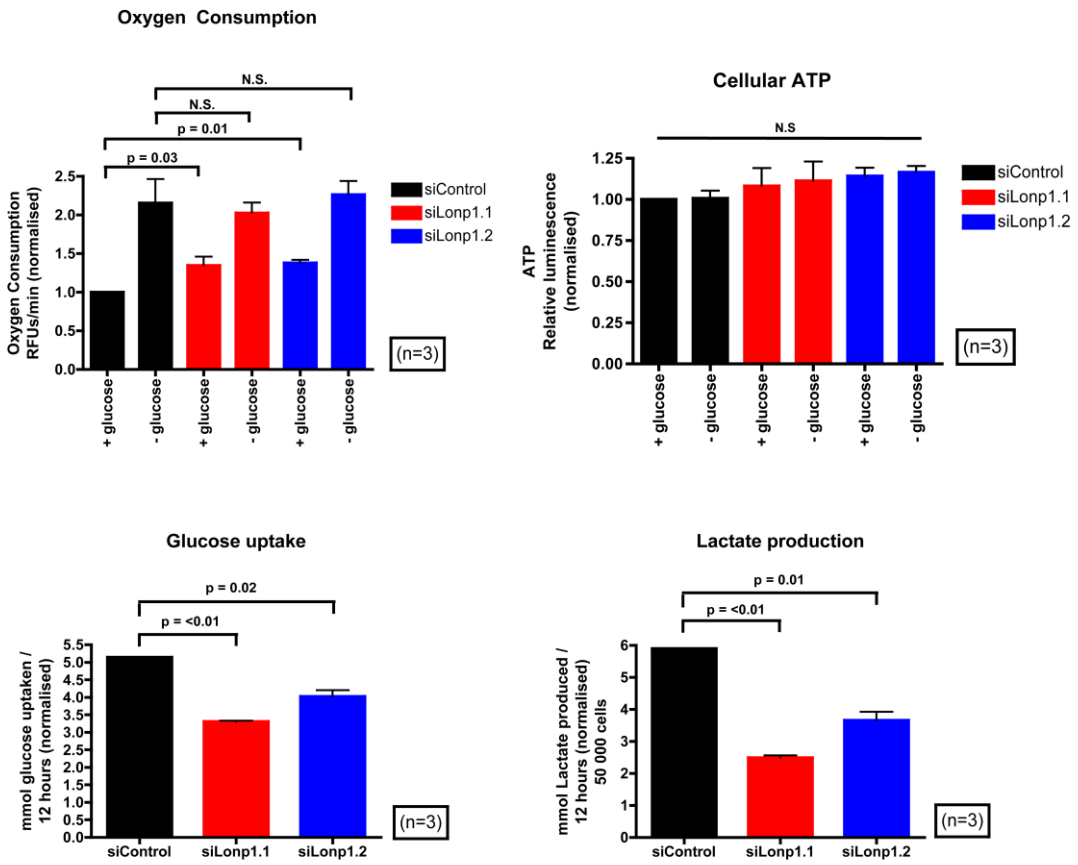

Figure 4.6 Reducing levels of Lon by siRNA in MCF7 cells increases oxygen consumption, decreases glucose uptake and lactate production without affecting overall ATP levels. Graphs show the means of three independent experiments, error bars indicate standard deviation and *p* values quoted are the result of unpaired Student's t-tests. Normalisation is by absolute cell numbers as detemined by CyQUANT assay which measures DNA content.

Targeting Lon by siRNA elicits changes in mitochondrial morphology in MCF7 cells expressing a mitochondrial targeted fluorescent protein

As we had seen changes in basal oxygen consumption, and hypoxia has been reported to influence mitochondrial morphology (Chiche *et al.*, 2010), we used MCF7 cells constitutively expressing mitochondrial-tagged red fluorescent protein to perform live cell confocal imaging of mitochondria, with and without Lon protease. We found that cells treated with siRNA against Lon showed mitochondria which were more interconnected and tubular, whilst those in control cells were more rounded and fragmented from the main mitochondrial

mass (Figure 4.7). A similar change in appearance has been described to be associated with HIF-α subunit stabilisation: 786-o cells, deficient in VHL activity, show enlarged mitochondria which revert to a tubular network when VHL is re-expressed (Chiche *et al.*, 2010).

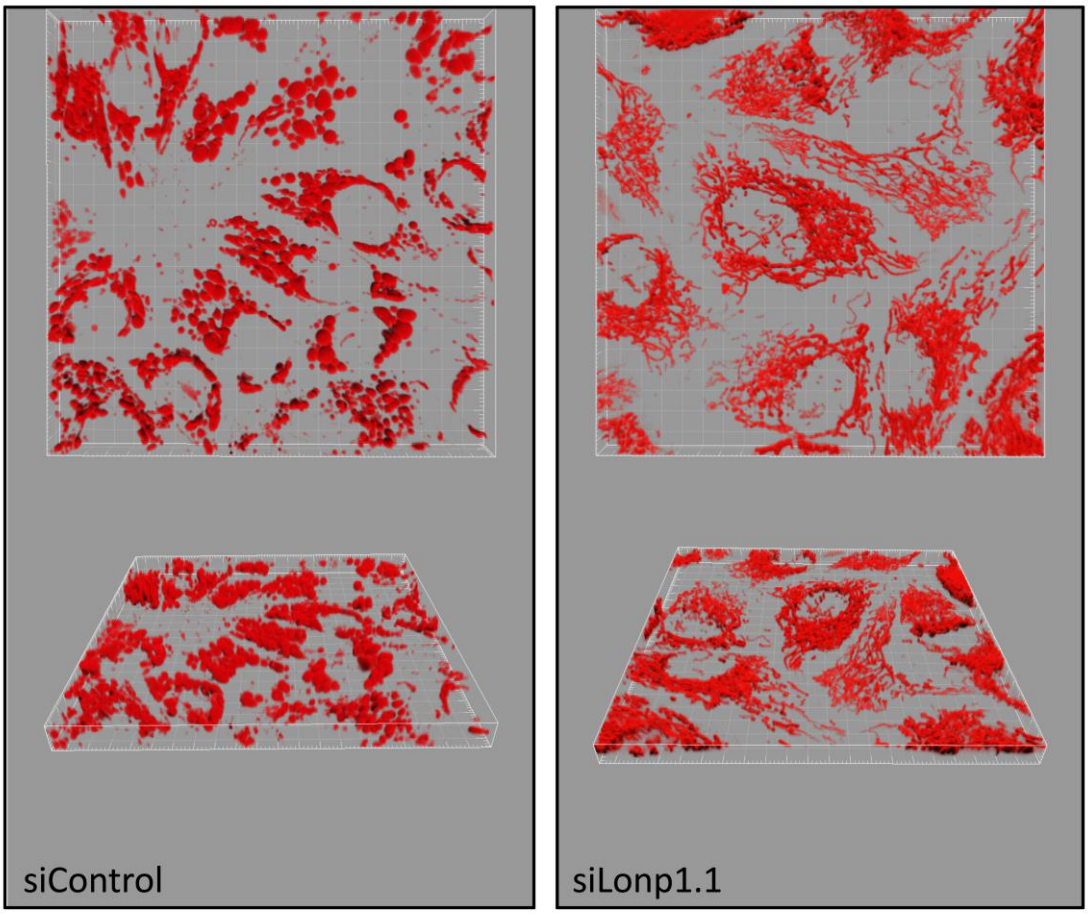

Figure 4.7 Targeting the Lon protease causes mitochondrial to become more interconnected, effectively increasing mitochondrial length. MCF7 cells stably expressing a mitochondrial-targeted fluorescent protein (dsRed2) were transfected with either siRNA targeting Lon protease (siLonp1.1) or non-targeting control (siControl) and imaged live using a laser-scanning confocal microscope. Stacked images were rendered into three-dimensional pictures (top). Mid-cell sections were used for quantification of longest mitochondrial elements (10) per cell (bottom). Mean of three biologic replicates is represented in bar chart. Error bars indicate standard deviation and *p* value quoted is the result of unpaired Student's t-test.

Discussion

Targeting Lon by stable expression of shRNA reduces HIF-1α stabilisation in normoxia and hypoxia

In Chapter 3 we demonstrated that, despite reducing Lon levels to undetectable levels, some siRNA sequences could reduce stabilised HIF-1α in normoxia with varying efficacy (Figure 3.2). This observation was consistent with effects on HIF-α stability requiring a high efficacy of Lon knockdown. We were able to reduce HIF-1α stability with shRNA (sh03) targeted against the Lon protease, whilst another sequence (sh04) did not show this change in western blotting lysed cells, cultured in plates in normoxia and hypoxia (in U87, MCF7 and MDA-MB-468 cells). When we embedded and sectioned MDA-MB-468 spheroids stably expressing shRNA targeting the Lon protease (Figure 4.4), we saw reductions in HIF-1α and CA9 in all but the most central (hypoxic) areas of spheroids for both Lon shRNA sequences (sh03 and sh04), whereas western blotting in plates showed effects only on HIF-1α (and CA9) for sh03.

The spheroid model, with a gradient of hypoxia, may be more suited to demonstrating subtle effects on HIF-α stabilisation that may not be apparent when cells are simply either cultured in normoxia or 1% hypoxia. Demonstrating that HIF-1α expression can be decreased with reducing levels of Lon by shRNA (as opposed to siRNA) additionally suggests that this effect is not transient.

Reducing levels of Lon can inhibit proliferation, but appears to be cell line dependent

To determine effects on growth, we stably knocked down the Lon protease with shRNA and cultured in normoxia and hypoxia. Inhibition of growth with Lon knockdown was seen most prominently in U87 cells, followed by significant reductions in MDA-MB-468, and no effect was seen in MCF7 cells. The reductions in growth with Lon knockdown, where present, were seen in normoxia and hypoxia, and in spheroid growth assays.

Previous studies have reported inhibited growth with depletion of Lon protease in human lung fibroblasts (Bota *et al.*, 2005). Lon knockdown also inhibits growth and promotes death in Granta cells (mantle cell lymphoma cell lines) while having no effect on LS174T (colorectal carcinoma) cells (Bernstein *et al.*, 2012).

The reason for cell-specific sensitivity to Lon depletion is not clear. There is a reduction in HIF-1α stabilisation in MCF7 cells, suggesting that the growth inhibition is not dependent on HIF-α levels with Lon knockdown. Also, U87 cells with reduced Lon levels but no apparent differences in HIF-1α stabilisation (sh04) still show severe reductions in proliferation. Mitochondrial toxicity may affect some cell lines more than others, and this may be related to a differential accumulation of toxic modified mitochondrial proteins, or the accumulation of regulatory proteins such as StAR or TFAM (Granot *et al.*, 2007) (Lu *et al.*, 2012).

The inability to propagate Lon deficient MDA-MB-468 and U87 cells was the primary reason not to investigate the growth in *in vivo* xenograft models. These cell lines eventually gave rise to resistant clones, necessitating the transduction and use of newly-created Lon deficient cells for each experiment.

Lon expression in tumour cells contributes to the Warburg effect

Reducing levels of Lon using siRNA had minimal effects on toxicity and proliferation, likely due to the transient knockdown effect of siRNA. We did notice, however, that there was a failure to acidify the media with siRNA targeted against Lon, leading us to investigate this metabolic phenotype. Despite no alterations in overall energy (by measurement of ATP), we determined that oxygen consumption increased, and lactate production and glucose consumption were decreased, in cells deficient in Lon. These measurements are consistent with a partial reversal of the Warburg effect, i.e. a switch from aerobic glycolysis to oxidative phosphorylation.

The switch to oxidative phosphorylation with depletion of Lon is not the expected consequence of removing a key enzyme involved in protein quality control in the mitochondrial matrix. Indeed it has been previously reported that lung fibroblasts treated with Lon antisense oligonucleotide have severely reduced rates of oxygen consumption (Bota *et al.*, 2005). Also, yeast deficient for Lon are also unable to grow on a non-fermentale carbon source (Guha *et al.*, 2011). This effect may be dependent on cell type, and we report the first metabolic changes with depletion of Lon in cancer cell lines.

The transcriptional effect of HIF target genes is responsible, in part, for the switch to aerobic glycolysis. HIF-1 activates the transcription of glucose transporters (GLUT1 and GLUT3), the enzyme required to convert glucose to glucose-6-phosphate (G6P) (hexokinase), the enzyme required for the subsequent conversion to 6-phosphogluconolactone to support the pentose phosphate shunt (G6PD), and the enzyme required to support the conversion of pyruvate into lactate (LDHA) (Semenza, 2010b). In addition, HIF-1 activates the transcription of pyruvate dehydrogenase kinase-1 (PDK-1), which phosphorylates and inactivates pyruvate dehydroxgenase (PDH), a key enzyme which converts pyruvate to acetyl coenzyme A for entry into the TCA cycle (Kim *et al.*, 2006) (Papandreou *et al.*, 2006). To facilitate the metabolic shift to glycolysis, HIF-1 also promotes efficient lactacte transport out of the cell via transcription of MCT4 (Ullah *et al.*, 2006) and enzymes involved in the maintenance of pH regulation (CA9 and CAXII) (Wykoff *et al.*, 2000). In this way, reducing levels of stabilised HIF-α subunits by reducing levels of Lon may be sufficient to reverse the switch to aerobic glycolysis.

Besides HIF-1, activated oncogenes (MYC and RAS) and activation of the PI3K/Akt/mTOR pathway can promote the switch in cellular energetics to favour glycolysis (Gillies *et al.*, 2008). Pyruvate has been shown to stabilise HIF-1α and promote glycolysis (Lu *et al.*, 2002), raising the possibility that Lon may affect HIF-α stability secondary to re-activation of the TCA cycle.

Reducing levels of Lon promotes the formation of tubular mitochondria

We found that reducing the levels of Lon in MCF7 cells caused a more tubular and interconnected mitochondrial network in cells constitutively expressing a mitochondrial targeted fluorescent protein. Mitochondrial networks are shaped through the regulated events of fusion, fission, distribution and autophagy (Palmer *et al.*, 2011). A small number of proteins have been described to be involved in shaping mitochondrial morphology (such as the mitochondrial fusion proteins Mfn1 and OPA1) (Cipolat *et al.*, 2004).

Of the mitochondrial proteins that shape mitochondrial morphology, only one has any evidence for a potential interaction with the Lon protease. The mitochondrial chaperone DnaJA3 (Tid1) induces mitochondrial fragmentation when either overexpressed or depleted and this effect is dependent on the DnaJ domain and fission factor dynamin-related protein 1 (Drp1) (Elwi *et al.*, 2012). DnaJA3 is a J-protein that promotes the ATPase activity of mtHSP70 and the two co-operate to refold aggregated proteins (Iosefson *et al.*, 2012). In bacteria, the DnaJA3 homologue DnaJ co-operates with Lon to degrade some proteins that cannot be refolded (keeping them in a soluble form) (Jubete *et al.*, 1996).

If Lon was responsible for the degradation of Drp1 (possibly with the chaperone activity of DnaJA3), one would expect an accumulation of this protein when Lon was depleted. Drp1 promotes mitochondrial fission (Smirnova *et al.*, 2001) and we saw a phenotype that resembles increased mitochondrial fusion (Figure 4.7). In reality, Lon is likely to have a large number of uncharacterised substrates and

chaperone partners, some of which may be recognised (or are yet to be recognised) as being involved in shaping mitochondrial morphology.

Morphological changes in mitochondria are induced in hypoxia in a HIF-1 dependent manner (Chiche *et al.*, 2010). In 786-o cells, with deficient VHL activity, mitochondria are enlarged, and these revert to a more tubular form when VHL activity is reintroduced (Chiche *et al.*, 2010). Together, we conclude that Lon can affect the morphology of mitochondria, and this may be related to alterations in normoxic HIF-α subunit stability.

The expected effect of small-molecule inhibition of Lon protease function in tumours

From the results presented in this chapter, we conclude that targeting the Lon protease in tumour cells can severely inhibit tumour cell proliferation in a cell-dependent manner, reverse the glycolytic phenotype of tumour cells, inhibit hypoxic signalling and potentially alter mitochondrial morphology. One unanswered question, however, is whether these phenotypic effects are related to the chaperone or proteolytic activites of Lon. In terms of designing a therapeutic against Lon, this may not matter, since inhibiting the ATPase activity of Lon will inhibit both chaperone and proteolytic activities of the enzyme (van Dijl *et al.*, 1998). Whilst the growth effects of Lon are dependent on cell-line, it appears that reducing levels of Lon inhibits growth, independent of effects on HIF-α stability. It is not clear however, whether reducing Lon affects aerobic glycolysis secondary to changes in HIF transcriptional activity.

In conclusion, we predict that inhibiting the Lon protease would have a substantial anti-tumour effect, both by directly inhibiting growth, and by indirectly inhibiting hypoxic signalling – reducing invasion, metastasis and angiogenesis.

Chapter 5 : Proline-hydroxylated hypoxia-inducible factor 1α (HIF-1α) upregulation in human tumours

We have determined that Lon can promote stabilisation of the proline-hydroxylated form of HIF-1α (Chapter 3). In this chapter we sought to determine whether proline-hydroxylated HIF-1α existed in tumour cells and, thus, whether targeting the Lon protease would have an effect on HIF signalling in human tumours.

Overview

The stabilisation of HIF-α is central to the transcriptional response of animals to hypoxia, regulating the expression of hundreds of genes, including those involved in angiogenesis, metabolism and metastasis. *In vitro*, under conditions of hypoxia, HIF proline hydroxylation is limited, so that HIF is not recognised and ubiquitinated by the von-Hippel-Lindau (VHL) E3 ligase complex. The aim of our study was to investigate the post-translational modification of HIF-1α in tumours, to assess whether there are additional mechanisms besides reduced hydroxylation leading to stability. To this end we optimised antibodies against the proline-hydroxylated forms of HIF-1α for use in formalin fixed paraffin embedded (FFPE) immunohistochemistry to assess effects in tumour cells *in vivo*. We found that HIF-1α, proline-hydroxylated at both VHL binding sites

(Pro402 and Pro564), was present in hypoxic regions of a wide range of tumours, tumour xenografts and in moderately hypoxic cells *in vitro.* Staining for hydroxylated HIF-1α can identify a subset of breast cancer patients with poorer prognosis, similar to total HIF-1α levels. The expression of proline-hydroxylated HIF-1α does not correlate with levels of the proline hydroxylase enzymes or VHL in breast cancer. Our conclusions are that the degradation of proline-hydroxylated HIF-1α may be rate-limited in tumours and therefore provides new insights into mechanisms of HIF upregulation. The persistence of proline-hydroxylated HIF-1α in perinecrotic areas suggests there is adequate oxygen to support PHD activity, and proline-hydroxylated HIF-1α may be the predominant form associated with the poorer prognosis that higher levels of HIF-1α confer.

Introduction

The activation of hypoxic signalling has a critical role in the pathogenesis of solid malignancies. Hypoxia-inducible factor 1 (HIF-1) consists of HIF-α and HIF-β subunits which heterodimerise and bind to discrete HIF-binding response elements in DNA, which in turn mediate changes in transcription. In hypoxia, the increased activity of HIF-1 leads to the increased transcription of multiple genes (Mole *et al.*, 2009) involved in genetic instability (Huang *et al.*, 2007), angiogenesis (Couvelard *et al.*, 2005), metabolism (Finley *et al.*, 2011), pH regulation (Swietach *et al.*, 2007), invasion, metastasis, epithelial-mesenchymal transition (Lu & Kang, 2010) and radiation resistance (Moeller *et al.*, 2007). The

HIF transcriptional responses have been largely attributed to HIF-1α and HIF-2α, although there is a third HIF-α subunit, HIF-3α (Makino *et al.*, 2002).

The HIF-α isoforms are normally efficiently degraded under normoxic conditions. This process firstly requires that HIF-1α is hydroxylated at one of two proline sites within two oxygen-dependent degradation domains (NODD Pro402, CODD Pro564), as catalysed by one or more of the three members of the prolyl hydroxylase domain (PHD) isoforms. Hydroxylation of either proline residue renders HIF-α susceptible to binding by the von Hippel-Lindau tumour suppressor (pVHL) E3 ligase complex, leading to ubiquitination and degradation by the proteasome (Jaakkola *et al.*, 2001). In hypoxia, HIF-1α and/or HIF-2α accumulate. One cause of this accumulation is that the PHDs are inhibited in hypoxia (Kaelin & Ratcliffe, 2008). In a second method of oxygen-dependent regulation of HIF activity, an aspargine residue in the *C*-terminal transactivation domain of HIF-α is hydroxylated by factor inhibitor HIF (FIH), a process that reduces binding of HIF to transcriptional coactivators.

Whether HIF-1α requires one or both proline sites hydroxylated *in vivo* in order to be efficiently degraded is not clear. Cells deficient in HIF-1α that are subsequently transfected with HIF-1α, with either proline sites substituted within the *C*- and *N*-terminal ODD, show approximately equal amounts of increased stability and reduced upregulation in hypoxia. If both proline sites are substituted, HIF-1α shows further increases in stability and no induction in hypoxia (Masson *et al.*, 2001) (Chan *et al.*, 2005). The ODD domain of HIF-1α with both proline sites mutated fused to *E.coli* cytosine deaminase can still

undergo VHL-dependent degradation, suggesting additional mechanisms of regulation to those for which hydroxylation is essential (Chan *et al.*, 2005). The *C*- and *N*- terminal proline sites have different susceptibilities to hypoxia such that Pro402 hydroxylation is inhibited under higher oxygen tensions than Pro564 (Tian *et al.*, 2011b). The observation of accumulated HIF-1α hydroxylated at Pro564 in cells under hypoxia suggests that VHL-mediated degradation may, at least under some conditions, be dependent on recognition of hydroxylation within the NODD (Tian *et al.*, 2011b).

In cell culture, inhibition of HIF-1α proline-hydroxylation requires levels of hypoxia below 1% oxygen (Tian *et al.*, 2011b), whilst the accumulation of HIF-1α is seen to exponentially rise below 6% oxygen (Jiang *et al.*, 1996). The kinetic properties of the PHDs, in particular PHD2, are proposed to be related to their roles as oxygen sensors. PHD2 has an apparently slow reaction with oxygen (Flashman *et al.*, 2010). However, it is notable that the K_m (oxygen) for PHD activity using recombinant enzymes is well above (100μM) the 10-30μM oxygen levels typically available to tissues (Ehrismann *et al.*, 2007) (Kaelin & Ratcliffe, 2008). Although in cells it is the overall flux through the pathways that is important, this observation suggests that PHD-independent mechanisms for HIF-α degradation may be relevant.

Modulators of PHD activity, beside oxygen, have been described; these may account, at least in part, for the disparities between the biochemical properties of the PHDs and the observed HIF-1α levels. These modulators include mitochondrial derived reactive oxygen species (ROS) (Finley *et al.*, 2011)

(Masson *et al.*, 2012), elevated levels of Krebs cycle intermediates such as succinate and fumarate (Selak *et al.*, 2005) (Hewitson *et al.*, 2007), iron and ascorbate (Knowles *et al.*, 2003). Although these factors can affect hydroxylation of HIF-1α, whether they modulate the degrading activity of the VHL-containing complex is not clear. Other factors can also affect the amount of HIF-1α available for transcription. These include increased HIF-1α production by activated mTOR signalling (Del Bufalo *et al.*, 2006) and VHL-independent degradation by heat shock protein 70 (Hsp70) and carboxyl terminus of HSP-interaction protein (CHIP) (Luo *et al.*, 2010).

In this study, we aimed to determine if proline-hydroxylated HIF-1α formed a component of upregulated HIF-1α expressed *in vivo* in tumours. As HIF-1α in reoxygenated tissue has a half-life of less than one minute (Yu *et al.*, 1998), we would not expect to see this unless there were other factors that regulate degradation.

In order to assess expression of proline-hydroxylated HIF-1α, we have validated commercially available hydroxylation-specific antibodies against the two proline-hydroxylation sites in HIF-1α for use in FFPE immunohistochemistry. These antibodies have previously been validated for their use in western blotting (Tian *et al.*, 2011b). Although not directly quantitative, we found that a proportion of HIF-1α in tumours was indeed hydroxylated, at both proline hydroxylation sites, revealing that the PHD-independent degradation processes are limiting. In addition, the expression of hydroxylated HIF-1α, as well as total HIF-1α, was predictive of poorer prognosis in breast cancer.

Materials and methods

Cells and culturing conditions

MCF7, 786-O, RCC4, U87, HCT-116 and MDA-MB-468 cells were cultured in DMEM (Lonza), supplemented with 10% foetal calf serum (Life Technologies) and 2 mM L-glutamine. MCF7 cells were treated with 1mM dimethyloxalylglycine (DMOG) (Sigma-Aldrich), 10mM of the proteasome inhibitor MG-132 (Millipore) or DMSO alone for four hours. RCC4 cells stably expressing a wild-type VHL (RCC+VHL) or empty vector (RCC-VHL) have been previously described (Maxwell *et al.*, 1999). Tumour spheroids were created from cell lines by plating cells in non-adherent round-bottomed 96-well dishes (Corning) and centrifuging at 2000xG for 10 minutes.

Cell pellet preparation

Cells were trypsinised, pelleted and washed, prior to resuspension in 10% neutral-buffered formalin for 24 hours. The formalin was removed and cells were then resuspended in 2% molten agarose dissolved in 10% formalin. The cells and agarose suspension was then centrifuged in a 1.5ml tube and transferred to ice to form a cell pellet. The pellet was removed from the tube and placed within a cassette for overnight processing, after which the pellet was wax embedded and sectioned.

Plasmid mutagenesis and transfection

The full-length HIF-1α expression vector was purchased from OriGene. The P402A mutation was produced by using the Quikchange site-directed mutagenesis kit XL (Stratagene) and the primers CTCCAGCGGCTGCGGCCAGCAAAGT (Forward) and ACTTTGCTGGCCGCAGCCGCTGGAG (Reverse). The P564G mutation was generated in the same way using the primers TAGACTTGGAGATGTTAGCTGGCTATAGCCCAATGGATGATG (Forward) and CATCATCCATTGGGATATAGCCAGCTAACATCTCCACGTCTA (Reverse). Primers were purchased from Eurogentec. Cells were transfected using Turbofect (Thermo Scientific) according to the manufacturer's protocol.

Mouse xenografts

Mice were housed at the Cancer Research UK Laboratories (Clare Hall) or at the Biomedical Sciences department (University of Oxford), and all procedures were carried out under a Home Office license. Cells were injected into the flank of BALB/c *nu/nu* mice subcutaneously. Mice were sacrificed when tumours reached 1.44 cm^3 by cervical dislocation. Tumours were excised, fixed in 10% formalin overnight, cut-up and processed in the same way as resected human diagnostic tissue.

Antibodies

The antibody against HIF-1α, insensitive to hydroxylation, was a mouse monoclonal from BD Biosciences (Catalogue Number 610958). Hydroxylation-

specific HIF-1α antibodies were raised in rabbit; P402 was from Millipore (07-1585) and P564 from Cell Signaling Technologies (3434S). Antibodies against PHD-1, PHD-2 and PHD-3 were previously produced and characterised by this group (Soilleux *et al.*, 2005). The antibody against VHL for immunohistochemistry was a mouse monoclonal from BD Biosciences (Catalogue Number 556347) and for western blotting was from Cell Signaling Technologies (2738S).

Immunohistochemistry

4μM sections of cells and tissue were deparaffinised and antigen retrieved in Target Retrieval Solution (S1699, Dako), using a Biocare decloaking chamber. Sections were blocked with 2.5% normal horse serum for 30 minutes and then incubated with primary antibody diluted in RPMI overnight at 4°C. Dilutions for primary antibodies used were: anti-HIF-1α total 1:100; anti-hydroxylated HIF-1α P402 1:1000; anti-hydroxylated HIF-1α P564 1:800; anti-VHL 1:500. Bound antibody was detected using the Novalink Polymer Detection System (Leica) for mouse antibodies and the two-step rabbit HRP polymer (Menarini Diagnostics) for rabbit antibodies, counterstained with haematoxylin. Conditions for PHD staining were as previously described.

Patient Material

Formalin-fixed paraffin-embedded (FFPE) tumour tissue from 109 patients with head and neck cancer, 144 patients with breast cancer, 20 patients with lung cancer and 47 patients with bladder cancer was assembled into tissue

microarrays (TMAs) as described previously (Bubendorf *et al.*, 2001). Local ethical committee approval was obtained for the use of de-identified patient material (CO2.216 and 09/H0606/5 for breast cancer).

Immunoblots

Cells were lysed on the bench (for normoxic samples) or within the hypoxic chamber (for hypoxic samples) with equilibrated Complete Lysis-M with protease inhibitors (Roche), and quantified using the BCA assay kit (Pierce). Protein was separated using Novex Bis-Tris 4-12% gels (Life technologies) and transferred to nitrocellulose membrane. Membranes were blocked with 5% non-fat milk powder dissolved in PBS-T, and incubated with primary antibodies overnight.

Cell line sequencing data

The data was obtained from the Wellcome Trust Sanger Institute Cancer Genome Project web site, http://www.sanger.ac.uk/genetics/CGP.

Results

HIF-1α proline hydroxylation in cancer cell lines in hypoxia

Initially, we tested a panel of cell lines to determine whether cells *in vitro* showed increased quantities of proline-hydroxylated HIF-1α at physiologically relevant levels of hypoxia. Cells were grown and lysed within a hypoxic chamber at 1% atmospheric oxygen using equilibrated buffers. HIF-1α proline hydroxylation was determined using antibodies specific for each proline-hydroxylation site (Figure 5.1) (Tian *et al.*, 2011b).

We found that, at 1% oxygen, there was a diverse pattern of proline-hydroxylation of HIF-1α between different cell lines. At these conditions, RCC4 cells, deficient in VHL activity (RCC4-VHL), showed inhibition of hydroxylation at Pro402, but not at Pro564. RCC4 cells with active VHL (RCC4+VHL) demonstrated robust induction of total HIF-1α in hypoxia, with a slight increase in the hydroxylated form at Pro564 and Pro406. MDA-MB-468 cells showed increased hydroxylated HIF-1α just at Pro564, whereas HCT-116 showed large increases in total HIF-1α, which was not accompanied by increases in proline hydroxylation at either site. MCF7 cells showed an increase in total HIF-1α in hypoxia that was accompanied by a decrease in the amount of proline-hydroxylated HIF-1α at Pro564, with none detectable at Pro406. U87 cells showed increased proline-hydroxylated HIF-1α at both Pro564 and Pro406, and a slight decrease in total HIF-1α.

We assessed whether the differences in induction in hydroxylated HIF-1α were associated with levels of the PHD enzymes, VHL, or Lon. Consistent with previous reports, PHD1 was expressed at very low levels (Appelhoff *et al.*, 2004). PHD2 levels were mildly induced by hypoxia in HCT-116 and MCF7 cells. PHD3 was strongly upregulated by hypoxia in all cell lines (apart from RCC4+VHL). VHL levels were not significantly altered in hypoxia. No correlation between the pattern of hydroxylated HIF-1α accumulation and levels of PHD enzymes, Lon or VHL was identified.

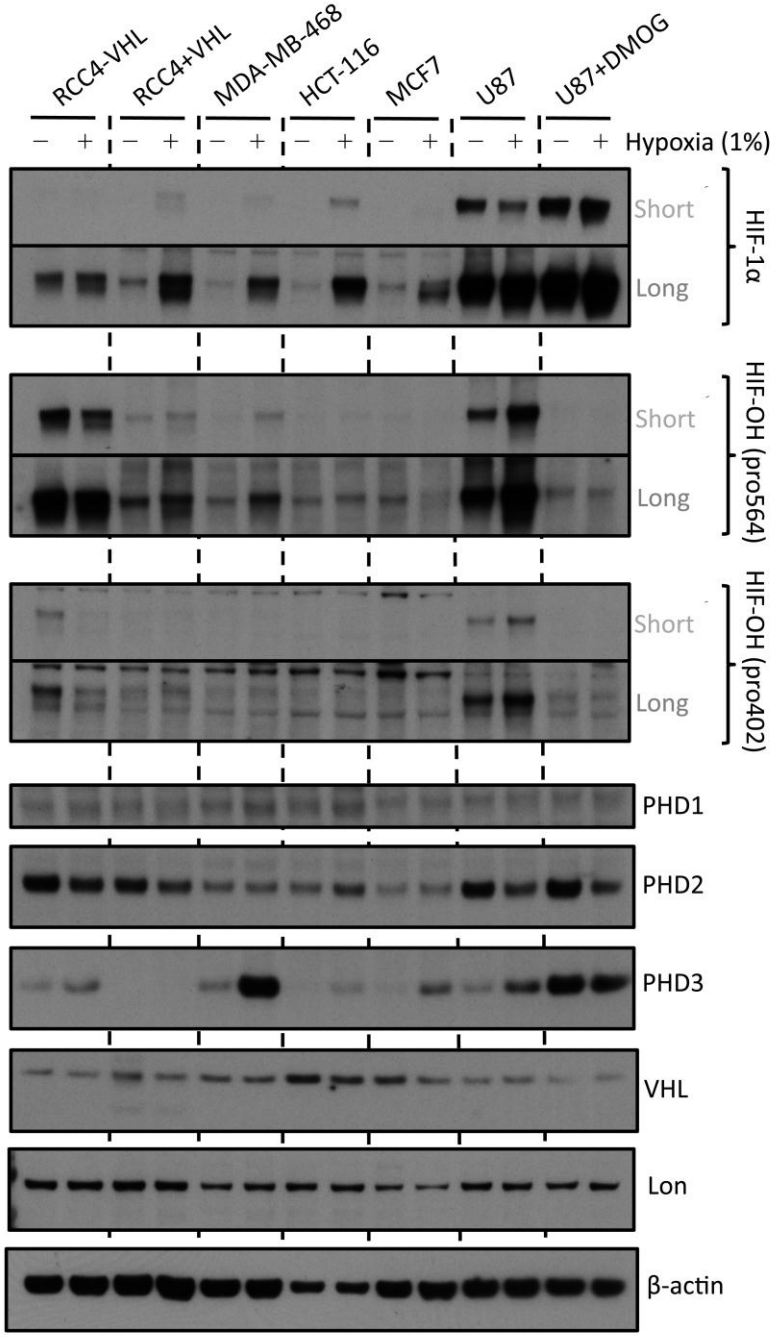

Figure 5.1 Cell lines show a heterogenous pattern of induction of the expression of proline-hydroxylated HIF-1α in moderate (1%) hypoxia. A panel of cell lines were incubated in 1% hypoxia for 16 hours, and probed with the indicated antibodies by western blot.

Validation of proline-hydroxylated specific HIF-1α antibodies

In order to determine that HIF-1α antibodies were specific for the hydroxylated form for use in immunohistochemistry, we treated MCF7 cells with a cell-penetrating prodrug form of a 2-oxoglutarate oxygenase / PHD inhibitor (dimethyloxalylglycine, DMOG) and the proteasomal inhibitor MG132. The cells were fixed and processed in the same way as tissue samples. The hydroxylated-specific antibodies recognised only HIF-1α that accumulated with proteasomal inhibition, and not that which accumulated with PHD inhibition, whereas the total HIF-1α antibody recognised the hydroxylated and non-hydroxylated forms (Figure 5.2A.). It can be assumed that the HIF-1α that accumulated with MG-132 treatment was entirely hydroxylated (since this modification is the target for the ubiquitinating complex with VHL), though the staining with the hydroxylated-specific antibodies was weaker than the total HIF-1α antibody. This indicates that the hydroxylated HIF-1α antibodies are less sensitive than the total HIF-1α antibody.

To investigate whether each hydroxy-specific antibody was specific to the individual prolines in HIF-1α, we used 786-o cells that are defective in VHL and have a HIF-1α homozygous deletion. We transfected a full length HIF-1α construct into these cells, one with a mutated proline 402 (P402A) and another with a mutated proline 564 (P564G). The hydroxy-specific antibodies did not bind when their respective proline sites were mutated (Figure 5.2B.) Mutation of either proline did not affect the hydroxylation of the other proline or the ability of these to be detected. 786-o cells have high levels of HIF-2α (Maxwell *et al.*, 1999), and the lack of staining with hydroxy-specific antibodies in cells

transfected with mutant plasmids shows there is no appreciable cross-reactivity to hydroxylated HIF-2α. The binding location of the total HIF-1α antibody is between proline 610 and serine 727. The location of antibody binding in relation to HIF-1α domains is illustrated in Figure 5.2C.

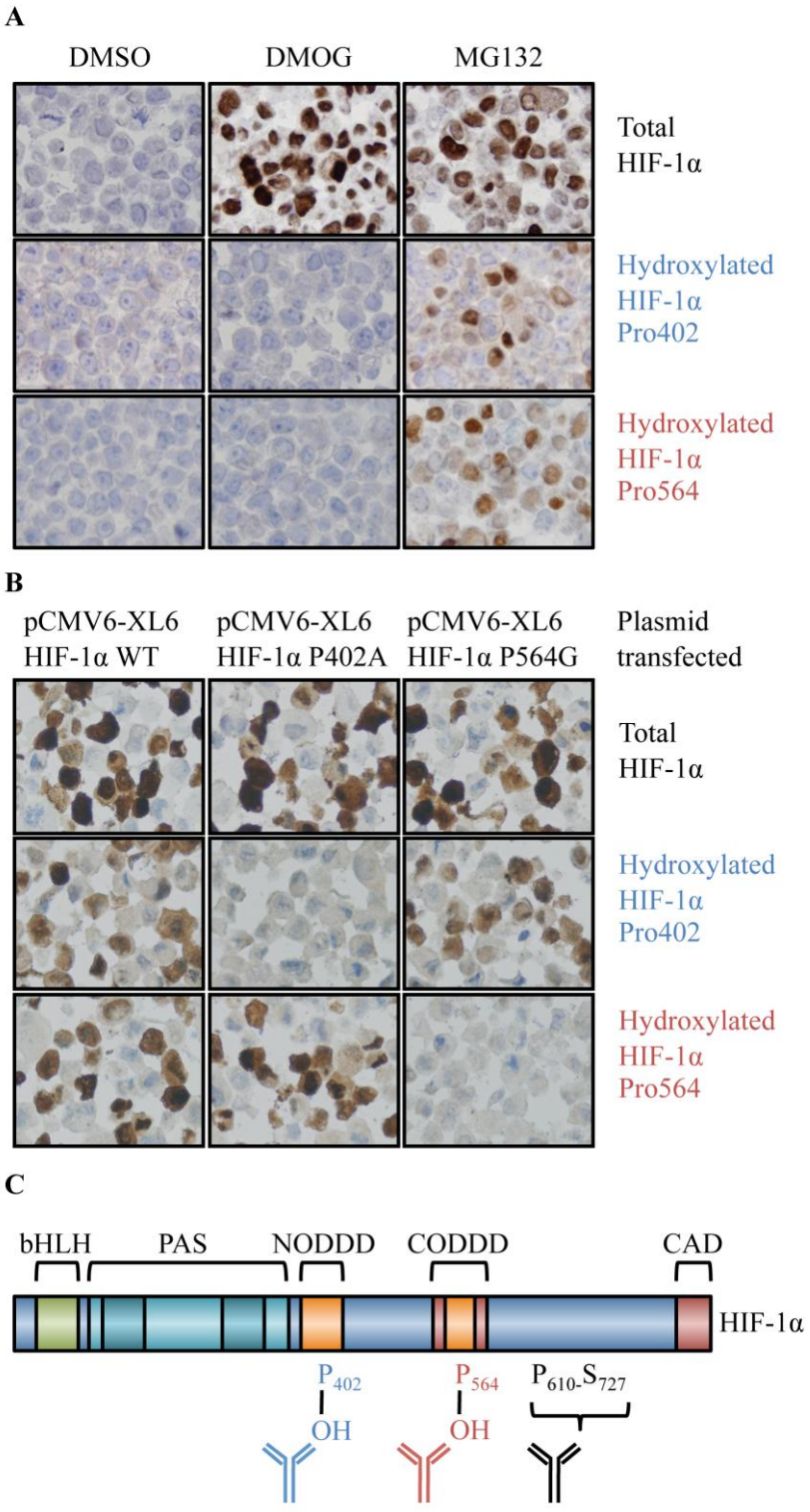

Figure 5.2 Validation of proline-hydroxylated HIF-1α specific antibodies on formalin-fixed paraffin embedded cell pellets. A. MCF7 cells treated with vehicle (DMSO), DMOG or MG132 and probed with the indicated antibodies. **B.** 786-o cells transfected with either HIF-1α WT, P402A or P564G and probed with the indicated antibodies. **C.** Domain structure of HIF-1α and antibody binding regions. The figure highlights: basic helix-loop-helix (bHLH) domains; PAS domain; the amino-terminal oxygen-dependent degradation domain (NODDD); the carboxy-terminal oxygen-dependent degradation domain (CODDD) and the carboxy-terminal activation domain (CAD).

Expression of proline-hydroxylated HIF-1α in tumour models

Having established the specificity of hydroxylated HIF-1α antibodies, we determined the expression *in vitro* and *in vivo* in tumour models. Two cell lines (U87 and MDA-MB-468) derived from glioblastoma and breast adenocarcinoma were used, and both have wild-type VHL, as determined by sequencing. In tumour spheroids, U87 cells showed an accumulation of HIF-1α substantially hydroxylated at both Pro402 and Pro564 (Figure 5.3.). MDA-MB-468 cells show a greater degree of central necrosis when cultured as spheroids. There was significant accumulation of hydroxylated HIF-1α at Pro564, though hydroxylation at Pro402 was not detected. The hydroxylation at Pro564 extended up to the necrotic core of the spheroid.

In U87 xenografts, hydroxylated HIF-1α at Pro402 and Pro564 showed increasing staining towards the necrotic areas, similar in pattern to that of total HIF-1α (Figure 5.3.). Cells that juxtapose necrosis show the strongest hydroxylated HIF-1α staining at both proline hydroxylation sites. The intensity of staining is less for the hydroxylated HIF-1α antibodies, consistent with being less sensitive than total HIF-1α staining. Areas of tumour close to blood vessels were negative for both total and hydroxylated HIF-1α. Tumour xenografts created from MDA-MB-468 cells showed the same pattern as that seen in spheroids. There was increased hydroxylated HIF-1α at Pro564, but none detectable at Pro406. The hydroxylated HIF-1α was observed to extend to the viable cells that juxtaposed the necrotic area.

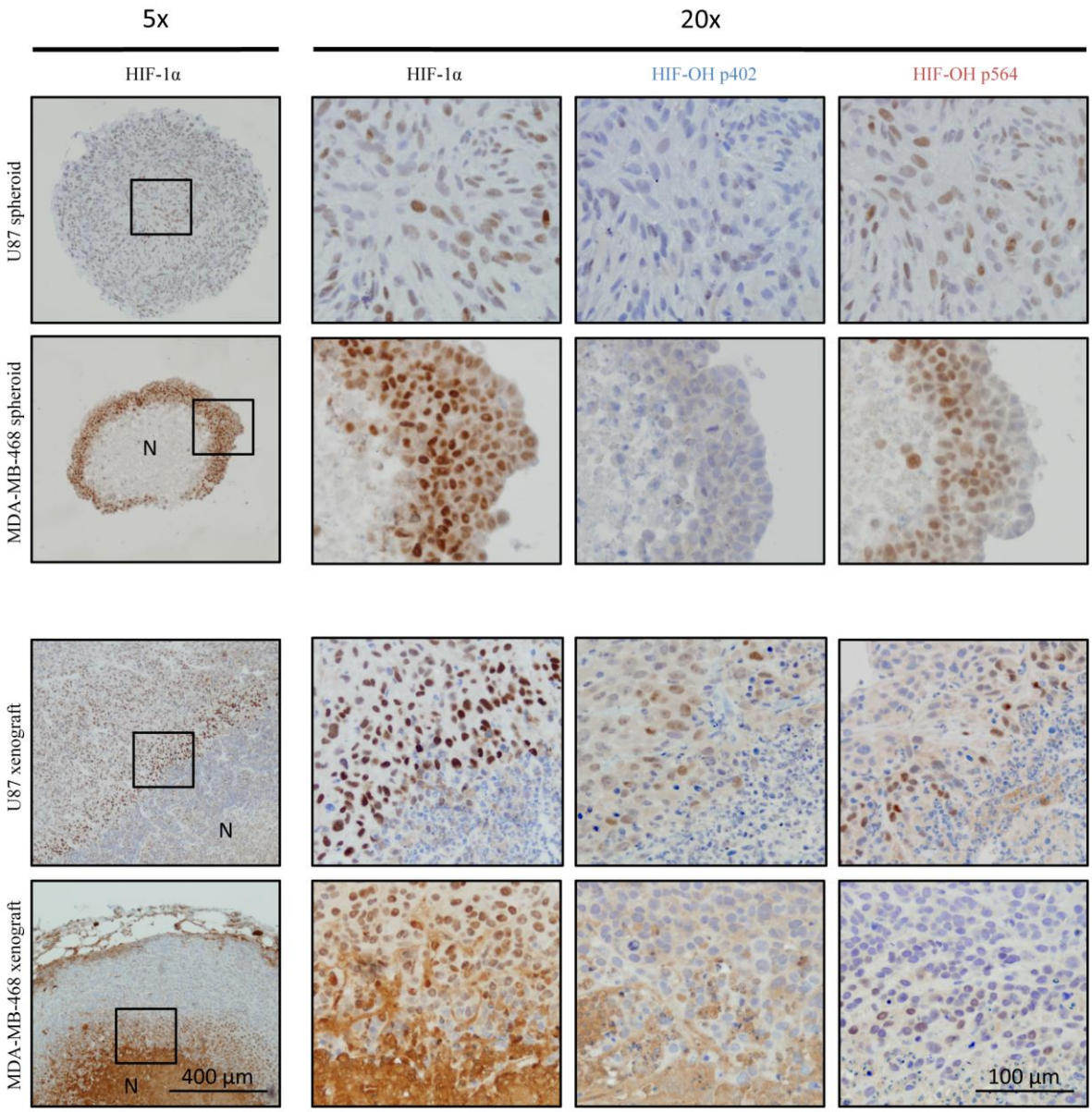

Figure 5.3 The expression of proline-hydroxylated and total HIF-1α in tumour models. Top two rows: U87 and MDA-MB-468 tumour spheroids. Left-most panel is a low power view (5x magnification) of spheroid stained with total HIF-1α. Box indicates area of enlargement for next three images. Right three images are high (20X) power serial sections stained with the indicated antibodies. Bottom two rows: U87 and MDA-MB-468 mouse tumour xenografts. N = necrosis. Scale bars apply to all images of the same magnification.

Expression of hydroxylated HIF-1α in hypoxic human tumours

Having determined variability in the expression of proline-hydroxylated HIF-1α in VHL competent cell lines, we used a panel of tissue microarrays to evaluate the expression of total and proline-hydroxylated HIF-1α in head and neck, breast, lung and bladder carcinomas (Figure 5.4). Overall, 50% of tumours had detectable HIF-1α (47% head and neck, 58% breast, 45% lung and 38% bladder). Of the tumours evaluated that had detectable HIF-1α, 68% also had proline-hydroxylated HIF-1α (71% head and neck, 59% breast, 100% lung and 89% bladder). Of the cases that had only one hydroxylation site detectable, 66% were hydroxylated just at proline 402 and 34% just at proline 564, within limits of detection. The different patterns of proline-hydroxylated HIF-1α in tumours are represented in Figure 5.4.

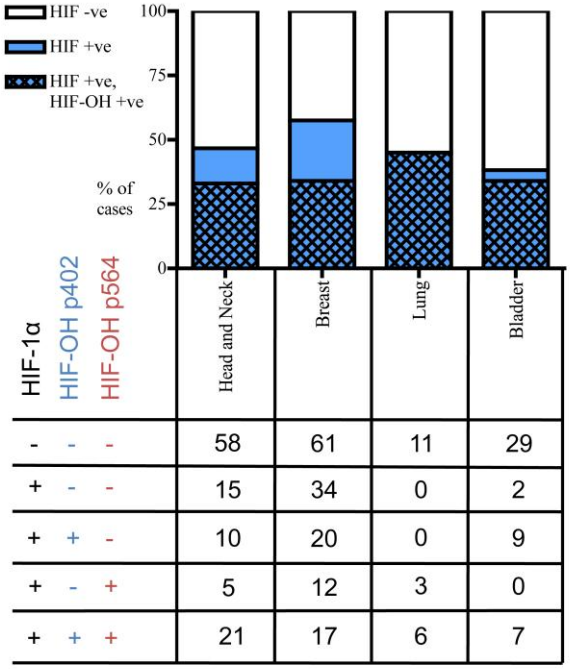

HIF-1α	HIF-OH p402	HIF-OH p564	Head and Neck	Breast	Lung	Bladder
-	-	-	58	61	11	29
+	-	-	15	34	0	2
+	+	-	10	20	0	9
+	-	+	5	12	3	0
+	+	+	21	17	6	7

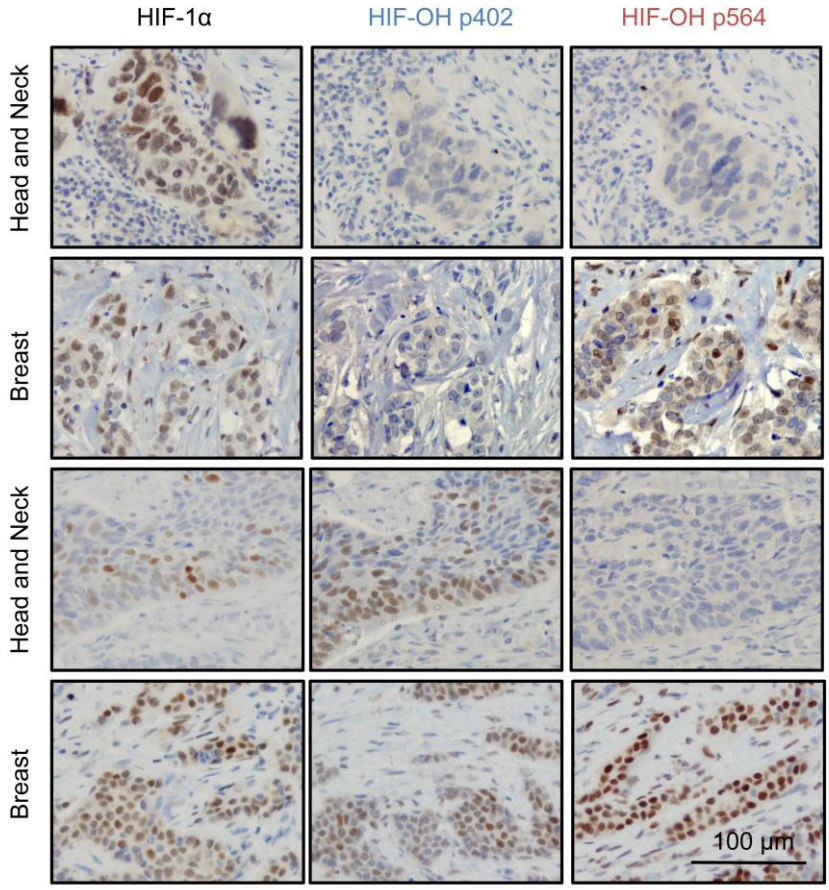

Figure 5.1 Proline-hydroxylated HIF-1α is present in a high proportion and wide range of tumours. Graph indicates relative proportion of HIF-1α positive tumours, and the proportion which also show detectable staining for proline-hydroxylated HIF-1α. Numbers below represent cases with that particular staining pattern. Photomicrographs are representative of cases showing different patterns of expression of proline-hydroxylated HIF-1α. Scale bar applies to all images.

Expression of proline-hydroxylated HIF-1α predicts adverse prognosis in breast cancer

We then evaluated whether proline-hydroxylated HIF-1α was prognostic in primary breast cancer. In this cohort, 86/147 patients had detectable HIF-1α in their primary resected tumours. The expression of HIF-1α was associated with a non-significant trend towards shorter overall survival (8.65 vs 7.43 years, p = 0.089) (Figure 5.5). When these patients were split into those with tumours containing detectable proline-hydroxylated HIF-1α versus those with HIF-1α without hydroxylation, patients with primary tumours containing hydroxylated HIF-1α had significantly worse overall survival (7.06 years) compared to patients with HIF-1α negative tumours (8.63 years, p = 0.04) (Figure 5.6). No significant differences in survival were observed between patients with HIF-1α positive tumours, comparing hydroxylated and hydroxylation-negative HIF-1α.

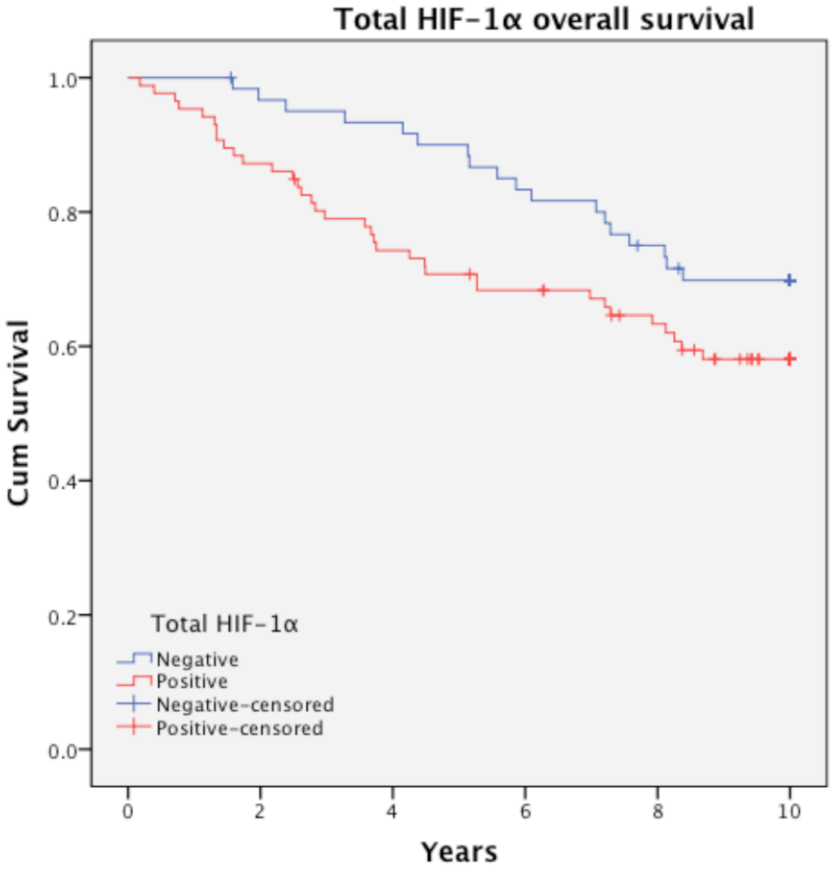

Case Processing Summary

Total HIF-1α	Total N	N of Events	Censored	
			N	Percent
Negative	61	18	43	70.5%
Positive	86	35	51	59.3%
Overall	147	53	94	63.9%

Total HIF-1α	Mean survival			
	Estimate	Std. Error	95% Confidence Interval	
			Lower Bound	Upper Bound
Negative	8.653	.305	8.055	9.250
Positive	7.426	.376	6.688	8.164
Overall	7.934	.259	7.427	8.441

	Total HIF-1α	Positive	
		Chi-Square	Sig.
Log Rank (Mantel-Cox)	Negative	2.891	.089

Figure 5.2 Expression of proline-hydroxylated HIF-1α shows a non-significant trend towards poorer overall survival in primary breast cancer. Kaplan-Meier curve is for overall survival comparing patients with tumours that are HIF-1α +ve or –ve. P value quoted is the result of the logrank test for comparison of survival curves.

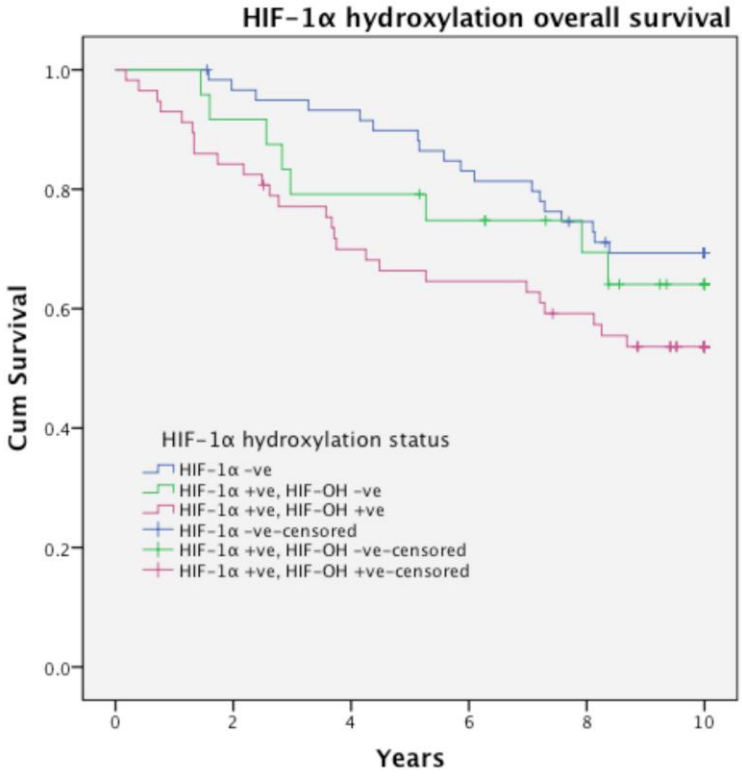

Case Processing Summary

HIF-1α hydroxylation status	Total N	N of Events	Censored	
			N	Percent
HIF-1α -ve	60	18	42	70.0%
HIF-1α +ve, HIF-OH -ve	24	8	16	66.7%
HIF-1α +ve, HIF-OH +ve	57	26	31	54.4%
Overall	141	52	89	63.1%

HIF-1α hydroxylation status	Mean survival (years)			
	Estimate	Std. Error	95% Confidence Interval	
			Lower Bound	Upper Bound
HIF-1α -ve	8.630	.309	8.024	9.236
HIF-1α +ve, HIF-OH -ve	7.986	.643	6.725	9.246
HIF-1α +ve, HIF-OH +ve	7.061	.483	6.114	8.008
Overall	7.884	.267	7.362	8.407

Pairwise Comparisons

	HIF-1α hydroxylation status	HIF-1α +ve, HIF-OH -ve		HIF-1α +ve, HIF-OH +ve	
		Chi-Square	Sig.	Chi-Square	Sig.
Log Rank (Mantel-Cox)	HIF-1α -ve	.349	.554	4.210	**.040**
	HIF-1α +ve, HIF-OH -ve			.926	.336
	HIF-1α +ve, HIF-OH +ve				

Figure 5.3 Expression of proline-hydroxylated HIF-1α predicts poorer overall survival in primary breast cancer. Kaplan-Meier curve compares patients with tumours that are negative for HIF-1α, HIF-1α+ve but hydroxylated HIF-1α –ve and HIF-1α+ve and hydroxylated HIF-1α+ve. P values quoted are the result of the logrank test for comparison of survival curves.

Correlation of the expression of proline-hydroxylated HIF-1α with the expression of proline hydroxylase enzymes, VHL and Lon in breast cancer

We stained and scored expression of the PHD enzymes (1-3), Lon and VHL, and evaluated whether levels of these correlated with expression of total, proline-hydroxylated, or unhydroxylated HIF-1α (Table 5.1). We found, as expected, HIF-1α and hydroxylated HIF-1α positivity correlated. The levels of PHD1 correlated with PHD2, and the levels of PHD2 and PHD3 also correlated with each other. The levels of VHL significantly correlated with the expression of HIF-1α in cases that did not show detectable proline-hydroxylated HIF-1α (unhydroxylated HIF-1α) (r = 0.201, p = 0.030). Lon correlated with the expression levels of VHL as previously described in Chapter 2, but not with the levels of hydroxylated HIF-1α.

Table 5.1 Correlations between total, proline-hydroxylation and unhydroxylated HIF-1α and enzymes involved in HIF-1α degradation.

Pearson's *r* ***p-value***		HIF-1α Pro402	HIF-1α Pro564	Hydroxylated HIF-1α	Unhydroxylated HIF-1α	PHD1	PHD2	PHD3	VHL	Lon
HIF-1α	*r*	0.330	0.680	0.700	0.395	-0.018	-0.047	0.010	0.167	-0.054
	p	**<0.0001**	**<0.0001**	**<0.0001**	**<0.0001**	**0.857**	**0.621**	**0.914**	**0.067**	**0.551**
HIF-1α Pro402	*r*		0.420	0.480	-0.182	0.147	-0.021	0.038	-0.027	-0.095
	p		**<0.0001**	**<0.0001**	**0.030**	**0.140**	**0.830**	**0.695**	**0.766**	**0.293**
HIF-1α Pro564	*r*			0.971	-0.368	-0.134	-0.050	-0.050	-0.008	-0.064
	p			**<0.0001**	**<0.0001**	**0.181**	**0.604**	**0.607**	**0.935**	**0.484**
Hydroxylated HIF-1α	*r*				-0.379	-0.163	-0.015	-0.025	-0.004	-0.054
	p				**<0.0001**	**0.105**	**0.878**	**0.796**	**0.962**	**0.557**
Unhydroxylated HIF-1α	*r*					0.173	-0.027	0.059	0.201	-0.021
	p					**0.085**	**0.785**	**0.545**	**0.030**	**0.821**
PHD1	*r*						0.292	0.179	0.208	0.059
	p						**0.001**	**0.052**	**0.034**	**0.545**
PHD2	*r*							0.501	0.154	0.044
	p							**<0.0001**	**0.100**	**0.636**
PHD3	*r*								0.062	0.099
	p								**0.511**	**0.290**
VHL	*r*									0.158
	p									**0.037**

■ = significant positive correlation, ■ = significant negative correlation

Discussion

Overall, whilst the results are not fully quantitative, our observations on the physiology of stabilised HIF-1α in tumours and cancer cell lines reveal that a substantial component of stabilised HIF-1α in tumours is proline-hydroxylated, and in many cases is seen hydroxylated at both potential proline-hydroxylation sites within the ODD. Data from both cells lines and tumour xenograft models extend this observation, demonstrating conclusively that accumulation of proline-hydroxylated HIF-1α occurs in tumours and cell lines that express wild-type VHL. The large numbers and wide range of tumours that express proline-hydroxylated HIF-1α suggest that the increased level of hydroxylated HIF-1α, which is likely transcriptionally active, is an important part of the physiological hypoxia-sensing mechanism in moderate levels of hypoxia. It is possible that the transcriptional activity of differently proline-hydroxylated HIF-1α varies, possibly as a consequence of altered protein-protein interactions involving pVHL, as is the case for CAD-hydroxylation, which reduces binding of HIF-α to coactivator proteins.

In cell lines exposed to hypoxia we observe heterogeneity in the accumulation of proline-hydroxylated HIF-1α, suggesting that tumour cells have major differences in their degradation pathways. Clearly, there is thus another mechanism of HIF regulation that occurs post proline-hydroxylation which is important in tumours and which is differentially exploited by different cell lines. Importantly, the level of VHL or PHD enzymes does not correlate with the

propensity of cells to accumulate hydroxylated HIF in hypoxia. The stabilisation of hydroxylated HIF-1α at Pro564 in normoxia has been described in cells expressing a constitutively active Akt (Chan *et al.*, 2002). Interestingly, both U87 and MDA-MB-468 cells have homozygous mutations in PTEN, a negative regulator of the Akt pathway. Furthermore, hypoxia activates Akt at moderate levels of hypoxia (5% oxygen and below) (Beitner-Johnson *et al.*, 2001). HCT116 and MCF7 cells, which do not show increases in hydroxylated HIF-1α in hypoxia, have wild-type PTEN. This suggests that activation of Akt versus other oncogenically activated pathways may potentially contribute towards the observed differential responses.

In vivo, we observed staining for proline-hydroxylated HIF-1α, even in the most hypoxic regions of MDA-MB-468 and U87 xenografts, demonstrating hypoxic inhibition of hydroxylated HIF-1α degradation *in vivo*. This staining extended up to the areas of necrosis, suggesting that the oxygen levels were sufficient to support HIF hydroxylation in these tumours. We were able to detect HIF-1α proline-hydroxylation in 68% of human tumours expressing HIF-1α. In the other 32%, tumours had HIF-1α yet no detectable hydroxylated HIF-1α. The data supports the notion that a substantial proportion of HIF-1α in the majority of tumours is proline-hydroxylated, and that hypoxia can cause the degradation of proline-hydroxylated HIF-1α to be rate limiting.

Our finding that hydroxylated HIF-1α in primary breast cancer is associated with poorer outcome (as is HIF-1α) suggests that a more moderate level of hypoxia that allows for continued HIF-1α hydroxylation may favour malignant

progression. Tumours are able to stabilise the proline-hydroxylated form of HIF-1α, providing another mechanism for regulating HIF in cancer. The activation of oncogenes associated with the stabilisation of hydroxylated HIF-1α may alternatively contribute to poor outcome. The expression of proline-hydroxylated and non-hydroxylated HIF-1α may explain why some studies fail to find a correlation between high HIF-1α tumour levels and adverse clinical outcome (Miyake *et al.*, 2008) (Beasley *et al.*, 2002). The presence of proline-hydroxylated HIF-1α may also explain why there is a lack of correlation in tumours between HIF-1α levels and pO_2 levels (Hutchison *et al.*, 2004) (Evans *et al.*, 2004).

A previous study detected an increase in proline-hydroxylated HIF-1α under hypoxia *in vitro,* in the tumour cell lines HeLa and HT1080 at Pro564, using similar methodology (Tian *et al.*, 2011b). We found a number of tumours (and the MDA-MB-468 cell line) in which we detected proline-hydroxylated HIF-1α at only one site, although this was not universally at proline site 402 or 564. In tumours where proline-hydroxylated HIF-1α is detected, 29% are mono-hydroxylated at Pro402, 20% at Pro564 and 51% of tumours are proline-hydroxylated at both sites, highlighting biological heterogeneity between tumours.

The underlying mechanism(s) leading to the accumulation of proline-hydroxylated HIF-1α in tumours is unknown. The identification of these mechanisms is important because they may present new therapeutic possibilities by targeting increased HIF-1α degradation. Recent evidence

suggests that overexpression of the oncogene c-Myc can also cause the accumulation of proline-hydroxylated HIF-1α in cell lines, by decreasing the interaction of VHL with HIF-1α (Doe *et al.*, 2012). Post-translational modification of VHL, such as SUMOylation, may cause oligomerisation and reduce its ability to recognise and degrade HIF-1α in hypoxia (Cai *et al.*, 2010). Alternatively, Lon may promote a post-translational modification through interaction with VHL (Chapter 3). We found that higher levels of VHL were associated with the presence of HIF-1α, without detectable proline hydroxylation, supporting the possibility that high levels of VHL may prevent the accumulation of hydroxylated HIF-1α.

The PHD isoforms differentially hydroxylate HIF-1α. In cell lines, PHD2 is the most abundant HIF prolyl hydroxylase, and performs a non-redundant role in HIF degradation (Appelhoff *et al.*, 2004) (Berra *et al.*, 2003). PHD3 preferentially hydroxylates Pro564 (CODD), while PHD1 and 2 can hydroxylate both NODD and CODD sites, although Pro564 is hydroxylated prior to Pro402 (Chan *et al.*, 2005) (Berra *et al.*, 2003). The regulation is complicated by the hypoxic induction of PHD2 and PHD3, and additional mechanisms to promote HIF accumulation may be required to prevent complete HIF degradation in the chronic hypoxic conditions found in tumours (Appelhoff *et al.*, 2004). Our analysis of PHDs found no relationship to levels of proline-hydroxylated HIF-1α, consistent with post-hydroxylation regulation.

In conclusion, we have demonstrated that a significant proportion of HIF-1α that accumulates in hypoxia *in vitro* and *in vivo* is proline-hydroxylated. This is seen

in tumours that do not have known VHL mutations, and this represents a novel mechanism of HIF-1α accumulation. Determining the pathways by which the degradation of proline-hydroxylated HIF-1α is blocked may allow for targeted therapy to reverse this adaptation and reduce the tumourigenic phenotypes that are associated with higher levels of HIF signalling.

Chapter 6 : Conclusions

This final chapter brings together the results, discussions and implications of the research. In particular, it highlights the pathophysiological role of Lon upregulation in cancer, including a proposed mechanism of aberrant HIF-α stabilisation. I also explore the potential utility of developing inhibitors of the Lon protease for use in cancer therapy. Finally, specific suggestions are offered as to how this project can be enhanced and extended.

The differential expression of Lon in tumours

In Chapter 2 we showed that Lon is upregulated in breast and lung cancer, and demonstrated that higher levels of expression, as occurs frequently in breast cancer, correlates with poorer overall survival breast cancer at 10 years follow up (Figure 2.5). Lon has a wide range of differential expression in tumours, suggesting that its upregulation is not essential to tumour development. The level of Lon varied significantly between different cell lines, and while we did see subtle up-regulation in hypoxia, it appears that different cell lines and tumours have intrinsically different levels of expression of Lon.

Whilst the expression of Lon has been described to be induced by hypoxia and dependent on HIF-1α (Fukuda *et al.*, 2007), other factors appear to exert a greater influence on the level of expression of Lon. This is most apparent in the renal cell carcinoma cell line RCC4, which has a similar expression of Lon with or

without functional VHL (Figure 3.6), despite have greatly reduced levels of HIF-1α when expressing a functional VHL (RCC+VHL).

The differential expression of Lon in tumours may be accounted for by its described physiologic role. Lon is required for the degradation of misfolded and oxidatively modified proteins in the mitochondrial matrix (Bota & Davies, 2002). Misfolded proteins in this compartment arise from damage incurred over time by ROS, mutations in mtDNA, and mismatches in the assembly between nuclear and mitochondrial protein translation and transport in the assembly of electron transport chain complexes (Baker & Haynes, 2011). The conditions that promote misfolded proteins in the mitochondrial matrix are increased in cancer, including the common finding of mutations in mtDNA (Chatterjee *et al.*, 2011) and the increased production of ROS (Szatrowski & Nathan, 1991) (Kawanishi *et al.*, 2006) in tumour cells.

Different tumours and cancer cell lines may accumulate misfolded and damaged proteins in the mitochondrial matrix to a greater or lesser degree, which may account for differences in the expression of Lon. As part of the quality control mechanism of the mitochondrial matrix, one might expect that the expression of Lon would increase with the quantity of misfolded or damaged proteins, as part of the mtUPR. This prediction is supported by the observation that overexpression of a terminally misfolded form of ornithine transcarbamylase (OTC) targeted to the mitochondrial matrix, which initiates the mtUPR, causes the increased expression of Lon (Zhao *et al.*, 2002). The same laboratory later published evidence that Lon was in fact not upregulated by the mtUPR, on the

basis that it lacked a CHOP element in the promoter (Aldridge *et al.*, 2007) required for mtUPR (Horibe & Hoogenraad, 2007). The disparity between these published observations has not been specifically addressed. The other mitochondrial matrix AAA+ protease ClpP is induced by mtUPR (Aldridge *et al.*, 2007). Furthermore, in mtUPR reporter worms (*C. elegans*) Lon knockdown does not induce the mtUPR (Nargund *et al.*, 2012).

The factors that regulate the expression of Lon are therefore not clear. We also found that high expression of Lon correlated with the tumour being positive for oestrogen receptor (Chapter 2). Oestrogen can regulate the expression of nuclear- and mtDNA-encoded mitochondrial proteins in breast cancer cells and upregulates mitochondrial biogenesis via NRF-1 (Mattingly *et al.*, 2008). Oestrogen signalling also promotes an increase in TFAM expression and mitochondrial transcripton (Mattingly *et al.*, 2008). Our findings raise the possibility that Lon may be upregulated in response to oestrogen signalling, and hence this is why it is correlated with ER status in the patient series we examined.

The role of Lon in mediating the hypoxic response of tumour cells

We found that the expression of Lon and VHL in breast cancer was positively correlated (Chapters 2 and 5). Targeting Lon reduces the expression of HIF-1α, an effect that was mediated post-hydroxylation, and we provide evidence for a direct interaction between Lon and VHL (Chapter 3). Interestingly, overexpression of c-Myc can increase the stabilisation of proline-hydroxylated

HIF-1α, despite increasing the expression of VHL (Doe *et al.*, 2012). VHL may be subjected to as-yet unidentified post-translational modification inhibiting its activity, allowing for the widespread stabilisation of proline hydroxylated HIF-1α in tumours, as we identified in Chapter 5.

We were unable to find any correlation between the levels of Lon and the expression of HIF-1α or the hydroxylated form. The effect of Lon on the hypoxic response may be produced by the (small) proportion of cytoplasmic Lon, which may interact with VHL in such a way as to modulate the levels of HIF-α. Immunohistochemistry provides only an indication of the overall levels of Lon, confounding any correlation with an effect on HIF stabilisation. The cytoplasmic role of Lon may explain why we could get only some siRNA and shRNA sequences to elicit effects on HIF-α stabilisation, despite achieving extremely good overall levels of Lon protein depletion.

Although when Lon and VHL were co-transfected in 293T cells there was destabilisation of VHL, reversible with bortezomib treatment and transfection of catalytic inactive Lon, we saw no changes in VHL with Lon targeting siRNA or shRNA. We do not have compelling evidence for the physiologic degradation of VHL by Lon and, certainly, effects on HIF-1α are independent of overall VHL levels. Our evidence of a direct interaction of Lon and VHL is limited to mutants of Lon with impaired mitochondrial import, an interaction that appears to be dependent on ATPase activity, and therefore Lon may have specific chaperone activity towards VHL. Clearly there are mechanisms of regulating the degradation of proline-hydroxylated HIF-1α, as we find it present in cell lines,

hypoxic regions of mouse xenografts and in human tumours. Our model of the regulation of the hypoxic response by Lon is illustrated in Figure 6.1.

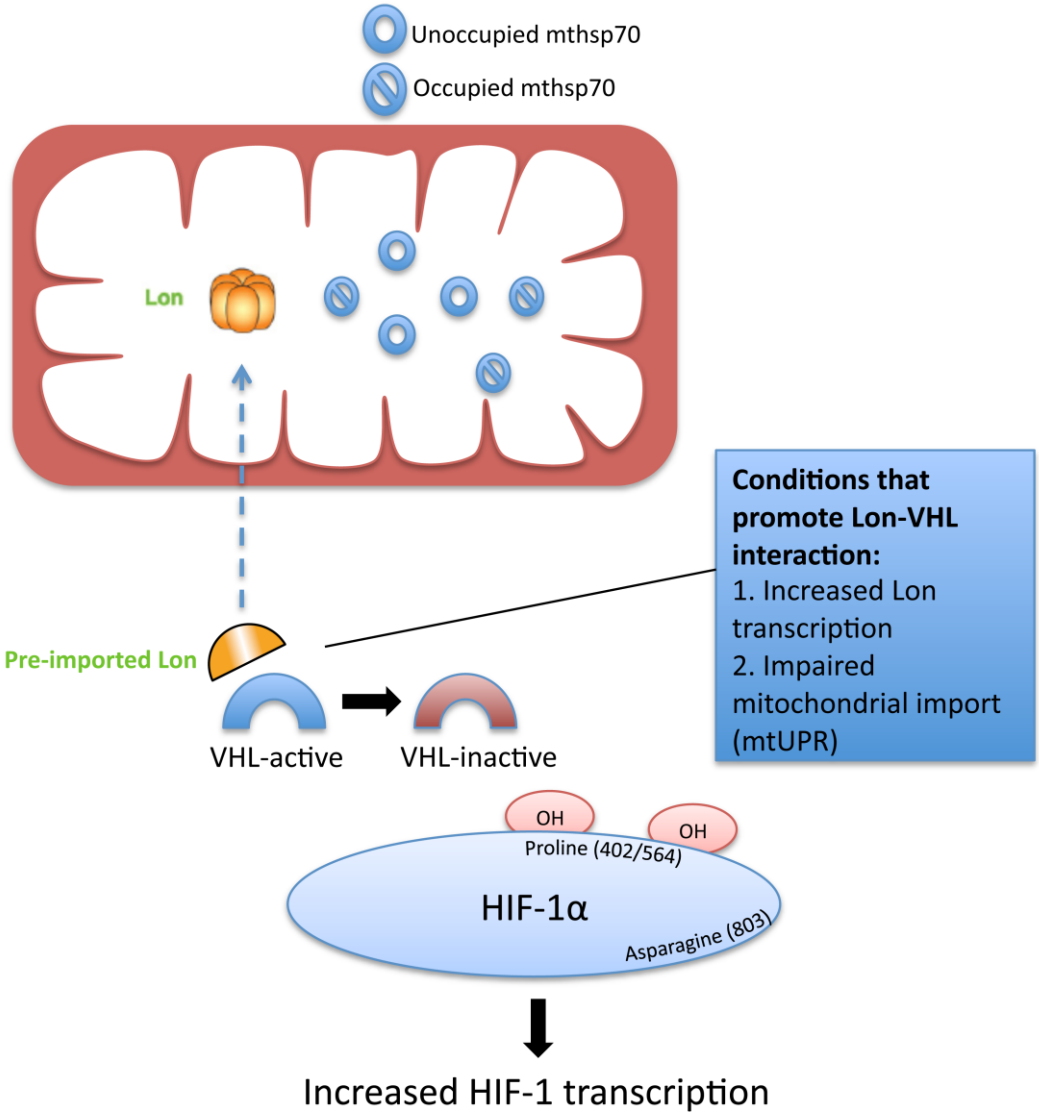

Figure 6.1 Model of mechanism by which Lon modulates the hypoxic response. The mitochondrial import of Lon is regulated by the rate of import, which may be affected by chaperone occupancy, principally mtHsp70, which itself it part of the mitochondrial import machinery (Becker *et al.*, 2012). Pre-imported Lon can interact with VHL in an ATPase-dependent fashion. Targeting Lon with siRNA may reduce this activity and reduce HIF-1α stabilisation independent of proline-hydroxylase activity. Targeting Lon with siRNA consequently reduces the rate of HIF-1 dependent transcription.

The expected utility of targeting the Lon protease in tumours

In growth studies *in vitro* we found that reducing the levels of Lon had divergent effects dependent on cell line (Chapter 4). Targeting Lon in U87 and MD-MB-468

cells caused severe growth suppression, whereas we saw very little effect in the breast cancer cell line MCF7. Although exploring the differences between cell lines contributing to this differential response would require analysis of many more than three, MCF7 cells are ER-positive, whereas U87 and MDA-MB-468 cells are ER-negative (Sareddy *et al.*, 2012). It may be that the mitochondrial-biogenesis promoting property of ER-signalling prevents the inhibited growth characteristics that the other two cell lines display.

Despite differential effects on growth, all three cell lines show decreased HIF stabilisation in normoxia and hypoxia and in spheroid models. This suggests that effects of targeting Lon on growth and effects on HIF stabilisation are independent. In the renal cell carcinoma cell line, we were unable to elicit any change in HIF stabilisation. This suggests that targeting Lon may not be efficacious in tumours with a mutant VHL. The effect of reducing HIF signalling in tumour cell lines has been shown to inhibit the growth of tumour xenografts (Li *et al.*, 2005b), although loss of function xenograft experiments are limited because the host stromal cells retain HIF activity (Semenza, 2010a). Agents that target HIF-1α and HIF-2α in tumour and stroma will likely have the highest therapeutic efficacy in cancer treatment (Semenza, 2010a), and our data indicates that targeting Lon may fulfil this criteria.

Reducing HIF signalling by targeting Lon is predicted to inhibit angiogenesis, chemotherapy and radiotherapy resistance, invasion and metastasis, proliferation, survival and metabolism and pH regulation (Semenza, 2010a). We

demonstrated partial reversal of the Warburg effect (Chapter 4), an effect which may be due to alteration in HIF signalling (Semenza, 2009).

The proteasome inhibitor Bortezomib has recently been shown to be an inhibitor of the Lon protease in human cells (Lu *et al.*, 2012). Bortezomib is effective in the treatment of multiple myeloma and mantle cell non-Hodgkin's lymphoma (Li *et al.*, 2010), although it has not been shown to have consistent therapeutic benefit in solid tumours (Piperdi *et al.*, 2011). This may be due to a narrow therapeutic index, or possibly that a proportion of therapeutic effect may be due to the inhibition of Lon rather than the proteasome. Bortezomib treatment has been shown to reduce HIF signalling *in vivo* (Birle & Hedley, 2007), an effect that is potentially mediated by inhibiting Lon.

A new mechanism of HIF regulation by stabilisation of proline hydroxylated HIF-1α

In Chapter 5 we demonstrated that a significant proportion of HIF-1α stabilised *in vitro* and *in vivo* is proline-hydroxylated in VHL competent cell lines and tumours. This observation is not consistent with the accepted model of HIF-1α stabilisation, in which proline-hydroxylation is inhibited under increasing levels of hypoxia (Kaelin & Ratcliffe, 2008). We are the first group to explore the extent of post-hydroxylation regulation of HIF-1α in tumours. This effect is not seen in all cell lines and tumours, and the accumulation of proline-hydroxylated HIF-1α may correlate with the activation of certain oncogenic signalling pathways.

Lon may promote the stabilisation of proline-hydroxylated HIF-1α in tumours. The two cell lines that showed robust increases in proline-hydroxylated HIF-1α in hypoxia also showed significant decreases in HIF-1α stabilisation with targeting of Lon (U87 and MDA-MB-468). We did see evidence for inhibition of proline-hydroxylation in hypoxia contributing to HIF-1α accumulation (MCF7, HCT-116), suggesting the accumulation of HIF in hypoxia may be regulated by different mechanisms, depending on cell line.

Future directions

We are currently exploring whether the mtUPR promotes the stabilisation of HIF-1α, and whether this affects levels of hydroxylated or unhydroxylated HIF-1α. The problems in trying to explore this question include the limited tools to induce and measure endogenous levels of mtUPR. Overexpression of misfolded OTC is one model that has been used in mammalian cell culture (Zhao *et al.*, 2002), but whether this is representative of physiological mtUPR is debatable. Measurements of endogenous mtUPR are limited to genes induced by such manipulations (Aldridge *et al.*, 2007). Immunohistochemical markers to quantify the degree of mtUPR in tumours may be useful as biomarkers predicting response to mitochondrial-targeted therapies (such as anti-Lon therapy).

To increase our understanding of the physiological role of Lon, we have begun to create a Lon knockout mouse. We aim to determine whether HIF stabilisation is affected in mice deficient for Lon, and whether mice knockout for Lon are viable.

This will also provide useful information on the likely toxicities associated with targeting the Lon protease pharmacologically.

Lastly, we are exploring the possibility of creating specific small molecule inhibitors for Lon for use as anti-cancer agents. The ability to target HIF-1α and HIF-2α in tumours would be predicted to have good therapeutic efficacy in solid malignancies. We are also currently trying to define the cell lines which respond most to anti-Lon therapy in terms of direct growth inhibition.

Bibliography

Accili D, Arden KC (2004) FoxOs at the crossroads of cellular metabolism, differentiation, and transformation. *Cell* **117:** 421-6

Adam J, Hatipoglu E, O'Flaherty L, Ternette N, Sahgal N, Lockstone H, Baban D, Nye E, Stamp GW, Wolhuter K, Stevens M, Fischer R, Carmeliet P, Maxwell PH, Pugh CW, Frizzell N, Soga T, Kessler BM, El-Bahrawy M, Ratcliffe PJ, Pollard PJ (2011) Renal cyst formation in Fh1-deficient mice is independent of the Hif/Phd pathway: roles for fumarate in KEAP1 succination and Nrf2 signaling. *Cancer Cell* **20:** 524-37

Adighibe O, Micklem K, Campo L, Ferguson M, Harris A, Pozos R, Gatter K, Pezzella F (2006) Is nonangiogenesis a novel pathway for cancer progression? A study using 3-dimensional tumour reconstructions. *Br J Cancer* **94:** 1176-9

Ahn BY, Trinh DLN, Zajchowski LD, Lee B, Elwi AN, Kim S-W (2010) Tid1 is a new regulator of p53 mitochondrial translocation and apoptosis in cancer. *Oncogene* **29:** 1155-66

Aldridge JE, Horibe T, Hoogenraad NJ (2007) Discovery of genes activated by the mitochondrial unfolded protein response (mtUPR) and cognate promoter elements. *PLoS ONE* **2:** e874

Allen JF (2003) The function of genomes in bioenergetic organelles. *Philos Trans R Soc Lond, B, Biol Sci* **358:** 19-37; discussion 37-8

Appelhoff RJ, Tian Y-M, Raval RR, Turley H, Harris AL, Pugh CW, Ratcliffe PJ, Gleadle JM (2004) Differential function of the prolyl hydroxylases PHD1, PHD2, and PHD3 in the regulation of hypoxia-inducible factor. *J Biol Chem* **279:** 38458-65

Bae M-K, Jeong J-W, Kim S-H, Kim S-Y, Kang HJ, Kim D-M, Bae S-K, Yun I, Trentin GA, Rozakis-Adcock M, Kim K-W (2005) Tid-1 interacts with the von Hippel-Lindau protein and modulates angiogenesis by destabilization of HIF-1alpha. *Cancer Res* **65:** 2520-5

Bai R-K, Chang J, Yeh K-T, Lou MA, Lu J-F, Tan D-J, Liu H, Wong L-JC (2011) Mitochondrial DNA content varies with pathological characteristics of breast cancer. *J Oncol* **2011:** 496189

Baker A, Payne CM, Briehl MM, Powis G (1997) Thioredoxin, a gene found overexpressed in human cancer, inhibits apoptosis in vitro and in vivo. *Cancer Res* **57:** 5162-7

Baker BM, Haynes CM (2011) Mitochondrial protein quality control during biogenesis and aging. *Trends Biochem Sci* **36:** 254-61

Bayot A, Basse N, Lee I, Gareil M, Pirotte B, Bulteau A-L, Friguet B, Reboud-Ravaux M (2008) Towards the control of intracellular protein turnover: mitochondrial Lon protease inhibitors versus proteasome inhibitors. *Biochimie* **90:** 260-9

Bayot A, Gareil M, Rogowska-Wrzesinska A, Roepstorff P, Friguet B, Bulteau A-L (2010) Identification of novel oxidized protein substrates and physiological partners of the mitochondrial ATP-dependent Lon-like protease Pim1. *The Journal of biological chemistry* **285:** 11445-57

Beasley NJP, Leek R, Alam M, Turley H, Cox GJ, Gatter K, Millard P, Fuggle S, Harris AL (2002) Hypoxia-inducible factors HIF-1alpha and HIF-2alpha in head and neck cancer: relationship to tumor biology and treatment outcome in surgically resected patients. *Cancer Res* **62:** 2493-7

Becker T, Böttinger L, Pfanner N (2012) Mitochondrial protein import: from transport pathways to an integrated network. *Trends Biochem Sci* **37:** 85-91

Befani CD, Vlachostergios PJ, Hatzidaki E, Patrikidou A, Bonanou S, Simos G, Papandreou CN, Liakos P (2012) Bortezomib represses HIF-1α protein expression and nuclear accumulation by inhibiting both PI3K/Akt/TOR and MAPK pathways in prostate cancer cells. *J Mol Med* **90:** 45-54

Beitner-Johnson D, Rust RT, Hsieh TC, Millhorn DE (2001) Hypoxia activates Akt and induces phosphorylation of GSK-3 in PC12 cells. *Cell Signal* **13:** 23-7

Bell EL, Emerling BM, Ricoult SJH, Guarente L (2011) SirT3 suppresses hypoxia inducible factor 1α and tumor growth by inhibiting mitochondrial ROS production. *Oncogene* **30:** 2986-96

Bell EL, Klimova TA, Eisenbart J, Moraes CT, Murphy MP, Budinger GRS, Chandel NS (2007) The Qo site of the mitochondrial complex III is required for the transduction of hypoxic signaling via reactive oxygen species production. *J Cell Biol* **177:** 1029-36

Bellot G, Garcia-Medina R, Gounon P, Chiche J, Roux D, Pouysségur J, Mazure NM (2009) Hypoxia-induced autophagy is mediated through hypoxia-inducible factor induction of BNIP3 and BNIP3L via their BH3 domains. *Mol Cell Biol* **29:** 2570-81

Bender T, Lewrenz I, Franken… S (2011) Mitochondrial enzymes are protected from stress-induced aggregation by mitochondrial chaperones and the Pim1/LON protease. *Molecular Biology of …*

Bento CF, Fernandes R, Ramalho J, Marques C, Shang F, Taylor A, Pereira P (2010) The chaperone-dependent ubiquitin ligase CHIP targets HIF-1α for degradation in the presence of methylglyoxal. *PLoS ONE* **5:** e15062

Bernstein SH, Venkatesh S, Li M, Lee J, Lu B, Hilchey SP, Morse KM, Metcalfe HM, Skalska J, Andreeff M, Brookes PS, Suzuki CK (2012) The mitochondrial ATP-dependent Lon protease: a novel target in lymphoma death mediated by the synthetic triterpenoid CDDO and its derivatives. *Blood*

Berra E, Benizri E, Ginouvès A, Volmat V, Roux D, Pouysségur J (2003) HIF prolyl-hydroxylase 2 is the key oxygen sensor setting low steady-state levels of HIF-1alpha in normoxia. *EMBO J* **22:** 4082-90

Berridge MV, Herst PM, Tan AS (2010) Metabolic flexibility and cell hierarchy in metastatic cancer. *Mitochondrion* **10:** 584-8

Birle DC, Hedley DW (2007) Suppression of the hypoxia-inducible factor-1 response in cervical carcinoma xenografts by proteasome inhibitors. *Cancer Res* **67:** 1735-43

Birner P, Schindl M, Obermair A, Plank C, Breitenecker G, Oberhuber G (2000) Overexpression of hypoxia-inducible factor 1alpha is a marker for an unfavorable prognosis in early-stage invasive cervical cancer. *Cancer Res* **60:** 4693-6

Bota DA, Davies KJA (2002) Lon protease preferentially degrades oxidized mitochondrial aconitase by an ATP-stimulated mechanism. *Nat Cell Biol* **4:** 674-80

Bota DA, Ngo JK, Davies KJA (2005) Downregulation of the human Lon protease impairs mitochondrial structure and function and causes cell death. *Free Radic Biol Med* **38:** 665-77

Botos I, Melnikov EE, Cherry S, Khalatova AG, Rasulova FS, Tropea JE, Maurizi MR, Rotanova TV, Gustchina A, Wlodawer A (2004) Crystal structure of the AAA+ alpha domain of E. coli Lon protease at 1.9A resolution. *J Struct Biol* **146:** 113-22

Brand MD (2010) The sites and topology of mitochondrial superoxide production. *Exp Gerontol* **45:** 466-72

Brinkman K, Smeitink JA, Romijn JA, Reiss P (1999) Mitochondrial toxicity induced by nucleoside-analogue reverse-transcriptase inhibitors is a key factor in the pathogenesis of antiretroviral-therapy-related lipodystrophy. *Lancet* **354:** 1112-5

Brugarolas JB, Vazquez F, Reddy A, Sellers WR, Kaelin WG (2003) TSC2 regulates VEGF through mTOR-dependent and -independent pathways. *Cancer Cell* **4:** 147-58

Brunelle JK, Bell EL, Quesada NM, Vercauteren K, Tiranti V, Zeviani M, Scarpulla RC, Chandel NS (2005) Oxygen sensing requires mitochondrial ROS but not oxidative phosphorylation. *Cell Metab* **1:** 409-14

Bruning U, Cerone L, Neufeld Z, Fitzpatrick SF, Cheong A, Scholz CC, Simpson DA, Leonard MO, Tambuwala MM, Cummins EP, Taylor CT (2011) MicroRNA-155 promotes resolution of hypoxia-inducible factor 1alpha activity during prolonged hypoxia. *Mol Cell Biol* **31:** 4087-96

Bubendorf L, Nocito A, Moch H, Sauter G (2001) Tissue microarray (TMA) technology: miniaturized pathology archives for high-throughput in situ studies. *J Pathol* **195:** 72-9

Cai Q, Robertson ES (2010) Ubiquitin/SUMO modification regulates VHL protein stability and nucleocytoplasmic localization. *PLoS ONE* **5**

Cai Q, Verma SC, Kumar P, Ma M, Robertson ES (2010) Hypoxia inactivates the VHL tumor suppressor through PIASy-mediated SUMO modification. *PLoS ONE* **5:** e9720

Carbia-Nagashima A, Gerez J, Perez-Castro C, Paez-Pereda M, Silberstein S, Stalla GK, Holsboer F, Arzt E (2007) RSUME, a small RWD-containing protein, enhances SUMO conjugation and stabilizes HIF-1alpha during hypoxia. *Cell* **131:** 309-23

Carbonell WS, Ansorge O, Sibson N, Muschel R (2009) The vascular basement membrane as "soil" in brain metastasis. *PLoS ONE* **4:** e5857

Cha S-S, An YJ, Lee CR, Lee HS, Kim Y-G, Kim SJ, Kwon KK, De Donatis GM, Lee J-H, Maurizi MR, Kang SG (2010) Crystal structure of Lon protease: molecular architecture of gated entry to a sequestered degradation chamber. *The EMBO journal*

Chamboredon S, Ciais D, Desroches-Castan A, Savi P, Bono F, Feige J-J, Cherradi N (2011) Hypoxia-inducible factor-1α mRNA: a new target for destabilization by tristetraprolin in endothelial cells. *Mol Biol Cell* **22:** 3366-78

Chan DA, Sutphin PD, Denko NC, Giaccia AJ (2002) Role of prolyl hydroxylation in oncogenically stabilized hypoxia-inducible factor-1alpha. *J Biol Chem* **277:** 40112-7

Chan DA, Sutphin PD, Yen S-E, Giaccia AJ (2005) Coordinate regulation of the oxygen-dependent degradation domains of hypoxia-inducible factor 1 alpha. *Mol Cell Biol* **25:** 6415-26

Chandel NS, Maltepe E, Goldwasser E, Mathieu CE, Simon MC, Schumacker PT (1998) Mitochondrial reactive oxygen species trigger hypoxia-induced transcription. *Proc Natl Acad Sci U S A* **95:** 11715-20

Chandel NS, McClintock DS, Feliciano CE, Wood TM, Melendez JA, Rodriguez AM, Schumacker PT (2000) Reactive oxygen species generated at mitochondrial complex III stabilize hypoxia-inducible factor-1alpha during hypoxia: a mechanism of O2 sensing. *The Journal of biological chemistry* **275:** 25130-8

Charette MF, Henderson GW, Doane LL, Markovitz A (1984) DNA-stimulated ATPase activity on the lon (CapR) protein. *J Bacteriol* **158:** 195-201

Chatterjee A, Dasgupta S, Sidransky D (2011) Mitochondrial subversion in cancer. *Cancer Prev Res (Phila)* **4:** 638-54

Chen C, Pore N, Behrooz A, Ismail-Beigi F, Maity A (2001) Regulation of glut1 mRNA by hypoxia-inducible factor-1. Interaction between H-ras and hypoxia. *The Journal of biological chemistry* **276:** 9519-25

Chen S-H, Suzuki CK, Wu S-H (2008) Thermodynamic characterization of specific interactions between the human Lon protease and G-quartet DNA. *Nucleic Acids Res* **36:** 1273-87

Chiche J, Rouleau M, Gounon P, Brahimi-Horn MC, Pouyssegur J, Mazure NM (2010) Hypoxic enlarged mitochondria protect cancer cells from apoptotic stimuli. *J Cell Physiol* **222:** 648-57

Christofk HR, Vander Heiden MG, Harris MH, Ramanathan A, Gerszten RE, Wei R, Fleming MD, Schreiber SL, Cantley LC (2008) The M2 splice isoform of pyruvate kinase is important for cancer metabolism and tumour growth. *Nature* **452:** 230-3

Chung CH, Goldberg AL (1982) DNA stimulates ATP-dependent proteolysis and protein-dependent ATPase activity of protease La from Escherichia coli. *Proc Natl Acad Sci U S A* **79:** 795-9

Cipolat S, Martins de Brito O, Dal Zilio B, Scorrano L (2004) OPA1 requires mitofusin 1 to promote mitochondrial fusion. *Proc Natl Acad Sci USA* **101:** 15927-32

Claros MG, Vincens P (1996) Computational method to predict mitochondrially imported proteins and their targeting sequences. *Eur J Biochem* **241:** 779-86

Colozza M, Azambuja E, Cardoso F, Sotiriou C, Larsimont D, Piccart MJ (2005) Proliferative markers as prognostic and predictive tools in early breast cancer: where are we now? *Ann Oncol* **16:** 1723-39

Confalonieri F, Duguet M (1995) A 200-amino acid ATPase module in search of a basic function. *Bioessays* **17:** 639-50

Copeland E, Balgobin S, Lee CM, Rozakis-Adcock M (2011) hTID-1 defines a novel regulator of c-Met Receptor signaling in renal cell carcinomas. *Oncogene* **30:** 2252-63

Couvelard A, O'Toole D, Leek R, Turley H, Sauvanet A, Degott C, Ruszniewski P, Belghiti J, Harris AL, Gatter K, Pezzella F (2005) Expression of hypoxia-inducible factors is correlated with the presence of a fibrotic focus and angiogenesis in pancreatic ductal adenocarcinomas. *Histopathology* **46:** 668-76

Dang CV, Kim J-w, Gao P, Yustein J (2008) The interplay between MYC and HIF in cancer. *Nat Rev Cancer* **8:** 51-6

Dansen TB, Burgering BMT (2008) Unravelling the tumor-suppressive functions of FOXO proteins. *Trends Cell Biol* **18:** 421-9

David CJ, Chen M, Assanah M, Canoll P, Manley JL (2010) HnRNP proteins controlled by c-Myc deregulate pyruvate kinase mRNA splicing in cancer. *Nature* **463:** 364-8

Del Bufalo D, Ciuffreda L, Trisciuoglio D, Desideri M, Cognetti F, Zupi G, Milella M (2006) Antiangiogenic potential of the Mammalian target of rapamycin inhibitor temsirolimus. *Cancer Res* **66:** 5549-54

Delpuech O, Griffiths B, East P, Essafi A, Lam EW-F, Burgering B, Downward J, Schulze A (2007) Induction of Mxi1-SR alpha by FOXO3a contributes to repression of Myc-dependent gene expression. *Mol Cell Biol* **27:** 4917-30

di Tomaso E, Snuderl M, Kamoun WS, Duda DG, Auluck PK, Fazlollahi L, Andronesi OC, Frosch MP, Wen PY, Plotkin SR, Hedley-Whyte ET, Sorensen AG, Batchelor TT, Jain RK (2011) Glioblastoma recurrence after cediranib therapy in patients: lack of "rebound" revascularization as mode of escape. *Cancer Res* **71:** 19-28

Doe MR, Ascano JM, Kaur M, Cole MD (2012) Myc posttranscriptionally induces HIF1 protein and target gene expression in normal and cancer cells. *Cancer Res* **72:** 949-57

Duan D, Humphrey J, Chen… D (1995) Characterization of the VHL tumor suppressor gene product: localization, complex formation, and the effect of natural inactivating mutations. *Proceedings of the …*

Duman RE, Löwe J (2010) Crystal structures of Bacillus subtilis Lon protease. *J Mol Biol* **401:** 653-70

Ehrismann D, Flashman E, Genn DN, Mathioudakis N, Hewitson KS, Ratcliffe PJ, Schofield CJ (2007) Studies on the activity of the hypoxia-inducible-factor hydroxylases using an oxygen consumption assay. *Biochem J* **401:** 227-34

Elwi AN, Lee B, Meijndert HC, Braun JEA, Kim S-W (2012) Mitochondrial chaperone DnaJA3 induces Drp1-dependent mitochondrial fragmentation. *Int J Biochem Cell Biol* **44:** 1366-76

Emerling BM, Weinberg F, Liu J-L, Mak TW, Chandel NS (2008) PTEN regulates p300-dependent hypoxia-inducible factor 1 transcriptional activity through Forkhead transcription factor 3a (FOXO3a). *Proc Natl Acad Sci U S A* **105:** 2622-7

Esch F, Baird A, Ling N, Ueno N, Hill F, Denoroy L, Klepper R, Gospodarowicz D, Böhlen P, Guillemin R (1985) Primary structure of bovine pituitary basic fibroblast growth factor (FGF) and comparison with the amino-terminal sequence of bovine brain acidic FGF. *Proc Natl Acad Sci U S A* **82:** 6507-11

Evans SM, Judy KD, Dunphy I, Jenkins WT, Nelson PT, Collins R, Wileyto EP, Jenkins K, Hahn SM, Stevens CW, Judkins AR, Phillips P, Geoerger B, Koch CJ (2004) Comparative measurements of hypoxia in human brain tumors using needle electrodes and EF5 binding. *Cancer Res* **64:** 1886-92

Evidence for novel non-angiogenic pathway in breast-cancer metastasis. Breast Cancer Progression Working Party. (2000) *Lancet* **355:** 1787-8

Feldman D, Thulasiraman V, Ferreyra… R (1999) Formation of the VHL–elongin BC tumor suppressor complex is mediated by the chaperonin TRiC. *Mol Cell*

Feldman DE, Spiess C, Howard DE, Frydman J (2003) Tumorigenic mutations in VHL disrupt folding in vivo by interfering with chaperonin binding. *Mol Cell* **12:** 1213-24

Ferber EC, Peck B, Delpuech O, Bell GP, East P, Schulze A (2011) FOXO3a regulates reactive oxygen metabolism by inhibiting mitochondrial gene expression. *Cell Death Differ*

Ferrara N, Henzel WJ (1989) Pituitary follicular cells secrete a novel heparin-binding growth factor specific for vascular endothelial cells. *Biochem Biophys Res Commun* **161:** 851-8

Figg WD, Folkman MJ (2008) *Angiogenesis : an integrative approach from science to medicine*. New York, NY: Springer

Finley LWS, Carracedo A, Lee J, Souza A, Egia A, Zhang J, Teruya-Feldstein J, Moreira PI, Cardoso SM, Clish CB, Pandolfi PP, Haigis MC (2011) SIRT3 Opposes Reprogramming of Cancer Cell Metabolism through HIF1α Destabilization. *Cancer Cell* **19:** 416-28

Fischer H, Glockshuber R (1994) A point mutation within the ATP-binding site inactivates both catalytic functions of the ATP-dependent protease La (Lon) from Escherichia coli. *FEBS Lett* **356:** 101-3

Fishovitz J, Li M, Frase H, Hudak J, Craig S, Ko K, Berdis AJ, Suzuki C, Lee I (2011) Active-site directed chemical tools for profiling mitochondrial Lon protease. *ACS Chem Biol*

Flashman E, Hoffart LM, Hamed RB, Bollinger JM, Krebs C, Schofield CJ (2010) Evidence for the slow reaction of hypoxia-inducible factor prolyl hydroxylase 2 with oxygen. *FEBS J* **277:** 4089-99

Folkman J (1971) Tumor angiogenesis: therapeutic implications. *N Engl J Med* **285:** 1182-6

Folkman J, Cole P, Zimmerman S (1966) Tumor behavior in isolated perfused organs: in vitro growth and metastases of biopsy material in rabbit thyroid and canine intestinal segment. *Ann Surg*

Folkman J, Long Jr D, Becker F (1963) Growth and metastasis of tumor in organ culture. *Cancer*

Forbes SA, Bhamra G, Bamford S, Dawson E, Kok C, Clements J, Menzies A, Teague JW, Futreal PA, Stratton MR (2008) The Catalogue of Somatic Mutations in Cancer (COSMIC). *Curr Protoc Hum Genet* **Chapter 10:** Unit 10 11

Frase H, Hudak J, Lee I (2006) Identification of the proteasome inhibitor MG262 as a potent ATP-dependent inhibitor of the Salmonella enterica serovar Typhimurium Lon protease. *Biochemistry (Mosc)* **45:** 8264-74

Fu GK, Markovitz DM (1998) The human LON protease binds to mitochondrial promoters in a single-stranded, site-specific, strand-specific manner. *Biochemistry (Mosc)* **37:** 1905-9

Fu GK, Smith MJ, Markovitz DM (1997) Bacterial protease Lon is a site-specific DNA-binding protein. *The Journal of biological chemistry* **272:** 534-8

Fukuda R, Zhang H, Kim J-w, Shimoda L, Dang CV, Semenza GL (2007) HIF-1 regulates cytochrome oxidase subunits to optimize efficiency of respiration in hypoxic cells. *Cell* **129:** 111-22

García-Nafría J, Ondrovičová G, Blagova E, Levdikov VM, Bauer JA, Suzuki CK, Kutejová E, Wilkinson AJ, Wilson KS (2010) Structure of the catalytic domain of the human mitochondrial Lon protease: Proposed relation of oligomer formation and activity. *Protein Sci*

Giatromanolaki A, Koukourakis MI, Pezzella F, Sivridis E, Turley H, Harris AL, Gatter KC (2008) Phosphorylated VEGFR2/KDR receptors are widely expressed in B-cell non-Hodgkin's lymphomas and correlate with hypoxia inducible factor activation. *Hematol Oncol* **26:** 219-24

Gil J, Kerai P, Lleonart M, Bernard D, Cigudosa JC, Peters G, Carnero A, Beach D (2005) Immortalization of primary human prostate epithelial cells by c-Myc. *Cancer Res* **65:** 2179-85

Gillies RJ, Robey I, Gatenby RA (2008) Causes and consequences of increased glucose metabolism of cancers. *J Nucl Med* **49 Suppl 2:** 24S-42S

Golinska M, Troy H, Chung Y-L, McSheehy PM, Mayr M, Yin X, Ly L, Williams KJ, Airley RE, Harris AL, Latigo J, Perumal M, Aboagye EO, Perrett D, Stubbs M, Griffiths JR (2011) Adaptation to HIF-1 deficiency by upregulation of the AMP/ATP ratio and phosphofructokinase activation in hepatomas. *BMC Cancer* **11:** 198

Gonzalez M, Frank EG, Levine AS, Woodgate R (1998) Lon-mediated proteolysis of the Escherichia coli UmuD mutagenesis protein: in vitro degradation and identification of residues required for proteolysis. *Genes Dev* **12:** 3889-99

Granot Z, Geiss-Friedlander R, Melamed-Book N, Eimerl S, Timberg R, Weiss AM, Hales KH, Hales DB, Stocco DM, Orly J (2003) Proteolysis of normal and mutated steroidogenic acute regulatory proteins in the mitochondria: the fate of unwanted proteins. *Mol Endocrinol* **17:** 2461-76

Granot Z, Kobiler O, Melamed-Book N, Eimerl S, Bahat A, Lu B, Braun S, Maurizi MR, Suzuki CK, Oppenheim AB, Orly J (2007) Turnover of mitochondrial steroidogenic acute regulatory (StAR) protein by Lon protease: the unexpected effect of proteasome inhibitors. *Mol Endocrinol* **21:** 2164-77

Gray MW, Burger G, Lang BF (1999) Mitochondrial evolution. *Science* **283:** 1476-81

Greer SN, Metcalf JL, Wang Y, Ohh M (2012) The updated biology of hypoxia-inducible factor. *EMBO J* **31:** 2448-60

Guha S, López-Maury L, Shaw M, Bähler J, Norbury CJ, Agashe VR (2011) Transcriptional and cellular responses to defective mitochondrial proteolysis in fission yeast. *J Mol Biol* **408:** 222-37

Gur E, Sauer RT (2008) Recognition of misfolded proteins by Lon, a AAA(+) protease. *Genes Dev* **22:** 2267-77

Gur E, Sauer RT (2009) Degrons in protein substrates program the speed and operating efficiency of the AAA+ Lon proteolytic machine. *Proc Natl Acad Sci USA* **106:** 18503-8

Hanahan D, Folkman J (1996) Patterns and emerging mechanisms of the angiogenic switch during tumorigenesis. *Cell* **86:** 353-64

Hanahan D, Weinberg RA (2011) Hallmarks of cancer: the next generation. *Cell* **144:** 646-74

Hansen WJ, Ohh M, Moslehi J, Kondo K, Kaelin WG, Welch WJ (2002) Diverse effects of mutations in exon II of the von Hippel-Lindau (VHL) tumor suppressor gene on the interaction of pVHL with the cytosolic chaperonin and pVHL-dependent ubiquitin ligase activity. *Mol Cell Biol* **22:** 1947-60

Haynes CM, Petrova K, Benedetti C, Yang Y, Ron D (2007) ClpP mediates activation of a mitochondrial unfolded protein response in C. elegans. *Dev Cell* **13:** 467-80

Haynes CM, Ron D (2010) The mitochondrial UPR - protecting organelle protein homeostasis. *J Cell Sci* **123:** 3849-55

Haynes CM, Yang Y, Blais SP, Neubert TA, Ron D (2010) The matrix peptide exporter HAF-1 signals a mitochondrial UPR by activating the transcription factor ZC376.7 in C. elegans. *Mol Cell* **37:** 529-40

Heffelfinger SC, Hawkins HH, Barrish J, Taylor L, Darlington GJ (1992) SK HEP-1: a human cell line of endothelial origin. *In Vitro Cell Dev Biol* **28A:** 136-42

Hervouet E, Cízková A, Demont J, Vojtísková A, Pecina P, Franssen-van Hal NLW, Keijer J, Simonnet H, Ivánek R, Kmoch S, Godinot C, Houstek J (2008) HIF and reactive oxygen species regulate oxidative phosphorylation in cancer. *Carcinogenesis* **29:** 1528-37

Hervouet E, Demont J, Pecina P, Vojtísková A, Houstek J, Simonnet H, Godinot C (2005) A new role for the von Hippel-Lindau tumor suppressor protein: stimulation of mitochondrial oxidative phosphorylation complex biogenesis. *Carcinogenesis* **26:** 531-9

Hervouet E, Pecina P, Demont J, Vojtísková A, Simonnet H, Houstek J, Godinot C (2006) Inhibition of cytochrome c oxidase subunit 4 precursor processing by the hypoxia mimic cobalt chloride. *Biochem Biophys Res Commun* **344:** 1086-93

Hewitson KS, Liénard BMR, McDonough MA, Clifton IJ, Butler D, Soares AS, Oldham NJ, McNeill LA, Schofield CJ (2007) Structural and mechanistic studies on the inhibition of the hypoxia-inducible transcription factor hydroxylases by tricarboxylic acid cycle intermediates. *J Biol Chem* **282:** 3293-301

Hirsilä M, Koivunen P, Günzler V, Kivirikko KI, Myllyharju J (2003) Characterization of the human prolyl 4-hydroxylases that modify the hypoxia-inducible factor. *The Journal of biological chemistry* **278:** 30772-80

Hoffman DL, Salter JD, Brookes PS (2007) Response of mitochondrial reactive oxygen species generation to steady-state oxygen tension: implications for hypoxic cell signaling. *Am J Physiol Heart Circ Physiol* **292:** H101-8

Hori O, Ichinoda F, Tamatani T, Yamaguchi A, Sato N, Ozawa K, Kitao Y, Miyazaki M, Harding HP, Ron D, Tohyama M, M Stern D, Ogawa S (2002) Transmission of cell stress from endoplasmic reticulum to mitochondria: enhanced expression of Lon protease. *J Cell Biol* **157:** 1151-60

Horibe T, Hoogenraad NJ (2007) The chop gene contains an element for the positive regulation of the mitochondrial unfolded protein response. *PLoS ONE* **2:** e835

HOWARD-FLANDERS P, SIMSON E, THERIOT L (1964) A LOCUS THAT CONTROLS FILAMENT FORMATION AND SENSITIVITY TO RADIATION IN ESCHERICHIA COLI K-12. *Genetics* **49:** 237-46

Hu J, Bianchi F, Ferguson M, Cesario A, Margaritora S, Granone P, Goldstraw P, Tetlow M, Ratcliffe C, Nicholson AG, Harris A, Gatter K, Pezzella F (2005) Gene expression signature for angiogenic and nonangiogenic non-small-cell lung cancer. *Oncogene* **24:** 1212-9

Huang LE, Bindra RS, Glazer PM, Harris AL (2007) Hypoxia-induced genetic instability--a calculated mechanism underlying tumor progression. *J Mol Med* **85:** 139-48

Hutchison GJ, Valentine HR, Loncaster JA, Davidson SE, Hunter RD, Roberts SA, Harris AL, Stratford IJ, Price PM, West CML (2004) Hypoxia-inducible factor 1alpha expression as an intrinsic marker of hypoxia: correlation with tumor oxygen, pimonidazole measurements, and outcome in locally advanced carcinoma of the cervix. *Clin Cancer Res* **10:** 8405-12

Hynes J, O'Riordan TC, Zhdanov AV, Uray G, Will Y, Papkovsky DB (2009) In vitro analysis of cell metabolism using a long-decay pH-sensitive lanthanide probe and extracellular acidification assay. *Anal Biochem* **390:** 21-8

Iliopoulos O, Ohh M, Kaelin WG (1998) pVHL19 is a biologically active product of the von Hippel-Lindau gene arising from internal translation initiation. *Proc Natl Acad Sci USA* **95:** 11661-6

Iosefson O, Sharon S, Goloubinoff P, Azem A (2012) Reactivation of protein aggregates by mortalin and Tid1--the human mitochondrial Hsp70 chaperone system. *Cell Stress Chaperones* **17:** 57-66

Isaacs JS, Jung YJ, Mole DR, Lee S, Torres-Cabala C, Chung Y-L, Merino M, Trepel J, Zbar B, Toro J, Ratcliffe PJ, Linehan WM, Neckers L (2005) HIF overexpression correlates with biallelic loss of fumarate hydratase in renal cancer: novel role of fumarate in regulation of HIF stability. *Cancer Cell* **8:** 143-53

Ito T, Ando H, Suzuki T, Ogura T, Hotta K, Imamura Y, Yamaguchi Y, Handa H (2010) Identification of a primary target of thalidomide teratogenicity. *Science* **327:** 1345-50

Jaakkola P, Mole DR, Tian YM, Wilson MI, Gielbert J, Gaskell SJ, Av K, Hebestreit HF, Mukherji M, Schofield CJ, Maxwell PH, Pugh CW, Ratcliffe PJ (2001) Targeting of HIF-alpha to the von Hippel-Lindau ubiquitylation complex by O2-regulated prolyl hydroxylation. *Science* **292:** 468-72

Jiang BH, Semenza GL, Bauer C, Marti HH (1996) Hypoxia-inducible factor 1 levels vary exponentially over a physiologically relevant range of O2 tension. *Am J Physiol* **271:** C1172-80

Jubete Y, Maurizi MR, Gottesman S (1996) Role of the heat shock protein DnaJ in the lon-dependent degradation of naturally unstable proteins. *The Journal of biological chemistry* **271:** 30798-803

Kaelin WG, Ratcliffe PJ (2008) Oxygen sensing by metazoans: the central role of the HIF hydroxylase pathway. *Mol Cell* **30:** 393-402

Kaluz S, Kaluzová M, Stanbridge EJ (2006) Proteasomal inhibition attenuates transcriptional activity of hypoxia-inducible factor 1 (HIF-1) via specific effect on the HIF-1alpha C-terminal activation domain. *Mol Cell Biol* **26:** 5895-907

Kampinga HH, Craig EA (2010) The HSP70 chaperone machinery: J proteins as drivers of functional specificity. *Nat Rev Mol Cell Biol* **11:** 579-92

Karbowski M, Kurono C, Wozniak M, Ostrowski M, Teranishi M, Soji T, Wakabayashi T (1999) Cycloheximide and 4-OH-TEMPO suppress chloramphenicol-induced apoptosis in RL-34 cells via the suppression of the formation of megamitochondria. *Biochim Biophys Acta* **1449:** 25-40

Karihtala P, Kauppila S, Puistola U, Jukkola-Vuorinen A (2011) Divergent behaviour of oxidative stress markers 8-hydroxydeoxyguanosine (8-OHdG) and 4-hydroxy-2-nonenal (HNE) in breast carcinogenesis. *Histopathology* **58:** 854-62

Karihtala P, Soini Y, Vaskivuo L, Bloigu R, Puistola U (2009) DNA adduct 8-hydroxydeoxyguanosine, a novel putative marker of prognostic significance in ovarian carcinoma. *Int J Gynecol Cancer* **19:** 1047-51

Kawanishi S, Hiraku Y, Pinlaor S, Ma N (2006) Oxidative and nitrative DNA damage in animals and patients with inflammatory diseases in relation to inflammation-related carcinogenesis. *Biol Chem* **387:** 365-72

Keith B, Johnson RS, Simon MC (2012) HIF1α and HIF2α: sibling rivalry in hypoxic tumour growth and progression. *Nat Rev Cancer* **12:** 9-22

Keniry M, Parsons R (2008) The role of PTEN signaling perturbations in cancer and in targeted therapy. *Oncogene* **27:** 5477-85

Kikuchi M, Hatano N, Yokota S, Shimozawa N, Imanaka T, Taniguchi H (2004) Proteomic analysis of rat liver peroxisome: presence of peroxisome-specific isozyme of Lon protease. *The Journal of biological chemistry* **279:** 421-8

Kim HS, Patel K, Muldoon-Jacobs K, Bisht KS, Aykin-Burns N, Pennington JD, van der Meer R, Nguyen P, Savage J, Owens KM, Vassilopoulos A, Ozden O, Park SH, Singh KK, Abdulkadir SA, Spitz DR, Deng CX, Gius D (2010) SIRT3 is a mitochondria-localized tumor suppressor required for maintenance of mitochondrial integrity and metabolism during stress. *Cancer Cell* **17:** 41-52

Kim J-w, Gao P, Liu Y-C, Semenza GL, Dang CV (2007) Hypoxia-inducible factor 1 and dysregulated c-Myc cooperatively induce vascular endothelial growth factor and metabolic switches hexokinase 2 and pyruvate dehydrogenase kinase 1. *Mol Cell Biol* **27:** 7381-93

Kim J-w, Tchernyshyov I, Semenza GL, Dang CV (2006) HIF-1-mediated expression of pyruvate dehydrogenase kinase: a metabolic switch required for cellular adaptation to hypoxia. *Cell Metab* **3:** 177-85

Kim J-w, Zeller KI, Wang Y, Jegga AG, Aronow BJ, O'Donnell KA, Dang CV (2004) Evaluation of myc E-box phylogenetic footprints in glycolytic genes by chromatin immunoprecipitation assays. *Mol Cell Biol* **24:** 5923-36

Kinnula VL, Crapo JD (2004) Superoxide dismutases in malignant cells and human tumors. *Free Radic Biol Med* **36:** 718-44

Kishida T, Stackhouse TM, Chen F, Lerman MI, Zbar B (1995) Cellular proteins that bind the von Hippel-Lindau disease gene product: mapping of binding domains and the effect of missense mutations. *Cancer Res* **55:** 4544-8

Kita K, Suzuki T, Ochi T (2012) Diphenylarsinic Acid promotes degradation of glutaminase C by mitochondrial lon protease. *The Journal of biological chemistry* **287:** 18163-72

Knowles HJ, Raval RR, Harris AL, Ratcliffe PJ (2003) Effect of ascorbate on the activity of hypoxia-inducible factor in cancer cells. *Cancer Res* **63:** 1764-8

Köhler G, Milstein C (1975) Continuous cultures of fused cells secreting antibody of predefined specificity. *Nature* **256:** 495-7

Kondo K, Kim WY, Lechpammer M, Kaelin WG (2003) Inhibition of HIF2alpha is sufficient to suppress pVHL-defective tumor growth. *PLoS Biol* **1:** E83

Kops GJPL, Dansen TB, Polderman PE, Saarloos I, Wirtz KWA, Coffer PJ, Huang T-T, Bos JL, Medema RH, Burgering BMT (2002) Forkhead transcription factor FOXO3a protects quiescent cells from oxidative stress. *Nature* **419:** 316-21

Koumenis C (2006) ER stress, hypoxia tolerance and tumor progression. *Curr Mol Med* **6:** 55-69

Kuroda A, Nomura K, Ohtomo R, Kato J, Ikeda T, Takiguchi N, Ohtake H, Kornberg A (2001) Role of inorganic polyphosphate in promoting ribosomal protein degradation by the Lon protease in E. coli. *Science* **293:** 705-8

Kwast KE, Burke PV, Poyton RO (1998) Oxygen sensing and the transcriptional regulation of oxygen-responsive genes in yeast. *J Exp Biol* **201:** 1177-95

Lando D, Peet DJ, Gorman JJ, Whelan DA, Whitelaw ML, Bruick RK (2002) FIH-1 is an asparaginyl hydroxylase enzyme that regulates the transcriptional activity of hypoxia-inducible factor. *Genes Dev* **16:** 1466-71

Landy A (1989) Dynamic, structural, and regulatory aspects of lambda site-specific recombination. *Annu Rev Biochem* **58:** 913-49

Leclercq G, Bojar H, Goussard J, Nicholson RI, Pichon MF, Piffanelli A, Pousette A, Thorpe S, Lonsdorfer M (1986) Abbott monoclonal enzyme immunoassay measurement of estrogen receptors in human breast cancer: a European multicenter study. *Cancer Res* **46:** 4233s-4236s

Lee AY-L, Hsu C-H, Wu S-H (2004) Functional domains of Brevibacillus thermoruber lon protease for oligomerization and DNA binding: role of N-terminal and sensor and substrate discrimination domains. *The Journal of biological chemistry* **279:** 34903-12

Lee HJ, Chung K, Lee H, Lee K, Lim JH, Song J (2011) Downregulation of mitochondrial lon protease impairs mitochondrial function and causes hepatic insulin resistance in human liver SK-HEP-1 cells. *Diabetologia*

Lee I, Suzuki CK (2008) Functional mechanics of the ATP-dependent Lon protease- lessons from endogenous protein and synthetic peptide substrates. *Biochim Biophys Acta* **1784:** 727-35

Lee S-J, Hwang AB, Kenyon C (2010) Inhibition of respiration extends C. elegans life span via reactive oxygen species that increase HIF-1 activity. *Curr Biol* **20:** 2131-6

Lewis MD, Roberts BJ (2004) Role of the C-terminal alpha-helical domain of the von Hippel-Lindau protein in its E3 ubiquitin ligase activity. *Oncogene* **23:** 2315-23

Li F, Wang Y, Zeller KI, Potter JJ, Wonsey DR, O'Donnell KA, Kim J-w, Yustein JT, Lee LA, Dang CV (2005a) Myc stimulates nuclearly encoded mitochondrial genes and mitochondrial biogenesis. *Mol Cell Biol* **25:** 6225-34

Li L, Lin X, Staver M, Shoemaker A, Semizarov D, Fesik SW, Shen Y (2005b) Evaluating hypoxia-inducible factor-1alpha as a cancer therapeutic target via inducible RNA interference in vivo. *Cancer Res* **65:** 7249-58

Li M, Rasulova F, Melnikov EE, Rotanova TV, Gustchina A, Maurizi MR, Wlodawer A (2005c) Crystal structure of the N-terminal domain of E. coli Lon protease. *Protein Sci* **14:** 2895-900

Li T, Ho L, Piperdi B, Elrafei T, Camacho FJ, Rigas JR, Perez-Soler R, Gucalp R (2010) Phase II study of the proteasome inhibitor bortezomib (PS-341, Velcade) in chemotherapy-naïve patients with advanced stage non-small cell lung cancer (NSCLC). *Lung Cancer* **68:** 89-93

Liao J-H, Lin Y-C, Hsu J, Lee AY-L, Chen T-A, Hsu C-H, Chir J-L, Hua K-F, Wu T-H, Hong L-J, Yen P-W, Chiou A, Wu S-H (2010) Binding and cleavage of E. coli HUbeta by the E. coli Lon protease. *Biophys J* **98:** 129-37

Lidgren A, Hedberg Y, Grankvist K, Rasmuson T, Vasko J, Ljungberg B (2005) The expression of hypoxia-inducible factor 1alpha is a favorable independent prognostic factor in renal cell carcinoma. *Clinical cancer research : an official journal of the American Association for Cancer Research* **11:** 1129-35

Lim J-H, Lee Y-M, Chun Y-S, Chen J, Kim J-E, Park J-W (2010) Sirtuin 1 modulates cellular responses to hypoxia by deacetylating hypoxia-inducible factor 1alpha. *Mol Cell* **38:** 864-78

Lin X, Ruan X, Anderson MG, McDowell JA, Kroeger PE, Fesik SW, Shen Y (2005) siRNA-mediated off-target gene silencing triggered by a 7 nt complementation. *Nucleic Acids Res* **33:** 4527-35

Ling Y-H, Liebes L, Zou Y, Perez-Soler R (2003) Reactive oxygen species generation and mitochondrial dysfunction in the apoptotic response to Bortezomib, a novel proteasome inhibitor, in human H460 non-small cell lung cancer cells. *The Journal of biological chemistry* **278:** 33714-23

Liu T, Lu B, Lee I, Ondrovicová G, Kutejová E, Suzuki CK (2004) DNA and RNA binding by the mitochondrial lon protease is regulated by nucleotide and protein substrate. *J Biol Chem* **279:** 13902-10

Liu Y, Cox SR, Morita T, Kourembanas S (1995) Hypoxia regulates vascular endothelial growth factor gene expression in endothelial cells. Identification of a 5' enhancer. *Circ Res* **77:** 638-43

Lowth BR, Kirstein-Miles J, Saiyed T, Brötz-Oesterhelt H, Morimoto RI, Truscott KN, Dougan DA (2012) Substrate recognition and processing by a Walker B mutant of the human mitochondrial AAA+ protein CLPX. *J Struct Biol* **179:** 193-201

Lu B, Garrido N, Spelbrink JN, Suzuki CK (2006) Tid1 isoforms are mitochondrial DnaJ-like chaperones with unique carboxyl termini that determine cytosolic fate. *The Journal of biological chemistry* **281:** 13150-8

Lu B, Lee J, Nie X, Li M, Morozov YI, Venkatesh S, Bogenhagen DF, Temiakov D, Suzuki CK (2012) Phosphorylation of Human TFAM in Mitochondria Impairs DNA Binding and Promotes Degradation by the AAA(+) Lon Protease. *Mol Cell*

Lu B, Yadav S, Shah PG, Liu T, Tian B, Pukszta S, Villaluna N, Kutejová E, Newlon CS, Santos JH, Suzuki CK (2007) Roles for the human ATP-dependent Lon protease in mitochondrial DNA maintenance. *J Biol Chem* **282:** 17363-74

Lu H, Dalgard CL, Mohyeldin A, McFate T, Tait AS, Verma A (2005) Reversible inactivation of HIF-1 prolyl hydroxylases allows cell metabolism to control basal HIF-1. *The Journal of biological chemistry* **280:** 41928-39

Lu H, Forbes RA, Verma A (2002) Hypoxia-inducible factor 1 activation by aerobic glycolysis implicates the Warburg effect in carcinogenesis. *The Journal of biological chemistry* **277:** 23111-5

Lu X, Kang Y (2010) Hypoxia and hypoxia-inducible factors: master regulators of metastasis. *Clin Cancer Res* **16:** 5928-35

Luo W, Hu H, Chang R, Zhong J, Knabel M, O'Meally R, Cole RN, Pandey A, Semenza GL (2011) Pyruvate kinase M2 is a PHD3-stimulated coactivator for hypoxia-inducible factor 1. *Cell* **145:** 732-44

Luo W, Zhong J, Chang R, Hu H, Pandey A, Semenza GL (2010) Hsp70 and CHIP selectively mediate ubiquitination and degradation of hypoxia-inducible factor (HIF)-1alpha but Not HIF-2alpha. *J Biol Chem* **285:** 3651-63

Maher ER, Neumann HP, Richard S (2011) von Hippel-Lindau disease: a clinical and scientific review. *Eur J Hum Genet* **19:** 617-23

Major T, von Janowsky B, Ruppert T, Mogk A, Voos W (2006) Proteomic analysis of mitochondrial protein turnover: identification of novel substrate proteins of the matrix protease pim1. *Mol Cell Biol* **26:** 762-76

Makino Y, Kanopka A, Wilson WJ, Tanaka H, Poellinger L (2002) Inhibitory PAS domain protein (IPAS) is a hypoxia-inducible splicing variant of the hypoxia-inducible factor-3alpha locus. *J Biol Chem* **277:** 32405-8

Maniotis AJ, Folberg R, Hess A, Seftor EA, Gardner LM, Pe'er J, Trent JM, Meltzer PS, Hendrix MJ (1999) Vascular channel formation by human melanoma cells in vivo and in vitro: vasculogenic mimicry. *Am J Pathol* **155:** 739-52

Mansfield KD, Guzy RD, Pan Y, Young RM, Cash TP, Schumacker PT, Simon MC (2005) Mitochondrial dysfunction resulting from loss of cytochrome c impairs cellular oxygen sensing and hypoxic HIF-alpha activation. *Cell Metab* **1:** 393-9

Masson N, Singleton RS, Sekirnik R, Trudgian DC, Ambrose LJ, Miranda MX, Tian Y-M, Kessler BM, Schofield CJ, Ratcliffe PJ (2012) The FIH hydroxylase is a cellular peroxide sensor that modulates HIF transcriptional activity. *EMBO Rep* **13:** 251-7

Masson N, Willam C, Maxwell PH, Pugh CW, Ratcliffe PJ (2001) Independent function of two destruction domains in hypoxia-inducible factor-alpha chains activated by prolyl hydroxylation. *EMBO J* **20:** 5197-206

Matsushima Y, Goto Y-I, Kaguni LS (2010) Mitochondrial Lon protease regulates mitochondrial DNA copy number and transcription by selective degradation of mitochondrial transcription factor A (TFAM). *Proc Natl Acad Sci USA*

Mattingly KA, Ivanova MM, Riggs KA, Wickramasinghe NS, Barch MJ, Klinge CM (2008) Estradiol stimulates transcription of nuclear respiratory factor-1 and increases mitochondrial biogenesis. *Mol Endocrinol* **22:** 609-22

Maxwell PH, Wiesener MS, Chang GW, Clifford SC, Vaux EC, Cockman ME, Wykoff CC, Pugh CW, Maher ER, Ratcliffe PJ (1999) The tumour suppressor protein VHL targets hypoxia-inducible factors for oxygen-dependent proteolysis. *Nature* **399:** 271-5

McClellan AJ, Scott MD, Frydman J (2005) Folding and quality control of the VHL tumor suppressor proceed through distinct chaperone pathways. *Cell* **121:** 739-48

McNeill LA, Hewitson KS, Gleadle JM, Horsfall LE, Oldham NJ, Maxwell PH, Pugh CW, Ratcliffe PJ, Schofield CJ (2002) The use of dioxygen by HIF prolyl hydroxylase (PHD1). *Bioorg Med Chem Lett* **12:** 1547-50

McShane LM, Altman DG, Sauerbrei W, Taube SE, Gion M, Clark GM, Diagnostics SSotN-EWGoC (2005) REporting recommendations for tumour MARKer prognostic studies (REMARK). *Br J Cancer* **93:** 387-91

Melville MW, McClellan AJ, Meyer AS, Darveau A, Frydman J (2003) The Hsp70 and TRiC/CCT chaperone systems cooperate in vivo to assemble the von Hippel-Lindau tumor suppressor complex. *Mol Cell Biol* **23:** 3141-51

Mick DU, Fox TD, Rehling P (2011) Inventory control: cytochrome c oxidase assembly regulates mitochondrial translation. *Nat Rev Mol Cell Biol* **12:** 14-20

Min J-H, Yang H, Ivan M, Gertler F, Kaelin WG, Pavletich NP (2002) Structure of an HIF-1alpha -pVHL complex: hydroxyproline recognition in signaling. *Science* **296:** 1886-9

Miyake K, Yoshizumi T, Imura S, Sugimoto K, Batmunkh E, Kanemura H, Morine Y, Shimada M (2008) Expression of hypoxia-inducible factor-1alpha, histone deacetylase 1, and metastasis-associated protein 1 in pancreatic carcinoma: correlation with poor prognosis with possible regulation. *Pancreas* **36:** e1-9

Moeller BJ, Richardson RA, Dewhirst MW (2007) Hypoxia and radiotherapy: opportunities for improved outcomes in cancer treatment. *Cancer Metastasis Rev* **26:** 241-8

Mole DR, Blancher C, Copley RR, Pollard PJ, Gleadle JM, Ragoussis J, Ratcliffe PJ (2009) Genome-wide association of hypoxia-inducible factor (HIF)-1alpha and HIF-2alpha DNA binding with expression profiling of hypoxia-inducible transcripts. *J Biol Chem* **284:** 16767-75

Murtas D, Piras F, Minerba L, Ugalde J, Floris C, Maxia C, Demurtas P, Perra MT, Sirigu P (2010) Nuclear 8-hydroxy-2'-deoxyguanosine as survival biomarker in patients with cutaneous melanoma. *Oncol Rep* **23:** 329-35

Nargund AM, Pellegrino MW, Fiorese CJ, Baker BM, Haynes CM (2012) Mitochondrial import efficiency of ATFS-1 regulates mitochondrial UPR activation. *Science* **337:** 587-90

Ngo JK, Davies KJA (2009) Mitochondrial Lon protease is a human stress protein. *Free Radic Biol Med* **46:** 1042-8

Noguera R, Fredlund E, Piqueras M, Pietras A, Beckman S, Navarro S, Påhlman S (2009) HIF-1alpha and HIF-2alpha are differentially regulated in vivo in neuroblastoma: high HIF-1alpha correlates negatively to advanced clinical stage and tumor vascularization. *Clinical cancer research : an official journal of the American Association for Cancer Research* **15:** 7130-6

Nomura K, Kato J, Takiguchi N, Ohtake H, Kuroda A (2004) Effects of inorganic polyphosphate on the proteolytic and DNA-binding activities of Lon in Escherichia coli. *The Journal of biological chemistry* **279:** 34406-10

O'Flaherty L, Adam J, Heather LC, Zhdanov AV, Chung Y-L, Miranda MX, Croft J, Olpin S, Clarke K, Pugh CW, Griffiths J, Papkovsky D, Ashrafian H, Ratcliffe PJ, Pollard PJ (2010) Dysregulation of hypoxia pathways in fumarate hydratase-deficient cells is independent of defective mitochondrial metabolism. *Hum Mol Genet* **19:** 3844-51

Oberley TD, Zhong W, Szweda LI, Oberley LW (2000) Localization of antioxidant enzymes and oxidative damage products in normal and malignant prostate epithelium. *Prostate* **44:** 144-55

Ogura T, Wilkinson AJ (2001) AAA+ superfamily ATPases: common structure--diverse function. *Genes Cells* **6:** 575-97

Okumoto K, Kametani Y, Fujiki Y (2011) Two proteases, trypsin domain-containing 1 (Tysnd1) and peroxisomal lon protease (PsLon), cooperatively regulate fatty acid β-oxidation in peroxisomal matrix. *The Journal of biological chemistry* **286:** 44367-79

Okumura F, Matsuzaki M, Nakatsukasa K, Kamura T (2012) The Role of Elongin BC-Containing Ubiquitin Ligases. *Front Oncol* **2:** 10

Ondrovicová G, Liu T, Singh K, Tian B, Li H, Gakh O, Perecko D, Janata J, Granot Z, Orly J, Kutejová E, Suzuki CK (2005) Cleavage site selection within a folded substrate by the ATP-dependent lon protease. *The Journal of biological chemistry* **280:** 25103-10

Ostersetzer O, Kato Y, Adam Z, Sakamoto W (2007) Multiple intracellular locations of Lon protease in Arabidopsis: evidence for the localization of AtLon4 to chloroplasts. *Plant Cell Physiol* **48:** 881-5

Ozbabacan SEA, Engin HB, Gursoy A, Keskin O (2011) Transient protein-protein interactions. *Protein Eng Des Sel* **24:** 635-48

Palmer CS, Osellame LD, Stojanovski D, Ryan MT (2011) The regulation of mitochondrial morphology: Intricate mechanisms and dynamic machinery. *Cell Signal*

Pan Y, Mansfield KD, Bertozzi CC, Rudenko V, Chan DA, Giaccia AJ, Simon MC (2007) Multiple factors affecting cellular redox status and energy metabolism modulate hypoxia-inducible factor prolyl hydroxylase activity in vivo and in vitro. *Mol Cell Biol* **27:** 912-25

Panaretou B, Prodromou C, Roe SM, O'Brien R, Ladbury JE, Piper PW, Pearl LH (1998) ATP binding and hydrolysis are essential to the function of the Hsp90 molecular chaperone in vivo. *The EMBO journal* **17:** 4829-36

Papandreou I, Cairns RA, Fontana L, Lim AL, Denko NC (2006) HIF-1 mediates adaptation to hypoxia by actively downregulating mitochondrial oxygen consumption. *Cell Metab* **3:** 187-97

Pastoreková S, Závadová Z, Kostál M, Babusíková O, Závada J (1992) A novel quasi-viral agent, MaTu, is a two-component system. *Virology* **187:** 620-6

Patan S, Munn LL, Jain RK (1996) Intussusceptive microvascular growth in a human colon adenocarcinoma xenograft: a novel mechanism of tumor angiogenesis. *Microvasc Res* **51:** 260-72

Paulis YWJ, Soetekouw PMMB, Verheul HMW, Tjan-Heijnen VCG, Griffioen AW (2010) Signalling pathways in vasculogenic mimicry. *Biochim Biophys Acta* **1806:** 18-28

Pellegrino MW, Nargund AM, Haynes CM (2013) Signaling the mitochondrial unfolded protein response. *Biochim Biophys Acta* **1833:** 410-6

Pezzella F, Pastorino U, Tagliabue E, Andreola S, Sozzi G, Gasparini G, Menard S, Gatter KC, Harris AL, Fox S, Buyse M, Pilotti S, Pierotti M, Rilke F (1997) Non-small-cell lung carcinoma tumor growth without morphological evidence of neo-angiogenesis. *Am J Pathol* **151:** 1417-23

Pfaffl MW (2001) A new mathematical model for relative quantification in real-time RT-PCR. *Nucleic Acids Res* **29:** e45

Phillips T, VanBogelen… R (1984) lon gene product of Escherichia coli is a heat-shock protein. *J Bacteriol*

Pinheiro C, Sousa B, Albergaria A, Paredes J, Dufloth R, Vieira D, Schmitt F, Baltazar F (2011) GLUT1 and CAIX expression profiles in breast cancer correlate with adverse prognostic factors and MCT1 overexpression. *Histol Histopathol* **26:** 1279-86

Pinti M, Gibellini L, De Biasi S, Nasi M, Roat E, O'Connor J-E, Cossarizza A (2010a) Functional characterization of the promoter of the human Lon protease gene. *Mitochondrion*

Pinti M, Gibellini L, Guaraldi G, Orlando G, Gant TW, Morselli E, Nasi M, Salomoni P, Mussini C, Cossarizza A (2010b) Upregulation of nuclear-encoded mitochondrial LON protease in HAART-treated HIV-positive patients with lipodystrophy: implications for the pathogenesis of the disease. *AIDS* **24:** 841-50

Piperdi B, Ling Y-H, Liebes L, Muggia F, Perez-Soler R (2011) Bortezomib: understanding the mechanism of action. *Mol Cancer Ther* **10:** 2029-30

Pollard PJ, Brière JJ, Alam NA, Barwell J, Barclay E, Wortham NC, Hunt T, Mitchell M, Olpin S, Moat SJ, Hargreaves IP, Heales SJ, Chung YL, Griffiths JR, Dalgleish A, McGrath JA, Gleeson MJ, Hodgson SV, Poulsom R, Rustin P, Tomlinson IPM (2005) Accumulation of Krebs cycle intermediates and over-expression of HIF1alpha in tumours which result from germline FH and SDH mutations. *Hum Mol Genet* **14:** 2231-9

Pore N, Gupta AK, Cerniglia GJ, Maity A (2006) HIV protease inhibitors decrease VEGF/HIF-1alpha expression and angiogenesis in glioblastoma cells. *Neoplasia* **8:** 889-95

Raffel J, Bhattacharyya AK, Gallegos A, Cui H, Einspahr JG, Alberts DS, Powis G (2003) Increased expression of thioredoxin-1 in human colorectal cancer is associated with decreased patient survival. *J Lab Clin Med* **142:** 46-51

Ramachandran A, Moellering DR, Ceaser E, Shiva S, Xu J, Darley-Usmar V (2002) Inhibition of mitochondrial protein synthesis results in increased endothelial cell susceptibility to nitric oxide-induced apoptosis. *Proc Natl Acad Sci U S A* **99:** 6643-8

Rasulova FS, Dergousova NI, Mel'nikov EE, Ginodman LM, Rotanova TV (1998a) [Synthesis and characterisation of ATP-dependent forms of Lon-proteinase with modified N-terminal domain from Escherichia coli]. *Bioorg Khim* **24:** 370-5

Rasulova FS, Dergousova NI, Starkova NN, Melnikov EE, Rumsh LD, Ginodman LM, Rotanova TV (1998b) The isolated proteolytic domain of Escherichia coli ATP-dependent protease Lon exhibits the peptidase activity. *FEBS Lett* **432:** 179-81

Ravi R, Mookerjee B, Bhujwalla ZM, Sutter CH, Artemov D, Zeng Q, Dillehay LE, Madan A, Semenza GL, Bedi A (2000) Regulation of tumor angiogenesis by p53-induced degradation of hypoxia-inducible factor 1alpha. *Genes Dev* **14:** 34-44

Rep M, van Dijl JM, Suda K, Schatz G, Grivell LA, Suzuki CK (1996) Promotion of mitochondrial membrane complex assembly by a proteolytically inactive yeast Lon. *Science* **274:** 103-6

Ribatti D, Vacca A, Dammacco F (2003) New non-angiogenesis dependent pathways for tumour growth. *Eur J Cancer* **39:** 1835-41

Risler JL, Delorme MO, Delacroix H, Henaut A (1988) Amino acid substitutions in structurally related proteins. A pattern recognition approach. Determination of a new and efficient scoring matrix. *J Mol Biol* **204:** 1019-29

Roe J-S, Kim H-R, Hwang I-Y, Ha N-C, Kim S-T, Cho E-J, Youn H-D (2011) Phosphorylation of von Hippel-Lindau protein by checkpoint kinase 2 regulates p53 transactivation. *Cell Cycle* **10**

Rotanova TV, Botos I, Melnikov EE, Rasulova F, Gustchina A, Maurizi MR, Wlodawer A (2006) Slicing a protease: structural features of the ATP-dependent Lon proteases gleaned from investigations of isolated domains. *Protein Sci* **15:** 1815-28

Rotanova TV, Melnikov EE, Khalatova AG, Makhovskaya OV, Botos I, Wlodawer A, Gustchina A (2004) Classification of ATP-dependent proteases Lon and comparison of the active sites of their proteolytic domains. *Eur J Biochem* **271:** 4865-71

Sareddy GR, Nair BC, Gonugunta VK, Zhang Q-g, Brenner A, Brann DW, Tekmal RR, Vadlamudi RK (2012) Therapeutic significance of estrogen receptor β agonists in gliomas. *Mol Cancer Ther* **11:** 1174-82

Scarpulla RC (2008) Transcriptional paradigms in mammalian mitochondrial biogenesis and function. *Physiol Rev* **88:** 611-38

Schmitz KJ, Müller CI, Reis H, Alakus H, Winde G, Baba HA, Wohlschlaeger J, Jasani B, Fandrey J, Schmid KW (2009) Combined analysis of hypoxia-inducible factor 1 alpha and metallothionein indicates an aggressive subtype of colorectal carcinoma. *Int J Colorectal Dis* **24:** 1287-96

Schoenfeld AR, Davidowitz EJ, Burk RD (2000) Elongin BC complex prevents degradation of von Hippel-Lindau tumor suppressor gene products. *Proc Natl Acad Sci U S A* **97:** 8507-12

Schofield CJ, Ratcliffe PJ (2004) Oxygen sensing by HIF hydroxylases. *Nat Rev Mol Cell Biol* **5:** 343-54

Schulze A, Harris AL (2012) How cancer metabolism is tuned for proliferation and vulnerable to disruption. *Nature* **491:** 364-73

Selak MA, Armour SM, MacKenzie ED, Boulahbel H, Watson DG, Mansfield KD, Pan Y, Simon MC, Thompson CB, Gottlieb E (2005) Succinate links TCA cycle dysfunction to oncogenesis by inhibiting HIF-alpha prolyl hydroxylase. *Cancer Cell* **7:** 77-85

Semenza GL (2009) Regulation of cancer cell metabolism by hypoxia-inducible factor 1. *Semin Cancer Biol* **19:** 12-6

Semenza GL (2010a) Defining the role of hypoxia-inducible factor 1 in cancer biology and therapeutics. *Oncogene* **29:** 625-34

Semenza GL (2010b) HIF-1: upstream and downstream of cancer metabolism. *Curr Opin Genet Dev* **20:** 51-6

Semenza GL (2012) Hypoxia-inducible factors in physiology and medicine. *Cell* **148:** 399-408

Semenza GL, Jiang BH, Leung SW, Passantino R, Concordet JP, Maire P, Giallongo A (1996) Hypoxia response elements in the aldolase A, enolase 1, and lactate dehydrogenase A gene promoters contain essential binding sites for hypoxia-inducible factor 1. *The Journal of biological chemistry* **271:** 32529-37

Shackelford DB, Vasquez DS, Corbeil J, Wu S, Leblanc M, Wu C-L, Vera DR, Shaw RJ (2009) mTOR and HIF-1alpha-mediated tumor metabolism in an LKB1 mouse model of Peutz-Jeghers syndrome. *Proc Natl Acad Sci U S A* **106:** 11137-42

Sheridan J, Wang L-M, Tosetto M, Sheahan K, Hyland J, Fennelly D, O'Donoghue D, Mulcahy H, O'Sullivan J (2009) Nuclear oxidative damage correlates with poor survival in colorectal cancer. *Br J Cancer* **100:** 381-8

Shiao YH, Resau JH, Nagashima K, Anderson LM, Ramakrishna G (2000) The von Hippel-Lindau tumor suppressor targets to mitochondria. *Cancer Res* **60:** 2816-9

Shieh Y-S, Lee H-S, Shiah S-G, Chu Y-W, Wu C-W, Chang L-C (2004) Role of angiogenic and non-angiogenic mechanisms in oral squamous cell carcinoma: correlation with histologic differentiation and tumor progression. *J Oral Pathol Med* **33:** 601-6

Shin DH, Chun Y-S, Lee DS, Huang LE, Park J-W (2008) Bortezomib inhibits tumor adaptation to hypoxia by stimulating the FIH-mediated repression of hypoxia-inducible factor-1. *Blood* **111:** 3131-6

Shinojima T, Oya M, Takayanagi A, Mizuno R, Shimizu N, Murai M (2007) Renal cancer cells lacking hypoxia inducible factor (HIF)-1alpha expression maintain vascular endothelial growth factor expression through HIF-2alpha. *Carcinogenesis* **28:** 529-36

Shou Z, Lin L, Liang J, Li J-L, Chen H-Y (2012) Expression and prognosis of FOXO3a and HIF-1α in nasopharyngeal carcinoma. *J Cancer Res Clin Oncol* **138:** 585-93

Sievers F, Wilm A, Dineen D, Gibson TJ, Karplus K, Li W, Lopez R, McWilliam H, Remmert M, Söding J, Thompson JD, Higgins DG (2011) Fast, scalable generation of high-quality protein multiple sequence alignments using Clustal Omega. *Mol Syst Biol* **7:** 539

Sikora S, Godzik A (2004) Combination of multiple alignment analysis and surface mapping paves a way for a detailed pathway reconstruction--the case of VHL (von Hippel-Lindau) protein and angiogenesis regulatory pathway. *Protein Sci* **13:** 786-96

Smirnova E, Griparic L, Shurland DL, van der Bliek AM (2001) Dynamin-related protein Drp1 is required for mitochondrial division in mammalian cells. *Mol Biol Cell* **12:** 2245-56

Smith MA, Schnellmann RG (2011) Mitochondrial calpain 10 is degraded by Lon protease after oxidant injury. *Arch Biochem Biophys*

Söderberg O, Gullberg M, Jarvius M, Ridderstråle K, Leuchowius K-J, Jarvius J, Wester K, Hydbring P, Bahram F, Larsson L-G, Landegren U (2006) Direct observation of individual endogenous protein complexes in situ by proximity ligation. *Nat Methods* **3:** 995-1000

Soilleux EJ, Turley H, Tian YM, Pugh CW, Gatter KC, Harris AL (2005) Use of novel monoclonal antibodies to determine the expression and distribution of the hypoxia regulatory factors PHD-1, PHD-2, PHD-3 and FIH in normal and neoplastic human tissues. *Histopathology* **47:** 602-10

Song J-Y, Marszalek J, Craig EA (2012) Cysteine desulfurase Nfs1 and Pim1 protease control levels of Isu, the Fe-S cluster biogenesis scaffold. *Proc Natl Acad Sci U S A*

Sova H, Jukkola-Vuorinen A, Puistola U, Kauppila S, Karihtala P (2010) 8-Hydroxydeoxyguanosine: a new potential independent prognostic factor in breast cancer. *Br J Cancer* **102:** 1018-23

Stahlberg H, Kutejová E, Suda K, Wolpensinger B, Lustig A, Schatz G, Engel A, Suzuki CK (1999) Mitochondrial Lon of Saccharomyces cerevisiae is a ring-shaped protease with seven flexible subunits. *Proc Natl Acad Sci U S A* **96:** 6787-90

Stickle NH, Chung J, Klco JM, Hill RP, Kaelin WG, Ohh M (2004) pVHL modification by NEDD8 is required for fibronectin matrix assembly and suppression of tumor development. *Mol Cell Biol* **24:** 3251-61

Sun Q, Chen X, Ma J, Peng H, Wang F, Zha X, Wang Y, Jing Y, Yang H, Chen R, Chang L, Zhang Y, Goto J, Onda H, Chen T, Wang M-R, Lu Y, You H, Kwiatkowski D, Zhang H (2011) Mammalian target of rapamycin up-regulation of pyruvate kinase isoenzyme type M2 is critical for aerobic glycolysis and tumor growth. *Proc Natl Acad Sci U S A* **108:** 4129-34

Suzuki CK, Suda K, Wang N, Schatz G (1994) Requirement for the yeast gene LON in intramitochondrial proteolysis and maintenance of respiration. *Science* **264:** 273-6

Swietach P, Vaughan-Jones RD, Harris AL (2007) Regulation of tumor pH and the role of carbonic anhydrase 9. *Cancer Metastasis Rev* **26:** 299-310

Swinson DEB, Jones JL, Cox G, Richardson D, Harris AL, O'Byrne KJ (2004) Hypoxia-inducible factor-1 alpha in non small cell lung cancer: relation to growth factor, protease and apoptosis pathways. *Int J Cancer* **111:** 43-50

Szatrowski TP, Nathan CF (1991) Production of large amounts of hydrogen peroxide by human tumor cells. *Cancer Res* **51:** 794-8

Talks KL, Turley H, Gatter KC, Maxwell PH, Pugh CW, Ratcliffe PJ, Harris AL (2000) The expression and distribution of the hypoxia-inducible factors HIF-1alpha and HIF-2alpha in normal human tissues, cancers, and tumor-associated macrophages. *Am J Pathol* **157:** 411-21

Tao R, Coleman MC, Pennington JD, Ozden O, Park S-H, Jiang H, Kim H-S, Flynn CR, Hill S, Hayes McDonald W, Olivier AK, Spitz DR, Gius D (2010) Sirt3-mediated deacetylation of evolutionarily conserved lysine 122 regulates MnSOD activity in response to stress. *Mol Cell* **40:** 893-904

Tarpey MM, Wink DA, Grisham MB (2004) Methods for detection of reactive metabolites of oxygen and nitrogen: in vitro and in vivo considerations. *Am J Physiol Regul Integr Comp Physiol* **286:** R431-44

Tian Q, Li T, Hou W, Zheng J, Schrum LW, Bonkovsky HL (2011a) Lon Peptidase 1 (LONP1)-dependent Breakdown of Mitochondrial 5-Aminolevulinic Acid Synthase Protein by Heme in Human Liver Cells. *J Biol Chem* **286:** 26424-30

Tian Y-M, Yeoh KK, Lee MK, Eriksson T, Kessler BM, Kramer HB, Edelmann MJ, Willam C, Pugh CW, Schofield CJ, Ratcliffe PJ (2011b) Differential sensitivity of HIF hydroxylation sites to hypoxia and hydroxylase inhibitors. *J Biol Chem* **286:** 13041-51

Tomoyasu T, Mogk A, Langen H, Goloubinoff P, Bukau B (2001) Genetic dissection of the roles of chaperones and proteases in protein folding and degradation in the Escherichia coli cytosol. *Mol Microbiol* **40:** 397-413

Trinh DLN, Elwi AN, Kim S-W (2010) Direct interaction between p53 and Tid1 proteins affects p53 mitochondrial localization and apoptosis. *Oncotarget* **1:** 396-404

Tsai J-P, Liou J-H, Yeh K-T, Tai H-C, Cheng Y-W, Chang H-R (2011) Intensity of cytosol expression of 8-OHdG in normal renal tubules is associated with the severity of renal fibrosis. *Swiss Med Wkly* **141:** w13268

Tsilibaris V, Maenhaut-Michel G, Van Melderen L (2006) Biological roles of the Lon ATP-dependent protease. *Res Microbiol* **157:** 701-13

Ullah MS, Davies AJ, Halestrap AP (2006) The plasma membrane lactate transporter MCT4, but not MCT1, is up-regulated by hypoxia through a HIF-1alpha-dependent mechanism. *The Journal of biological chemistry* **281:** 9030-7

Van den Eynden GG, Bird NC, Majeed AW, Van Laere S, Dirix LY, Vermeulen PB (2012) The histological growth pattern of colorectal cancer liver metastases has prognostic value. *Clin Exp Metastasis* **29:** 541-9

van Dijl JM, Kutejová E, Suda K, Perecko D, Schatz G, Suzuki CK (1998) The ATPase and protease domains of yeast mitochondrial Lon: roles in proteolysis and respiration-dependent growth. *Proc Natl Acad Sci USA* **95:** 10584-9

van Dyck L, Neupert W, Langer T (1998) The ATP-dependent PIM1 protease is required for the expression of intron-containing genes in mitochondria. *Genes Dev* **12:** 1515-24

Van Melderen L, Thi MH, Lecchi P, Gottesman S, Couturier M, Maurizi MR (1996) ATP-dependent degradation of CcdA by Lon protease. Effects of secondary structure and heterologous subunit interactions. *The Journal of biological chemistry* **271:** 27730-8

Vaupel P (2004) The role of hypoxia-induced factors in tumor progression. *Oncologist* **9 Suppl 5:** 10-7

Venkatesh S, Lee J, Singh K, Lee… I (2011) Multitasking in the mitochondrion by the ATP-dependent Lon protease. *Biochimica et Biophysica …*

Wagner I, Arlt H, van Dyck L, Langer T, Neupert W (1994) Molecular chaperones cooperate with PIM1 protease in the degradation of misfolded proteins in mitochondria. *The EMBO journal* **13:** 5135-45

Wagner I, van Dyck L, Savel'ev AS, Neupert W, Langer T (1997) Autocatalytic processing of the ATP-dependent PIM1 protease: crucial function of a pro-region for sorting to mitochondria. *The EMBO journal* **16:** 7317-25

Wang N, Gottesman S, Willingham MC, Gottesman MM, Maurizi MR (1993) A human mitochondrial ATP-dependent protease that is highly homologous to bacterial Lon protease. *Proc Natl Acad Sci USA* **90:** 11247-51

Wang Y, Porter WW, Suh N, Honda T, Gribble GW, Leesnitzer LM, Plunket KD, Mangelsdorf DJ, Blanchard SG, Willson TM, Sporn MB (2000) A synthetic triterpenoid, 2-cyano-3,12-dioxooleana-1,9-dien-28-oic acid (CDDO), is a ligand for the peroxisome proliferator-activated receptor gamma. *Mol Endocrinol* **14:** 1550-6

Warburg O, Wind F, Negelein E (1926) Ueber den Stoffwechsel von Tumoren im körper. *J Mol Med*

Wesseling P, van der Laak JA, de Leeuw H, Ruiter DJ, Burger PC (1994) Quantitative immunohistological analysis of the microvasculature in untreated human glioblastoma multiforme. Computer-assisted image analysis of whole-tumor sections. *J Neurosurg* **81:** 902-9

Willingham M, Gottesman… M (1993) A human mitochondrial ATP-dependent protease that is highly homologous to bacterial Lon protease. *Proceedings of the …*

Wu WF, Zhou Y, Gottesman S (1999) Redundant in vivo proteolytic activities of Escherichia coli Lon and the ClpYQ (HslUV) protease. *J Bacteriol* **181:** 3681-7

Wykoff CC, Beasley NJ, Watson PH, Turner KJ, Pastorek J, Sibtain A, Wilson GD, Turley H, Talks KL, Maxwell PH, Pugh CW, Ratcliffe PJ, Harris AL (2000) Hypoxia-inducible expression of tumor-associated carbonic anhydrases. *Cancer Res* **60:** 7075-83

Yamamoto M, Hiroi T, Kohno H, Yamamoto Y, Hara M, Tanaka T, Mamba K, Watabe S (2005) Nucleotide sequence for cDNA of bovine mitochondrial ATP-dependent protease and determination of N-terminus of the mature enzyme from the adrenal cortex. *DNA Seq* **16:** 474-8

Yamamoto Y, Ibusuki M, Okumura Y, Kawasoe T, Kai K, Iyama K, Iwase H (2008) Hypoxia-inducible factor 1alpha is closely linked to an aggressive phenotype in breast cancer. *Breast Cancer Res Treat* **110:** 465-75

Yang J, Staples O, Thomas LW, Briston T, Robson M, Poon E, Simões ML, El-Emir E, Buffa FM, Ahmed A, Annear NP, Shukla D, Pedley BR, Maxwell PH, Harris AL, Ashcroft M (2012) Human CHCHD4 mitochondrial proteins regulate cellular oxygen consumption rate and metabolism and provide a critical role in hypoxia signaling and tumor progression. *J Clin Invest* **122:** 600-11

Yang Y, Cimen H, Han M-J, Shi T, Deng J-H, Koc H, Palacios OM, Montier L, Bai Y, Tong Q, Koc EC (2010) NAD+-dependent deacetylase SIRT3 regulates mitochondrial protein synthesis by deacetylation of the ribosomal protein MRPL10. *The Journal of biological chemistry* **285:** 7417-29

Yarborough A, Zhang YJ, Hsu TM, Santella RM (1996) Immunoperoxidase detection of 8-hydroxydeoxyguanosine in aflatoxin B1-treated rat liver and human oral mucosal cells. *Cancer Res* **56:** 683-8

Yoneda T, Benedetti C, Urano F, Clark SG, Harding HP, Ron D (2004) Compartment-specific perturbation of protein handling activates genes encoding mitochondrial chaperones. *J Cell Sci* **117:** 4055-66

Yu AY, Frid MG, Shimoda LA, Wiener CM, Stenmark K, Semenza GL (1998) Temporal, spatial, and oxygen-regulated expression of hypoxia-inducible factor-1 in the lung. *Am J Physiol* **275:** L818-26

Zelko IN, Mariani TJ, Folz RJ (2002) Superoxide dismutase multigene family: a comparison of the CuZn-SOD (SOD1), Mn-SOD (SOD2), and EC-SOD (SOD3) gene structures, evolution, and expression. *Free Radic Biol Med* **33:** 337-49

Zhang H, Bosch-Marce M, Shimoda LA, Tan YS, Baek JH, Wesley JB, Gonzalez FJ, Semenza GL (2008) Mitochondrial autophagy is an HIF-1-dependent adaptive metabolic response to hypoxia. *The Journal of biological chemistry* **283:** 10892-903

Zhang H, Gao P, Fukuda R, Kumar G, Krishnamachary B, Zeller KI, Dang CV, Semenza GL (2007) HIF-1 inhibits mitochondrial biogenesis and cellular respiration in VHL-deficient renal cell carcinoma by repression of C-MYC activity. *Cancer Cell* **11:** 407-20

Zhang J, Sattler M, Tonon G, Grabher C, Lababidi S, Zimmerhackl A, Raab MS, Vallet S, Zhou Y, Cartron M-A, Hideshima T, Tai Y-T, Chauhan D, Anderson KC, Podar K (2009) Targeting angiogenesis via a c-Myc/hypoxia-inducible factor-1alpha-dependent pathway in multiple myeloma. *Cancer Res* **69:** 5082-90

Zhao Q, Wang J, Levichkin IV, Stasinopoulos S, Ryan MT, Hoogenraad NJ (2002) A mitochondrial specific stress response in mammalian cells. *The EMBO journal* **21:** 4411-9

Zhao S, Lin Y, Xu W, Jiang W, Zha Z, Wang P, Yu W, Li Z, Gong L, Peng Y, Ding J, Lei Q, Guan K-L, Xiong Y (2009) Glioma-derived mutations in IDH1 dominantly inhibit IDH1 catalytic activity and induce HIF-1alpha. *Science* **324:** 261-5

Zhong H, Chiles K, Feldser D, Laughner E, Hanrahan C, Georgescu MM, Simons JW, Semenza GL (2000) Modulation of hypoxia-inducible factor 1alpha expression by the epidermal growth factor/phosphatidylinositol 3-kinase/PTEN/AKT/FRAP pathway in human prostate cancer cells: implications for tumor angiogenesis and therapeutics. *Cancer Res* **60:** 1541-5

Zhu Y, Wang M, Lin H, Huang C, Shi X, Luo J (2002) Epidermal growth factor up-regulates the transcription of mouse lon homology ATP-dependent protease through extracellular signal-regulated protein kinase- and phosphatidylinositol-3-kinase-dependent pathways. *Exp Cell Res* **280:** 97-106

Zundel W, Schindler C, Haas-Kogan D, Koong A, Kaper F, Chen E, Gottschalk AR, Ryan HE, Johnson RS, Jefferson AB, Stokoe D, Giaccia AJ (2000) Loss of PTEN facilitates HIF-1-mediated gene expression. *Genes Dev* **14:** 391-6